# Conceptual, Algorithmic, and Statistical Exploration of Relations Between Runoff Generation, Stream Geomorphology, and Watershed Topography in West Texas

by

George R. Herrmann

A Dissertation

In

Civil Engineering

Department of Civil and Environmental Engineering

Submitted to the Graduate Faculty
of Texas Tech University in
Partial Fulfillment of
the Requirements for
the Degree of

Doctor of Philosophy

Approved

Theodore G. Cleveland, Ph.D., P.E.
Chair of Committee

William H. Asquith, Ph.D., Ph.D., P.G.

David B. Thompson, Ph.D., P.E., P.H., D.WRE, CFM

Venkatesh Uddameri, Ph.D., P.E.

Dominick Joseph Casadonte, Jr.
Interim Dean of the Graduate School

December, 2013

# Acknowledgments

The number of people and entities to which I am very grateful is long, and it will probably be an incomplete list. In no order of priority, but somewhat grouped together, I would like to express my deepest thanks to the following people for the reasons mentioned:

My parents, the late Dr. George H. Herrmann, M.D. (July 25, 1928–January 22, 2011) and Gloria Jones Herrmann, R.N., for providing financial assistance and encouragement for continuing my formal education throughtout my life, as well as providing me genetically with a sound mind and a keen curiosity about the world around me.

My good friends in engineering and the sciences, Theodore G. Cleveland, Ph.D., P.E., William H. Asquith, Ph.D., Ph.D., P.G., David B. Thompson, Ph.D., P.E., P.H, D.WRE, CFM, and Xing Fang, Ph.D., P.E. These gentlemen have provided me with many hours of conversation, education, intellectual stimulation, discussion, laughter, and relaxation since about 1997. Without their confidence and encouragement, I would never have considered returning to the university environment for further enlightenment. They have inspired and assisted me in ways that I cannot even begin to describe. These four individuals were my mentors in the graduate academic, research, and publishing endeavors. Among them as well are my academic advisors for my Master's thesis (2002), my academic advisor for this Doctoral dissertation, and committee members for this Doctorate.

My friends and associates in the Texas Department of Transportation during a 24-year career with that agency, the agency that supported my Master's degree and provided me with the opportunity to become an expert in a field in which I have had a lifelong interest, even before I knew that it was called hydrology. Among those people are David Stolpa, P.E.(Ret.), Amy Ronnfeldt, P.E., John R. DeWitt P.E., Walter McCullough, P.E.(Ret.), and many others.

Particularly in the context of the third technical chapter of this document, and even more specifically with respect to my familiarity with the lower Pecos River in Texas, I must

mention the great debt I owe to Roy D. Cash (July 19, 1923–December 15, 2010), who ranched along the Pecos in northwest Val Verde County, Texas for his entire life. In the summer of 1974, at 16 years old, I began working for him for the summer as a ranch hand, and continued for four summers and many weekends and holidays. While working for him and with him and others in the area, I developed a deep affection for the rough and rugged country of the lower Pecos area, as well as all of the surrounding area of western Val Verde County, southern Crockett County, and southern Terrell County of Texas. While working as a ranch hand in that area, I witnessed first hand many amazing thunderstorms and the resulting runoff events, and saw the results of massive sediment transport by those events. I was sufficiently impressed that I can see those events in my mind's eye some 40 years later.

I owe much to Bill C. and Jeannie Lewis of Del Rio, family friends from my childhood, who talked me into going back to college for undergraduate work after a hiatus of four years. After two years as a Geology student at Texas Tech and several years in the tooling industry, I was disillusioned and looking for something else to do with my life. Over lunch one day in September, 1981, they convinced me that I should not neglect further education. It was a long road to my Bachelor's degree, but I made it. Their encouragement at that time was invaluable to me.

Most of all, I am grateful to my wonderful wife, Bonnie. Since the day we met, she has been a constant source of inspiration, encouragement, support, council, patience, strength, love, and friendship. She has been, without a doubt, the most profound and positive influence on my life. We have supported each other through good and bad, health and sickness, joy and sorrow, for many years now, and will for many more...

# Table of Contents

# List of Tables

# List of Figures

# Abstract

This Dissertation contains four separate, free-standing, but related documents. The common theme is the relation between geomorphology and hydrologic response.

1. *Moving Substrate in an Ephemeral Stream: A Case Study in Bridge Survival*
   (Republished with permission of the Transportation Research Board.)

   A case study concerns a small bridge site in an arid area where ongoing inhibition of the transport of bed load sediment has caused chronic problems and maintenance issues for many years. The crossing of Guadalupe Arroyo by coaligned US[1] Highways 62 and 180 exhibits many unusual and important characteristics that are seldom seen in one place. Evidence exists of large magnitude transport of very large particles on a regular basis, to the extent of requiring protection of the piles from boulder impacts. A large lens of bed material has accumulated upstream and extends approximately 1,000 ft (305 m) from the bridge. This site presents a rare opportunity to study an extreme case of the inadvertent inhibition of the transport of bed material in an ephemeral desert stream by the construction of an otherwise ordinary and innocuous highway bridge.
2. *A Generalized Additive Model (GAM) for Stream Discharge and Velocity Estimation from Stream Geomorphology*

   A discussion of work that was inspired by and resulted from discussions between the author and colleagues from various universities and from the U.S. Geological Survey (USGS) during and after the study of Guadalupe Arroyo documented in the previous chapter of this dissertation. The focus is on the validation of hydrologic techniques, hydraulic modeling, and bridge scour analyses.

[1] Prefixes for highways, US and SH, as used in this dissertation without periods, are system designators for the U. S. Federal and State Highway systems, respectively, rather than the initials for United States and State Highway.

3. *The Effect of Terrain Ruggedness on Runoff Generation and Flood Magnitude*

   This chapter constitutes a study of the influence of both terrain ruggedness and areal proximity on flood magnitude. Discussion and conceptualization of the influence on the runoff process of parts of a watershed far distant, versus those more proximate, to a point of interest. Case studies illustrating the point are observed by the fact that distinct differences in proximal influence are magnified by the ruggedness the terrain of proximate areas. The case examined involves increase in the ruggedness of the proximal terrain through which the main stem of the lower Pecos River flows.

4. *A Probabilistically Based Alternative to Unit Hydrograph Watershed Modeling*

   This chapter discusses conventional Unit Hydrograph modeling, then presents an alternative method of watershed modeling. The alternative method is based on the concept that the survival of a raindrop to traverse the watershed and exit is a random variable. The proposed model replaces the unit hydrograph and loss model with a time-area relationship, randomly generated variates from the either the exponential or the Weibull distribution, and a comparison between variate magnitude and the time needed to exit the watershed. A conceptual study and case studies demonstrate that the model can reasonably represent real rainfall-runoff data.

# Chapter 1
# Introduction

## 1.1 Prologue

In the early fall of 2008, as a recognized subject matter expert in hydraulic and hydrologic issues, I was asked to render an opinion with regard to a chronically problematic bridge site on the western edge of Culberson County, Texas. The site in question is where US Highways 62 and 180 (running the same alignment) cross an ephemeral stream known as Guadalupe Creek, or alternatively Guadalupe Arroyo. The bridge had been in place since 1959, 48 years at the time I became involved, and had been plagued with problems threatening the safety of the bridge for as long as any TxDOT employees could remember. The critical problem as seen in 2008 was bank erosion and meander migration.

An engineering consulting firm (I will not name which) had previously been engaged to do a study and report, and to make recommendations. This firm is a general firm rather than a firm specializing in water issues, and the people involved were transportation oriented in contrast to being water oriented. I was asked to review that report, do my own research, and render an opinon on suitable treatment. The report as it had been written was among the better reports I have read, especially considering the circumstances. This dissertation exists because of critical evaluation of that work, and is intended to answer questions stimulated by that report.

What was revealed to me by review of the report, by site visits, and by all available data collection, was (from a hydrologic and hydraulic standpoint) a pathologically diffiicult stream, a pathologically difficult watershed, and a pathologically difficult bridge site, all compounding one another. Added to those factors, ultimately, was a pathologically difficult funding mechanism, the American Reinvestment and Recovery Act (ARRA), which put very tight time constraints on process, and precluded the ability to work beyond the TxDOT right-of-way line.

Out of the study performed by the author, several lines of thought emerged. All involved the relationship between stream behavior and topography—topography of the watershed as a whole, topography of the watershed close to a point of interest, and the local topography of the stream itself, normally falling under the specific science of *fluvial geomorphology*, the study of the physical form of streams and features associated with streams. The lines of thought provoked by the Guadalupe Arroyo site resulted in this dissertation.

## 1.2 Historical Perspective of Hydrologic Research

From time out of mind, man has been dependent on surface water for many things. Other than the obvious purposes of drinking, cooking, and washing, mankind has depended on surface water for transportation, power, security, navigation, the delineation of boundaries, food supplies, irrigation, and countless other things. In particular, fresh water in the form of rivers and streams has been especially important.

The relationship between man and surface water has historically carried mixed blessings. The river that supplies all of the necessities of life to a thriving civilization will, eventually betray that civilization by way of massive floods and the attendant death and destruction, or by capriciously drying up at the time when it is most needed. Rivers and streams are intimately dependent on climate, and climate is notably unreliable.

For millenia, man often called upon divine inspiration or intervention when questioning the future state of flow in a stream. It was usually easy to observe the relationship between rain or snow and the flow in a stream, but little else was known. The scientific study of water, what we now call hydrology, began in fairly recent times. Much progress has been made, and much remains to be revealed. The scientific study of the past 100 years has focused on applying mathematics and the laws of physics to the study of water, its occurrence, and its movement.

Much of that study has been geared toward isolating clean, mathematically tractable, physical phenomena that are easily understood, described and simulated in the office, from the dirty inconvenient, chaotic, and ultimately disappointing occurrences that reality shows us on even the simplest of watersheds. Researchers in the field of hydrology such as Clarke, Sherman, Horton, Leinhard, Betson, Eagleson, Asquith, Thompson, Cleveland, Herrmann, and many more have developed and published very technical methods based on physics and mathematics. A theme that is common, and occasionally openly stated is the desire to develop methods that are based in theory alone, and do not require physiographic informa-

tion from the watershed under study. Some widely used and very popular methods, such as the SCS method (USDA-SCS, 1972), are based on the assumption that all watersheds behave the same, and that response to a rainfall event is, within reason, independent of the topography or geomorphology of a particular watershed.

Another very popular method for the estimation of instantaneous peak streamflow, the USGS regional regression equations, (Asquith et al., 1996; Asquith and Slade, 1997; Asquith, 1998; Raines, 1998; Asquith and Thompson, 2008; Asquith and Roussel, 2009) along with the web-based program StreamStats (U. S. Geological Survey, 2013), also rely upon the assumption that similar watersheds behave similarly. These equations typically have several explanatory variables. Almost without exception, one of the variables used is watershed area. Other popular variables that do constitute physiographic information about watersheds are stream slope, shape factor, altitude, and mean annual precipitation. There are hundreds of explanatory variables availalble for the developer of the equation to use to establish statistical relationships. However, by their very nature, the equations represent expected response to expected conditions.

The Guadalupe Arroyo site presented a situation of unexpected conditions, and the analyst was confronted with the challenge that there was not an appropriate method of hydrologic estimation available. Some reasons for the inadequacy of available methods are the extreme elevation difference and ruggedness of the watershed, its remoteness and isolation from areas of dense data collection, and the orographic effects of mountains. Any one of the issues of isolation from sites of either rainfall or streamflow data collection, known inconsistency with surrounding areas because of orographic effects, and known inconsistency with surrounding areas because of terrain ruggedness would create discordance with nearby watersheds that would make hydrologic estimation questionable. All of these factors combined were present at the site in question.

The Guadalupe Arroyo site is not the only site in west Texas that stimulates questions about hydrologic estimation. During an engineering study conducted by the author for internal (TxDOT) discussion, a succession of streamgauges on the Pecos River in west Texas was noticed, the data from which exhibited unexpected behavior. In the case of this group of gauges, annual peak series along a major stream exhibited leaps in magnitude and disjunction in peak flow dates that made them appear to be on completely different streams. By chance, the author was personally familiar with the terrain and conditions of these streamgauge situations because of time spent in the area many years past.

At best, the sites described (Guadalupe Arroyo and the lower Pecos River) present confusing, unexpected results to conventional analysis. The Guadalupe Arroyo watershed is

involves an unusual degree of change in elevation and stream slope, along with localized anomalous rainfall because of orographic effects. No historical rainfall data could be located for the watershed, and no streamflow data for similar conditions nearby could be located. The lower Pecos River exhibits diminishing annual peak flow rates past several gauges, then a very dramatic increase in annual peak flow rate past the lowest two gauges. These two phenomona represent situations that are outside of the boundaries of the assumptions of similarity that dominate in hydrologic analyses.

This dissertation is not intended to criticize the use of accepted, standard methods for the majority of hydrologic analyses. It is intended to document and describe the unexpected, with the idea that hydrologists should always be mindful that unexpected situations do exist and can be documented and explained, whether they can be accommodated by conventional methods of hydrology or not. The cases in point are real cases, not theoretical ones. Proposed theoretical explanations are put forth, with the hope that future research will expand the knowledge base.

## 1.3 Description of Chapters

The bulk of this dissertation is composed of four separate, but related research topics.

1. The first (Chapter 2) is a republication of a paper by G. R. Herrmann and T. G. Cleveland. It is a case study on the Guadalupe Arroyo bridge site. The study done for this site stimulated the following three chapters in this dissertation, all of which deal with the effects of terrain on hydrologic response, and on hydraulic performance.
2. The second (Chapter 3) is a discussion of the topics, motivations, and value to the profession of a paper by Asquith, Herrmann, and Cleveland. The article is discussed, and attached in Appendix A, with deletion of a notation section and a list of gauges used in the analysis, is a study that draws connections and implies boundaries on the hydraulic flow characteristics of natural streams, such as velocity, depth, top width, and discharge. In essence, it makes use of the fact that the topographic characteristics of a stream channel are durable artifacts of the hydraulics of past flood (direct runoff) events. By analyzing those characteristics, we can better understand the nature of flood events on a stream.
3. The third (Chapter 4) is new work by the author. The chapter examines in some detail a known case of multiple stream gauges on the same stream that exhibit unexpectedly disjoint behavior over reasonably short distances. An explanation is proposed by examining

the apparent strong influence of terrain proximate to the gauge combined with the effects of rugged terrain within the proximate area.

4. The fourth (Chapter 5) also is new work by the author. Building on the idea of proximate area exerting more influence than distal area, and alternative approach is proposed, then demonstrated, that accounts for the diminishing of influence with distance by equating distance with residence time. A conceptual model is built and demonstrated, then simple case studies are performed to demonstrate the applicability and viability of the model.

Chapter 2 and Appendix A were previously published in journals. Chapters 4 and 5 will be submitted to appropriate journals. Each chapter begins with a prologue giving a brief explanation of context within the dissertation. Chapter 6 is a conclusions and recommendations chapter for the entire dissertation as a collective body of work. Computer codes written for the **R** programming environment for two different probability distributions (the exponential and the Weibull) are included in Appendices B and C, respectively.

# Chapter 2

# Moving Substrate in an Ephemeral Stream: A Case Study in Bridge Survival

## 2.1 Prologue

This chapter contains the entirety of a paper written for the Transportation Research Board 7th International Bridge Engineering Conference, held in San Antonio, Texas, in December, 2010. During the preceding year, the authors (George R. Herrmann, principal author, and Theodore G. Cleveland, coauthor) had examined the bridge site at Guadalupe Arroyo because of mutual interest in the instability shown by this site. Mr. Herrmann had been asked to consult on this case by representatives of the Bridge Division Geotechnical Section of the Texas Department of Transportation (TxDOT). The problem as originally cast was thought to be bank erosion and meander migration. It was subsequetly decided that these problems were the result of aggradation and overall instability.

An engineering study of the site had resulted in a report, performed by a consulting firm. Contained in that report was output from standard step backwater computations performed using a widely accepted modeling system. Considering the nature of the bed material at the site (sand, gravel, cobbles, and boulders; no cohesive material), and the obvious long-term problem with deposition in the bridge opening, the calculated velocities from the model, in the range of 20 feet per second, did not seem to make sense. Had velocities been that high, the expectation would be to see indurated rock exposed, or at least only large boulders remaining. Core borings taken prior to the construction of the bridge and shown on the plan sheet indicated granular alluvium to a depth of at least 22 feet from the original surface of the streambed. Length of driven piling foundations were shown as 50 feet for interior bents, indicating the absence of indurated rock for at least that depth.

Referring to available literature on stream geomorphology and sediment transport, oblique reference (without citation) to a study by the USGS on velocities measured in the U. S. by USGS personnel was discovered (Leopold, 1994). A colleague in the USGS

(William H. Asquith) was consulted in order to locate the referenced study. The study mentioned in Leopold (1994) was not located, however, an ad-hoc study was begun on Texas data. The result of that study, and subsequent research work, is documented in a later chapter of this disseration and in Appendix A. The origin of that study, and the inspiration for all work in this dissertation, was the study that resulted in the article on Guadalupe Arroyo.

The Guadalupe Arroyo bridge site brings to light at least three related topics. Those are:

1. The unusually high sediment transport that occurs in this area;
2. The ruggedness of the terrain in this area; and
3. The absence of appropriate hydrologic estimation techniques, because of ruggedness of the terrain, the lack of rainfall data considering orographic effects, and the lack of streamgauges.

This paper was presented by the principal author on December 3, 2010. It is republished with changes in format and minor revisions, with permission of the Transportation Research Board. Previously published in the Transportation Research Record: Journal of the Transportation Research Board, No. 2201, pp. 3–9. None of this material implies endorsement by the Transportation Research Board of any product, method, practice, or policy.

## 2.2 Chapter Abstract

A case study concerns a small bridge site in an arid area where ongoing inhibition of the transport of bed load sediment has caused chronic problems and maintenance issues for many years. The crossing of Guadalupe Arroyo by coaligned US Highways 62 and 180 (US 62/180) exhibits many unusual and important characteristics that are seldom seen in one place. Guadalupe Arroyo is an ephemeral stream in a very arid area. The stream originates high on the east slopes of the Guadalupe Mountains of Texas, where the watershed is subject to rainfall generated by orographic lift. The stream traverses several miles of arid land and ultimately disappears into a dry lake. It is subject to severe flash flooding because of the slope and orographic effects of the mountains, and it apparently transports large amounts of widely graded material (silt to boulder sized). A bridge across this stream was constructed for US 62/180 in 1959. Since that construction, the stream has exhibited symptoms of instability in the reach around the bridge, manifesting as chronic, severe aggradation accompanied by widening, avulsion, and bank erosion. Evidence exists of large magnitude transport of very large particles on a regular basis, to the extent of requiring protection of the piles from boulder impacts. Maintenance forces have continually removed accumulated bed material from the bridge opening and the reach immediately upstream. A large lens of bed material has accumulated upstream and extends approximately 1,000 ft (305 m) from the bridge. This site presents a rare opportunity to study an extreme case of the inadvertent inhibition of the transport of bed material in an ephemeral desert stream by the construction of an otherwise ordinary and innocuous highway bridge.

## 2.3 Introduction

Guadalupe Arroyo is an unusual Texas stream, with several interesting qualities. Streams that flow into dry lakes are not uncommon in states like Arizona and Nevada, but there are few in Texas. This ephemeral stream arises from the southeastern flank of the Guadalupe Mountains and the adjacent Delaware Mountains to the east, traverses a region of Chihuahuan desert at the foot of a mountain known as El Capitan from east to west, and disappears into a dry lake. It is characterized by relatively steep slopes, sparse desert scrub vegetation and “flashy” flood response typical of streams in arid regions.

This area of west Texas is arid and sparsely populated. There are few rainfall measurement stations, and even fewer streamflow-gauging stations. While the mean annual

precipitation in the area is low, the nearby Guadalupe Mountains exerts a strong orographic effect, locally increasing rainfall on the mountain flanks directly contributing to this stream. Flash floods at the site are anecdotally considered more common and severe than in the surrounding desert. These floods often occur from rainfall confined to the mountains, resulting in flows at the bridge in the absence of rainfall at the site itself.

## 2.4 Hydrology

A reliable method of hydrologic estimation for this watershed does not exist because of the unusual and relatively unique nature of this stream. Statistical methods, such as regression equations, rely on a consistency between the watershed being analyzed and gauged watersheds used to develop the equations. Such consistency does not exist in this case. Watershed modeling requires a similar consistency between rainfall measured at weather stations and the rainfall that generates runoff on a watershed. Again, that condition cannot be met for this watershed because of the orographic influence on the dominant flood-producing rainfall.

The contributing watershed area to the site is about 40 square miles (104 square kilometers) (Figure 2.1). The crossing is approximately at elevation 3,850 feet (1,174 meters). The uppermost point of the watershed is Guadalupe Peak, the highest point in Texas, at approximately 8,550 feet (2,606 meters). The total drop is on the order of 4,700 feet (1,433 meters) in about 12.5 miles (20 kilometers) of stream, with 3,500 feet (1,067 meters) of that elevation change occurring in the upper 1/3 of the drainage. The physical characteristics of this watershed are therefore unusual. Such a stream can be considered as a conveyor belt of the mass wasting process; the stream exists mainly to move the products of mass wasting downhill.

## 2.5 Site Character

In 1959, the existing bridge crossing Guadalupe Arroyo on US 62/180 was constructed. During the more than 50 years since that construction, maintenance effort necessary to keep the bridge serviceable has been increasing. Recently, erosion of the south bank of the stream to the east of the bridge has presented a threat to the south abutment. For many years (as long as current maintenance employees recall), there has been a chronic need for maintenance forces to remove bed material from the bridge opening and the reach

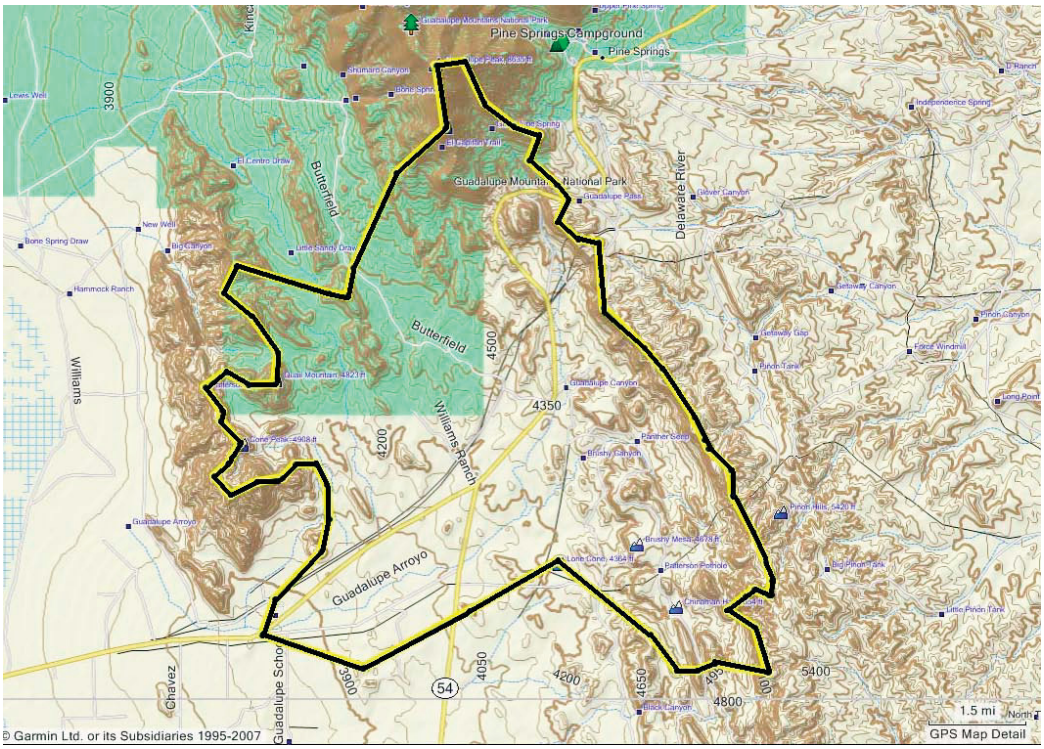


**Figure 2.1.** Drainage area map. (Source: Garmin Ltd., 2010)

immediately above it. The lateral migration of the south bank and other visible indicators, suggests that bedload sediment is inhibited from passing the bridge site on the stream, and has clogged and aggraded the streambed. These observations further suggest that instability in the reach adjacent to the crossing is related to the crossing in some way, possibly from the influences of the crossing on bedload sediment transport potential.

A trace of darker material appears on the surface of the widened bed in a meandering pattern that coincides with areas of apparent bank erosion in overhead imagery. That meander pattern appears to be of shorter wavelength and smaller radius of curvature than the rest of the stream, at least until the stream gradient drops as it enters the terminal lake downstream. Unusual widening of the visible streambed is often an indicator of localized aggradation, and a shortening of meander wavelength can be an indicator of lessening of relative stream gradient.

The particular problem at the site has developed as bank erosion along the outside of a gentle meander, adjacent to and threatening the adjacent south abutment of the bridge. An important observation about this site is found in the overhead imagery (Google Earth). Tracking Guadalupe Creek along all tributaries from origin to destination, the stream reach immediately adjacent to the crossing of US 62/180 stands out as anomalous. The stream

exhibits an obvious widening at the crossing, which continues downstream approximately 300 feet (91 meters) before disappearing, and extends upstream approximately 1,600 feet (488 meters). This widening is seen in Figure 2.2.

The image shows an already conspicuously wide reach of the stream is further widening to the south. No similar reach is in evidence from imagery along this stream. This widening appears to be associated with the highway crossing. Numerous other sites have been identified in recent years where highway stream crossings have exhibited an adverse impact on stream stability in central and west Texas (Herrmann, 2007, 2008; Heitmuller and Asquith, 2008; Thompson et al., 2009) so such an association is not unusual. At this site, the highway crosses the stream at a fairly acute angle (greater than 45 deg.) and in a bend of the stream. The exact angle of skew is ambiguous because of the curvature of the stream, and because the streambed is tapering at this point. The bridge bents are skewed with respect to the roadway to more nearly align with the stream. The supporting foundations are driven steel H-piling.


**Figure 2.2.** Current (2009) overhead image (note overwidened section upstream of bridge and appearance of shorter wavelength). (Google Earth)

## 2.6 Hydraulic Factors

The original design of the bridge clearly attempted to align the bents with flow streamlines, but the location of the bridge in a bend of the stream is a complicating factor. Approaching and departing streamlines are at angles to the bents, and to each other. A further complication is that flow under the existing conditions appears to converge through the bridge opening. Hydraulic geometry at the crossing has been altered from the natural conditions by construction activities such that arriving bedload material does not readily proceed through to the adjacent reach. The approach reach has become a sediment sink; as more sediment arrives, it adds to sediment already residing there. The accumulation has caused the streambed aggradation, forcing widening and avulsion.

A review of the bridge layouts indicates that the stream cross section through the bridge opening may have been shaped or "improved" to enhance hydraulic capacity by providing greater area of flow. This kind of effort to enhance hydraulic capacity is ubiquitous in bridge hydraulic design. Although well-intentioned, it often adversely affects the hydraulic geometry of the stream, a critical variable in bedload sediment transport (Heitmuller, 2009), and disrupts stream power at the point in the stream profile occupied by the bridge.

This particular stream is apparently extremely sensitive to such changes, as it appears to have been destabilized at that time, with chronic problems resulting. The nature of the existing bents and the angles of approach and departure of water and sediment are compounding factors to an unknown degree. Altogether, the result is severe stream instability.

Streams are invariably the avenues of movement of at least two media; water and sediment. Sediment is composed of two components; suspended load and bed load. In ephemeral streams such as this one, the fraction of total sediment load that moves as bed load is necessarily higher than it is in perennial streams, simply because bed load movement is a result of flood flow, and all flow in an ephemeral stream is flood flow. What specific condition triggered the onset of aggradation and the subsequent destabilization of the stream is now difficult to determine.

The ability of a stream to move bed material is apparently related to both velocity and depth. When a stream aggrades and widens, stream power available to move bed material is reduced. However, at locations downstream where more favorable geometry exists, the stream may be thought of as deficient in bed load sediment. Under those conditions, the stream will still mobilize the available material from the bed and banks, resulting in scour or degradation of the streambed in that reach. Such scour may also manifest itself as lateral movement and erosion of the stream banks.

**Figure 2.3.** Bridge pile (note evidence that bed material has been at least 4 ft higher than it is under conditions at time of the photograph (2009)).(12 in by 12 in steel H piling)

At this site, the streambed in the immediate vicinity of the crossing (600 feet (183 meters) upstream and 300 feet (91 meters) downstream) has been further influenced by ongoing mechanical efforts to prevent further damage to the bridge. Unknown quantities of bed material have been moved from the stream under and near the bridge to the banks. There are physical indications of material having been approximately 4 feet (1.2 meters) deeper at the bridge itself in the past (see Figure 2.3) than when the site was visited. Material has been mechanically removed in order to enlarge the bridge opening.

The construction plans for the bridge indicate a general height of the bridge low chord above the streambed at the time of construction of 12 feet (3.6 meters). The roadway profile at the bridge is both on a grade and in a superelevated curve, making reference to such a height ambiguous. Thus it is difficult to state with certainty how much the streambed has aggraded. A rough estimate based on observation is that net aggradation at the bridge has been, in the recent past, between 5 and 8 feet (1.5 and 2.4 meters) of depth of bed material, which has been mechanically removed. As the removal of such material has apparently been ongoing for many years, the amount of material that has already passed through the reach cannot be estimated. However, on the basis of this degree of aggradation at the bridge and the distance upstream that impact is visible, the amount of material remaining in a lens upstream of the bridge is estimated at between 10,000 and 20,000 cubic yards (7,650 and 15,300 cubic meters). A minimum of approximately 300 cubic yards (230 cubic meters) of bed material per year appears to be the average arriving at the site and being detained since original construction in 1959.

The steel H-pilings supporting the bridge bear indications of having been buried numerous times, and bear damage indicating impacts from boulders. Some time after the original construction, concrete walls connecting the piling of each bent and semi-circular nose elements on the upstream side of the upstream pilings were constructed, evidently to prevent damage from boulder impacts, or machine impacts during removal operations.

A hydraulic study conducted of this site by others using step-backwater techniques, extending approximately 300 feet (91 meters) upstream and downstream of the structure, indicated very high calculated velocities (20 ft/sec, 6.1 m/sec). An ad-hoc study by a USGS employee (William H. Asquith) indicated that out of 58,724 measured discharge and velocity values in Texas, roughly 20 exceed 10 ft/sec (3 m/sec) and none approach 20 ft/sec (6.1 m/sec). Whereas this is an unusual case, we concluded that the simplifying assumptions necessary for such hydraulic analyses are incompatible with actual flow conditions. In particular, the assumptions of rigid channel boundaries and single-phase flow are likely not representative of sites such as this. High-magnitude bed load movement may be a transitional phenomenon between ordinary fluid flow and debris-type flow.

## 2.7 Bed Material

Site reconnaissance demonstrated that the bed material is composed of particles ranging from silt size up to several feet in size (Figures 2.4 and 2.5). This gradation is also an

indication of the magnitude of forces driving movement; such particles are not moved easily. Conditions permitting their movement would necessarily result in the movement of huge quantities of cobbles and gravel as well. By volume, the preponderance of material is fine sand. Larger particles, including a wide range of gravel, cobble, and boulder sizes, appear embedded in a matrix of fine sand. One plausible model is that the apparent throughput of material might be related to some optimal proportion of large particles embedded in a matrix of more easily mobilized sand.

In locations where the undisturbed stream banks that are subject to erosion were visible, the material in them appears to be alluvium consistent with the bed material; sand, gravel, and cobbles. Erosion of the banks results in material indistinguishable from that already in the streambed (Figure 2.6), thus at least some of the material present at the site is material recently liberated from these banks. However, considerable quantities of material have had to be removed mechanically; this argues in favor of a net positive change in storage of the bed material in this reach over time, as opposed to simply liberation from adjacent alluvial deposits.

Imagery indicates that the over-widened reach dissipates in less than 400 feet (122 meters) downstream of the bridge. A reconnaissance of that distance and greater downstream revealed that features consistent with bankfull geometry emerge from the bed material and are consistently maintained proceeding downstream. Using these features, a bankfull width of 50 feet and a depth of 4 feet (1.2 meters) is estimated to be the natural stream channel configuration near the crossing.

Upstream approximately 1,200 feet from the bridge, the emergence of similar features of similar dimension from the downstream bed was observed. Using a parabolic approximation for area of flow and assuming a Froude number of 0.5 (Heitmuller and Asquith, 2008), these dimensions result in a bankfull discharge of approximately 600 cfs (17 cubic meters/sec). In the reach adjacent to the bridge, no such features are in evidence. Morphologic structures existing prior to the bridge construction may be buried under bed material, or may have been obliterated by construction and maintenance efforts. Rather than being streambanks, the features now defining the channel have probably been floodplain terraces until recently. Similar terraces exist in the reaches where the smaller bankfull features are visible. The bank on which erosion is currently a problem appears to actually be a floodplain terrace, rather than a stream bank associated with bankfull channel geometry dictated by current climatic and runoff conditions.

**Figure 2.4.** Streambed material (view of streambed looking downstream toward bridge).

The stream reach adjacent to the bridge (approximately 300 feet (91 meters) downstream and 600 feet (183 meters) upstream) has been severely altered by maintenance activities such that identification of bankfull features is impossible.

Locating actual bankfull features and geometry are important for several reasons. In diagnosing stream instability, estimating what bankfull geometry should be is essential. In addressing unstable sites, it is desirable to re-establish and maintain bankfull geometry approximating what should occur at a location in order to stabilize the stream. It is logical that bankfull configuration through the bridge reach was similar to the configuration above and below the bridge where features are still identifiable today.

## 2.8 Stream Morphology and Surrounding Terrain

Several miles above the site in question, Guadalupe Arroyo is crossed by Texas State Highway 54 (SH 54), which ends where it intersects US 62/180 several miles east of the bridge in question. At this crossing, bed material is predominantly sand-size. The boulder-

**Figure 2.5.** Large bed material (4 ft. Philadelphia level rod for scale).

size particles seen at the US 62/180 site are not in evidence in quantities similar to the problematic site, although occasional large cobbles do appear (Figure 2.7).

The watershed contributing to the SH 54 site primarily drains from the Delaware Mountains, an adjacent range much lower, less impressive, and geologically different from the Guadalupes. Several tributaries cross US 62/180 between the intersection of SH 54 and flow into Guadalupe Arroyo upstream of the site of interest. These crossings allow the examination of associated streams in similar conditions, but with other crossing types. It is evident from the examination of one of these crossings that the cobble- and boulder-size particles seen at the site of interest are the result of concentration of those particles in the area of a crossing by preferential transport. The smaller particles move through the crossing more easily, whereas the large particles are delayed, resulting in an anomalously large presence of them at the site of a crossing. This preferential segregation was observed at the SH 54 site also.

The crossings at SH 54 and of US 62/180 at a tributary to Guadalupe Arroyo present comparisons to the crossing in question. The former is an open-span bridge, similar to the structure of interest, but smaller. In that location, bankfull width is approximately 40 feet

**Figure 2.6.** Undisturbed streambank showing character of bank material

(12 meters). The latter is a 6-barrel 10 ft. by 10 ft. (3 meter by 3 meter) box culvert, and the bankfull width is approximately 35 feet (10.7 meters) (Figure 2.8).

Meander amplitude is usually confined to a "meander belt" between floodplain terraces or the valley banks that define the floodplain, while meander wavelength is related to the overall topographic slope of the valley. Steep valley slopes are characterized by small meander amplitude relative to meander wavelength. When aggradation occurs, a localized decrease in stream slope accompanies it. The meander wavelength tends to diminish, and meander amplitude tends to increase, in response to that change in slope (Rosgen, 1996; Leopold, 1994).

According to the Rosgen classification system (Rosgen, 1996), this stream falls into the classification of G3. This classification is noted as being "highly unstable due to the very high sediment supply available form both upslope and channel derived sources." It is further described as: "very sensitive to disturbance and tend to make significant adverse channel adjustments to changes in flow regime and sediment supply from the watershed." These descriptions encapsulate the problem as it is presented here quite thoroughly. A relatively slight disturbance (the construction of a bridge and change in hydraulic geometry) 50 years

**Figure 2.7.** Guadalupe Arroyo at upstream crossing of SH 54 looking downstream (larger material in bridge vicinity; bankfull configuration is evident in stream adjacent to this bridge).

ago has echoed with instability and channel adjustments ever since. Of this stream type, Rosgen also states "The ratio of bedload to total sediment load often exceeds 50 percent. (Rosgen, 1996)" Such large bedload movement is consistent with observation and history at this site.

A series of overhead images extending back in time approximately 13 years shows that the stream immediately above the bridge has been exhibiting essentially identical instability at least that long. Imagery from 1996 (Figure 2.9) indicate that the meander character of the stream immediately upstream of the bridge is in a state of change. Where there had previously been a long, gentle meander, meander reversal has occurred, resulting in the development of a short-wavelength meander anomalous for the stream. The avulsion attendant to this meander change has been seen and interpreted only in the context of bank erosion that threatens the southwest bridge abutment.

This image, and others from the years between 1996 and the present, show the signs of repeated and chronic attempts to rebuild and stabilize the stream banks, as well as removing material from the bridge opening itself. Figure 2.10 is an image from 2005, which shows

**Figure 2.8.** US 62/180 at a tributary to Guadalupe Arroyo

bed material piled adjacent to the stream from efforts to deal with the accumulating bed material.

## 2.9 Discussion and Conclusions

This site has been a chronic maintenance problem for many years, possibly decades. In 1996, the problem was already well developed. Thus far, efforts to keep the bridge in service have done so, but have clearly not solved the problem. Indications are that the problem is getting worse with time; the severity of bank erosion along the southwest abutment of the bridge increases with each flood event. Repeated efforts to rebuild and reinforce the banks have failed. This long and chronic history of problems should be an indicator that the situation has not been understood. The visible problem is one of bank erosion; however the underlying problem is one of stream stability.

Stability and instability with regard to stream geomorphology are terms that are much more commonly thought of in the context of perennial streams, fisheries biology, and


**Figure 2.9.** Overhead Image from 1996 (shortening of meander wavelength is evident at this time). (Google Earth)

riparian habitat. Many engineers and environmental scientists would view the application of these terms to an ephemeral stream in a desert area such as this with some doubt. However, this case demonstrates that the terms are applicable, and that ephemeral desert streams may be even more sensitive to disturbance than those streams where the science of fluvial geomorphology evolved. General fluvial geomorphic concepts such as the progression of riffles, runs, pools, and glides, the relationship of these profile features to plan features such as meanders and a bankfull channel are much more difficult to identify with certainty when a stream lacks base flow.

Stream restoration is an activity that is of increasing importance in the general civil engineering field. In its traditional form, dealing with the preservation or restoration of habitat and the mitigation of environmental damage, it has often been used to address the long-term aftermath of prior civil engineering works. As the general civil engineering profession has begun to examine the long-term implications of our works, stream stability and stream restoration have begun entering into the vocabulary of the profession. However, it is still difficult for many engineers to accept that these concepts might extend to desert streams like Guadalupe Arroyo (Bull and Kirkby, 2002).


**Figure 2.10.** Overhead Image from 2005 (note bed material piled along stream upstream of bridge location, indicated by closed shapes). (Google Earth)

In spite of that, it appears that an approach to this problem should be sought through stream restoration. Clearly, the simple armoring of the banks has not solved the problem; there is no reason to believe that it will in the future. A more thorough solution would involve the manipulation of the stream geometry in a manner that would allow bed material arriving at the site to pass, and encourage bed material accumulated at the site to re-mobilize and continue downstream.

Both hydrology and hydraulic analysis at this site (and others like it) are particularly difficult because of a lack of appropriate data under similar conditions. At this time, a computational approach to stream restoration is severely hampered by those difficulties. However, the "reference reach" approach to stream restoration would be a viable option for addressing this site. The reference reach approach involves locating a similar reach of stream in close proximity, and transferring certain physical characteristics from that stream to the stream of interest. In this case, reaches immediately above and below the impacted reach were examined for features including bankfull channel and potential riffles. At intervals along the stream in the reaches upstream and downstream of the bridge are features thought to be riffles during flow events. The nature of the material, as well as

**Figure 2.11.** Riffle location (looking downstream from a location thought to be head of a riffle).

visibly higher slopes over short distances, are thought to be indicative of riffles. Figure 2.11 shows one of these locations.

Riffles are important features in the profile of any stream, and are used as important points of reference for the assessment of a stream. Locating them is a vital part of finding a reference reach.

The important conclusion that can be drawn from an examination of this site is that stream type, stability, and sediment transport considerations should be emphasized to engineers designing and constructing bridges and roadways. While it is easy to dismiss factors such as this in an arid area subject to 10 inches of rainfall per year on average, to do so obviously risks severe long-term problems and maintenance costs.

The authors contend that the ultimate cause of the problem plaguing the crossing of Guadalupe Arroyo by US 62/180 is the re-shaping of the stream channel that occurred during the construction of the bridge. This re-shaping was compounded by the severe skew of the crossing, which extended the affected area along the stream for more distance than would be found in a normal crossing. Such re-shaping is a common practice in bridge

construction, under the hypothesis that it increases the conveyance through the bridge. Streams, particularly ephemeral ones, are often re-shaped to that of a simple trapezoid, destroying the shape that the stream has assumed in order to transport bed sediment. While it should increase conveyance of water by increasing flow area, this re-shaping destroys the natural hydraulic geometry for varying distances upstream and downstream. Sediment transport through the reach involved is inhibited, and the reach becomes a sink for sediment. All bed sediment is inhibited, but particles that are most difficult to move (the largest ones) reside in the reach for long periods, effectively segregating from the remainder of the load as it moves through the reach. This has been perpetuated and compounded by continued re-shaping by maintenance activities.

This segregation hypothesis is supported by the presence of large particles in the structure vicinity at the other two sites examined, where a more natural bed form and sediment gradation could be observed nearby. At the SH 54 location, maintenance is necessary, but to a much smaller degree than at US 62/180. At the nearby tributary stream, maintenance activities are not in evidence at all. Both of these structures cross at smaller or nonexistent skews, and the structures are closer to in length to the bankfull width of the stream at there locations.

This site should be periodically re-examined or monitored long-term. Large particle movement and ongoing maintenance activities endanger traditional monitoring equipment placed at the site, and data collection may require innovative monitoring techniques.

# Chapter 3

# A Generalized Additive Model (GAM) for Stream Discharge and Velocity Estimation from Stream Geomorphology

## 3.1 Prologue

This chapter consists of a discussion of the background and utility of a paper by Asquith, Herrmann, and Cleveland published in the American Society of Civil Engineers (ASCE) Journal of Hydrologic Engineering. The article is republished in Appendix A to this dissertation, with permission from ASCE. This material may be downloaded for personal use only. Any other use requires prior permission of the American Society of Civil Engineers. The full citation is as follows:

Asquith, W. H., Herrmann, G. R., and Cleveland, T. G., *Generalized Additive Regression Models of Discharge and Mean Velocity Associated with Direct-Runoff Conditions In Texas: Utility of the U.S. Geological Survey Discharge Measurement Database*, American Society of Civil Engineers, Journal of Hydrologic Engineering, volume 18, no. 10, October, 2013, pp 1331–1348.

The above paper is discussed as relates to the historical development of the research leading to the paper, and to emphasize the practical aspects of estimating velocity for bridge scour estimation and hydraulic model validation. Initial encouragement for this idea came from the TxDOT Bridge Division Geotechnical Section, as well as the TxDOT Design Division Hydraulics Section for validation of hydraulic modeling.

The primary aspect of this paper is that it places reasonable restraint on, and provides methods of computing, important hydraulic characteristics of a stream, based on the existing cross section geometry. Stream geometry is invariably a product of past events, and can therefore provide information on the behavior of future events.

## 3.2 Chapter Abstract

A discussion of work that was inspired by and resulted from discussions between the author and colleagues from various universities and from the U.S. Geological Survey (USGS) during and after the study of Guadalupe Arroyo documented in the previous chapter of this dissertation. The focus is on the validation of hydrologic techniques, hydraulic modeling, and bridge scour analyses.

## 3.3 Introduction

During the preliminary engineering phase of a proposed TxDOT construction project intended to mitigate a chronically troublesome bridge site in Culberson County, Texas, at US Highway 62 and 180 aand Guadalupe Arroyo (Herrmann and Cleveland, 2010), the review of a report including hydraulic analyses, prepared by an outside consultant, resulted in a conversation between TxDOT personnel and USGS personnel. Leopold (1994) alluded to, but did not cite, a USGS report discussing the range of stream velocity measurements by USGS personnel. The discussion in Leopold (1994) appeared inconsistent with velocities frequently reported in bridge scour analyses that is, velocities resulting from hydraulic model computations. Insufficient information on the USGS report mentioned made it impossible to locate, however the question of the distribution of measured velocities remained.

Hydraulic analyses for bridge hydraulic opening design and for foundation scour estimation are ubiquitous in the bridge and highway engineering profession. Normally undertaken with readily available standard-step one-dimensional hydraulic models, these analyses have great impact on the initial cost of construction of bridges, as well as long-term performance and suitability. In the opinion and observation of the author, poor hydraulic analyses may result in needless initial cost expenditure, introduction or exacerbation of stream instability problems, long-term excessive maintenance cost, loss of servicability, or even catastrophic failure of bridge structures.

On April 5, 1987, a bridge over Schoharie Creek in New York collapsed under traffic, resulting in several deaths, because of the undermining of bridge pier foundations by scour. In the years after the Schoharie Creek bridge collapse, the U.S. Department of Transportation (USDOT) Federal Highway Administration (FHWA), under legislative mandate,[1] began requiring the evaluation of all stream crossing bridges, or bridges over tidally influ-

[1] Fall 2013 version 23 CFR 650, subpart C, historical reference unavailable.

enced estuaries, for potential scour collapse. Scour collapse was seen to be a tangible threat to public safety, so the program proceeded with high priority through FHWA to the various state Departments of Transportation. By Federal Aid Policy (FAP), states are required to oversee the inspection of all publicly traveled bridges within the state, regardless of the owner of the bridge (bridges may be owned and operated by city, county, state, toll road franchise, or other entity).

Between FHWA and individual states, research into scour mechanisms, scour evaluation and modeling, and scour failures consumed many research dollars. FHWA published Hydrologic Engineering Circular 18 (HEC-18) *Evaluating Scour at Bridges* soon after the mandate for scour evaluation, as a guide for scour evaluations. HEC-18 is currently (2013) in the fifth edition (Arneson et al., 2013). Early editions promoted the use of one-dimensional step backwater analysis as the only reliable source of velocities for scour evaluation. Mean velocity is a very important parameter for the equations used to estimate scour.

The Texas Department of Transportation (TxDOT) manages inspections, files, and data on over 45,000 stream crossing bridges, on and off the state system (Ramsey, 2011). As such, Texas has the largest inventory of bridges in the United States. The task of evaluating all 45,000 bridges for scour potential was daunting. Many engineers (including the author) were trained to perform the necessary engineering analyses for hydraulic modeling, and scour calculations. However, topographic data necessary to perform backwater computations reliably was unavailable for most bridges (known from personal involvement by the author). The necessary funds, time, and manpower were not available to meet the FHWA mandate in the time frame required. The Texas Secondary Evaluation and Analysis for Scour (TSEAS) (The Division of Bridges and Structures Hydraulics Section, 1993) program was initiated in order to meet the mandate. TSEAS used very general information to screen and categorize the scour vulnerability of bridges.

Each stream crossing bridge in Texas was screened, and a code describing the scour vulnerability was entered into the computer database used to manage bridge information. The screening was done in each of 24 districts (at that time; there are now 25 districts) by district personnel. The result is that the codes entered for scour vulnerability are inconsistent over the state, and depend to a high degree on the risk aversion or risk tolerance of individual engineers. Some districts have many bridges coded as scour vulnerable; some do not. The initial mandate from FHWA was only that bridges be screened and coded; no further action was required at the time.

After the initial mandate and coding, a second mandate followed that required all bridges coded as scour vulnerable be further evaluated and that some action be taken—either treated to mitigate vulnerablility (if evaluation confirms vulnerability) or re-coded to indicate lower vulnerability. Re-coding requires that a valid reason for doing so be documented in the inspection files. FHWA continued to recommend hydraulic modeling as the tool for evaluation.

The situation with funding and manpower had not changed in Texas. For that and various other engineering reasons, the administration of the TxDOT Bridge Division (BRG) resisted FHWA mandates and recieved numerous extensions. Texas was not alone in resisting; other states were in similar situations. Compliance was sufficiently difficult that FHWA had to extend deadlines repeatedly.

All new bridges are evaluated for scour potential during the design process; hydraulic models are assembled for the design of the bridge, and evaluating them for scour is an extension of the design hydraulic analysis. The more difficult aspect of FHWA mandates is the evaluation of in-service bridges (those that have been in service since before scour evaluation was a design requirement). There remain thousands such bridges carrying undesirable scour codes. To date there has been no relief from the problems of funding and manpower.

In addition to funding and manpower, the difficulty of obtaining topographic information for hydraulic modeling has chronically been a major stumbling block to hydraulic modeling for scour in Texas. Even with the advent of modern technology such as Global Positioning Systems (GPS) and LIDAR, ground survey is still vital for obtaining topographic data for modeling. Property law in Texas does not require a landowner to cooperate by allowing access for ground surveys, or for the placement of control for aerial surveys, upon request. Access can be acquired against the wishes of a landowner, but to do so is a lengthy and arduous process that is usually reserved for cases preceding the acquisition of additional right-of-way property.

TxDOT funded considerable research into the mechanics of scour, particularly in cohesive soils. The results of that research was to develop methods for estimating scour (Briaud et al., 2009, 2007, 2003). All of the methods developed require velocity as an input. The cost and manpower of hydraulic modeling, the lack of reliable access to land for surveys, and the number of bridges needing evaluation have been ongoing issues in Texas.

The author has been involved in the oversight of numerous research projects with scour as the subject; and was recognized as a subject matter expert in hydraulic and hydrologic

subjects. Among persons internal to TxDOT [2] many methods were discussed to estimate velocity at bridges without the need for hydraulic modeling, so that the methods developed by by TxDOT-funded research could be applied in a cost-effective manner. In addition to avoiding hydraulic modeling it was considered desireable to avoid delineating a watershed, as doing so requires considerable time and effort by a knowledgeable person. Avoiding delineation of the watershed equated to avoiding hydrologic estimation, a process that carries a high degree of uncertainty. A method was needed that used geometry/topography, stream information, and bridge information obtainable at the bridge site only. Prior to the development of QGAM and VGAM, no such method existed.

## 3.4 Historical Background

Upon finding the reference in Leopold (1994), one of the TxDOT personnel involved in the Guadalupe Arroyo assessment (the author) recognized the inconsisency between the referenced velocities and those resulting from routine hydraulic studies by standard-step. It was decided that hydraulic modelers, regardless of experience level, tend to judge the validity of their hydraulic models by comparing to previous hydraulic models, rather than to any independent information. Few comparisons of velocity from hydraulic models to known velocities exist. Comparison between water-surface elevations and assumed or indirectly computed discharge rates is occasionally done when such data are available, however the validity of the modeled discharges is subject to question in many of those cases. In effect, little information flow occurs between modeling and measurement. Modeling is judged by consistency with other modeling.

It became clear to both TxDOT and USGS personnel that to possess any information on the distribution of measured velocities would be valuable by providing hydraulic modelers with an independent check of the consistency of their model results with measured, field conditions. Thus began the development of the statistical models described here. In addition, such information would provide the tool needed for the cost-effective evaluation of bridge scour on in-service bridges statewide.

The immediate result of the discussions mentioned above was development of Figure 3.1. Figure 3.1 contaned information prevously unavailable to hydraulic modelers; reference of the validity of computed average velocities. A brief (two page) unpublished white paper

[2] Mark McClelland, P.E., (Ret.) BRG geotechnical branch, John Delphia, P.E., BRG geotechnical branch, Keith L. Ramsey, P.E., formerly Bridge Inspection group, BRG, David Stolpa, P.E., (Ret.) Design Division (DES) hydraulics branch, the author, and others

resulted, as a prospect for future research. The content of that white paper follows in its entirety.

Past experience with hydraulic models by TxDOT personnel mentioned herein had led to a prevailing opinion that velocities produced by hydraulic models were characteristically higher than should be expected. Figure 3.1 provided support for that opinion. The case of the Guadalupe Arroyo study was consistent with prior observation. Numerous reasons for the tendency were discussed among TxDOT personnel and with the USGS personnel consulted. Numerous undocumented discussions took place during development of the models presented subsequently in Appendix A.

While the initial desire was velocity, ancillary discussions included discharge. One of the (unverified) opinions commonly discussed among TxDOT personnel involved a common tendency to estimate discharge *conservatively*, meaning to the large side of the range of uncertainty; a result of the tendency to do so (it was thought, and still is by those involved) was to necessitate modeling the conveyance of larger discharges through cross sections than they actually carry. High calculated velocities are the result. The ability to estimate discharge, as well as velocity, from site features is a very desirable tool. The involvement of the author was driven by these issues.

## 3.5 Early Investigation (White Paper)

An early document to be distributed for the purposes of discussion and comment by colleagues was written in 2009. The document is included for historical reference and logical context. Under discussion was the inference that mean velocity is reasonably bounded and exhibits some central tendencies; that is, mean velocity in natural channels exhibits certain statistical properties. Such information is not commonly provided to users of one-dimensional computer models for reference. Computed mean velocities that fall far from the central tendencies of measured data are seen in models frequently, particularly in those involving bridge openings.

### 3.5.1 Problem

The U.S. Geological Survey (USGS), through the streamflow-gaging station network in Texas, has collected and digitally archived about 140,000 streamflow measurements and

station inspections for more than 600 stations from Dec. 1897–Feb. 2009. For 435 selected stations, nearly 60,000 measurements of streamflow with concomitant cross-section area, mean velocity, and other properties exist. To date, systematic investigation of these data to generalize the distribution of observed mean velocity has not occurred. Such velocity generalization is important for reliable application of the step-backwater method for modeling flood elevations and mean velocities of design discharges such as 100-year peak streamflows. Mean velocity at a cross section often is the quantity of interest for subsequent computations of bridge scour or bank protection.

### 3.5.2 Motivation

Commonly, engineers involved in step-backwater modeling are taught to assemble models based on generalizations of parameter values from textbooks or literature of the method, from computer program documentation, and from experience. However, the aforementioned "experience" often is exclusive to *prior modeling experience*—an example of circular logic. Such a conclusion is drawn by the authors because typical engineering education as well as practice lacks physical (that is observational) experience or exposure to streamflow metrology.

In step-backwater modeling, parameters such as Manning's $n$ are selected from tables, graphs, published procedures, and ideally visual site assessments. Other parameter values, such as coefficients for expansion and contraction loss, often are left at program defaults. This practice (understandably) is made because typically there is scant information on which to base alternative values. As a result, modeling efforts by even experienced engineers are assembled and often judged to be valid based entirely on experiences from earlier modeling efforts for hydraulically similar settings.

Unfortunately, outside of circumstances in which a model is calibrated to data from one or more stations, there is seldom any independent information upon which to base a validity assessment. Many assessments of and discussions about model validity begin and end as expressions of individual professional opinion, with inadequate quantification to discriminate between valid and invalid models. Documentation of observed mean velocities could provide a fundamental link to physical reality and potentially could provide an authoritative and independent measure of consistency that will allow for enhanced assessment of step-backwater model reliability.

At the least, velocity generalizations would provide a tool to flag severely inconsistent situations for further scrutiny. In other words, "modeled mean velocities, which are inconsistent with the historical database, might suggest that an erroneous model has been made and alternative parameters or other changes should be considered."

### 3.5.3 Initial Foray

As an initial foray into the streamflow measurement database, an exercise was conducted in which all streamflow measurements with values greater than the 1st-percentile daily mean streamflow (a low-flow statistic) were considered if cross-section area and mean velocity data were available and their product within a tolerance matched the recorded discharge. The exercise considered the 620 stations described in USGS Data Series 372, *Summary of annual mean and annual harmonic mean statistics of daily mean streamflow for 620 U.S. Geological Survey streamflow-gaging stations in Texas through water year 2007* by W.H. Asquith and F.T. Heitmuller. The results of the exercise are shown in Figure 3.1. From the 620 candidate stations, 435 stations had sufficient data to produce the plot.

The figure contains 58,724 points. The figure—as well as potential analyses that could consider factors such as method of discharge measurement (wading, crane, indirect, ...), regional location (east Texas forest verses central Texas plateau), channel top width, proximal channel slope (as an expression of gravitational forces), and bed material classification (rock, gravel, sand, ...)—provides a potential tool for evaluation of limits on mean velocities from step-backwater models.

For example, suppose that a design discharge of 1,000 cubic feet per second has a modeled mean velocity at a cross section in excess of 10 feet per second. Such a coordinate would plot outside of an imaginary hull around the cloud of data points. Should the model be scrutinized for possible errors and improvement? The distribution of the observed mean velocity data suggests: Yes.

### 3.5.4 Continuation of Work

For the operational support of the streamflow-gaging station (streamgauge) network in Texas, USGS personnel collected and digitally archived about 140,000 discharge measurements (including zero-flow values) and streamgauge inspections for more than 600

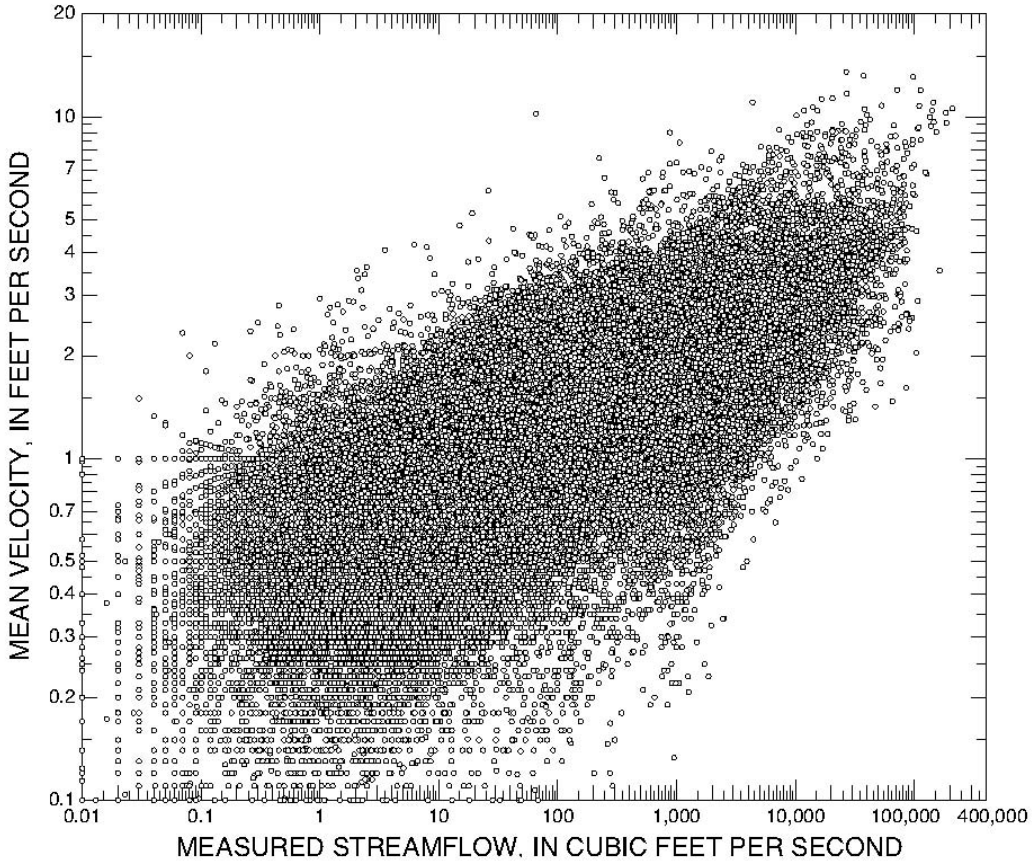


**Figure 3.1.** Relation between mean velocity and measured streamflow from the U.S. Geological Survey streamflow-gauging station network in Texas

streamgauges for the approximate period Dec. 1897–Feb. 2009. These discharge measurements, which are actually individual summaries of extensive field-collected data, reside within the USGS National Water Information System (NWIS) and are readily obtained (U.S. Geological Survey, 2009b) by streamgauge number (a unique numerical identifier). The vast majority of the data represent discharges $Q$ measured from current-meter-based (velocity-meter) techniques (Turnipseed and Sauer, 2010). For most of the discharge measurements concomitant hydraulic properties are also available, these are cross-section flow area $A$, water-surface top width $B$, reported mean velocity $V$, and other details. The basic relation between $Q$, $A$, and $V$ is $Q = AV$. The basic relation between hydraulic (mean) depth $D$ and $A$ and $B$ is $D = A/B$.

## 3.6 Sediment Transport, Discharge, and Velocity

### 3.6.1 Bedload Sediment Transport

At least one of the phenomena observed by the author at Guadalupe Arroyo is not an uncommon one—that of aggradation upstream of a bridge or other cross-drainage structure. Put simply, because of institutional policies and the high degree of uncertainty inherent in hydrologic estimation, it is common for the natural configuration of a stream to be disrupted during the construction of large roadway drainage structures such as bridges. In Chapter 2, it is referred to as "opening up" the bridge. When subjected to hydraulic modeling, the modeled performance of bridges treated in this way invariably appear enhanced, allowing more water to be conveyed at less cost in bridge structure. However, streams also transport sediment in bed load. The disruption of bedload transport, as occurred at Guadalupe Arroyo, is common in the experience of the author. The disruption results in subsequent stream instability in many cases, which may threaten the structure even more than a large flood. The tools published in the paper in Appendix A allow independent assessment of the conveyance available above and below a bridge site.

### 3.6.2 Discharge and Velocity Computations by GAM Equations

As a demonstration of the utility of the equations developed in Asquith et al. (2013), the dimensions presented in Herrmann and Cleveland (2010) for Guadalupe Arroyo will be used as input for the GAM models See Figure 3.2. The model for discharge, called QGAM, is of the following form:

$$\begin{aligned}\log(Q) = &-0.2896 + 1.269\log(A) - 0.2247\log(B) + 0.2865\Omega \\ &+ f_5(\text{longitude}, \text{latitude}) + f_6(P)\end{aligned} \tag{3.1}$$

where log is base-10 logarithm, $Q$ is discharge in cubic meters per second (cms), $A$ is cross-section flow area in $m^2$, $B$ is top width in m, $\Omega$ is the OmegaEM parameter from Figure A.3, $P$ is mean annual precipitation in mm, and $f_5$ and $f_6$ are "smooth functions" of the indicated predictor variables in graphs presented in the original document (Appendix A).

Values for the section discussed in Herrmann and Cleveland (2010) approximately 1200 feet upstream are (in SI units) for input into the equation:

$A$=40.7 m$^2$, $B$=15.25 m, $\omega$=-0.2, $f_5$=0.2, $f_6$=0.004

The resulting equation is

$$\log(Q) = -0.2896 + 1.269\log(40.7) - 0.2247\log(15.25) + 0.2865(-0.2) + 0.2 + 0.004 \tag{3.2}$$

Thus $\log(Q) = 1.633$ or $Q = 43.03$ cms.

In Herrmann and Cleveland (2010), discharge was estimated from this cross section and a speculated Froude number of 0.5 as being approximately 17 cubic meters per second (cms). The QGAM equation results in a larger discharge, 43.03 cms, without the speculative aspect,which converts to 1,520 cfs.

The GAM model for velocity (VGAM) is also presented in Asquith et al. (2013):

$$V^{1/5} = 0.9758 + 0.1588\log(Q) - 0.1820\log(B) + 0.0854\Omega + f_9(\text{longitude}, \text{latitude}) + f_{10}(P) \tag{3.3}$$

where log is base-10 logarithm, $V$ is mean velocity in m/s transformed by the fifth root, $Q$ is discharge in m$^3$/s, $B$ is top width in m, $\Omega$ is the OmegaEM parameter from Figure A.3 in Appendix A, $P$ is mean annual precipitation in mm, and $f_9$ and $f_{10}$ are "smooth functions" of the indicted predictor variables in Figures in the original document.

Using the value of discharge ($Q$) computed herein, $B$ is the same, $f_9$=0.15, $f_1$0=-0.02, the following equation results:

$$V^{1/5} = 0.9758 + 0.1588\log(43.03) - 0.1820\log(15.25) + 0.0854(-0.2) + 0.15 + -0.02 \tag{3.4}$$

Thus $V^{1/5} = 1.132$, $V = 1.865$ m/s, which converts to 6.1 ft/s.

The value computed using the methods in Asquith et al. (2013) is substantially smaller than was predicted by backwater modeling (value >20 ft/s), as was suspected initially by the author during the Guadalupe Arroyo study. The discharge computed by QGAM is larger that that estimated by expedient methods described in the study of Guadalupe Arroyo (Chapter 2). However, since no traditional method of hydrologic estimation was applicable at this site, the discharge resulting from QGAM constitutes the best estimate available.

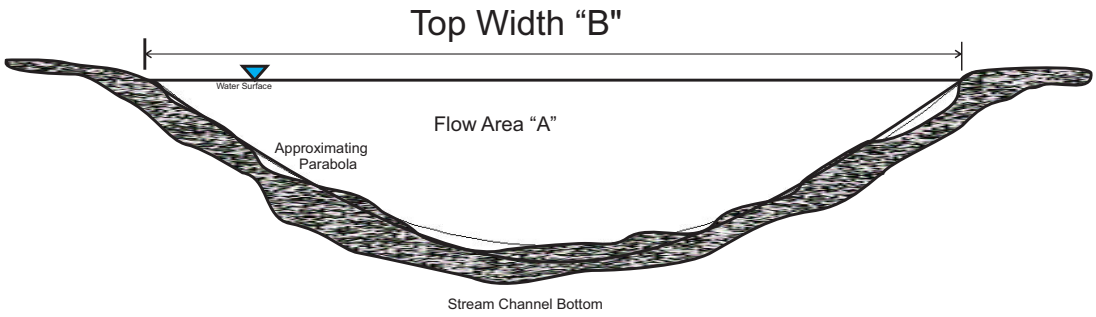


**Figure 3.2.** Reference drawing for QGAM and VGAM calculations. B is topwidth. Area is approximated as a parabola

## 3.7 Conclusions

The ability to assess stream performance and historical conveyance by measurement of stream geometry at a single site offers a tool that has not been available before. All calculations, hydraulic calculations for design, bridge scour, and bridge performance, are enhanced with independent verification. Estimated discharges from hydrologic methods and associated with design probabilities can be verified for consistency with measured values. The essentially unbounded nature of design hydraulic and hydrologic calculations that has resulted in problems like Guadalupe Arroyo are now subject to bounding estimates.

# Chapter 4

# The Effects of Proximity and Terrain Ruggedness on Runoff Generation and Flood Magnitude

## 4.1 Prologue

This chapter is the original work of the author. The particular situation studied in this chapter has been a source of intriguing study by the author for several years. The rugged canyon country of the lowest reachs of the Pecos River are a source of inspiration and beauty appreciated by few people. When it was noted that there was a dramatic increase in magnitude of annual peak flood flows, unexpected and inexplicable under common hydrologic assumptions, at a location in this area. The author, having spent much time there as a youth and being very familiar with the area, suspected an unusual explanation—ruggedness.

Ruggedness is a property of topography that is easy to visualize, but difficult to quantify. Standard hydrologic thought states that ruggedness affects runoff potential, (Maidment, 1993; Chow et al., 1988; House et al., 2001) but there are few ways of including that in modeling techniques.

In this analysis, a flood on the Pecos River in 1954 has been eliminated from the data analyzed. The listed magnitude of that flood is 948,000 cfs, or 958,000 cfs in some places (an insignificant difference). Local people describe this flood (from the remnants of Hurricane Alice) as being beyond belief (personal interviews, 1974–1978). Anecdotal, unverified rainfall estimates for the area northwest of the Shumla streamgauge are that there was 34 inches of rainfall in 24 hours, a significant fraction of Probable Maximum Precipitation. A NOAA website (Oceaninc and Administration, 2013) acknowledges 24.07 inches in 24 hours. When that amount of rain fell on the rugged terrain under discussion, the results were catastrophic. The 1954 event was eliminated from the present analysis in order to prevent bias, even though it was a real event. The elimination of the event described is

justified on the basis that extraordinary flood-producing mechanisms were in play relative to the normal population of conventional annual peak producing mechanisms.

## 4.2 Chapter Abstract

This chapter is an exploration of the influence of areal proximity to a point of interest on runoff generation, and hence on runoff magnitude. Discussion of basic hydrologic thought relating to runoff generation processes is followed by conceptualization of the influence on the runoff process of parts of a watershed far distant, versus those more proximate, to a point of interest. A case study is presented illustrating the hypothesis that the nature of terrain proximal to a point of interest exerts influence that is substantially different from the influence of terrain more distant from the point of interest. Greater contribution from proximate area is inferred. Another property thought to exhibit added influence is topographic ruggedness. A case is made that proximity and ruggedness magnify one another. The case study involves streamgauges along the Pecos River, primarily in Texas, and examines changes in the terrain through which the main stem of the Pecos River flows.

## 4.3 Introduction

The lumped parameter modeling of watershed response to rainfall input has traditionally been based on the assumption that area within the watershed uniformly contributes runoff to the point of interest. The general idea, with caveats, is that a small subarea of the watershed contributes runoff to a direct runoff hydrograph at the point of interest in the same manner, regardless of whether that subarea is located near to or far from the point of interest. The caveats generally relate to the abstraction of rainfall from the gross rainfall by each given subarea. A subarea with highly permeable soil is anticipated to produce less runoff than one with dense, low permeability soil. In lumped parameter modeling, the location of any small subarea is given no consideration with respect to what fraction of the rainfall it receives is returned as runoff. Modeling that does consider location by discretization of the watershed, distributed parameter modeling, typically considers only difference in arrival time from different subareas (USACE-HEC, 2012). All area is still basically considered to contribute evenly, or in a way weighted for the physical properties of the watershed (soil properties). Losses in transit, or dilution of contribution effects with time and distance, are not usually accounted for in distributed modeling.

### 4.3.1 Watershed Behavior and Modeling Principles

In contrast with the idea expressed above is the observation that flood discharge, either as peak rate or as total volume, does not increase linearly with area; in fact discharge *per unit area* diminishes as area increases, for a given probability. For example, regression equations developed for Texas (Asquith and Thompson, 2008) for flood peaks of a given probability of exceedance, using area as the only explanatory variable are of the following form:

$$Q = KA^{\beta} \tag{4.1}$$

where the exponent $\beta$ in the power law model is very near 0.5, or the square root of area (Asquith and Thompson, 2008).

The common explanation of the diminution of discharge per unit area is related to the response time of a watershed and rainfall averaging. Figure 4.1 is a diagram of two watersheds. In this Figure, the slope is assumed unchanged between the two watersheds, thus channel flow velocity is assumed the same. A reasonable assumption is that the rainfall averaging time is related to the main diagonal length and some flow velocity which is related to the slope; e.g. $T = \sqrt{A}/V$ (Cleveland et al., 2011). The characteristic time can be then replaced by the main diagonal length of a square of area equal to that of a watershed under discussion. The ideal watershed depicted on the right side of Figure 4.1, has four times the drainage area as that on the left. Main channel length is depicted as the diagonal lines in the two watersheds in this conceptual model. The main channel length of the watershed on the right is twice the length of that on the left.

Figures 4.2 and 4.3 are portions of two panels from Asquith and Roussel (2004). The rose-colored area approximates the Pecos River watershed in Texas. The two figures are depth estimates for an annual recurrence interval of 10 years for a one- and two-day storm. From the two figures the two-day depth is about 4 inches, whereas the one-day is about 3.5 inches. Thus in this location, doubling the rainfall averaging time only increases the depth from 3.5 inches to 4.0 inches; equivalent to a fractional increase of about 15 percent ($\frac{0.25}{3.5} \approx 0.15$).

Now one can discuss the anticipated increase in discharge for the two conceptual watersheds. Increasing the area fourfold increases the discharge fourfold if the rainfall depth and averaging time are held constant. However, the change in area doubles the averaging time, so if the rainfall depth is held constant, and only the area and time are compared, then the discharge is only doubled. Lastly, the rainfall depth is not constant, but also does not increase at the same rate as the averaging time. Using the conceptual diagram and the Pecos

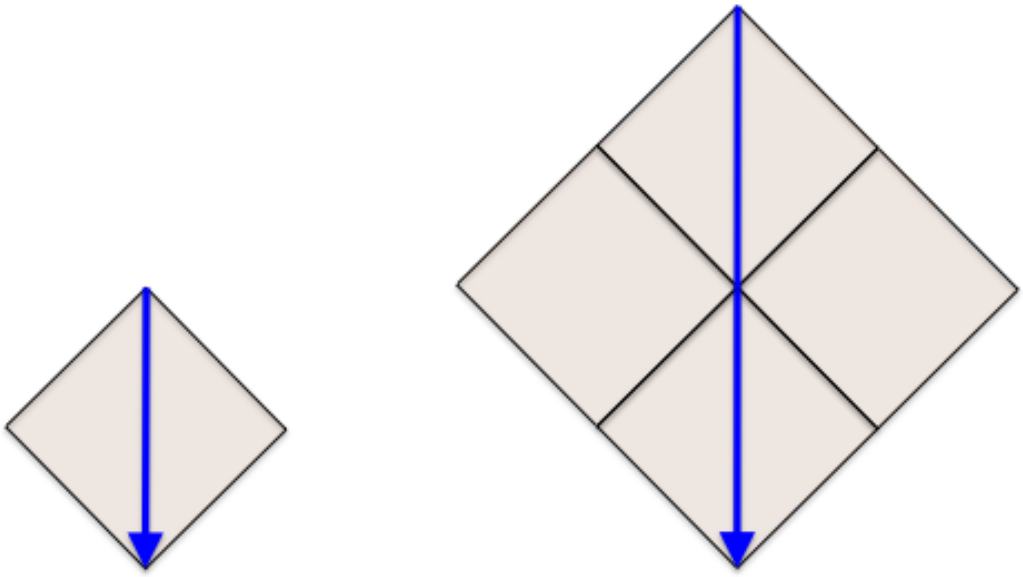

**Figure 4.1.** Two ideal, conceptual watersheds. The one on the right has four times the area of the one on the left, while the main channel length is two times that of the one on the left

River rainfall as an example, a four-fold increase in area increases discharge slightly more than double.

Equation 4.2 is a power law model that includes Mean Annual Precipitation (MAP) as an explanatory variable, also from Asquith and Thompson (2008).

$$Q = KA^{\beta_1}P^{\beta_2} \tag{4.2}$$

Through this equation, the influence of increasing or decreasing precipitation is displayed, by way of a general precipitation factor, the Mean Annual Precipitation depth for a given watershed. The exponent on the MAP value for the equations varies from 0.2366, a weak influence, on the 100-year AEP equation, to 0.9732, a nearly linear factor, for the 2 year AEP. The exponent decreases with increasing return period.

Equation 4.3 is Equation 4.1 parameterized with values appropriate to the Pecos River Region for an AEP of 10 years and area ranging from 100 to 1,000 square miles. Equation 4.4 is Equation 4.2, parameterized similarly, with precipitation held constant at 14 inches. The results of both are plotted in Figure 4.4, to illustrate the increase in discharge with increase in area. The inclusion of MAP produces a substantially different curve, however, both curves increase with area in a sublinear fashion. Both exhibit monotonic increase.

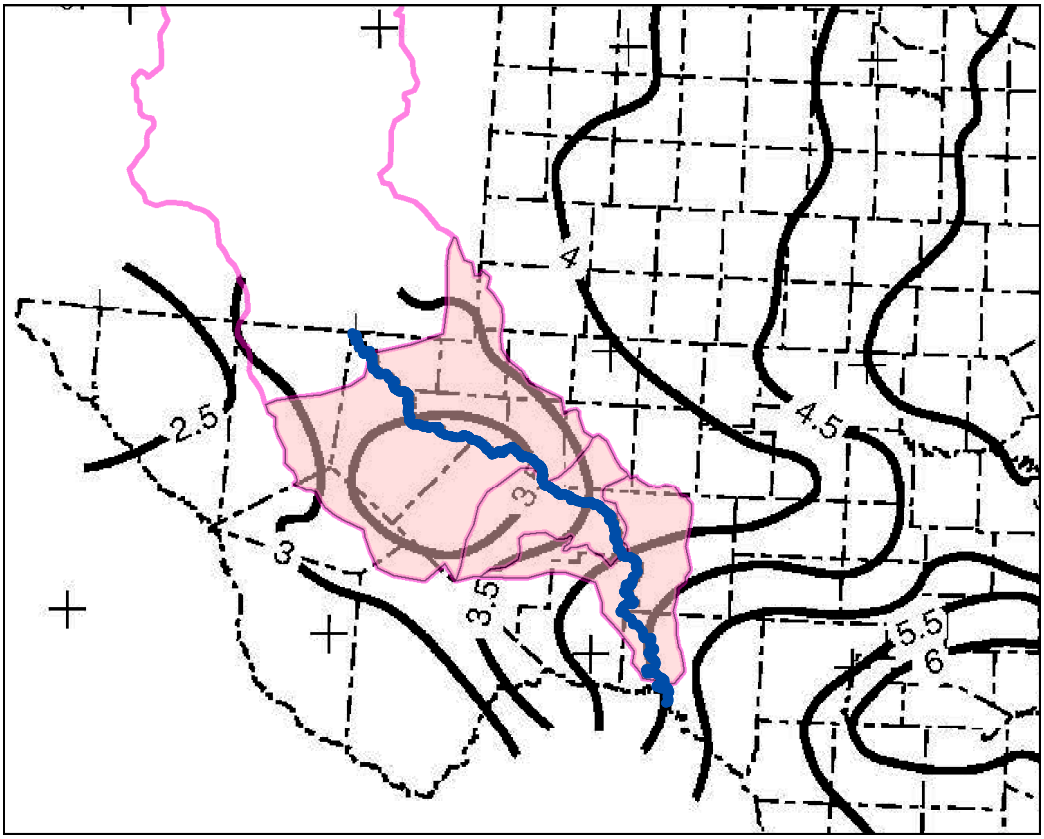


**Figure 4.2.** One–day depth of precipitation for the 10-year AEP for the lower Pecos River watershed in Texas. The rose-colored shading indicates the watershed contributing below Red Bluff Reservoir. This is a portion of Figure 35 from Asquith and Roussel (2004)

The idea behind Figure 4.4 is that, in general, peak discharge is expected to increase as contributing area increases.

Equation 4.4 was then evaluated with area held constant at 100 square miles and precipitation ranging from 9 to 17 inches, the range encountered in the Pecos River in Texas. The results of that evaluation, plotted in Figure 4.5, show the increase in discharge with increase in precipitation exhibited by Equation 4.4. Although the graph appears linear, there is slight curvature, with downward concavity.

$$Q = 780A^{0.510} \tag{4.3}$$

$$Q = 111A^{0.5311}P^{0.5469} \tag{4.4}$$

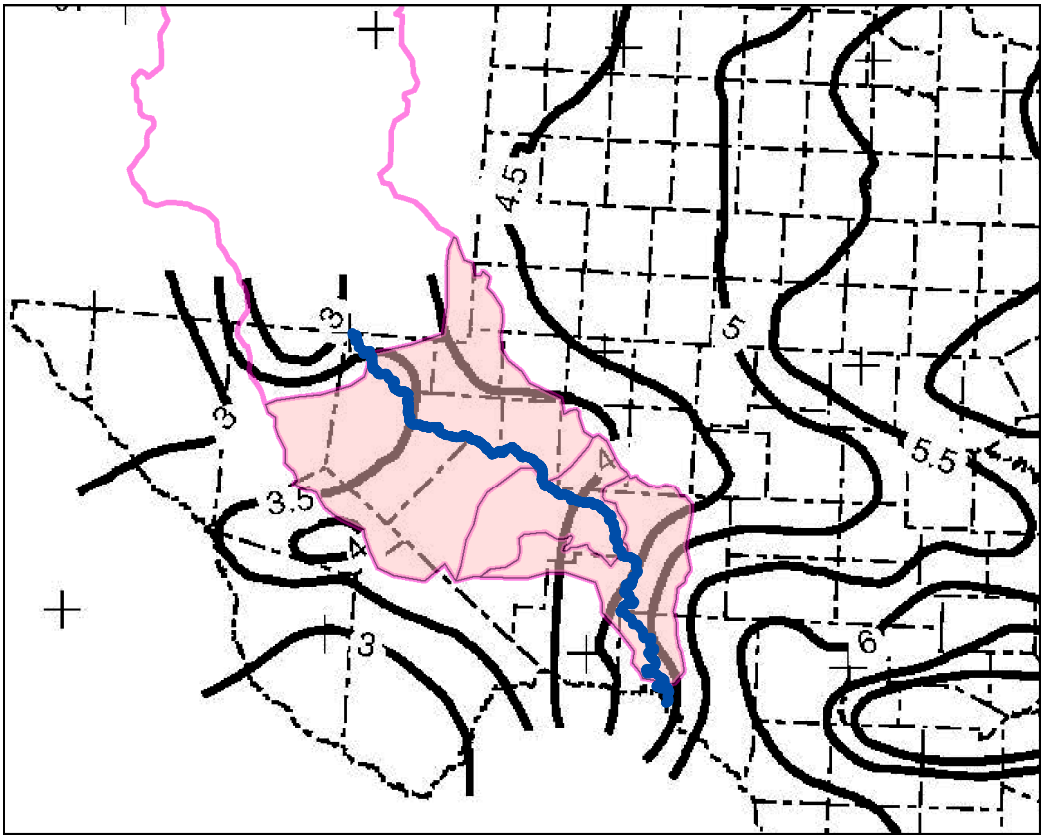


**Figure 4.3.** Two-day depth of precipitation for the 10-year AEP for the lower Pecos River watershed in Texas. The rose colored shading indicates the watershed contributing below Red Bluff Reservoir. This is a portion of Figure 36 from Asquith and Roussel (2004)

The idea expressed in Figure 4.5 is that peak discharge also increases as precipitation depth increases

### 4.3.2 Lumped Watershed Models

Hydrologic watershed models used for engineering purposes are often "lumped parameter" models in which a single value of any parameter is intended to represent the entire watershed (Maidment, 1993; Chow et al., 1988). If distinct areas of different values exist, for instance different soil types or land-use types, some weighting scheme is used to arrive at an areally weighted average value for the parameter; alternatively, in distributed models, the watershed may be divided into subwatersheds, or even gridded, and the results aggregated, for analysis. In the case of analyses where the watershed is divided into a number of sub-

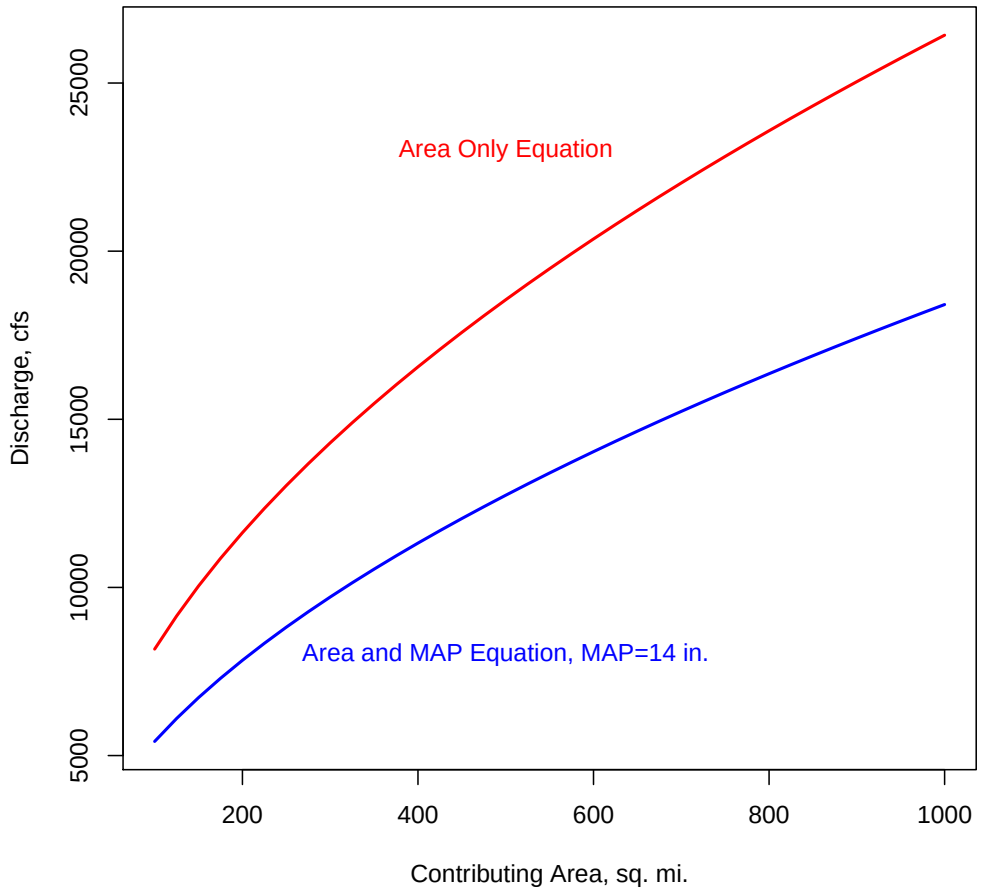


**Figure 4.4.** Graph of discharges estimated as contributing area changes from 100 to 1,000 square miles, according to equation 4.3, using area as the only explanatory variable, and equation 4.4, using area and Mean Annual Precipitation as explanatory variables, from Asquith and Thompson (2008)

areas, the problem can be likened to "nesting" of smaller areas with the same restrictions (Cleveland and Thompson, 2009). In this case, the outflow from each subarea is considered to be transmitted downstream with possible attenuation attributable to time and distance, but seldom is there considered to be any further loss of water from that outflow during the transmission downstream. Travel time and attenuation of the hydrograph from channel storage and transmission effects are often simulated by channel routing routines, but conservation of mass through a channel reach is usually assumed. Losses to channel and bank infiltration are not routinely considered in engineering modeling, even though they

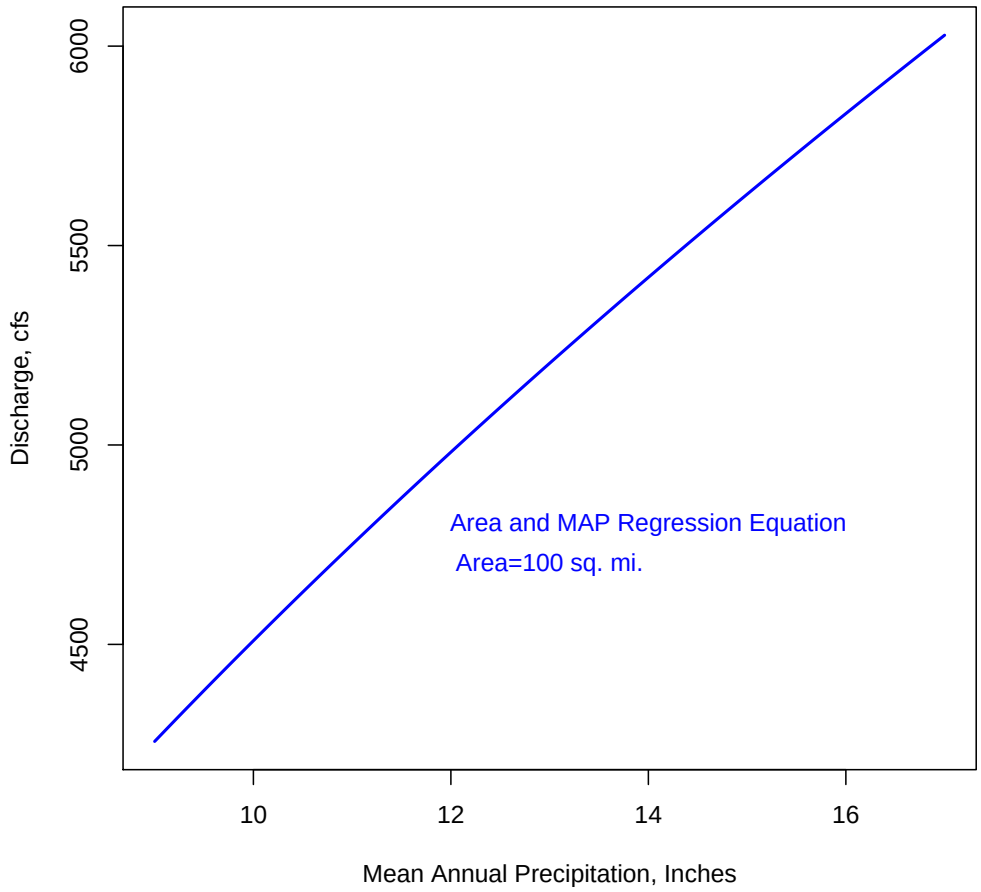


**Figure 4.5.** Graph of discharges estimated for contributing area of 100 square miles as Mean Annual Precipitation changes from 9 to 17 inches, using Equation 4.4, with area and Mean Annual Precipitation as explanatory variables, from Asquith and Thompson (2008). While the graph appears at this range of precipitation to be linear, there is actually slight curvature, with downward concavity.

undoubtedly occur in real streams. The current (2013) version of the popular hydrologic modeling software HEC-HMS (USACE-HEC, 2012) offers two methods of accounting for losses in channel routing. However, guidance for use of such methods is very sparse.

The idea that a property such as permeability matters, but location does not, is convenient in terms of visualizing and explaining watershed mechanics and processes; the idea is linear, and lends itself well to modeling and discussion. However, like many of the ideas used for research and engineering analysis, it is a simplification and generalization of what actually

occurs on watersheds. Study by direct observation and measurement is very difficult and expensive, and the resulting data are often difficult to interpret; most of what is common belief about these processes comes from indirect measurement, mathematical modeling, and conjecture. Many of the direct measurements that are available were collected on watersheds that are not entirely natural or necessarily representative; that is highly urbanized or agricultural, very small watersheds with man-made or man-altered physical features.

Contributing to the common idea of uniformity of areal response are other long-standing ideas regarding the effect of regulating structures within watersheds. The U.S. Geological Survey (USGS) uses the criterion that if 10 percent of a watershed is affected by a regulating structure, the watershed is considered regulated (Asquith and Slade, 1997), and a corresponding code accompanies each annual peak flood value for such watersheds, regardless of how the regulated area is situated with respect to the point of measurement (streamgauge).

Rainfall-runoff modeling relies heavily on the concept of "effective" or "excess" precipitation; precipitation that appears at the point of interest as runoff. Measurement generally shows that considerably less water is seen passing the point of interest than should be available from rainfall measurements. The common view is that gross rainfall landing on a watershed is reduced by various processes known as "abstractions" or "losses." These losses are usually categorized as infiltration, evaporation, evapotranspiration by plants, retention in depressions, or adherence to surfaces. As modeled many of these processes are time dependent; losses accumulate as time passes.

### 4.3.3 Partial and Variable Area Contribution

An alternate point of view is that the volume of runoff resulting from a rainfall event does not actually originate from uniform distribution across the extent of the watershed. Betson (1964) first described partial area contribution, the idea that the entire watershed *as defined topographically* does not contribute to all, or any, runoff event other than possibly the most extreme. Betson's suppositions were based on the failure of a rigorous mathematical procedure to adequately reflect measured runoff. He surmised that only a portion of the topographically defined watershed was actually contributing runoff. Much work followed on the partial area subject, including experimental watershed studies that attempted to measure actual contributing area during real and simulated events. Ragan (1968) selected a small watershed in Vermont for detailed instrumentation and study. Results of the study

indicated that most of the observed runoff originated in specific areas, proximate to (within 35 feet) the stream. Little or no overland flow was observed and Ragan concluded that rainfall directly on the channel and porous media flow in the lower layers of forest litter were important mechanisms of runoff for this small watershed.

Dunne and Black (1970), conducted a study, also in Vermont, to test contentions by Kirkby and Chorley (1967) that shallow, subsurface flow (throughflow) was a major contributor to flood hydrographs. The results of Dunne and Black indicate that hillslope overland flow accounts largely for observed runoff, and that a small portion of the watershed produces runoff, in general agreement with Betson's hypotheses. Hortonian flow, an often discussed mode of runoff, was not observed to occur. Dunne and Black concluded that, in the Vermont watershed studied, runoff was produced by small, saturated areas nearby to streams, and as overland flow. The remainder of the watershed stores water to be released as baseflow.

Amerman (1965) concluded from study of small watersheds in Ohio that runoff producing areas are located randomly about the watershed, and further observed that they did not necessarily contribute to the perennial stream by connected surface flow. The author observed that runoff may infiltrate into an adjacent area that it reaches subsequently as "run on." The fact that much of the runoff he observed and commented upon apparently did not actually contribute flow past the point of interest gives cause to discount areas distant from the stream as actually contributing flow as it interests the practicing hydrologist.

A common theme among these works of the 1960s and 1970s is the idea that partial area contribution is the dominant watershed runoff-producing mode. Many concluded that actual contributing area is not only partial, but variable (Hewlett and Hibbert, 1967; Ragan, 1968; Dunne and Black, 1970; Engman, 1974). The idea of partial area contribution contrasts with the fully contributing, lumped watershed model represented by traditional UH theory, with respect to area, loss, and characteristic time. The bulk of the studies done on partial area contribution using measured watershed data have revolved around identifying contributing areas, characterizing the mode of runoff, noting the physical attributes or properties that allow them to generate runoff, and delineating runoff producing areas. Many studies reached different conclusions with respect to the dominant transport process: overland flow, saturation flow, or throughflow. Some stduies were unable to identify the flow mechanism.

Evidence such as that presented by the researchers mentioned above strongly supports the idea of partial area contribution. The actual contributing areas are difficult to identify and delineate. There is evidence that contributing area is variable. All of the evidence presented

by the researchers above can be seen to refute the idea that uniform areal response by the watershed as presented by common thought.

### 4.3.4 Travel Time and Contribution

Almost all loss process models are, or include, a component of the total loss that is time-dependent. As time passes, more of the rain that has fallen enters the soil. The time rate of loss may diminish with increasing soil saturation, but the total depth infiltrated increases. As a necessary consequence of time-dependent loss processes, the time that has elapsed since water fell as rain on the watershed, the residence time, is related to the likelihood that it will flow past a point of interest. Therefore, the longer that water resides on the surface of the watershed, the smaller the chance of it being observed at the point of interest. The farther away an area recieving rainfall is from the point of interest, the longer the travel time for rain falling there to travel to the point of interest, and proportionally the smaller is the fraction of rainfall landing there that passes the point of interest. Conversely, rainfall landing on an area proximate to the point of interest requires less time to reach that point; the fraction that passes the point of interest is greater than for a more remote area. Supporting this assertion is the idea of a time-dependent component to the loss process—that idea alone implies that the fraction of rainfall lost prior to passing the point of interest is proportional to elapsed time, and elapsed time during travel is closely related to travel distance.

Even accounting for differences in loss from physically explainable phenomena such as soil texture, it can still be said that the longer a drop of water resides on the watershed, the more likely it is to be lost to the runoff process; that is, the lower the probability that it will be observed to pass the point of interest. In this hypothesis, a critical variable is travel time from where a drop of rain falls (originates) on the watershed until it is observed at the point of interest.

Travel time to the point of interest is related to travel distance, path, and average speed; thus both distance and speed are variables of interest in estimating runoff. Put simply, if water must travel along a path on the watershed for a long time in order to reach the point of interest, less of that water is observed at the point of interest than if the water can travel to the point of interest along a shorter path. Rain falling on a small area far from the point of interest is probably more difficult to detect, and likely exerts less influence on the resulting hydrograph, than does rain falling on a similar small area proximate to the point of interest.

This discussion illustrates that the conventional idea of uniform areal contribution ubiquitous in watershed modeling is an incomplete simplification of how real runoff is probably generated on a real watershed. A great deal of work, and much literature, has been generated based on the idea that only a small fraction of the watershed actually contributes under all but extraordinary conditions (Betson, 1964). Watershed studies (Ragan, 1968; Amerman, 1965; Engman, 1974) supported this contention, but difficulties in identifying areal properties that consistently produce runoff have limited the development of models to simulate the partial area idea. A more tractable idea includes the possibility that the influence of a small differential element of watershed area on the outflow hydrograph is inversely proportional to its distance from the point of interest.

Many of the authors mentioned herein were critical of the methods of their day and advocated for further development in modeling methods that would reflect partial area concepts. The general methods that these researchers critiqued are still in common use today, and are still subject to the same criticisms as they were at the time. Desktop computing capability has eased the computational burden on hydrologists, but the fundamental modeling assumptions have changed little.

## 4.4 Thought Experiments

### 4.4.1 Uniform Areal Contribution

Assuming a simple, near-ideal watershed that is relatively homogeneous in topography, a series of informative thought experiments can be conducted. Under the assumption of uniform areal contribution found in unit hydrograph based watershed modeling, if 10 percent of the watershed is regulated by a retention structure such as a dam, and considering the regulated portion as non-contributing, *all else being equal*, the volume of discharge would be expected to diminish by 10 percent, and by the principle of proportionality, the peak discharge to be reduced by 10 percent under regulation. If peak discharges before and after regulation were estimated with a regression equation such as those mentioned (using area only) under the same conditions, the estimated peak discharge would be reduced by something less than 10 percent; if the exponent is 0.5, the reduction is closer to 5 than to 10 percent (Equation 4.5).

$$Q = KA^{0.5} = K(0.9)^{0.5} = K(0.948) \tag{4.5}$$

Both of the reductions computed above (the linear scaling of unit hydrograph and the reduction computed by regression equation) do not consider where the regulated area occurs within the watershed because all area is considered equal in contribution. It is noteworthy that two commonly used and sound methods reach different conclusions about something as simple as changing contributing area by a small factor (10 percent).

### 4.4.2 Influence of Travel Time

Returning to the contention that the travel time on the watershed is of consequence in runoff production, the possibility is revealed that reduction in peak volume and discharge because of the regulation of 10 percent of the watershed would depend on where that 10 percent is located with respect to the point of interest. If the regulated portion is located far up the watershed, its effects may be difficult to observe, whereas if the regulated area is located on a small tributary that contributes to the stream proximate to the point of interest, the effects may be close to the 10 percent expected by UH-type modeling. The actual magnitudes computed would be subject to influence by the time/loss relation chosen, but in any case the influence of area distant from the point of interest would, under this set of assumptions, be less than that of a more proximate area.

Figure 4.6 is a conceptual map of an ideal watershed, showing different subareas to be considered. Both subareas represent 10 percent of the total topographic watershed. Subarea A is at the distal end of the watershed. Runoff from the distant area must travel a great distance to pass the point of interest. Subarea B is a tributary that contributes to the stream proximate to the point of interest. Under conventional, "lumped parameter" unit hydrograph modeling (no subdivision of the watershed or routing), the introduction of control of either of the two subareas, for instance by the placement of a dam, would have effects on the hydrograph indistinguishable from one another. Under the idea of partial/variable area contribution as documented by research, the actual contributing areas are unknown, and the relative effects of control at either point are unclear.

Considering that losses are time-dependent even under conventional modeling assumptions, the effects of control of Subarea A should be less substantial than those of the control of Subarea B, simply by the fact that water traveling downstream from Subarea A to the point of interest is subject to the ongoing effects of time-dependent loss during the entire duration of the journey. Whereas, water traveling from Subarea B is not subject to the effects

of time-dependent loss for as long. The effects of control of area is inversely proportional to travel time, and thus to travel distance.

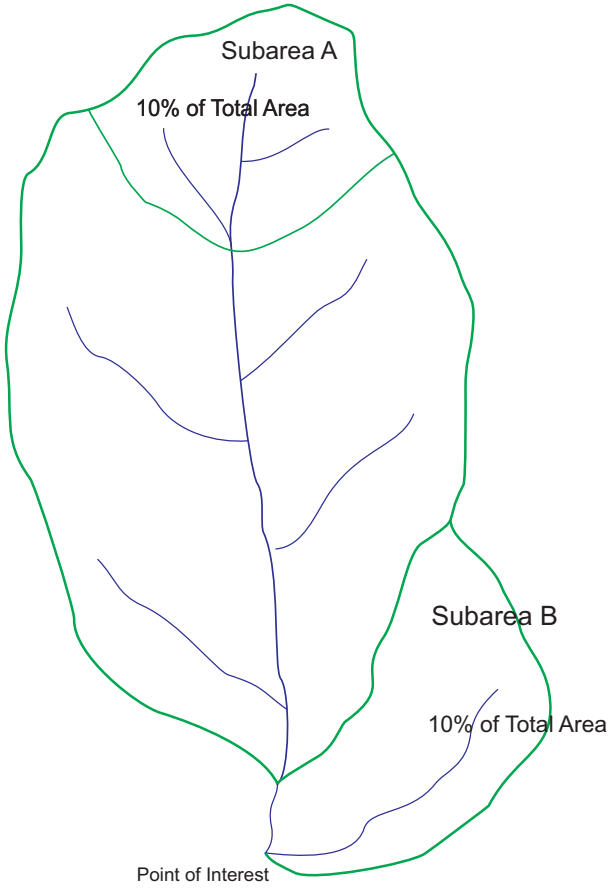


**Figure 4.6.** Conceptual map of a watershed, showing different subareas to be considered. Both subareas represent ten percent of the total topographic watershed. Subarea A is at the distal end of the main stem. Water from it must travel a great distance to pass the point of interest. Subarea B is a tributary that contributes to the main stem proximate to the point of interest.

### 4.4.3 Discussion of Thought Experiments

Whereas the approach presented departs from the assumptions usually made for watershed models, the idea of influence being inversely proportional to distance is ubiquitous in physics and mathematics. Examples of inversely proportional physical phenomena are gravitational fields, electrical fields, light intensity with distance from source, and the optical resolution of distant objects. Many waves or wave-like phenomena are known to diminish in magnitude with distance (and thus with time). The movement of water down a watershed has wave-like properties. Assuming that it diminishes as it moves downstream is consistent with first principles of physics.

For the purposes of the thought experiments shown, a near-ideal watershed was proposed, non-ideality was introduced by way of conceptual regulation (assume dams). Rather than dams, a different variety of non-ideality may be assumed; topographic ruggedness. If Subarea A in Figure 4.6 was composed of an area of high topographic ruggedness, whereas the remainder is ordinary topography as defined arbitrarily, some change in the hydrograph would be expected. High topographic ruggedness is associated, in most if not all cases, with increased volume, rate of discharge, and travel velocity as compared to lower topographic ruggedness, all else being equal (House et al., 2001). The increase in travel velocity equates to a decrease in travel time.

As with regulated area, if the area of high topographic ruggedness is located on the far distal edge of the watershed (Subarea A), increased runoff generated there must traverse a long distance before being observed at the point of interest; it is therefore subject to "decimation" by travel time; the influence it exerts on the flood hydrograph is diluted. Also as with regulated area, if the area of high topographic ruggedness is located proximate to the point of interest (Subarea B), the effects of high relief and proximity magnify one another. *As compared to a topographically homogeneous watershed, one with a small concentration of high topographic ruggedness proximate to the point of interest would show reinforcement of the influence of that proximate area on flood generation, as compared to ruggedness in a distal area.*

The series of thought experiments above led to further examination of watershed mechanics, particularly as related to several of the simplifications and assumptions that are axiomatic in hydrology. The intent is not to undermine the usefulness of these simplifications and assumptions, but to demonstrate that their fidelity to real processes is not without limits, and that there are times and situations where there is need to maintain sight of

their limitations. In particular, the following assumptions and simplifications are considered brought under scrutiny by the thought experiments:

- All contributing area contributes uniformly, according to the parameters of whatever loss model is being used;
- Discharge monotonically increases with increasing contributing area, regardless of the nature of that area;
- Maximum watershed response is observed when the entire watershed is contributing to discharge; and
- Effective precipitation (that resulting in runoff) can be thought of as separate and distinct from other precipitation.

## 4.5 Example From Historical Streamgauge Data

The model considerations expressed in the discussion above are illustrated with a case study that presents evidence of this effect in the real world. The example to be shown involves the lower Pecos River in Texas. It will be stated initially that the example shown consists of a very large watershed. The likelihood of uniform rainfall over those areas is, in practical terms, nonexistent. However, uniform rainfall and full watershed contribution are not necessary conditions for the demonstration of the phenomenon of interest; it is sufficient to show that actual recorded flood data reflects dramatic change from one streamgauge to the next with respect to changes in topography.

### 4.5.1 Lower Pecos River, Texas

Figure 4.7 is a map of the Pecos River watershed in Texas and New Mexico, showing locations of the streamgauges referenced in this study, and some of the subareas of interest in this example. The Pecos River begins in the Rocky Mountains of northern New Mexico. It drains the eastern flank of the mountains, and portions of the adjacent eastern plains of New Mexico and western Texas. It crosses into Texas, flowing southeast, and ultimately joins with the Rio Grande in Val Verde County, Texas.

For years 1900–1966, a streamgauge existed at the crossing of the Pecos by US 90 in Val Verde County near a railroad ghost town called Shumla. This streamgauge became ineffective when Amistad Reservoir on the Rio Grande began to impound water up the

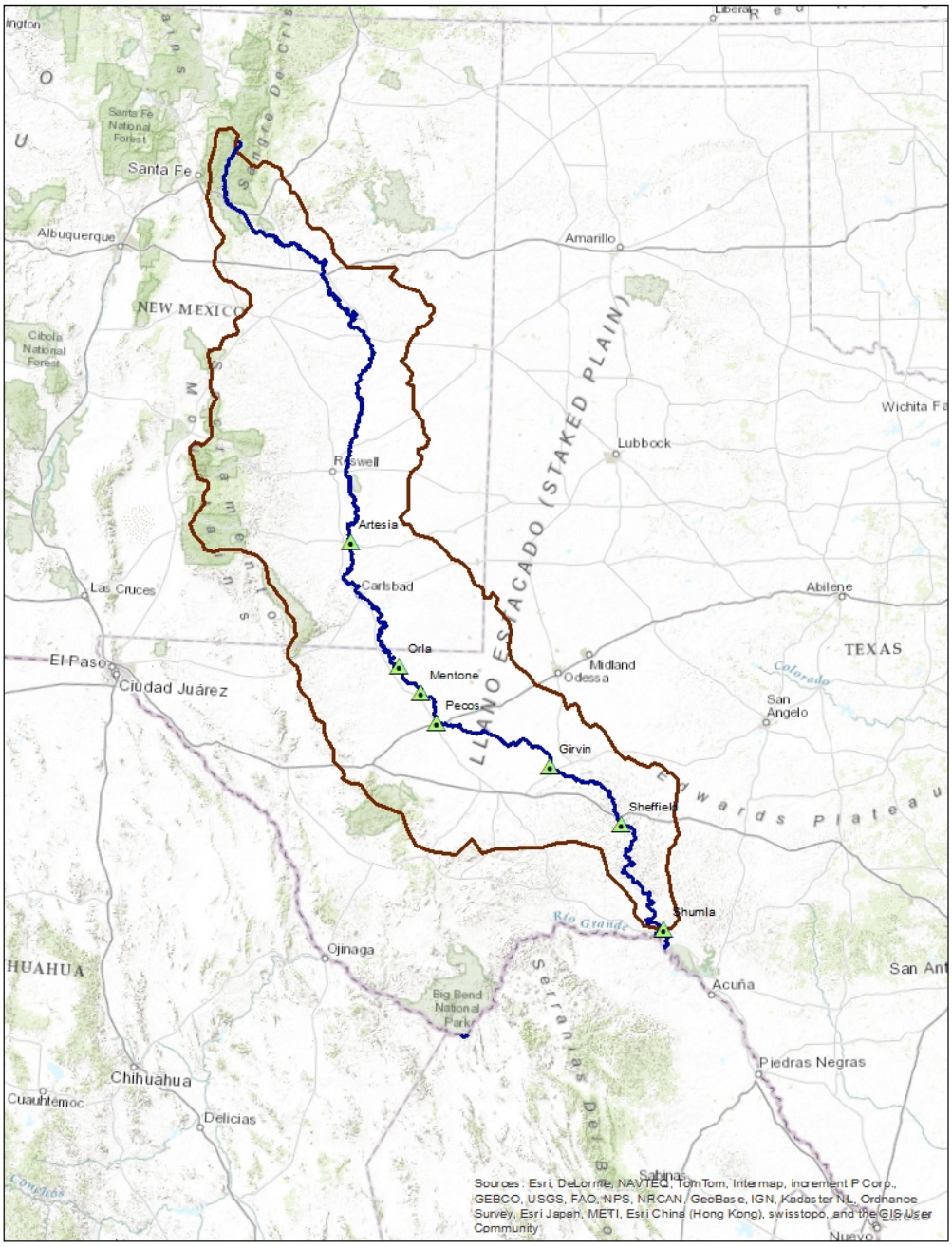


**Figure 4.7.** Map of the watershed of the Pecos River, showing full watershed extent and the location of the stream streamgauges referenced in the text and tables.

Pecos, and was discontinued. Intermittently, several other streamgauges have been operated on the Pecos River in Texas, located at or near Orla, Pecos, Mentone, Girvin, and Sheffield, Texas, all of which are very small towns or ghost towns.

In 1936, a dam near Orla, Texas began impounding water in Red Bluff Reservoir, very near the Texas-New Mexico state line. A streamgauge Artesia, New Mexico, has existed, also intermittently, spanning the construction of the dam impounding Red Bluff. The streamgauge at Artesia was included in this analysis to include data upstream from that reservoir as well as spanning the unregulated/regulated time. The Artesia gauge was retained for the purpose of assessing the effects of the construction of Red Bluff Reservoir, and for the assessment of system-wide responses. The streamgauges at Orla and at Girvin were both placed subsequent to the construction of Red Bluff Reservoir, and thus collected no unregulated data. The streamgauge at Orla is immediately downstream from the Red Bluff dam. Tables 4.1, 4.2, and 4.3 contain annual peak discharge series for streamgauges on the lower Pecos River in Texas, broken at water years 1935 and 1936, the periods before and after the construction of Red Bluff Reservoir. Streamgauges were operated intermittently during the period 1900 to 1966, however the gauge at Shumla operated during the entire time. The Shumla gauge, and the apparently anomalous series of discharges recorded there, is the central subject of the discussion.

### 4.5.2 Temporal Association of Annual Peak Data

Tables 4.4, 4.5 and 4.6 list annual peak data, including dates, for periods before and after the construction of Red Bluff Reservior. Several gauges were operated only for a few years, or have been operated intermittently, during the period of interest, that of the existence of the gauge at Shumla, water years 1900–1966. Data from a gauge at Artesia, New Mexico, which is located above Red Bluff Reservoir, spans a period beginning in water year 1906 and continuing until after the period of interest, with gaps in water years 1909, 1915, 1927–1928, and 1933–1934. Prior to the construction of Red Bluff Reservoir, gauges existed at Mentone in water years 1922–1926, at Pecos from water year 1900–1904, 1906, 1917–1918, 1920, and 1923–1925. The gauge at Sheffield operated from water year 1922–1924. The gauges at Orla and Girvin were not in operation prior to the construction of Red Bluff Reservoir.

After the construction of Red Bluff Reservoir, the gauge at Orla began operating in water year 1938 and operated through the remainder of the period of interest. The gauge at Pecos

**Table 4.1.** Table of annual peak discharges 1900–1935 for two Texas gauges, in cfs

| Water Year | Pecos Date | Pecos Discharge | Shumla Date | Shumla Discharge |
|---|---|---|---|---|
| 1900 | 9/23/1900 | 2350 | 4/6/1900 | 107000 |
| 1901 | 10/18/1900 | 2600 | 9/8/1901 | 9200 |
| 1902 | 11/7/1901 | 4270 | 5/18/1902 | 33500 |
| 1903 | 6/22/1903 | 2670 | 6/29/1903 | 2140 |
| 1904 | 9/25/1904 | 1260 | 6/27/1904 | 72000 |
| 1905 | - | - | 4/23/1905 | 47000 |
| 1906 | 7/18/1906 | 2340 | 8/11/1906 | 90000 |
| 1907 | - | - | 12/10/1906 | 880 |
| 1908 | - | - | 7/7/1908 | 68000 |
| 1909 | - | - | 8/1/1909 | 1780 |
| 1910 | - | - | 9/6/1910 | 102000 |
| 1911 | - | - | 4/4/1911 | 27000 |
| 1912 | - | - | 4/7/1912 | 1110 |
| 1913 | - | - | 5/4/1913 | 63000 |
| 1914 | - | - | 5/23/1914 | 9280 |
| 1915 | - | - | 10/23/1914 | 67000 |
| 1916 | - | - | 9/1/1916 | 97000 |
| 1917 | 10/15/1916 | 2820 | 5/12/1917 | 1590 |
| 1918 | 1/15/1918 | 176 | 8/15/1918 | 7140 |
| 1919 | - | - | 9/16/1919 | 87000 |
| 1920 | 10/14/1919 | 4000 | 10/4/1919 | 5220 |
| 1921 | - | - | 6/13/1921 | 18500 |
| 1922 | - | - | 6/18/1922 | 77000 |
| 1923 | 9/17/1923 | 2900 | 9/17/1923 | 1500 |
| 1924 | 10/15/1923 | 5000 | 9/21/1924 | 12800 |
| 1925 | 8/13/1925 | 4720 | 5/28/1925 | 61000 |
| 1926 | - | - | 7/23/1926 | 4380 |
| 1927 | - | - | 6/13/1927 | 14600 |
| 1928 | - | - | 5/13/1928 | 19800 |
| 1929 | - | - | 6/30/1929 | 3970 |
| 1930 | - | - | 10/14/1929 | 6320 |
| 1931 | - | - | 10/14/1930 | 20100 |
| 1932 | - | - | 9/1/1932 | 116000 |
| 1933 | - | - | 10/16/1932 | 6360 |
| 1934 | - | - | 6/4/1934 | 8220 |
| 1935 | - | - | 9/4/1935 | 84400 |

**Table 4.2.** Table of annual peak discharges 1936–1966 for gauges at Orla, Pecos, and Shumla, with dates, in cfs.

| Water Year | Orla Date | Orla Discharge | Pecos Date | Pecos Discharge | Shumla Date | Shumla Discharge |
|---|---|---|---|---|---|---|
| 1936 | - | - | - | - | 9/27/1936 | 31100 |
| 1937 | - | - | - | - | 5/10/1937 | 2800 |
| 1938 | 6/28/1938 | 2280 | - | - | 7/24/1938 | 31500 |
| 1939 | 6/21/1939 | 2690 | - | - | 5/5/1939 | 5800 |
| 1940 | 6/29/1940 | 770 | 6/30/1940 | 528 | 6/25/1940 | 5610 |
| 1941 | 9/29/1941 | 23700 | 9/30/1941 | 22200 | 9/18/1941 | 18700 |
| 1942 | 10/5/1941 | 15700 | 10/27/1941 | 4800 | 10/10/1941 | 14300 |
| 1943 | 11/11/1942 | 2060 | 11/12/1942 | 1590 | 7/15/1943 | 11200 |
| 1944 | 8/18/1944 | 2470 | 8/19/1944 | 1220 | 9/6/1944 | 8960 |
| 1945 | 7/4/1945 | 2130 | 7/5/1945 | 828 | 7/8/1945 | 8730 |
| 1946 | 9/20/1946 | 1280 | 3/23/1946 | 418 | 10/7/1945 | 27700 |
| 1947 | 4/19/1947 | 562 | 4/18/1947 | 449 | 10/6/1946 | 65000 |
| 1948 | 6/1/1948 | 1320 | 9/10/1948 | 560 | 7/4/1948 | 51300 |
| 1949 | 9/11/1949 | 1380 | 4/14/1949 | 286 | 7/26/1949 | 98500 |
| 1950 | 7/19/1950 | 1790 | 7/20/1950 | 766 | 7/13/1950 | 44900 |
| 1951 | 5/3/1951 | 755 | 5/18/1951 | 506 | 5/24/1951 | 8180 |
| 1952 | 4/17/1952 | 2000 | 4/19/1952 | 888 | 5/27/1952 | 3570 |
| 1953 | 6/9/1953 | 460 | 7/15/1953 | 51 | 8/24/1953 | 14800 |
| 1954 | 10/23/1953 | 1830 | 10/24/1953 | 1060 | 6/28/1954 | 948000 |
| 1955 | 6/30/1955 | 804 | - | - | 7/19/1955 | 27100 |
| 1956 | 10/2/1955 | 8050 | - | - | 5/2/1956 | 4000 |
| 1957 | 7/2/1957 | 2110 | - | - | 5/10/1957 | 38400 |
| 1958 | 10/9/1957 | 3780 | - | - | 9/22/1958 | 38400 |
| 1959 | 6/29/1959 | 1010 | - | - | 9/30/1959 | 23700 |
| 1960 | 7/8/1960 | 2360 | - | - | 10/4/1959 | 47500 |
| 1961 | 10/17/1960 | 1030 | - | - | 6/17/1961 | 14700 |
| 1962 | 7/17/1962 | 524 | - | - | 9/7/1962 | 12500 |
| 1963 | 8/15/1963 | 1880 | - | - | 10/18/1962 | 18000 |
| 1964 | 6/24/1964 | 870 | - | - | 9/24/1964 | 51800 |
| 1965 | 9/1/1965 | 1350 | - | - | 5/31/1965 | 15600 |
| 1966 | 6/11/1966 | 3520 | - | - | 4/25/1966 | 15500 |

operated again from water year 1940 through the remainder of the period of interest, while the gage at Sheffield operated from 1940–1949.

The purpose of Tables 4.4–4.6 is to draw inference about the potential effects of the existence of Red Bluff Reservoir on annual peak floods on the river below the dam, after construction. Dates of annual peaks progressing in a downstream direction might imply a flood wave moving downstream, a general/regional weather system, or simply association

**Table 4.3.** Table of annual peak discharges 1936–1966 for gauges at Girvin, Sheffield, and Shumla, with dates, in cfs.

| Water Year | Girvin Date | Girvin Discharge | Sheffield Date | Sheffield Discharge | Shumla Date | Shumla Discharge |
|---|---|---|---|---|---|---|
| 1936 | - | - | - | - | 9/27/1936 | 31100 |
| 1937 | - | - | - | - | 5/10/1937 | 2800 |
| 1938 | - | - | - | - | 7/24/1938 | 31500 |
| 1939 | - | - | - | - | 5/5/1939 | 5800 |
| 1940 | 8/11/1940 | 469 | 6/24/1940 | 2870 | 6/25/1940 | 5610 |
| 1941 | 6/16/1941 | 6870 | 6/20/1941 | 5700 | 9/18/1941 | 18700 |
| 1942 | 10/5/1941 | 20000 | 10/8/1941 | 13800 | 10/10/1941 | 14300 |
| 1943 | 11/5/1942 | 1290 | 10/17/1942 | 3820 | 7/15/1943 | 11200 |
| 1944 | 8/22/1944 | 450 | 8/26/1944 | 1330 | 9/6/1944 | 8960 |
| 1945 | 7/8/1945 | 1080 | 7/7/1945 | 1480 | 7/8/1945 | 8730 |
| 1946 | 10/6/1945 | 201 | 5/9/1946 | 384 | 10/7/1945 | 27700 |
| 1947 | 5/16/1947 | 652 | 5/18/1947 | 3410 | 10/6/1946 | 65000 |
| 1948 | 5/25/1948 | 259 | 2/26/1948 | 1450 | 7/4/1948 | 51300 |
| 1949 | 6/13/1949 | 198 | 7/26/1949 | 5560 | 7/26/1949 | 98500 |
| 1950 | 5/26/1950 | 1800 | - | - | 7/13/1950 | 44900 |
| 1951 | 9/15/1951 | 189 | - | - | 5/24/1951 | 8180 |
| 1952 | 7/11/1952 | 164 | - | - | 5/27/1952 | 3570 |
| 1953 | 8/20/1953 | 43 | - | - | 8/24/1953 | 14800 |
| 1954 | 6/15/1954 | 784 | - | - | 6/28/1954 | 948000 |
| 1955 | 10/6/1954 | 2000 | - | - | 7/19/1955 | 27100 |
| 1956 | 7/5/1956 | 230 | - | - | 5/2/1956 | 4000 |
| 1957 | 4/26/1957 | 3800 | - | - | 5/10/1957 | 38400 |
| 1958 | 9/27/1958 | 5090 | - | - | 9/22/1958 | 38400 |
| 1959 | 7/18/1959 | 365 | - | - | 9/30/1959 | 23700 |
| 1960 | 6/7/1960 | 309 | - | - | 10/4/1959 | 47500 |
| 1961 | 3/28/1961 | 690 | - | - | 6/17/1961 | 14700 |
| 1962 | 5/21/1962 | 474 | - | - | 9/7/1962 | 12500 |
| 1963 | 11/21/1962 | 277 | - | - | 10/18/1962 | 18000 |
| 1964 | 9/23/1964 | 367 | - | - | 9/24/1964 | 51800 |
| 1965 | 6/13/1965 | 635 | - | - | 5/31/1965 | 15600 |
| 1966 | 8/30/1966 | 240 | - | - | 4/25/1966 | 15500 |

by way of region-wide seasonal similarity. Dates of annual peaks that are disjoint from one another might imply flood peaks that derive from more localized weather events, i.e. mesoscale or convective events, that affect a limited reach of the river. Nothing certain can be said about these implications, but the idea is to assess the overall impact of Red Bluff Reservoir on the river below it, and thus infer the influence of the watershed above the reservoir on the river below it.

Table 4.4 lists annual peak discharges and the associated dates prior to the construction of Red Bluff Reservoir. Water years during which there were common data between the gauge at Artesia, New Mexico, and one or more gauges between the Artesia gauge and Shumla are 1906, 1917–1918, 1920, and 1922–1926. Of those years, four (1906, 1920, 1924, and 1925) display some apparent association among dates between the Artesia gauge and those nearby in Texas. Three years (1918, 1923, and 1926) show date association with the Shumla gauge. In 1920, the peak in Shumla occurred close in date to others, but prior to them, possibly indicating a general or regional weather system. Thus, it can be said that prior to regulation by Red Bluff Reservoir, four years out of nine showed association of dates of annual peak flows. It is difficult to draw conclusions about flood waves or causal factors, but association of dates gives some idea of relative dependence. What is not seen is a consistent flood wave producing annual peaks progressing downstream, as might be expected.

Tables 4.5 and 4.6 list water year 1940–1966 annual peaks for the Artesia gauge compared to those of the Orla and Mentone gauges and the Girvin, Sheffield, and Shumla gauges, respectively, for comparison of dates after the construction of Red Bluff Reservoir. Water years 1942, 1943, and 1950 show a relation in peak dates that exhibit association that might be expected for a floodwave moving downstream through Red Bluff Reservoir, while water years 1955, 1960, and 1961 exhibit associations that are close in date, but adverse in that the peak at the downstream station precedes that at the upstream station. Such an association could be attributable to a common regional weather system, but probably not to a floodwave.

Of 15 water years during which both the Orla and Pecos gauges were in operation, nine exhibit close association. (1940–1941, 1943–1945, 1947, 1950, 1952, and 1954). Of 26 years of data comparing the Artesia to Girvin annual peaks after the construction of Red Bluff Reservoir, only three show dates close in time to one another; two are adverse (downstream preceding upstream) and one is on the same date. These occurrences would not lead to a conclusion of a floodwave moving through Red Bluff Reservoir. However, there are three years in which the annual peak at Shumla appears associated with that at Artesia, even though in all three cases, an annual peak at one of the gauges between the two is dissociated.

As might be expected, the annual peaks for gauges that are relatively close and sequential show closer association than of gauges further apart. The Orla and Pecos gauges show the highest degree of association, followed by the Sheffield and Shumla gauges. The Pecos

and Girvin gauges show only weak association; between 1940 and 1954 only water years 1943–1945 and 1953 appear associated.

A year in which an apparent floodwave swept down the system, water year 1942, appears broken up by the date of peak and magnitude of discharge at the Pecos gauge. All others are reasonably high discharges and are recorded early in October, while that at Pecos is moderate and recorded in late October, suggesting the possibility of misrecorded or mistranscribed record at that gauge for that year.

Other than those noted, annual peak discharges in this series of streamgauges exhibit a level of independence in dates and magnitudes that is surprising. In the vicinity of Girvin, the associations appear to weaken. Associations that might be suspected for regional weather systems appear, but connections indicating floodwave passage are few. Associations above Girvin, and those below Girvin appear stronger than those across Girvin.

In several cases, associations appear to be broken by a dissociated annual peak at an intervening gauge; a peak that does not produce an associated peak lower down. A conjecture to explain this is that large, regional weather systems of relatively low intensity produce a system-wide response that is relatively consistent, resulting in annual peaks at several gauges, while a localized, intense, mesoscale or convective event proximate to a specific gauge may produce a larger response at that gauge, yet be attenuated prior to reaching lower gauges. This phenomenon would result in the annual peak produced by the regional system being replaced in the record by a higher peak at one, or two, gauges.

Although common data prior to the construction of Red Bluff Reservoir are sparse, the influence of the construction is suggested in a change in the frequency of associated annual peak dates prior to and subsequent to the construction in 1936. However, the existence of the reservoir does not completely break the associations. This continuation of association suggests that at least part of the potential association is not because of hydraulic connection across the reservoir but because of meteorologic connection throughout all or part of the region.

Under the assumptions of uniform areal contribution and of optimal response occurring because of system-wide weather events, the general expectation on a river of the size and prominence of the Pecos River would be that annual peaks would frequently be associated with one another in time along a series of gauges. Finding isolated peaks dissociated in both time and magnitude speaks against system-wide responses. The temporal evidence presented in this subsection suggests that associated dates of annual peaks are more likely produced by local response to system-wide weather systems as opposed to system-wide responses to system-wide weather systems. Responses seen at different gauges do not, in

**Table 4.4.** Table of annual peak discharges for various years between 1906 and 1926 for gauges at Artesia, Mentone, Pecos, Sheffield, and Shumla, with dates, in cfs, for date comparison prior to the construction of Red Bluff Reservoir.

| Water Year | Artesia Date | Artesia Disch. | Mentone Date | Mentone Disch. | Pecos Date | Pecos Disch. | Shumla Date | Shumla Disch. |
|---|---|---|---|---|---|---|---|---|
| 1906 | 7/18/1906 | 8500 | - | - | 7/18/1906 | 2340 | 8/11/1906 | 90000 |
| 1917 | 8/20/1917 | 6220 | - | - | 10/15/1916 | 2820 | 5/12/1917 | 1590 |
| 1918 | 8/10/1918 | 6270 | - | - | 1/15/1918 | 176 | 8/15/1918 | 7140 |
| 1920 | 10/10/1919 | 4760 | - | - | 10/14/1919 | 4000 | 10/4/1919 | 5220 |
| 1922 | 6/4/1922 | 9200 | 4/26/1922 | 1660 | - | - | 6/18/1922 | 77000 |
| 1923 | 6/10/1923 | 3390 | 9/16/1923 | 4110 | 9/17/1923 | 2900 | 9/17/1923 | 1500 |
| 1924 | 10/6/1923 | 10200 | 10/11/1923 | 5250 | 10/15/1923 | 5000 | 9/21/1924 | 12800 |
| 1925 | 8/6/1925 | 5080 | 8/12/1925 | 5690 | 8/13/1925 | 4720 | 5/28/1925 | 61000 |
| 1926 | 7/13/1926 | 4000 | 5/30/1926 | 5140 | - | - | 7/23/1926 | 4380 |

general, appear to represent flood waves moving downstream. Frequently, annual peaks precede those at gauges located upstream; large discharges frequently appear dissociated in time, or only loosely associated with those on other gauges for the same water year. These associations and dissociations suggest that even under the influence of a common weather system, responses seen at various gauges are the result of partial area contribution local to the gauge site. In particular, there is appearance of a disconnect between what happens upstream from Girvin and what happens downstream from it.

Subareas were delineated for the portion above Orla (and Red Bluff Dam), area contributing between Orla and Girvin, where annual peak discharges diminish, between Girvin and Sheffield where annual peaks increase slightly, and between Sheffield and Shumla where annual peaks increase dramatically.

### 4.5.3 Flood Magnitude Comparisons

Table 4.7 is a listing of annual peak discharges 1940–1949 on five gauges along the Pecos River in Texas (in cfs), with the mean value for that interval. Table 4.8 lists the contributing area (in square miles) at each of the five gauges, the difference from one to the next in square miles, the percent change in area from one gauge to the next, and the percent change in the mean of the annual peak flow values from one gauge to the next. Table 4.9 lists annual peak discharges 1940–1954 for four of the gauges (in cfs), with the mean value for that interval. Table 4.10 lists the contributing area (in square miles) at each of the gauges, the difference

**Table 4.5.** Table of annual peak discharges 1940–1966 for gauges at Artesia, Orla, and Pecos, with dates, in cfs, for date comparison after the construction of Red Bluff Reservoir.

| Water Year | Artesia Date | Artesia Discharge | Orla Date | Orla Discharge | Pecos Date | Pecos Discharge |
|---|---|---|---|---|---|---|
| 1940 | 5/23/1940 | 6060 | 6/29/1940 | 770 | 6/30/1940 | 528 |
| 1941 | 9/25/1941 | 44300 | 9/29/1941 | 23700 | 9/30/1941 | 22200 |
| 1942 | 10/2/1941 | 25500 | 10/5/1941 | 15700 | 10/27/1941 | 4800 |
| 1943 | 11/5/1942 | 4620 | 11/11/1942 | 2060 | 11/12/1942 | 1590 |
| 1944 | 3/20/1944 | 1520 | 8/18/1944 | 2470 | 8/19/1944 | 1220 |
| 1945 | 4/8/1945 | 1160 | 7/4/1945 | 2130 | 7/5/1945 | 828 |
| 1946 | 6/28/1946 | 3190 | 9/20/1946 | 1280 | 3/23/1946 | 418 |
| 1947 | 10/5/1946 | 1160 | 4/19/1947 | 562 | 4/18/1947 | 449 |
| 1948 | 6/3/1948 | 4210 | 6/1/1948 | 1320 | 9/10/1948 | 560 |
| 1949 | 7/16/1949 | 5550 | 9/11/1949 | 1380 | 4/14/1949 | 286 |
| 1950 | 7/7/1950 | 4650 | 7/19/1950 | 1790 | 7/20/1950 | 766 |
| 1951 | 10/5/1950 | 2540 | 5/3/1951 | 755 | 5/18/1951 | 506 |
| 1952 | 7/20/1952 | 2340 | 4/17/1952 | 2000 | 4/19/1952 | 888 |
| 1953 | 7/19/1953 | 3280 | 6/9/1953 | 460 | 7/15/1953 | 51 |
| 1954 | 5/20/1954 | 5350 | 10/23/1953 | 1830 | 10/24/1953 | 1060 |
| 1955 | 10/8/1954 | 25200 | 6/30/1955 | 804 | - | - |
| 1956 | 10/3/1955 | 4200 | 10/2/1955 | 8050 | - | - |
| 1957 | 5/31/1957 | 3640 | 7/2/1957 | 2110 | - | - |
| 1958 | 7/7/1958 | 2930 | 10/9/1957 | 3780 | - | - |
| 1959 | 7/18/1959 | 2240 | 6/29/1959 | 1010 | - | - |
| 1960 | 7/11/1960 | 11700 | 7/8/1960 | 2360 | - | - |
| 1961 | 10/18/1960 | 3900 | 10/17/1960 | 1030 | - | - |
| 1962 | 8/1/1962 | 3260 | 7/17/1962 | 524 | - | - |
| 1963 | 6/3/1963 | 4230 | 8/15/1963 | 1880 | - | - |
| 1964 | 6/14/1964 | 5200 | 6/24/1964 | 870 | - | - |
| 1965 | 7/30/1965 | 4500 | 9/1/1965 | 1350 | - | - |
| 1966 | 8/24/1966 | 7000 | 6/11/1966 | 3520 | - | - |

from one to the next in square miles, the percent change in area from one gauge to the next, and the percent change in the mean of the annual peak flow values from one gauge to the next. Similarly, Table 4.11 is a listing of annual peak discharges 1940–1966 on three of the gauges (in cfs) with the mean value for that interval and Table 4.12 lists the contributing area (in square miles) at each of the gauges, the difference from one to the next in square miles, the percent change in area from one gauge to the next, and the percent change in the mean of the annual peak flow values from one gauge to the next. The streamgauges at Pecos, Mentone, and Sheffield have existed intermittently with some data before the regulation

**Table 4.6.** Table of annual peak discharges for various years between 1940 and 1966 for gauges at Artesia, Girvin, Sheffield, and Shumla, with dates, in cfs for date comparison after to the construction of Red Bluff Reservoir.

| Water Year | Artesia Date | Artesia Disch. | Girvin Date | Girvin Disch. | Sheffield Date | Sheffield Disch. | Shumla Date | Shumla Disch. |
|---|---|---|---|---|---|---|---|---|
| 1940 | 5/23/1940 | 6060 | 8/11/1940 | 469 | 6/24/1940 | 2870 | 6/25/1940 | 5610 |
| 1941 | 9/25/1941 | 44300 | 6/16/1941 | 6870 | 6/20/1941 | 5700 | 9/18/1941 | 18700 |
| 1942 | 10/2/1941 | 25500 | 10/5/1941 | 20000 | 10/8/1941 | 13800 | 10/10/1941 | 14300 |
| 1943 | 11/5/1942 | 4620 | 11/5/1942 | 1290 | 10/17/1942 | 3820 | 7/15/1943 | 11200 |
| 1944 | 3/20/1944 | 1520 | 8/22/1944 | 450 | 8/26/1944 | 1330 | 9/6/1944 | 8960 |
| 1945 | 4/8/1945 | 1160 | 7/8/1945 | 1080 | 7/7/1945 | 1480 | 7/8/1945 | 8730 |
| 1946 | 6/28/1946 | 3190 | 10/6/1945 | 201 | 5/9/1946 | 384 | 10/7/1945 | 27700 |
| 1947 | 10/5/1946 | 1160 | 5/16/1947 | 652 | 5/18/1947 | 3410 | 10/6/1946 | 65000 |
| 1948 | 6/3/1948 | 4210 | 5/25/1948 | 259 | 2/26/1948 | 1450 | 7/4/1948 | 51300 |
| 1949 | 7/16/1949 | 5550 | 6/13/1949 | 198 | 7/26/1949 | 5560 | 7/26/1949 | 98500 |
| 1950 | 7/7/1950 | 4650 | 5/26/1950 | 1800 | - | - | 7/13/1950 | 44900 |
| 1951 | 10/5/1950 | 2540 | 9/15/1951 | 189 | - | - | 5/24/1951 | 8180 |
| 1952 | 7/20/1952 | 2340 | 7/11/1952 | 164 | - | - | 5/27/1952 | 3570 |
| 1953 | 7/19/1953 | 3280 | 8/20/1953 | 43 | - | - | 8/24/1953 | 14800 |
| 1954 | 5/20/1954 | 5350 | 6/15/1954 | 784 | - | - | 6/28/1954 | 948000 |
| 1955 | 10/8/1954 | 25200 | 10/6/1954 | 2000 | - | - | 7/19/1955 | 27100 |
| 1956 | 10/3/1955 | 4200 | 7/5/1956 | 230 | - | - | 5/2/1956 | 4000 |
| 1957 | 5/31/1957 | 3640 | 4/26/1957 | 3800 | - | - | 5/10/1957 | 38400 |
| 1958 | 7/7/1958 | 2930 | 9/27/1958 | 5090 | - | - | 9/22/1958 | 38400 |
| 1959 | 7/18/1959 | 2240 | 7/18/1959 | 365 | - | - | 9/30/1959 | 23700 |
| 1960 | 7/11/1960 | 11700 | 6/7/1960 | 309 | - | - | 10/4/1959 | 47500 |
| 1961 | 10/18/1960 | 3900 | 3/28/1961 | 690 | - | - | 6/17/1961 | 14700 |
| 1962 | 8/1/1962 | 3260 | 5/21/1962 | 474 | - | - | 9/7/1962 | 12500 |
| 1963 | 6/3/1963 | 4230 | 11/21/1962 | 277 | - | - | 10/18/1962 | 18000 |
| 1964 | 6/14/1964 | 5200 | 9/23/1964 | 367 | - | - | 9/24/1964 | 51800 |
| 1965 | 7/30/1965 | 4500 | 6/13/1965 | 635 | - | - | 5/31/1965 | 15600 |
| 1966 | 8/24/1966 | 7000 | 8/30/1966 | 240 | - | - | 4/25/1966 | 15500 |

by Red Bluff Reservoir and some after. The streamgauge at Shumla extends across the time at which Red Bluff began to regulate the lower Pecos. A cursory examination of the magnitudes of annual peaks recorded by the streamgauges above Shumla and the Shumla streamgauge shows very little commonality on a 1:1 basis; there are few years in which annual peaks appear related in magnitude. A curious aspect of these time series of peak discharges is the apparent tendency for annual peak discharge to diminish in downstream direction from Orla to Sheffield, contrary to assumptions presented earlier in this chapter. The ubiquitous concept in hydrology is that peak flood discharge increases with increasing

contributing area, which translates directly to increasing discharge as the point of interest moves downstream.

As with many streams in west Texas, mean annual peak discharge diminishes as time passes. This diminution of discharge can be explained in several ways; for instance that the data in question are primarily from the post-regulation period, and that withdrawal for irrigated agriculture along the Pecos increased during the period of record. A commonly discussed cause is the thought that brush invasion of the watersheds increases uptake along with phreatophyte invasion of the riparian areas (Graf, 2002).

Conventional hydrologic thought is that discharge should increase with increasing area as exemplified by regression equations having positive exponents on the area term (Asquith and Thompson, 2008). In this streamgauge series is a counterexample to that thought; discharges from Orla to Girvin diminish steadily in magnitude, and appear to reach a nadir at Girvin. Annual peaks at the most downstream streamgauge, which is located at Shumla near the mouth of the Pecos, are approximately an order of magnitude greater than those at the streamgauges upstream. The increase in flood discharge between Girvin and Shumla is inexplicably large. Previous discussion herein alluded to regression on contributing area usually indicating that discharge increases proportional to the square root of area. The cases between Orla and Girvin, and between Girvin and Shumla, are both exceptions to that generalization, but contrasting in nature with one another.

**Table 4.7.** Table of annual peak discharges 1940–1949 for five Texas gauges, in cfs.

| Water Year | Orla | Pecos | Girvin | Sheffield | Shumla |
|---|---|---|---|---|---|
| 1940 | 770 | 528 | 469 | 2870 | 5610 |
| 1941 | 23700 | 22200 | 6870 | 5700 | 18700 |
| 1942 | 15700 | 4800 | 20000 | 13800 | 14300 |
| 1943 | 2060 | 1590 | 1290 | 3820 | 11200 |
| 1944 | 2470 | 1220 | 450 | 1330 | 8960 |
| 1945 | 2130 | 828 | 1080 | 1480 | 8730 |
| 1946 | 1280 | 418 | 201 | 384 | 27700 |
| 1947 | 562 | 449 | 652 | 3410 | 65000 |
| 1948 | 1320 | 560 | 259 | 1450 | 51300 |
| 1949 | 1380 | 286 | 198 | 5560 | 98500 |
| Mean | 5137 | 3288 | 3147 | 3980 | 31000 |

As with the discussion in Section 4.5.2, under the assumptions of uniform areal contribution and of optimal response occurring because of system-wide weather events, the

**Table 4.8.** Table of contributing areas in square miles (sq. mi.), difference in area, percentage increase in area, mean peak discharge, and percent increase in mean peak discharge for years 1940–1949 for five gauges.

| Gauge | Orla | Pecos | Girvin | Sheffield | Shumla |
|---|---|---|---|---|---|
| Contributing area | 21210 | 26236 | 29560 | 31600 | 35162 |
| Difference | - | 5026 | 3324 | 2040 | 3562 |
| Percent increase in area | | 24 | 13 | 7 | 11 |
| Mean peak discharge | 5137 | 3288 | 3147 | 3980 | 31000 |
| Percent change in peak discharge | - | -36 | -4 | 26 | 679 |

**Table 4.9.** Table of annual peak discharges 1940–1954 for four Texas gauges, in cfs. An extreme value of 958,000 cfs in 1954 was removed for averaging

| Water Year | Orla | Pecos | Girvin | Shumla |
|---|---|---|---|---|
| 1940 | 770 | 528 | 469 | 5610 |
| 1941 | 23700 | 22200 | 6870 | 18700 |
| 1942 | 15700 | 4800 | 20000 | 14300 |
| 1943 | 2060 | 1590 | 1290 | 11200 |
| 1944 | 2470 | 1220 | 450 | 8960 |
| 1945 | 2130 | 828 | 1080 | 8730 |
| 1946 | 1280 | 418 | 201 | 27700 |
| 1947 | 562 | 449 | 652 | 65000 |
| 1948 | 1320 | 560 | 259 | 51300 |
| 1949 | 1380 | 286 | 198 | 98500 |
| 1950 | 1790 | 766 | 1800 | 44900 |
| 1951 | 755 | 506 | 189 | 8180 |
| 1952 | 2000 | 888 | 164 | 3570 |
| 1953 | 460 | 51 | 43 | 14800 |
| 1954 | 1830 | 1060 | 784 | - |
| Mean | 3880 | 2410 | 2297 | 27246 |

general expectation on a river of the size and prominence of the Pecos River would be that annual peaks would frequently be associated with one another in magnitude along a series of gauges. The magnitude evidence presented suggests that little interaction occurs between the areas contributing to various gauge. Responses seen at different gauges do not, in general, appear to represent flood waves moving downstream. Frequently, large discharges appear dissociated or only loosely associated with those on other gauges for the same water year. These associations and dissociations, like those for timing, suggest that

**Table 4.10.** Table of contributing areas in square miles (sq. mi.), difference in area, percentage increase in area, mean peak discharge, and percent increase in mean peak discharge for years 1940–1954 for four gauges.

| Gauge | Orla | Pecos | Girvin | Shumla |
|---|---|---|---|---|
| Contributing area | 21210 | 26236 | 29560 | 35162 |
| Difference | - | 5026 | 3324 | 3562 |
| Percent increase in area | | 24 | 13 | 19 |
| Mean peak discharge | 5137 | 3288 | 3147 | 31000 |
| Percent change in peak discharge | - | -36 | -4 | 885 |

even under the influence of a common weather system, responses seen at various gauges are the result of partial area contribution local to the gauge site. Magnitude comparison is even more compelling than temporal comparison in suggesting that what happens above Girvin bears little on what happens below it, and that the area between Girvin and Shumla, a small fraction of total contributing area, is unusually productive of runoff.

At Girvin, the Pecos is a weak stream, apparently in danger of disappearing completely as surface flow. At Shumla, the same river tends to be a raging torrent at annual peak stage. That this river demonstrates such a dramatic change in character when the contributing area only changes by a relatively small amount is difficult to explain. In the years of overlapping data between Girvin and Shumla, measurements at the Shumla stream streamgauge exhibit an average peak flow rate 15 times greater than the average peak discharge observed at Girvin, although the contributing area at Shumla is only 19 percent than that at Girvin.[1] The 19 percent of total area between Girvin and Shumla appears to produce 14 times greater discharge at the Shumla streamgauge than the 81 percent of total area above Girvin. Total contributing area is as recorded in USGS streamgauge records.

If the area above Red Bluff is discounted because of regulation, and only the area below it considered, the increase in unregulated contributing area between Girvin and Shumla is 67 percent of the total unregulated area at Girvin. The increase between Girvin and Shumla is a noteworthy departure from the behavior that would be expected according to traditional assumptions.

The author has observed from past analyses as a professional that, at least in the state of Texas, it is common to encounter situations where, on major river systems in Texas such as

[1] The extreme high outlier of 1954 was removed from the Shumla data for averaging, as it exerted a disproportionally large influence.

**Table 4.11.** Table of annual peak discharges 1940–1966 for three Texas gauges. An extreme value of 958,000 cfs in 1954 was removed for averaging.

| Water Year | Orla | Girvin | Shumla |
|---|---|---|---|
| 1940 | 770 | 469 | 5610 |
| 1941 | 23700 | 6870 | 18700 |
| 1942 | 15700 | 20000 | 14300 |
| 1943 | 2060 | 1290 | 11200 |
| 1944 | 2470 | 450 | 8960 |
| 1945 | 2130 | 1080 | 8730 |
| 1946 | 1280 | 201 | 27700 |
| 1947 | 562 | 652 | 65000 |
| 1948 | 1320 | 259 | 51300 |
| 1949 | 1380 | 198 | 98500 |
| 1950 | 1790 | 1800 | 44900 |
| 1951 | 755 | 189 | 8180 |
| 1952 | 2000 | 164 | 3570 |
| 1953 | 460 | 43 | 14800 |
| 1954 | 1830 | 784 | - |
| 1955 | 804 | 2000 | 27100 |
| 1956 | 8050 | 230 | 4000 |
| 1957 | 2110 | 3800 | 38400 |
| 1958 | 3780 | 5090 | 38400 |
| 1959 | 1010 | 365 | 23700 |
| 1960 | 2360 | 309 | 47500 |
| 1961 | 1030 | 690 | 14700 |
| 1962 | 524 | 474 | 12500 |
| 1963 | 1880 | 277 | 18000 |
| 1964 | 870 | 367 | 51800 |
| 1965 | 1350 | 635 | 15600 |
| 1966 | 3520 | 240 | 15500 |
| Mean | 3166 | 1812 | 26487 |

the Nueces, Red, and Guadalupe, the quantile values of flood-frequency curves diminish in a downstream direction, primarily in the lower reaches of these rivers as they traverse the eastern, coastal plains sections of the state. Simplistically, this diminution can be ascribed to the attenuation of flood waves as they progress downstream. This simple explanation implies that at least a distinct fraction of annual peak floods originate in the distal areas of the watershed and travel downstream, past a series of gaging stations, diminishing with attenuation as they go. The interpretation of floods originating in distal areas and traveling downstream is consistent with the prevailing thought that the entire watershed contributes

**Table 4.12.** Table of contributing areas in square miles (sq. mi.), difference in area, percentage increase in area, mean peak discharge, and percent increase in mean peak discharge for years 1940–1966 for three gauges.

| Gauge | Orla | Girvin | Shumla |
|---|---|---|---|
| Contributing area | 21210 | 29560 | 35162 |
| Difference | - | 8350 | 5602 |
| Percent increase in area | | 39 | 19 |
| Mean peak discharge | 5137 | 3147 | 31000 |
| Percent change in peak discharge | - | -39 | 885 |

and exerts influence, but diminution of quantile valuest is inconsistent with the prevailing thought that, all else being equal, peak discharge increases with increasing contributing area. Accounting for this departure from expected behavior requires departure from standard assumptions.

At least one explanation for both of these inconsistencies is the influence of topography local to the point of interest (streamgauge). As stated earlier, standard thought treats all contributing area equally. Implied is that the influences of terrain can be lumped into a few descriptive parameters that can be computed from easily measured quantities. Some authors (Lienhard, 1964) seek "minimum knowledge of watershed properties" as a goal in developing a watershed response simulation tool. The implication of the examples shown here is that the influence of topographic ruggedness, and of geology, on flood development is amplified by proximity to the point of interest, or conversely diminishes with distance from the point of interest.

### 4.5.4 Measured Discharges Compared to Predicted Discharges

Some idea of the context of annual peak discharges recorded for the gauges shown can be derived by comparing the actual discharges to those that would be computed using regression equations such as those in Asquith and Thompson (2008). In order to do so, at least one of the measured values must be placed in some sort of probabilistic context. Annual exceedance values available through the regression equations are the 2-, 5-, 10-, 25-, 50-, and 100-year values. The 2-year value is that which is expected to be exceeded one year out of two, on average, over a long period of time, or half of years. The median of an annual peak flood series is the value at which half of the series are larger, and half

smaller. Equation 4.6 is Equation 4.2 with coefficients for the 2-year discharge and was used to compute values for comparison.

$$Q = 6.81A^{0.5534}P^{0.9732} \tag{4.6}$$

The median of each of the 9-year series from 1940–1949 (Table 4.7) was used to reflect as many gauges as possible, and to reflect conditions after the construction of Red Bluff Reservoir. Results are tabulated in Table 4.13.

Values computed using the regression equations for full contributing area listed with gauge data are much greater than the median of observed values. For interest, the discharge was also computed only for the area contributing *between* gauges. With the exception of the Shumla gauge, even this discharge is much greater than the median of observed values; that at the Shumla gauge is smaller than the measured discharge. As an additional comparison, discharge was computed for the Shumla gauge using the sum of areas contributing below Girvin. The computed discharge for that value of contributing area is 11,638 cfs, much closer to the 14,300 than other computations.

**Table 4.13.** Table of contributing areas in square miles (sq. mi.), difference in area, percentage increase in area, median peak discharge, MAP, and discharges (cfs) computed by Equation 4.6 for years 1940–1949 for five gauges.

| Quantity | Orla | Pecos | Girvin | Sheffield | Shumla |
|---|---|---|---|---|---|
| Contributing Area | 21210 | 26236 | 29560 | 31600 | 35162 |
| Difference | - | 5026 | 3324 | 2040 | 3562 |
| Percent increase in area | | 24 | 13 | 7 | 11 |
| Median Disch | 1380 | 560 | 469 | 2870 | 14300 |
| MAP (Inches) | 11 | 9 | 13 | 14 | 17 |
| Computed Disch. (Total Area) | 17415 | 16115 | 24622 | 27459 | 35189 |
| Computed Disch. (Difference) | - | 7850 | 7347 | 6027 | 9911 |

As a point of interest, Equation 4.6 was algebraically rearranged to solve for area in terms of the observed discharge, resulting in Equation 4.7

$$A = \left(\frac{Q}{6.81 \times P^{0.9732}}\right)^{1.8070} \tag{4.7}$$

Equation 4.7 was evaluated using the median discharge and mean annual precipitation values in Table 4.13. The resulting values of area represent estimates for the partial area

contributing to the median annual peak value for each gauge for the period 1940–1949, shown in Table 4.14.

**Table 4.14.** Table of median peak discharge, MAP, and partial area implied to produce the median by Equation 4.7 for years 1940–1949 for five gauges.

| Quantity | Orla | Pecos | Girvin | Sheffield | Shumla |
|---|---|---|---|---|---|
| Listed Contributing Area | 21210 | 26236 | 29560 | 31600 | 35162 |
| Median Disch | 1380 | 560 | 469 | 2870 | 14300 |
| MAP (Inches) | 11 | 9 | 13 | 14 | 17 |
| Computed Contributing Area | 217 | 60 | 23 | 533 | 6908 |

The values in Table 4.14 are dramatically smaller that the contributing areas listed for the gauges under discussion. The area for the Shumla gauge appears to be of the approximate magnitude of the combined area between Shumla and the gauge at Girvin. The diminutive size of the areas computed by the method above are further support for the partial area concept as described by Betson (1964), Amerman (1965), Hewlett and Hibbert (1967), Ragan (1968), Dunne and Black (1970), and others in the general literature. Computations at the Girvin gauge imply that the fraction of the topographic watershed contributing may be as small as 0.07 percent for the median annual peak discharge.

### 4.5.5 Rainfall Environment

Evidence was shown in Subsections 4.5.2 and 4.5.3 to suggest that annual peak discharges among the streamgauges shown exhibit variation in general character that is not explained by normal hydrologic expectation. General thought would suggest a gentle and monotonic increase in mean annual peak discharge with increase in contributing area, and would suggest that annual peaks at different points on the same stream would exhibit a high degree of temporal association. The streamgauges shown on the lower Pecos River exhibit gentle decrease, followed by rapid increase, in mean annual peak, as well as dissociated temporal behavior of floods. Such dissociation suggests examining rainfall data to estimate the influence of geographical variation in climate on this system.

Equation 4.2 suggests dependence of disharge on rainfall. That dependence was demonstrated in 4.3.1 and further in 4.5.4. In the case of Equation 4.2, the value used is mean

annual precipitation (MAP). For the purposes of reference, Figure 4.8 is a map of MAP for the area under discussion. While MAP is apparently a reasonable surrogate for precipitation influences, actual flood events are the products of actual rainfall events, and MAP carries little information about individual events themselves.

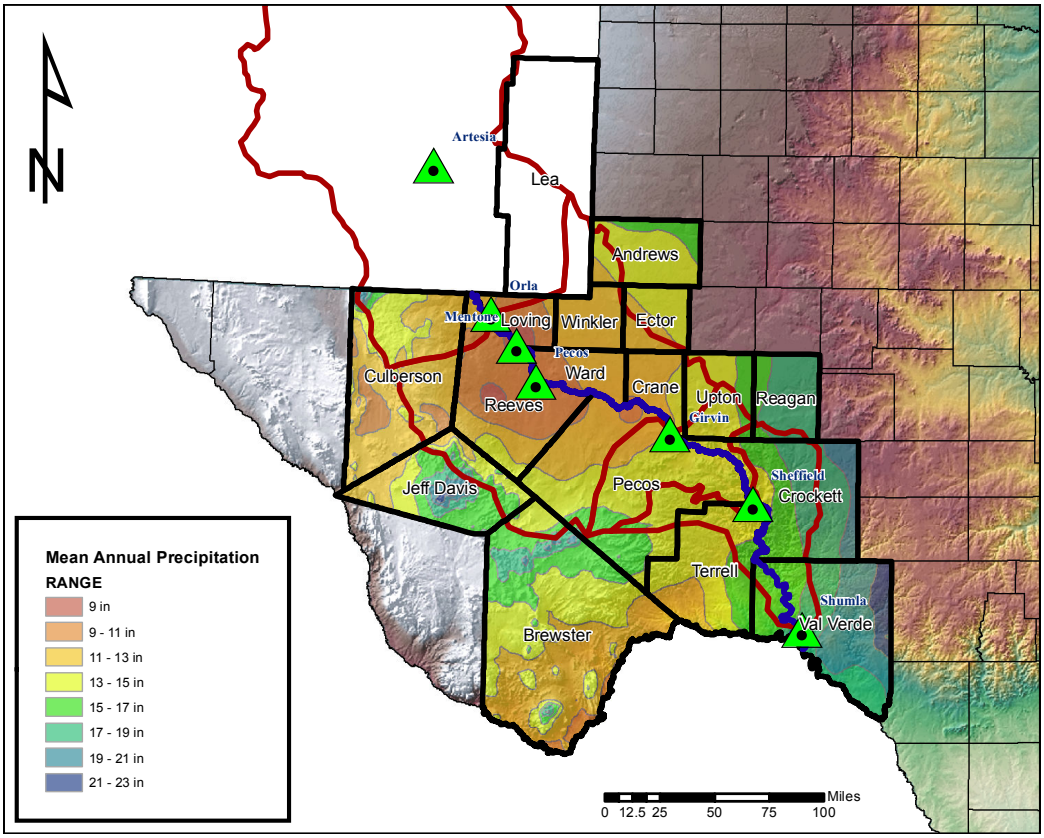


**Figure 4.8.** Map of Mean Annual Precipitatio(MAP)n for the lower Pecos River in Texas. Emphasized area is the area contributing below Red Bluff Reservoir. The small area in Lea County, New Mexico, is omitted, but rainfall there can be inferred from adjacent Texas counties. MAP is the surrogate rainfall quantity used in the regression equations of Asquith and Thompson (2008).

Climatic storm information for Eastern New Mexico, Oklahoma, and Texas has been compiled in Asquith et al. (2006). The counties containing contributing area for the lower Pecos River pertinent to the gauges under discussion are Lea County in New Mexico, and Brewster, Crane, Crockett, Culberson, Jeff Davis, Loving, Pecos, Reagan, Reeves, Terrell, Upton, Val Verde, Ward, and Winkler Counties in Texas. Asquith et al. (2006, Tables 13 and 19) for New Mexico and Texas list *mean storm depth* for *interevent durations* of 6, 8, 12, 18, 24, 48, and 72 hours. In order to compare rainfall characteristics of the region under

discussion, the above counties were divided into three categories by approximately where the area in them contributes to the Pecos River in the region under discussion. Lea County in New Mexico, and Andrews, Crane, Culberson, Loving, Reeves, Ward, and Winkler Counties in Texas were considered to contribute to the upper portion. Brewster, Jeff Davis, Pecos, and Upton Counties in Texas were considered to contribute to the middle portion, while Crockett, Reagan, Terrell, and Val Verde were considered to contribute to the lower portion.

Figure 4.9 is a map of the counties contributing to the lower Pecos River, classified as contributing to the upper, middle, or lower portion of the river within Texas; green for the upper, yellow for the middle, and blue for the lower portions of the reach under discussion. Figure 4.10 is a graph, related to Figure 4.9, showing the progression of mean storm depth for the counties and the interevent durations listed, generated from information in Asquith et al. (2006). Green lines are the values for counties contributing in the upper portion of the river reach; yellow lines for those contributing in the middle portion of the reach, and blue lines those contributing in the upper portion of the reach. The counties exhibiting the largest values are those contributing to the lower portion, where discharge increases dramatically. Table 4.15 lists the values for the counties, grouped as discussed. However, the increase of smallest to largest is from 0.497 to 0.788 inches at the 72-hour interevent time, an increase of 58 percent. The maximum increase in the middle range is from 0.497 to 0.631, a 27 percent increase. Annual peak streamflow, however, diminishes in the middle portion of the reach. The gradient in rainfall environment shown by Figure 4.10 and Table 4.15 appear inadequate to explain the behavior of the annual peak discharges of the river in this region. The counties as grouped are shown in colors in Figure 4.9.

Referring to the regression equations using area and MAP in Asquith and Thompson (2008) and the analysis performed in Subsection 4.5.4, whereas both MAP and the expected value of depth of precipitation for events increase in a downstream direction, the increase is insufficient to explain the observed increase in peak discharges. Precipitation by any metric shown approximately doubles, but a doubling in precipitation produces much less than a doubling of discharge, whereas observed discharges increase manyfold.

### 4.5.6 Runoff Generation from Soils and Rock Outcrops

The generation of runoff by rainfall on a watershed is dependent on at least two characteristics: the rainfall received by the watershed, and the tendency for rain to either run off,

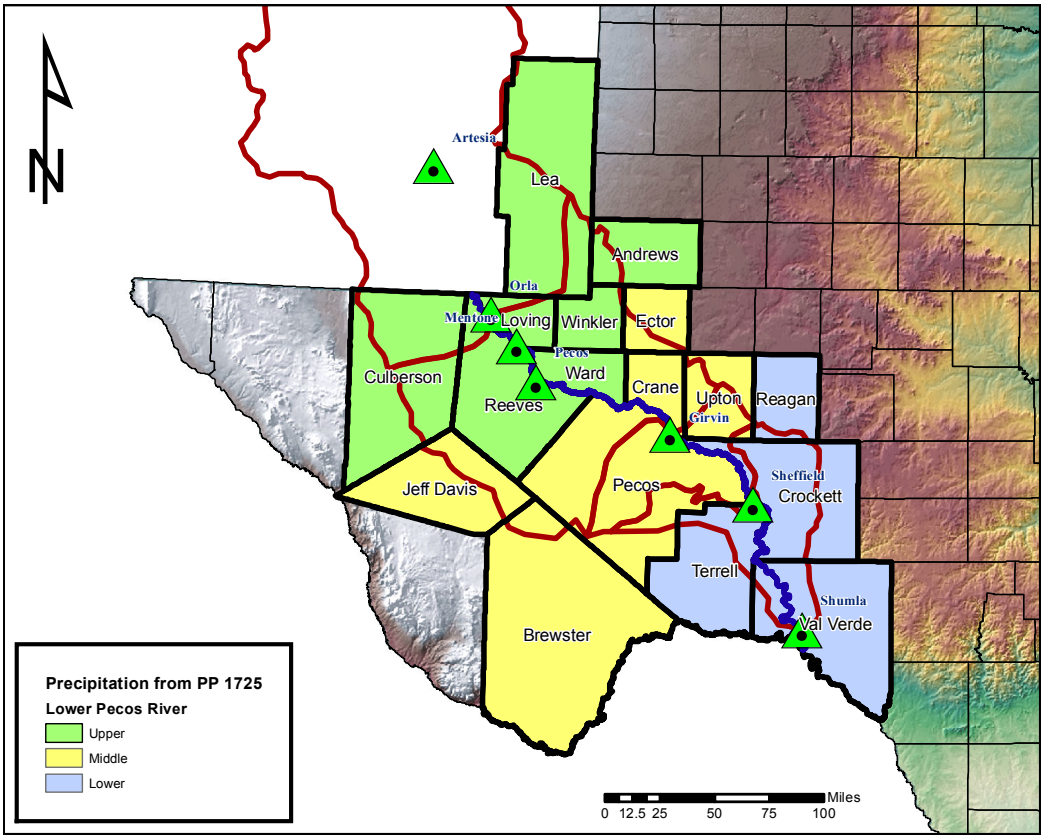


**Figure 4.9.** Map of counties classified as contributing to the upper, middle and lower contributing reaches of the Pecos River in Texas. Data from these counties, grouped by reach, is plotted on Figure 4.10. The rainfall quantities presented in this map and the associated graph are considered more closely associated with flood generation than is mean annual precipitation (MAP)

or be taken into the ground and be lost to the runoff process. Quantification of the latter of the two normally involves study of the soil within the watershed. Various types of soils allow the entry of water in different quantities and at different rates. Figure 4.11 is a map of soils in the lower Pecos River watershed of Texas. The areas contributing above Girvin are composed of a relatively normal array of soils. However, the areas contributing below Girvin, particularly proximate to Sheffield and Shumla, are dominated by rock outcrops. It is intuitive to conclude that rock outcrops, with very little and very thin soils, would be highly impervious and thus very productive of runoff. However, such a conclusion would be premature.

Asquith and Roussel (2007) found, in a study for a loss model to be used in unit hydrograph modeling, that runoff from rock areas is less than that from areas of soil. In this model, a binary variable of rock/not rock (denoted R in the reference) is used in compu-

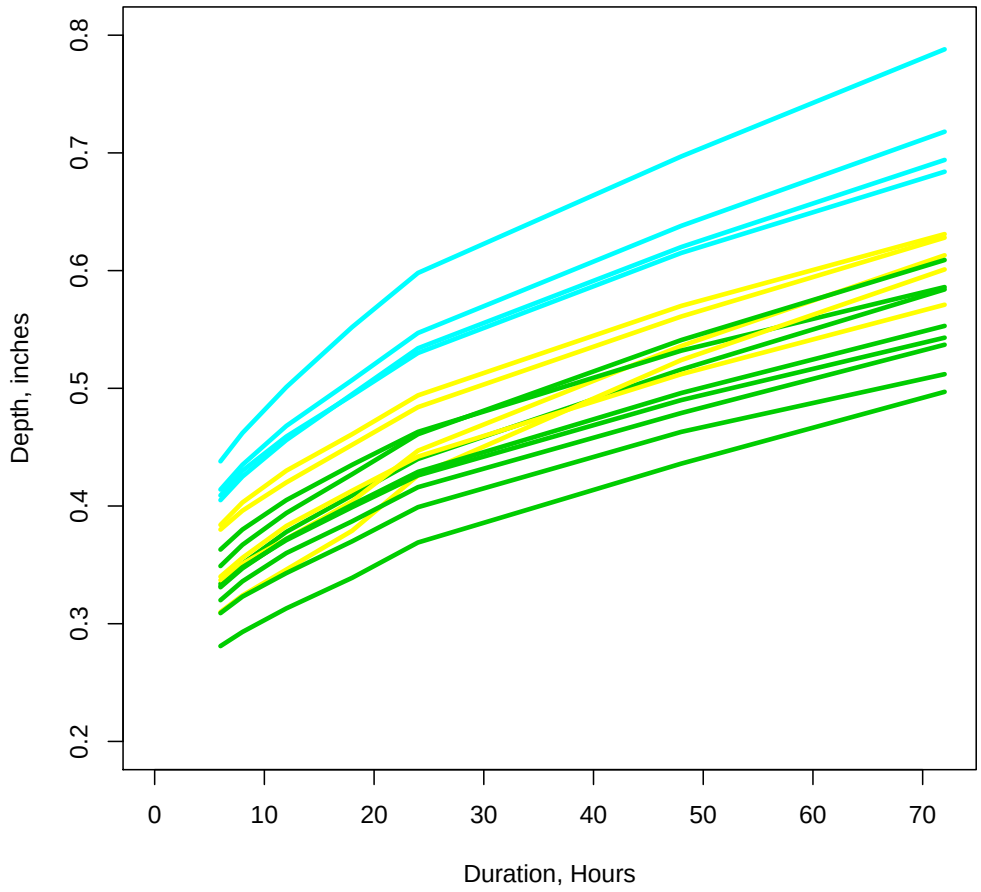


**Figure 4.10.** Graph of mean storm depth from Asquith et al. (2006) for various counties in New Mexico and Texas that contribute in the region under discussion. Green lines contribute to the upper portion, yellow lines to the middle portion and blue lines to the lower portion.

tations by equations (Equations 23 and 29 in the reference) for initial abstraction ($I_A$, a depth of rainfall accumulation prior to which no runoff occurs), and constant loss rate ($C_L$), respectively. The following is a quotation from Asquith and Roussel (2007):

> The coefficients on R for $I_A$ and $C_L$ are +0.2414 and +0.2271 watershed inch and watershed inch per hour, respectively. The positive signs mean that rock dominated, thin-soiled watersheds tend to have larger rainfall losses. This observation appears logically consistent with many watersheds in the Austin and San Antonio areas. In general, rock-dominated, thin-soiled,

**Table 4.15.** Table of mean storm depths for interevent durations of 6 hr to 72 hr for the counties in Texas contributing to the Pecos River, as well as Lea County, New Mexico. Each county is designated as contributing to the upper, middle, or lower portion of the river in Texas. Mean storm depth is considered to be more closely associated with flood generation than is MAP.

| County | 6 hr | 8 hr | 12 hr | 18 hr | 24 hr | 48 hr | 72 hr | Cont. Reach |
|---|---|---|---|---|---|---|---|---|
| Andrews | 0.334 | 0.351 | 0.378 | 0.409 | 0.440 | 0.516 | 0.584 | Upper |
| Culberson | 0.281 | 0.293 | 0.313 | 0.339 | 0.369 | 0.436 | 0.497 | Upper |
| Lea (NM) | 0.349 | 0.367 | 0.394 | 0.427 | 0.461 | 0.541 | 0.609 | Upper |
| Loving | 0.320 | 0.336 | 0.360 | 0.387 | 0.416 | 0.479 | 0.537 | Upper |
| Reeves | 0.309 | 0.323 | 0.343 | 0.370 | 0.399 | 0.463 | 0.512 | Upper |
| Ward | 0.332 | 0.348 | 0.371 | 0.399 | 0.426 | 0.490 | 0.543 | Upper |
| Winkler | 0.331 | 0.347 | 0.372 | 0.401 | 0.429 | 0.496 | 0.553 | Upper |
| Brewster | 0.337 | 0.351 | 0.372 | 0.404 | 0.447 | 0.536 | 0.613 | Middle |
| Crane | 0.363 | 0.380 | 0.405 | 0.435 | 0.463 | 0.532 | 0.586 | Middle |
| Ector | 0.340 | 0.356 | 0.383 | 0.413 | 0.442 | 0.512 | 0.571 | Middle |
| Jeff Davis | 0.310 | 0.324 | 0.346 | 0.379 | 0.426 | 0.524 | 0.601 | Middle |
| Pecos | 0.380 | 0.396 | 0.420 | 0.452 | 0.484 | 0.561 | 0.628 | Middle |
| Upton | 0.384 | 0.403 | 0.430 | 0.461 | 0.494 | 0.570 | 0.631 | Middle |
| Crockett | 0.414 | 0.435 | 0.468 | 0.507 | 0.547 | 0.638 | 0.718 | Lower |
| Reagan | 0.409 | 0.430 | 0.459 | 0.494 | 0.530 | 0.615 | 0.684 | Lower |
| Terrell | 0.405 | 0.425 | 0.456 | 0.495 | 0.534 | 0.620 | 0.694 | Lower |
| Val Verde | 0.438 | 0.462 | 0.501 | 0.552 | 0.598 | 0.697 | 0.788 | Lower |

karst watersheds represented by R = 1 in the database have about 1/4-inch larger $I_A$ or 1/4-inch per hour larger $C_L$ than other watersheds.

The observations in Asquith and Roussel (2007) contradict the assumption of increased runoff from rock outcrops with thin soil. The inconsistency between theory and observation is explained by detailed observation of the medium under discussion. Figures 4.12–4.14, depict features found in roadway cut sections through limestone in areas of the Edwards Plateau of Texas, similar in nature to the rock in the Pecos River watershed below Sheffield. Figures 4.15 and 4.16 show preferential flow paths in alluvium deposits in the same geographical region.

Figure 4.12 was taken within a few weeks of the widening of an existing rock cut on US Highway 83 (US 83) in Real County near Leakey, Texas. The funnel-shaped fracture and accompanying void in the limestone bears evidence of regular inflow of water by way of the presence of mud throughout the depth of the funnel, ending in a large void that continues downward out of sight. No evidence of this feature appeared in the land surface other than

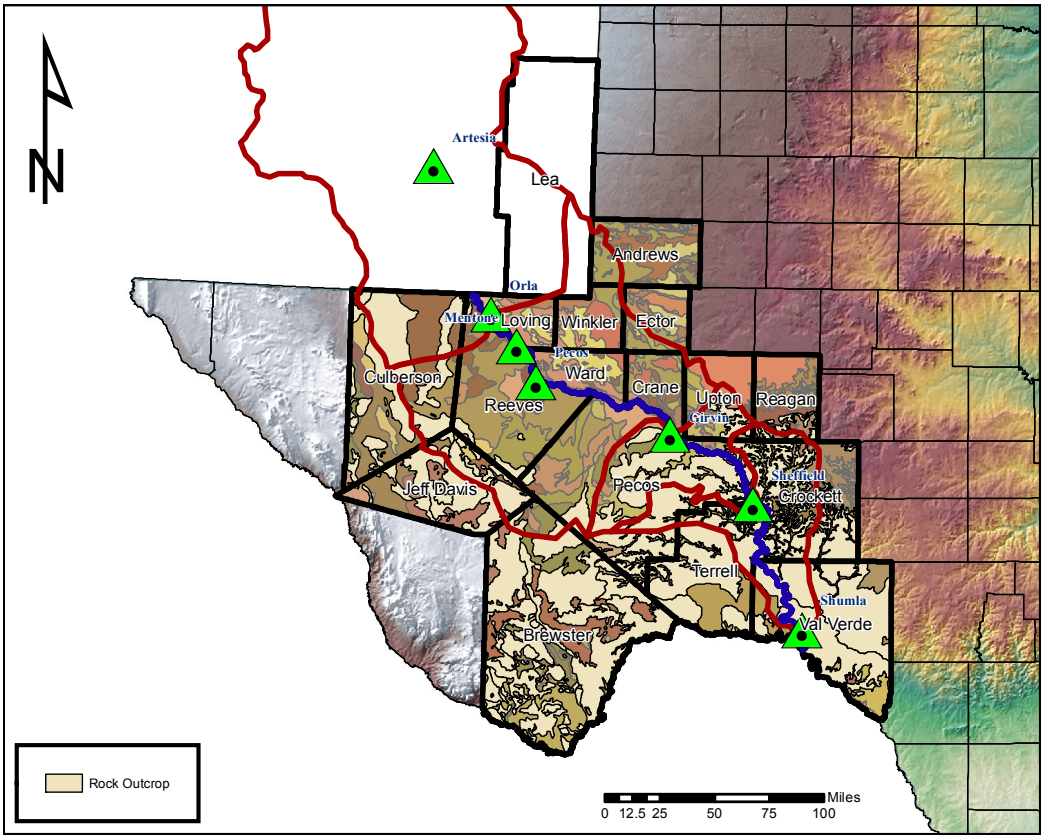


**Figure 4.11.** Soil Map of the Lower Pecos Watershed. Note that the areas contributing proximate to the Sheffield and Shumla gauges are dominated by rock outcrops. Above Sheffield, rock outcrops are less prevalent.

a slight depression and slight difference in vegetation. Numerous similar structures were revealed nearby in the same manner.

Figure 4.13 illustrates a pipe-like feature entering limestone from the surface in an existing rock cut on US 277 in Schleicher County, Texas. This feature was evident from the land surface. Evidence of large-scale entry of water is mud and debris accumulation along the length of the feature until it joins with a larger fracture. This feature had been exposed for 20+ years at the time of the photograph. This is one of many such features evident in rock cuts along US 277 in the area.

Figure 4.14 illustrates numerous pipe–like features entering along the top surface of limestone from the surface in an existing rock cut on US 277 in Schleicher County, Texas. Many of them follow a characteristic angle downward from the surface, possibly an artifact of a particular weathering mode of the limestone. Near the center of the photograph is a vertical feature that shows considerable evidence of large-scale entry of water by discoloration and

**Figure 4.12.** Photograph of feature in limestone showing obvious signs of large-scale water intake. Photograph taken by the author on US 83 in Real County, Texas.

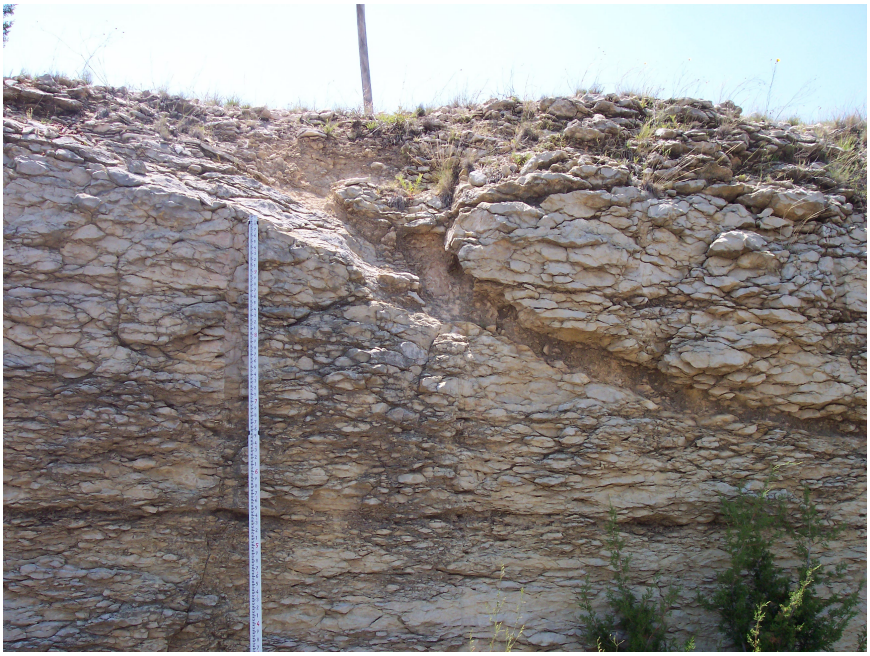

**Figure 4.13.** Photograph of feature in limestone showing obvious signs of large-scale water intake. Photograph taken by the author on US 277 in Schleicher County, Texas.

obvious weathering along the course of the feature. These features had been exposed for 20+ years at the time of the photograph. Features evident in rock cuts along US 277 in the area abound.

**Figure 4.14.** Photograph of feature in limestone showing obvious signs of large-scale water intake. Photograph taken by the author, US 277 in Schleicher County, Texas.

Figures 4.15 documents preferential flow paths in alluvium deposits in a mechanically made bank cut near a residential subdivision in southwest San Angelo, Tom Green County, Texas. These features were not evident from the land surface. They appear to have originated as tension cracks in alluvial deposits, through which water has entered the ground. Calcareous mineralization indicates that these flow paths have existed for an extended period of time, and have served as flow paths for much of that time. Alluvial deposits like that shown in the photographs are characteristic features in the rock outcrop areas of the Edwards Plateau and nearby regions of Texas. Figure 4.16 is a closer photograph of the features shown in 4.15, with a measuring device included to provide scale.

The purpose of the discussion of rock outcrops and inflow features is to demonstrate that, in spite of the intuitive assumption that runoff would increase under such conditions, it does not. In fact, runoff has been shown by Asquith and Roussel (2007) to be reduced in such areas relative to areas with substantial soil structure. Features such as those shown in Figures 4.12–4.16 provide an answer to the question of why this counterintuitive result

**Figure 4.15.** Photograph of a preferential flow feature in alluvium showing obvious signs of large-scale water intake over time. Photograph taken by the author, Tom Green County, Texas.

**Figure 4.16.** [Photograph of a preferential flow feature in alluvium showing obvious signs of large-scale water intake over time, Tom Green County, Texas.

would be true. The series of photographs shown illustrates both the need for metrics and the challenges of hydrologic modeling in an arid climate on rocky terrain. The intake and preferential flow features in the photographs are likely undetectable by current remote sensing technology. Furthermore, how to weight their contribution in a loss model is challenging.

Evidence presented in Asquith and Roussel (2007) and in the photographs herein contradict any contention that the prevalence of rock outcrops in the area contributing proximate to the Sheffield and Shumla gauges is an explanation for the dramatically higher discharges observed at the gauges located at those places as compared to those upstream.

### 4.5.7 Ruggedness and Rugged Terrain

Mean annual rainfall does, indeed, increase as the Pecos River traverses west Texas from northwest to southeast (Figure 4.8), but the amount by which it increases results in a small increase in runoff potential. Likewise, surface condition represented by soil or rock outcrop changes from soil to rock along the way, but it has been demonstrated that the nature of rock outcrop surface in the Edwards Plateau of Texas results in an overall decrease in runoff as compared to areas with significant soil structure. The purpose of the preceding discussions on rainfall and rock outcrops has been to answer speculation that either or both of those conditions explain the increase in discharge observed at the Sheffield and Shumla gauges. The increase observed at the Shumla gauge is substantial; the area between Girvin and Shumla is about 14 times more productive of peak discharge than the area that contributes to Girvin. Some property other than rainfall and surface condition must exert a profound influence on runoff production. The remaining factor is topography, particularly in the form of topographic ruggedness.

Along with the idea of inverse distance influence is the idea of terrain ruggedness. Landforms and the influence of landforms on hydrology are discussed in Sposito (1998) in considerable detail, without mentioning ruggedness by name. The work is oriented more toward scaling laws on landscapes than on metrics of relief. There is mention of the use of Geographical Information Systems (GIS) technology, including Digital Elevation Models (DEMs), in the analysis of landforms.

Riley et al. (1999), proposed a "Terrain Ruggedness Index" (TRI) derived by GIS from DEMs. That TRI had been developed on DEMs circa late 1990s of very coarse resolution. The included script was written in a form no longer compatible with modern systems. Cooley (2013) maintains a website called *GIS 4 Geomorphology* (URL

http://gis4geomorphology.com/), which describes 12 ways of measuring "Terrain Roughness." Of the 12 methods shown, some are claimed to be independent of scale. GIS holds great potential for the solution of problems such as terrain ruggedness; however the worldwide inconsistency of DEM cell size suggests that metrics of ruggedness derived by GIS techniques should independent of cell size in order to be universally comparable.

A technique comparing ranges of elevation difference in moving 5 cell by 5 cell windows on a 1-arc-second (commonly called 30 meter) grid cell size was explored for this paper—an adaptation of existing TRI technology. Results were still heavily dependent on cell size. The subject of a metric of terrain ruggedness is meaningful, and will be examined in more detail in wection 4.5.8.

### 4.5.8 Terrain Ruggedness Metrics

In the case of the lower Pecos River, the topography above Red Bluff Reservoir is that of the western Great Plains and the outwash plains of the Rocky Mountains. Whereas the headwaters of the Pecos are high in the Rockies of northern New Mexico, the river travels a great distance south along the plains of eastern New Mexico. As it approaches Texas, traverses Red Bluff Reservoir, and continues, the topography along and adjacent to the river is low rolling hills, with a moderate valley walls along a wide valley developed along the river itself. Agriculture along the river valley and nearby indicates substantial soil structure is present along most of this reach. The slow diminution of discharges as the stream proceeds south can be thought of as the influence of proximate terrain; in this case, the terrain draining between streamgauges is relatively gentle, shallow rolling plains terrain. If an analogy to sound is made, terrain with great ruggedness can be thought of as "loud," whereas gentle terrain can be thought of as "quiet;" the terrain above Red Bluff Reservoir is rather quiet by analogy. After passing Girvin, the terrain gradually begins to increase in ruggedness. Once reaching Sheffield, it is entering the northwest part of the massive limestone of the western edge of the Edwards Plateau.

The streamgauge at Sheffield shows a distinct increase in flood magnitude over that at Girvin. Downstream from Girvin, as Sheffield is approached, the character of the topography changes dramatically, from gently rolling hills to deeply incised canyon country with hundreds of feet of relief and thin or non-existent soil. The Pecos River traverses the transition between the Edwards Plateau and areas known as the Big Bend and the Trans-Pecos Mountain and Basin region of the state. The river has carved for itself a deep canyon

through massive limestone. The terrain in this area presented a substantial impediment to the construction of the Southern Pacific Railroad in the late 19th century. Initially, a tortuous route including two long tunnels was constructed to cross the Pecos River near river level at the confluence with the Rio Grande (local lore and firsthand observation of the abandoned route called the "loop line"). A second railroad bridge carrying the Southern Pacific across the Pecos was built in 1894 several miles upstream, and at 321 feet was the highest bridge in North America for decades.

Figure 4.17 is a map of the Pecos watershed in Texas. This map was the result of an exploratory study of terrain ruggedness conducted for this region, investigating GIS spatial analysis techniques. Overlaid on county data is the previous subarea map. A spatial analysis technique called "Focal Statistics" was used in this analysis. A statistic called "range" was the most enlightening of the standard tools available. The size and shape of the "neighborhood" to be used in computation of each cell value of the output raster can be specified, numerous sizes of regular quadrilaterals (squares) were tried. A $5 \times 5$ grid cell rectangle produced informative results. In essence, the output is the difference between the lowest and highest of 25 cells and that value is placed in the center cell of the grid to constitute the output raster. For presentation, these values were classified into five quantile groups, each containing 20 percent of the values. In that way, areas with different classes of change in elevation among 25 cells ($150 \times 150$ meters) can be visualized by color. This statistic appears to be informative, but it is dependent on the grid cell size of the DEM raster used; it should not be considered for general use because DEMs of the same resolution are not universally available worldwide. The raster data used was 1-arc-second (commonly referred to as 30 meter) resolution.

Geographically, tributary streams draining the surrounding area fall hundreds of feet in a few dozen miles. Soil structure is minimal, consisting mostly of rocky alluvium and colluvium. The river runs along the transition between upper and lower Chihuahuan Desert terrain, with the characteristic vegetation from both desert regions being sparse. Sparse vegetation, sparse soil, exposed rock, and high topographic ruggedness combine to present a terrain that produces rapid runoff.

In the case of the lower Pecos River, the flood series is decoupled in magnitude between gauges. What is seen to occur above some point is substantially obliterated by what occurs below that point. In effect one watershed dies and another is born from a statistical point of view. While there is no distinct point of change, an argument could be made that, for flood hydrology, the Pecos River below Girvin becomes a different stream entirely from that above Girvin.

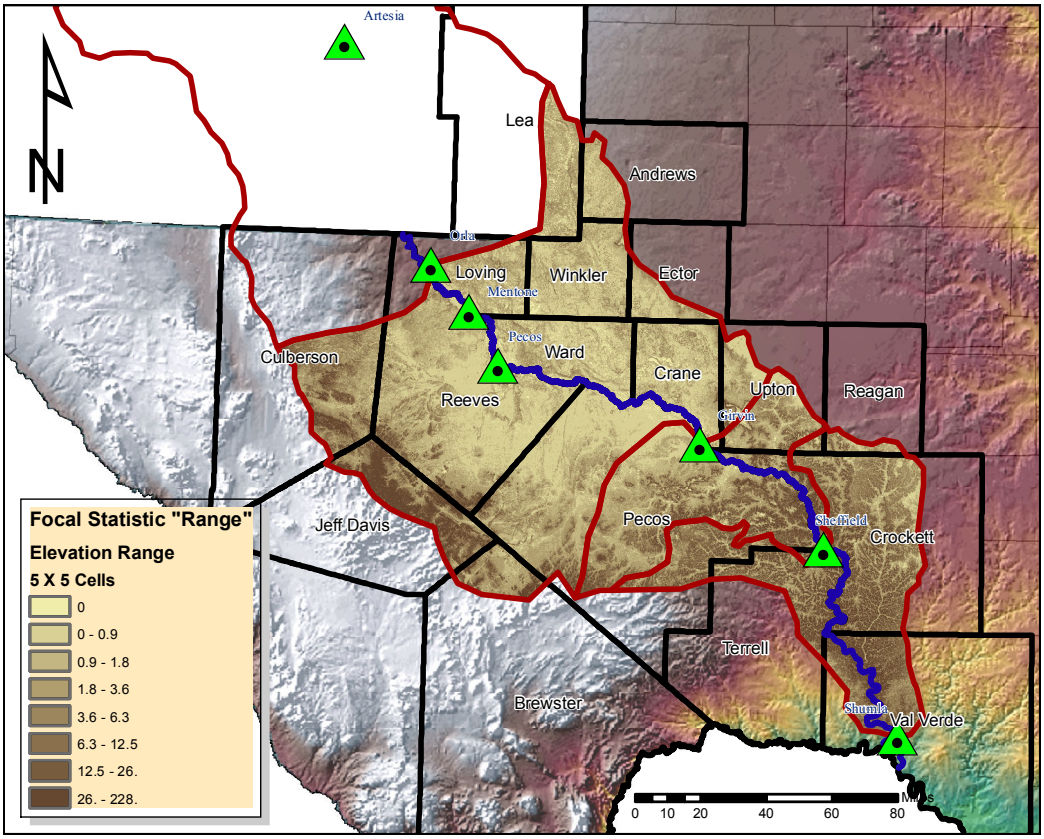


**Figure 4.17.** Map of the counties comprising the bulk of the Pecos River watershed in Texas. Shading represents the range in elevation of each 150m x 150m set of 25 grid cells in a DEM. Not the difference in range between the area contributing to the streamgauge at Girvin between Orla and Girvin compared to that contributing between Sheffield and Shumla.

## 4.6 Discussion

The case in point has been shown for several, related reasons. This case is an example of the influence of partial, proximate area on flood magnitude; demonstrates the influence of rugged terrain on flood magnitude; and demonstrates that the combination of proximity and ruggedness can dominate a flood series to such a degree that the appearance is of the emergence of an entirely different stream from one observed upstream. The example shown possesses a large watershed, where uniformity of rainfall over the entire watershed would never be expected. However, no assumption of uniformity is needed or appropriate; the flood series stand for themselves. In order to further document this phenomenon, a large watershed with multiple streamgauges facilitates recognition of anomalous behavior, as it possesses dramatic difference in terrain that is unlikely on a small watershed. Again, the

idea of both ruggedness of terrain and proximity exerting influence on runoff generation are independent of watershed size; yet relatively large size is a practical asset to observation.

The likelihood of encountering watersheds where the character of terrain changes radically in the downstream direction increases as the size of watersheds under consideration increases. This fact should not imply that partial area contribution or terrain ruggedness is only a concern in large watershed hydrology. The case studied is illustrative because of otherwise inexplicable changes in annual peak flood series, but credibility of the idea that both proximity and ruggedness of terrain exert great influence on flood magnitude is shown by in terms of real data. The common, general watershed form is for a stream to begin in relatively severe terrain at the headwaters, and for terrain adjacent to the stream and draining into it to become gentler with downstream progress (Heitmuller, 2009; Huggett, 2007; Bull and Kirkby, 2002).

Returning to the analogy previously made to sound, the Pecos River at Girvin can be thought of as flowing through a quiet environment. Loud sounds from upstream are audible as flood waves, and become less audible as they proceed downstream, even without locally generated sound to obscure them. At Sheffield on the Pecos River, some locally generated sound is heard, and sound from far away is nearly inaudible. At Shumla on the Pecos River, very loud sound produced locally drowns out almost all sound from far away.

The data used for this simple investigation are annual peak discharge values. Comparing the dates of annual peak can give some sense of association or dissociation; if they occur close in time, they may be associated, at least through the occurrence of a common weather system. Comparison of dates was performed for data used in these analyses and reported in detail in Subsection 4.5.2. In this case study, it appears that the assumption that peak discharges observed at an upstream streamgauge are transmitted downstream and should be seen at a downstream streamgauge is not supported. The explanation of why annual peak discharge recorded in a common year can be dramatically larger a relatively short distance downstream, and without close temporal association, is that the downstream peak discharge was generated in the portion of the watershed that contributes in the intervening distance. If streamgauges consistently show a dramatic difference, as between Girvin and Shumla, that intervening area must be seen to be unusually productive of runoff, relative to that contributing to the upstream streamgauge, even if the area contributing in the intervening distance is a small fraction of the total area contributing to the downstream streamgauge.

## 4.7 Observations and Conclusions

### 4.7.1 Observations

One very common technique for peak discharge estimation is the use of regional regression equations. In the United States, these equations are normally developed by U.S. Geological Survey personnel (Asquith and Slade, 1997; Asquith and Thompson, 2008; Asquith and Roussel, 2009). Survey personnel possess both the data and expertise to perform these regression analyses. A ubiquitous explanatory variable in regional regression equations is stream slope. The USGS and others have various definitions of slope, and the method of measurement has varied over time. In general, the slope used is the channel slope along the main channel, upstream of the point of interest. In the example shown, that slope would be very small; slope shown in Asquith and Slade (1997) is 4.09 feet per mile, or 0.00077 feet per foot, and would likely appear poorly related to observed peak discharge at those points. From the point of view of the apparent local origin of peak flows in the kind of terrain present, some type of local topographic slope, possibly slope up a tributary, would be more closely related to discharge at the gauges in question. In most cases, slope is the only topographic variable in the equations that influences time. In cases such as those shown, the slope of the main stream poorly represents the surrounding terrain; the utility of the equations may benefit from some additional morphologic metric that can capture the ruggedness of the terrain.

### 4.7.2 Conclusions

Evidence was presented in Subsection 4.5.5 that differences in rainfall between the areas contributing proximate to the Sheffield and Shumla gauges exist, but exert insufficient influence to account for the dramatic increase in discharge at those gauges compared to those upstream. Also, evidence was presented in Subsection 4.5.6 that the existence of rock outcrops in the areas contributing proximate to the Sheffield and Shumla gauges should exert an influence counter to the dramatic increase observed.

The evidence presented in this case study supports the partial area and variable area concepts. At some streamgauges, the area contributing appears to be much smaller by inference (Table 4.14) than the topographic watershed. Temporally dissociated peak discharges as discussed in Subsection 4.5.2 and magnitude dissociated annual peaks as discussed in

Subsection 4.5.3 support a conjecture of partial area contribution local to a gauge site rather than system-wide responses being the source of annual peak discharges. The conclusion is that that flood discharges at any point of interest are very likely the result of local influence, and subject to the subtleties of local topography.

The evidence presented also supports the idea that topographic ruggedness is an important quality in the production of flood discharge, particularly when rugged terrain is located hydrologically proximate to a point of interest. A conclusion from this case study is that a subset of area, contributing proximate to a point of interest such as a streamgauge, can and occasionally does dominate the behavior of the stream at that point, even if the area in question is a small fraction of the total contributing area. The effect of distal areas of the watershed is supressed with respect to the statistical character of the stream. Ultimately, examining, measuring, and quantifying the geomorphologic properties of a watershed is indispensible in hydrologic modeling of that watershed.

A metric of terrain ruggedness or roughness that is dimensionless, or at least not dependent on raster grid cell size, is necessary. A search of literature reflecting such a metric that is generally accepted was unsuccessful; some prior work was identified, but dependence on grid cell size rendered it unsuitable for this project. A practical complication of this idea is that metrics depending on areal properties are difficult to compute without the use of GIS, and may be dependent on size and shape of the area measured. An in-depth quest for this metric is a recommended future research topic.

Considerable use was made of inference encapsulated in regression equations developed by USGS personnel. It is possible that, upon the development of a ruggedness metric as recommended, the regression analysis done previously might be revisited to include the influence of local topography.

It is anecdotally accepted in hydrology (House et al., 2001) that in a qualitative sense, rugged terrain results in more rapid runoff and larger flood peak generation than does more gentle terrain. In that context, this paper demonstrates that commonly accepted axiom. The degree to which ruggedness affects flood generation is emphasized. However, whether or not ruggedness is adequately reflected in the processes and parameters used in watershed modeling and flood prediction is not readily apparent and is probably ignored in most applications.

Based on 25 years of experience using, training, and reviewing hydrologic modeling in the profession, the author concluded that hydrologic modeling often is done by analysts who have little or no knowledge of geomorphology and with little “on site” knowledge of the watershed being modeled. Nothing prevents someone from sitting in an office and

developing watershed characteristics and model parameters remotely, and constructing and operating a computer model; in fact, such practice is typical. However, there are many instances where departure from the expected behavior would result in vast differences between expected and observed flood frequency characteristics. An open question with respect to the training of users of modeling technology is how to train them to look for and recognize situations that may contradict expectations, and what to do when those situations are encountered.

Traditionally, those who are likely to have need to do hydrologic modeling and estimation for engineering works are unlikely to have more than an introductory knowledge of watershed geomorphology. However, at least in some cases, as illustrated in this study, geomorphology and hydrology are tightly coupled and inseparable. Future training and education in hydrology would benefit from increased emphasis on geomorphology and other field sciences.

# Chapter 5

# A Probabilistically Based Alternative to UH Watershed Modeling

## 5.1 Prologue

This chapter is the original work of the author and concerns the idea of a watershed model that, rather than assuming uniform contribution of rainfall to runoff from the entire watershed, assumes that the survival of water is a random, time-dependent variable. This conceptualization weights influence inversely with distance is a natural outgrowth of extensive experience with the hydrology of arid watersheds. Traditional modeling methods assume that runoff occurs only after the application of loss models to gross rainfall. It is implied that gross rainfall can be neatly parsed into lost rainfall and rainfall that results in runoff. Traditional methods are based on the rhetorical question: Given that rainfall occurs, how much of it is taken away by loss processes? What is not taken away by loss processes is considered to be runoff. Examining streamflow data from arid small watersheds typically shows far fewer runoff events than rainfall events. The conclusion that follows from such an observation is that the production of runoff cannot be assumed in all, or even a majority, of rainfall events. Rather than the rhetorical question above, arid lands support an alternate rhetorical question: Given that rainfall occurs, what conditions might allow it to run off rather than be lost? The philosophical difference lies in what is expected: Is runoff the expected result of rainfall, or is it the exceptional result of rainfall?

The logical exercise above leads directly to the issue of survival. It is serendipitous that the idea of survival versus loss also leads us to a model that weights area inversely with distance, through travel time. It seems that such weighting ties in well with the influence of proximate terrain discussed in the previous chapter.

## 5.2 Chapter Abstract

This chapter discusses conventional unit hydrograph (UH) modeling and the basic assumptions behind it, discusses the ideas of partial area contribution and of residence time distribution, and then presents an alternative method of watershed modeling. The alternative method is based on the concept that the survival of a raindrop to traverse the watershed and exit is a random variable. This model replaces the UH watershed response relationship and loss model with a time-area relationship, randomly generated variates from a probability distribution, and compares variate magnitude to the magnitude of time/distance needed to exit the watershed. A conceptual study demonstrates the technique, and case studies demonstrates that it can reasonably represent real rainfall-runoff data.

## 5.3 Introduction

The modeling of direct runoff from short-duration rainfall events is a key tool in practical hydrology. The modeling process is normally accomplished by of basic UH theory introduced by Sherman (1932) and Horton (1933), and refined over ensuing decades by Clarke (1945); Nash (1957, 1959); Dooge (1959); Eagleson et al. (1966); Dooge and Bruen (1989); Asquith et al. (2005) and many others. In its simplest form, UH theory consists of three parts: a temporal rainfall distribution (hyetograph), a loss model, and a representation of basin response, which is known as the unit hydrograph. It is called a "unit" hydrograph because it is scaled to represent the runoff produced by one unit depth of effective rainfall over the entire watershed.

The hyetograph (Williams-Sather et al., 2004) is used to simulate the temporal distribution of a specified amount of conceptual "gross rainfall," whereas the "loss model" reduces that conceptual rainfall by removing water from it according to some simulated physical process that is thought to represent actual losses attributable to a multitude of real processes, the largest of which is usually thought to be the infiltration of rainwater into the surface of the watershed.

Decades of work have gone into UH method development. Great effort has been spent in developing intricate models, and on engineering works that rely on those models. Despite the importance of UH modeling in support of engineering design, there are few modeling toolsets where all three of those parts were developed concurrently and tuned to work as a set; most models are assembled from component parts that were developed as independent

of one another as separate components. An exception to the component part paradigm is the integrated process developed for the U.S. Soil Conservation Service (SCS) (USDA-SCS, 1972). Although the SCS method is very popular and is possibly the most commonly used method, questions regarding the appropriateness of the method for general use and the effect of many compromises that were made in its development remain unresolved. The SCS method (now called the NRCS method) is used as frequently as it is, and is regularly implemented by many practicing hydrologists, simply because it is the only widely known, complete modeling toolset available. Nevertheless, many rainfall-runoff models for design storm computation are assembled from various parts that are theoretically based, or based on limited data from specific geographical areas. The parts used to assemble these models are invariably highly idealized and are based on gross simplifications and generalizations of what are known to be very complex processes, such as the conversion of rainfall into runoff, or the subsequent transport (routing) of that runoff.

## 5.4 A Brief Review of Unit Hydrograph Theory

A UH (Sherman, 1932) model consists of three parts: a hyetograph, a loss model, and a unit response model. For the purposes of discussion herein, all references to rainfall, losses, runoff, events, and time will not be to real rainfall-runoff events, but will be assumed purely conceptual. Modeling is a conceptual undertaking. The purpose of articulating this distinction is that the conceptual process can be discussed with certainty and definition, whereas the real process is highly complex and defies simple description, The models under discussion exist because they are practical, abstract simplifications of the real, complex, phenomenon that are difficult or impossible to describe with any degree of fidelity.

### 5.4.1 Hyetograph

In a UH model, conceptual rainfall is applied to the loss model according to the hyetograph, typically in multiple pulses (Chow et al., 1988). The loss model divides the conceptual rainfall into two parts; that which is considered "lost" in that it does not run off, and *effective rainfall*, that which is not lost. Early in an event, all of a pulse may be lost. As time progresses, the conceptual loss rate diminishes, the rainfall rate exceeds the loss rate, and effective rainfall, which is considered runoff, appears. Each pulse of effective rainfall is multiplied by the ordinates of the response model, and the ordinates resulting from

sequential pulses are summed at each time interval. The string of the sums of simultaneous ordinates resulting from sequential pulses is considered to be the string of ordinates of a runoff hydrograph.

### 5.4.2 Unit Hydrograph

The response function (UH) is variable in scale with amount of precipitation, but invariant in time (Chow et al., 1988; Viessmann and Lewis, 2003). Each pulse produces a sequence of runoff values proportional to the depth of effective precipitation. This principle of proportionality implies full, uniform, and proportional contribution from all parts of the watershed. Runoff is assumed be produced uniformly across the entire watershed. Runoff that originates in the most distal areas of the watershed is assumed to route along the entire flow path to the point of interest with no further probability of loss. Runoff produced by a unit area of watershed along the watershed boundary is distinguishable from runoff produced by a unit area proximate to the point of interest only by arrival time at the point of interest. Each successive pulse of effective rainfall is treated as a conceptual membrane of thickness equal to the depth of the effective rainfall. The membrane is pulled downstream by gravity to the outlet. The width of the membrane represents the ordinate of the UH at the corresponding time, rather than the shape of the watershed itself. At the next rainfall pulse, another membrane is laid on top of the first one, and begins being pullled downstream simultaneously. In effect, UH theory implies that runoff occurs in a manner analogous to a series of membranes as described. Like a stack of pancakes, each of depth equal to the depth of effective rainfall occurring within a given analytical time step. The UH shape represents the arrival time distribution from such a membrane as the membranes gather and move down gradient.

### 5.4.3 Characteristic Time

Each individual watershed is considered to have a characteristic time. For modeling purposes, characteristic time is normally called “basin lag time,” “time of concentration,” or one of several other time parameters described in hydrology texts (Maidment, 1993; Chow et al., 1988). Characteristic time is associated with the concept of “critical duration of rainfall.” The nature of depth/duration/frequency relationships is outside of the scope of this research. However, for frequency-based prediction for engineering purposes, the concept of critical duration is very important. In normal engineering hydrology, duration of effec-

tive rainfall approximately equal to the characteristic time of the watershed is assumed to produce the maximum watershed response associated with rainfall of a given probability.

## 5.5 Discussion of the Basic Tenets of Unit Hydrograph Theory and Extensions

### 5.5.1 Lumped Models and Uniformity of Response

Runoff being produced uniformly across the entire watershed is a dramatic simplification of reality. The idea results in the concept of effective rainfall, which is rainfall that is either lost uniformly across the watershed, or produces runoff uniformly across the watershed. The same idea also results in the concept of lumped parameter modeling, i.e. that differences in the uptake of rainfall into soil and rock, however it is represented by the loss model, can be averaged across the watershed and a single set of parameters used. Such simplified ideas warrant close scrutiny when real watersheds with real rainfall and real runoff are discussed. For these simplifications to mimic reality with any fidelity, several other things must also be true as well; topography of the watershed, soil and rock, vegetation, and land use must be reasonably uniform across the entire watershed for loss to be uniform across the watershed. In addition to watershed properties, rainfall must also be spatially uniform. In general, uniformity of the kind implied as being necessary is inconsistent with our knowledge and observation of real watershed properties.

### 5.5.2 Distributed Models

In contrast to the areally averaged values used in lumped parameter modeling is that of distributed modeling. In distributed modeling, the watershed is divided into small sub-elements, and each division is treated discretely (Maidment, 1993; Chow et al., 1988). Parameters for runoff generation and timing are estimated for each element, along with the timing of transmission of runoff produced by that element to the point of interest. Runoff is aggregated at the point of interest to produce a hydrograph. Subdivision of the watershed may take place by topographically guided subwatershed delineation, or by arbitrary gridded discretization of the watershed. Distributed modeling is thought by many modelers to more accurately represent the areal variation of runoff production within a watershed.

Pappenberger and Beven (2006) describe "types" of modelers; "modeler type 0" believes that the model is physically correct and that the system is thus fully determined. Distributed modeling is consistent with the"modeler type 0"; the attempt is being made to fully determine the physics of watershed behavior. Fang et al. (2005) demonstrated that topographic subdivision of watersheds for analysis increases the ability to represent measured runoff only when the watershed is subdivided into a small number of subwatersheds (less than 10). Subdivision beyond that degree seemingly produces no better results, and sometimes degrades results.

### 5.5.3 Partial Area and Variable Area Concepts

Betson (1964) first described partial area contribution, the idea that the entire watershed *as defined topographically* does not contribute to all, or any, runoff event other than possibly the most extreme. Betson's suppositions were based on the failure of a rigorous mathematical procedure to adequately reflect measured runoff. Betson (1964) surmised that only a portion of the topographically defined watershed was actually contributing runoff. Much work followed on the partial area subject, including experimental watershed studies that attempted to measure actual contributing area during real and simulated events. Ragan (1968) selected a small watershed in Vermont for detailed instrumentation and study. Results of the study indicated that most of the runoff seen originated in specific areas, proximate to (within 35 feet) the stream. Little or no overland flow was observed and Ragan concluded that rainfall directly on the channel and porous media flow in the lower layers of forest litter were among the important mechanisms of runoff for this small watershed.

Dunne and Black (1970), conducted a study, also in Vermont, to test contentions by Kirkby and Chorley (1967) that shallow, subsurface flow (throughflow) was a major contributor to flood hydrographs. The results of Dunne and Black indicate that hillslope overland flow accounts largely for observed runoff, and that a small portion of the watershed produces runoff, in general agreement with Betson's hypotheses. Hortonian flow, an often discussed mode of runoff, was not observed to occur. Dunne and Black concluded that, in the Vermont watershed studied, runoff was produced by small, saturated, marshy areas nearby to streams, and as overland flow. The remainder of the watershed stores water to be released as baseflow.

Amerman (1965) concluded from study of Ohio small watersheds that runoff producing areas were located randomly about the watershed, and observed that even thr runoff-

producing areas did not necessarily contribute to the perennial stream by connected surface flow, i.e. that runoff may infiltrate into a subsequent area that it reaches as "run on." Beven and Kirkby (1979) describe a model intended for use in humid, vegetated environments that accounts for variable partial area contribution, based on topography, soil, and vegetation.

Partial contributing area model concepts are well documented in the literature (Betson, 1964; Amerman, 1965; Hewlett and Hibbert, 1967; Ragan, 1968; Kirkby and Chorley, 1967; Dunne and Black, 1970; Beven and Kirkby, 1979; Engman, 1974). The researchers published on it predominantly focus on physically identifiable heterogeneity within the watershed, such as soil, land use, or topography. All still either explicitly or implicitly allude to the concept that effective rainfall can be conceptually separated from lost rainfall. Areas that do contribute are assumed to contribute uniformly, or in a way identifiable by physical differences. In this way, the focus has been on identification of the contributing areas, or in the case of variable areas, those likely to contribute under specific conditions. Taking the integrated standpoint specified in Section 5.6 and in Botter et al. (2011), for a hydrograph, parsimony dictates that if the identification and delineation of contributing areas can be avoided, nothing is lost. This dissertation will make a distinction between the *topographic watershed*, which can be identified on a map and has been used as the watershed area in traditional analysis, and the *hydrologic watershed*, which actually contributes under modeled conditions.

A common theme among these works of the 1960s and 1970s is the idea that partial area contribution is the dominant watershed runoff-producing mode. Many concluded that actual contributing area is not only partial, but variable (Hewlett and Hibbert, 1967; Ragan, 1968; Dunne and Black, 1970; Engman, 1974). The partial area contribution concept contrasts with the fully contributing, lumped watershed model represented by traditional UH theory, both with respect to area and with respect to characteristic time. The bulk of the studies done on partial area contribution using measured watershed data have revolved around identifying contributing areas, characterizing the mode of runoff, noting the physical attributes or properties that allow them to generate runoff, and delineating runoff producing areas. Many studies reached different conclusions with respect to the dominant transport process: infiltration excess, saturation excess, or throughflow. Some were unable to identify the flow mechanism.

The primary difficulty of modeling partial area contribution lies in defining or delineating the actual contributing area. Research did not *in general* agree with respect to dominant processes, modes of contribution, or important physical attributes. Most studies based on physical data did agree that saturated areas proximate to the stream, and the stream surface

itself, were important contributing areas (Ragan, 1968; Dunne and Black, 1970). Lumped watershed modeling requires that contributing area be delineable by some physical characteristic. Unfortunately, no such characteristic has been discovered that allows reliable delineation of partial contributing area (Van De Griend and Engman, 1985). Engman and Rogowski (1974) presented a model for a variable contributing area based on infiltration curves and rainfall curves. This model mapped the watershed to a simple geometry, then advanced the boundary of contributing area up the conceptual watershed using differences between accumulated precipitation and predicted infiltration.

During the 1960s and 1970, the time of high interest in partial area contribution, digital computers were primarily devices of research computation, although their utility was recognized and their use was increasing (IASH, 1969). In the past 25 years, computers and computational capacity have become ubiquitous in the sciences and in society. The availability of computation has led to a proliferation in interest in and use of distributed modeling, as it is computationally intensive. Distributed modeling has been presented as being adaptable to partial area modeling (Lee and Huang, 2013). By dividing the watershed into pieces and treating each piece individually, areas with different physical properties such as soil texture, topography, land use or cover, connection to the stream, proximity to the stream, and so forth, can be subject to individual computation. In theory, this allows contribution by each subarea to be proportional to the ratio of losses to rainfall simulated by loss and rainfall process models. In theory, the model is parameterized for each subarea with appropriate values. The assumption that distributed modeling will adequately represent partial area contribution is another expression of the "modeler type 0" as in Pappenberger and Beven (2006). Lee and Huang (2013) described a "semi-distributed" model to describe partial area contribution, postulating a relation between contributing area and "current precipitation index" (Smakhtin and Massey, 2000). The "semi-distributed" model was proposed to reduce the complexity of a fully distributed gridded model. Lee and Huang state that:

> ... a well-established distributed, physically-based model requires sound integration of many hydrological mechanisms and uses a large amount of on-site observed data for model development and parameters calibration (Lee and Huang, 2013).

This discussion illustrates that the conventional idea of uniform areal contribution ubiquitous in watershed modeling is an incomplete simplification of how real runoff is probably generated on a real watershed. A great deal of work and much literature has been generated based on the idea that only a small fraction of the watershed actually contributes under all by extraordinary conditions (Betson, 1964). Watershed studies (Ragan, 1968; Amerman,

1965; Engman, 1974) supported this contention, but attempts to identify areal properties that consistently produce runoff have been unsuccessful. An alternative idea includes the possibility that the influence of a small differential element of watershed area on the outflow hydrograph is inversely proportional to its distance from the point of interest.

Many of the authors mentioned herein were critical of the methods of their day and advocated for further development in modeling methods that would reflect partial area concepts. The general methods that these researchers critiqued are still in common use today, and are still subject to the same criticisms as they were at the time. Desktop computing capability has eased the computational burden on hydrologists, but the fundamental modeling assumptions have changed little.

### 5.5.4 Discussion of Various Modeling Ideas

Therein lies the largest condemnation of distributed modeling; complexity. Even given that claims of fidelity to physical processes were valid, the level of time, effort, and expertise necessary for their use is impractical for normal engineering computation. Distributed models are primarily tools of hydrologic research. Claims of fidelity in the arena of partial area contribution are not without challenge even by users (Lee and Huang, 2013).

From an overview perspective, watersheds can be said to be excellent process integrators (Thompson, 2001). Water that passes the point of interest has been accumulated from all contributing areas of the watershed, having fallen as rain at varying times from the time it passes the point of interest. No individual drop can be identified as having fallen on a specific area, or having been subject to a specific mode of runoff. At the point of interest, what is relevent is the hydrograph itself. In large part, the hydrograph can be said to be "memoryless" in that it contains no information on the intricacies of the physical processes on the watershed that resulted in the hydrograph. That information is irretreivably lost. Botter et al. (2011) states:

> The travel time PDF (probability density function), in fact, allows a description of how catchments retain and release water and pollutants in response to rainfall forcings, robustly integrating, — without the need to specify, — the spatial heterogeneities of hydrologic and morphologic features.

The same can be said of modeling; information that goes into the model in the form of parameters is lost in the sense that it cannot be retrieved from the hydrograph. If a lumped model with few parameters produces essentially the same hydrograph as a distributed model

with many parameters, neither can be declared better than the other, on the basis of model output. However, if one appeals to the principle of parsimony (Koutsoyiannis, 2009), the simpler, lumped parameter model is preferable. The hydrologic processes being what they are, and the self-smoothing nature of the spatial/temporal integration being what it is, the effort needed to parameterize distributed models is always challenged by parsimony. The same principle applies to the identification and delineation of partial or variable contributing areas. If they can be simulated at the point of interest by a simple model, with fidelity indistinguishable from a complex model, then parsimony dictates that the simple model is preferred. The idea of "accurate representation of physical processes" loses all advantage when viewed from the point of interest.

Distributed modeling aside, the concept of partial area contribution has piqued interest in the hydrologic research community for decades, and it has been stated by many researchers as the likely mechanism of runoff production. Yet, nearly 50 years after Betson introduced it, partial area contribution and its extension known as variable source area contribution have made very little progress in practical application. UH based modeling assuming full watershed contribution is still the norm for rainfall-runoff modeling. Assumptions such as these are inconsistent with what is known about reality, but simplifying and generalizing complex processes is a necessary step in the process of modeling them. Comparing modeling to reality objectively reveals the differences, and that there can be conceptual models other than the currently popular ones. There may even be models that offer advantages over the traditional ones in how they mimic reality with fidelity. One such alternative model is presented here.

## 5.6 A Story of Survival (or not)

Consider the perils faced by a raindrop on its journey downstream. Many possibilities present themselves: the raindrop may adhere to vegetation, it may infiltrate directly into the soil in an upland area, flow into a crack in rock, end up in a small depression from which it can only escape by evaporation or infiltration, or be absorbed into the alluvium in the channel of an ephemeral stream. The drop may travel all the way past the point of interest, or it may make it only partway before vanishing from one fate or another.

Traditionally, when rainfall-watershed interactions are conceptualized, they focus is on soil-water uptake processes that are implied to be point processes. Methods like Horton's and Green-Ampt (Chow et al., 1988) infiltration models are one-dimensional, point concep-

tual models, and are used as if they apply at all points on the watershed. In these models, the difference between the depth of rainfall and the depth of water absorbed into the soil at each discreet point is considered the depth of runoff. The one-dimensional view neglects that a drop that does not infiltrate at the point it lands on the surface does not travel along or above the surface without further interactions. Each drop of runoff leaves its point of impact and travels along the surface in a down gradient direction. In doing so, it crosses an uncountable number of other points, any one of which has the same ability to allow infiltration as the point on which it landed (Amerman, 1965). Wong (2007) discussed the relationship between selected loss models, runoff, and partial area effects on an ideal conceptual rectangular watershed. The effects discussed include those on critical duration of rainfall. Corradini et al. (1998) discussed similar relationships on the hillslope scale, using the idea of run on contributing to saturation of certain areas. Both Wong (2007) and Corradini et al. (1998) use physically based conceptual models of infiltration and runoff in their discussions, yet the idea of distinct separation of effective rainfall from other rainfall is still present.

Almost all loss process models include a component of the total loss that is time-dependent. As time passes, more and more of the rain that fell enters the soil. The rate of loss may diminish with increasing soil saturation, but the total depth absorbed increases. As a necessary consequence of such time-dependent loss processes, the probability of loss is related to the time that a drop resides on the watershed. The drop may travel all the way past the point of interest, or it may make it any fraction of the way there before vanishing from one fate or another. Considering the possibilities, the following can be said with reasonable certainty; the longer the time span that the drop resides on the surface of the watershed, the greater the probability is that it will be lost (conceptually die). Therefore, the longer the drop needs to travel on the watershed to make the journey to the outlet, the smaller is the probability is that it will survive the journey past the point of interest. Conversely, a shorter time of travel to the outlet would correspond to less chance of death. Supporting this assertion is the idea that a time-dependent component to the loss process implies that loss probability is proportional to elapsed time. Assuming a transitive law applies, then from physics it is known that elapsed time during travel is proportional to travel distance.

### 5.6.1 Travel Time and Residence Time

In contrast with traditional analytical techniques, such as discussed in Section 5.4.2 as an analogy to a membrane laid over the watershed, an alternative conceptual model of the

runoff process will be constructed and described. Similar to the concepts in Wong (2007) and Corradini et al. (1998), this model accounts for variation in loss over the watershed. Unlike others found by the author, the model accounts for variation in loss based on the length of time that a drop resides on the watershed (residence time) rather than trying to attribute variation to physical causes.

Because rain impacting on areas far removed from the point of interest must travel farther, that rain is assumed to remain on the watershed for a longer time. Rain impacting closer to the point of interest (outlet) moves past the outlet in less time. Because of losses being time dependent, the probability of loss is inversely proportional to "residence time." The net effect is that the model represents contribution weighted toward area proximate to the point of interest; distal areas contribute a much smaller fraction of the rain that they receive. In this way, a "residence time" approach is consistent with both the partial contributing area and the variable contributing area models discussed herein.

The idea of a residence time distribution is ubiquitous in fields other than hydrology. In particular, in chemical engineering for reactor process design and for testing of reactor vessels and other hardware, residence time distributions are often employed. In the hydrologic rainfall-runoff context, the analog to the model would be that of components undergoing first-order reaction during flow through a reactor vessel such as a filter. Rainfall into the reactor would be the stream of contaminant-containing fluid, losses would be the contaminants filtered out and staying in the vessel, and runoff would be the contaminants remaining in the fluid stream. A thorough discussion of residence time distribution with reactions is included in Clark (1996).

The discussion here is about direct runoff only, and furthermore that the time origin is such that the rate of rainfall exceeds the rate of infiltration, so that the fate (infiltrating or not infiltrating) of each raindrop is uncertain. For visualization, consider that rainfall depth and rate is uniform across the watershed, and that the population of discreet drops landing in a given instant that do not immediately infiltrate form a "layer" on the surface moving down gradient. In the next instant, more raindrops fall. This second group land atop the layer already in place and form a second layer on top of the first. The drops in the first layer are therefore beneath the second layer. Because of proximity to the soil surface, infiltration occurring during the second time instant is more likely to take in drops from the lower layer, that which fell earlier and traveled downgradient to "run on" to a point on the surface, than to take in drops landing at that point during that instant. In succeeding instants, layer upon layer of drops are laid on top of these earliest layers, "ponding" deeper and deeper. It is easy to visualize that in this model, at least a portion of drops that infiltrate at any given

point originally impacted up gradient and then “ran on,” rather than infiltrating where they impact.

Several interesting ideas are implied by the model, that are normally not discussed with traditional models. Returning briefly to the membrane analogy and visualizing the membrane as gravity is pulling it downstream, the membrane would start out full-depth of effective precipitation, and it would get thinner and thinner as it proceeded downstream, because it was being ”worn away” by time-dependent loss processes along the way. The edge that fell at the watershed boundary might be completely worn away before it reaches the outlet, in which case the more distal areas of the watershed have contributed nothing to the hydrograph.

The conceptual model under discussion assumes an ideal, homogeneous watershed with uniform soil properties. Under such conditions, it is possible to talk in generalities that are not necessarily applicable to any specific drop under real conditions. Under real conditions, or even more generalized conceptual models, at any point the rate of infiltration may exceed the combined rate of rainfall and run on. In that case, all rain that arrives there may infiltrate, resulting in no runoff at all from that point during that instant. Under the conceptual conditions of this exercise the situation of no runoff will be reserved for rainfall having ceased.

### 5.6.2 A Conceptual Model of Layers

If the watershed area immediately adjacent to the watershed boundary is considered, there is no “run on;” the only water available at those points is what impacts at each point. What does not infiltrate upon impact runs off, but will remain in the “lowest layer” of of water that will constitute “run on” to down gradient points. Therefore, the chances are large that a raindrop that falls promptly at the watershed boundary will infiltrate before it has traveled a great distance, by virtue of the position it occupies in a “low layer.” A drop landing slightly further from the watershed boundary and at a later time instant will land on top of drops “running on” from earlier, up gradient impacts, and will form a “higher layer.” Yet, as drops move down gradient, they are covered by succeeding layers, and the layers beneath are decimated by loss to those processes that constitute loss. In this scheme, as time progresses, each drop begins in a top layer and is covered by other layers in succession, whereas lower layers are ground away by infiltration and other landform loss processes.

Other than the special case of a conceptual rain gauge, all watersheds inherently possess the property of contributing area. Rain falls distributed over an area (not necessarily uniformly distributed) and runs off down gradient. Those down gradient paths converge into channels and streams. Streams converge into larger streams. At each point along any path leading from a point on the watershed to the outlet or point of interest, area contributing to that point increases compared to any point up gradient. Thus, it can be said that watersheds exhibit *spatial convergence* in the down gradient direction.

Because watersheds spatially converge in the down gradient direction, each layer is concentrated and must become deeper as it moves down gradient. Depth of ponding attributable to each layer increases in the down gradient direction from run on alone, while the area available for infiltration diminishes. In the conceptually ideal watershed of the exercise, these effects should result in preferentially earlier saturation of the soil in down gradient areas, attributable to the greater ponding depths. The fraction of rainfall either falling on, or running across, down gradient areas in later instants of time that infiltrates is smaller than that on up gradient areas at the same instants for two reasons; there is less area to accept infiltration because of spatial convergence, and likely lower infiltration rate because of greater saturation. Preferentially earlier saturation of more down gradient areas, and the accompanying higher runoff production from those areas is, incidentally, consistent with the observations of Ragan (1968), Dunne and Black (1970), and Engman (1974) in small watershed studies. Runoff from some areas being lost later as run on in other areas is consisent with the observations of Amerman (1965). Thus, the layered idea can be seen as consistent with the partial area and variable source area writings of the 1960s and 1970s.

From this layered conceptual model, the following statements pertaining to rainfall at rates greater than the infiltration rate may be considered:

- Rainfall infiltrating promptly at the watershed boundary did not land elsewhere and arrive there as run on because there is no up gradient area to serve as a source of run on water;
- The further a drop lands from the watershed boundary, the more competition it has for infiltration because of run on from up gradient locations and spatial convergence;
- Drops infiltrating at any point on the watershed likely impacted some distance up gradient and arrived at that point as run on, rather than having impacted at the point of infiltration;
- Each raindrop likely travels down gradient some distance as runoff/run on before it infiltrates;
- The further down gradient a drop impacts, the greater its chance of avoiding infiltration altogether;

- Soil located in down gradient areas will have a greater availability of water for infiltration and greater ponded depth, and thus may saturate more quickly and take in more total infiltration than soil located near the watershed boundary, soil properties permitting; and
- Earlier soil saturation in down gradient areas may combine with spatial convergence to reduce the likelihood of a drop falling on a down gradient area directly infiltrating at the point it impacts.

For simplicity and as a practical matter, it will be implied that average travel speed of a drop over any distance is relatively constant. The likelihood of a drop infiltrating is proportional to the time it resides on the watershed. Distance at a constant speed equates to time, therefore time and distance will be considered equivalent, used interchangeably throughout the exercise. Ironically and seemingly in conflict with the residence time idea, because of spatial convergence and increased soil saturation in down gradient areas, the further down gradient a drop travels from its point of impact, the greater is the likelihood of that drop not infiltrating. It can be thought that the longer a drop survives, the greater the chances of that drop surviving even even longer. There is therefore a reinforcing self-similarity to the survival process.

### 5.6.3 A Model of Survival

It is true that rain does not arrange itself in layers in the manner described; the layering described is simply a conceptual model. Raindrops impacting on a surface over which runoff is already in progress will mix randomly with runoff already there. However, the overall effects itemized in Section 5.6.2 are not dependent to the layering idea; they remain valid in the face of mixing. Travel distances mentioned in the list would be random functions of time.

The likelihood of any drop passing the outlet is proportional to two things; the distance it must travel to arrive there, and the likelihood that it will travel that far. According to the list of effects, drops impacting in down gradient areas have a higher likelihood of a large travel distance, and a smaller distance to travel. The implicit consequence of this list of effects is that the influence on runoff of any small area within the watershed is inversely proportional to the distance of that area from the outlet. This idea conflicts with the basic assumption of conventional watershed modeling, that gross rainfall can be divided into two distinct parts; "effective rainfall" that produces uniform runoff from the entire watershed analogous to a

membrane and "lost rainfall" that infiltrates at or very near the location of impact on the landscape.

If this story is repeated many times, with the conceptual raindrop landing at random locations all across the watershed, the likelihood of any given raindrop making it past the point of interest is inversely proportional to the time it is exposed to the hazards of the watershed. Because time to travel is closely coupled with distance to travel, it follows that when the drop falls in a very distal area, such as along the watershed boundary, it is much less likely to survive the trip all the way to the outlet than it is if it falls proximate to a channel and just upstream of the point of interest.

The exercise leads to the observation that in the model discussed, runoff is not generated evenly over the watershed as implied in conventional UH theory. Assuming some of the same simplifications used in other watershed modeling techniques, (uniform rainfall, uniform watershed characteristics, and others) a larger fraction of raindrops falling in areas close to the point of interest become runoff than do those falling in far distal areas of the watershed. Upland areas far from the point of interest may constitute a large fraction of the watershed area, but by the model under discussion they might contribute very little runoff compared to the amount of rain they receive. Conversely, areas proximate to streams that provide fast, efficient transport paths may contribute a much larger fraction of the rainfall that falls on them than do the upland areas.

It is also interesting to note that the idea of effective rainfall no longer has the same utility in this model that it does in traditional UH modeling. In this model, whether or not a drop becomes runoff is a matter of chance; it is not separable from other raindrops that fall concurrently by any identifiable physical-temporal criterion.

Assuming that the idea of residence time distribution for a non-conservative substance, exhibiting first-order decay, represents the rainfall-runoff process, the construction of a hydrograph would be accomplished by accounting for those drops that are not lost, as they travel past the point of interest. Those drops are represented as having survived the journey from where they fell, across the watershed, past the point of interest. As the accounting is of surviving drops, it will be called a "survival model." Survival analysis is a field with much work and rich literature. The case here is simple: of interest is the survival probability distribution raindrops as a function of residence time.

Residence time is encountered in the field of hydrology, typically with respect to water quality, stream base flow, and groundwater/surface water interactions (Soulsby et al., 2013; Langmuir, 1997; Drever, 1997). Residence time in the context other than storm runoff considers long-term residence and movement of water within the soil structure. Botter et al.

(2011) gives extensive details and citations of prior work on the travel time and residence time distributions of water within a watershed. These descriptions focus on water as a solvent of contaminants, and therefore consider the characteristics of water only *as it leaves the watershed.* Whereas very similar in concept to the survival idea, they do not explicitly account for rainfall/survival/outflow as a generator of a direct runoff hydrograph. Sayama and McDonnell (2009) presents a rather complicated, GIS-based, distributed model that tracks flow and residence time of both surface and subsurface water through a watershed. Residence time itself is the major goal of the models of Sayama and McDonnell (2009) and the equations of Botter et al. (2011). The model presented here uses residence time/distance to travel as a descriptor of the likelihood of survival or death of a drop of rain. For the model constructed, only those processes contributing to "direct runoff" will be considered.

## 5.7 Constructing a Conceptual Survival Model

In order to construct a model that will allow the discovery of anything from the conceptual journey of the intrepid drop of rainfall, at least two things must exist: an idea of the travel time of a drop from any point on the watershed to the outlet, and the ability to make many, many of those trips simulating the chances of surviving the journey.

### 5.7.1 The Time-Contributing Area Relationship

For the first part, the idea of a *time-area graph* is prevalent in the study of UHs, in particular a subset of that study focusing on *instantaneous unit hydrographs* (IUHs) (Cleveland et al., 2008). A time-area graph can be divided into pieces that represent uniform time steps. The size of those pieces will be proportional to the fraction of the total area that contributes in each time step, given an initial instantaneous rainfall pulse at $time = 0$. Time-area graphs are described seminally in Clarke (1945). Clarke described the derivation of a UH from the development of a time-area graph and *attenuation* of flow attributed to channel storage. Because of the attenuation component, an argument can be made that Clarke's time-area graph is not really time-area, but rather a graph of the quotient of distance and instantaneous velocity versus area.

A conceptual graphic of the relationship between time and area on a watershed is shown in Figure 5.1. Each line represents equal time of contribution (isochrone). The area between any two ischrones is taken to contribute at the mean of the times of the isochrones. The

result is a set of ordered pairs of time and area. The pairing can be even increments of time and corresponding area, or even increments of area and corresponding time. For purposes herein, it shall be considered as even increments of time as a fraction of total time, and fraction of total area corresponding to that time. An ordered triple will be impled, for instance, the first time step would have a time step-subarea number of 1, a travel time of one-half T1, and the area fraction as between the outlet and the T1 line on Figure 5.1.

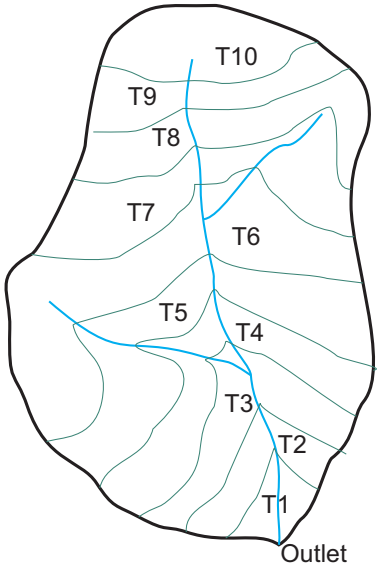


**Figure 5.1.** Conceptual Picture of Time-Area relationship. The green lines represent "isochrones", lines of equal travel time to the outlet. The time-area relationship is represented for analysis by the area between isochrones, assumed to contribute at an average of the two times.

Lienhard (1964) describes a process for deriving a dimensionless UH using a time-area histogram and fitting a specific probability distribution to represent the shape. Lienhard (1964) is an intriguing paper in the context of this research, because it describes the use of a probability distribution for response. However, it only uses the distribution to simulate shape, the membrane analogy of effective rainfall remains, and the fate of raindrops is not addressed directly as being probabilistic. Leinhard opens with a statement appearing to

categorically deny dependence of the UH shape on watershed characteristics. and he development is highly mathematically based, and appears in many ways similar to arguments in this research. However, survival is treated implicitly as being certain; Boltzmann statistics applied to real rainfall-runoff data are used to derive a UH shape.

Figure 5.2 is a cumulative time-area graph (Cleveland et al., 2008), and Figure 5.3 a bar chart of the fraction of total watershed area contributing in each of 20 equal time intervals, assuming an instantaneous pulse of rainfall. Figure 5.2 shows the amount of area contributing (as a fraction of the total topographic watershed) for a corresponding fraction of the total time of contribution of the topographic watershed. If water traveled without loss and without attenuation, by simple translation, the outflow hydrograph from a uniform rainfall event of duration longer than the total time of contribution would closely resemble this graph.

The first represents the accumulation of contributing area as time passes. Early in a runoff event, only the area immediately adjacent to the point of interest is contributing runoff. As time passes, water from areas further away reaches the point of interest. Considering the case of a single, short duration pulse of rainfall and moving forward in time, only runoff from the portion of the watershed that possesses travel time corresponding to the time elapsed since the pulse will be observed passing the point of interest at any point in time. In the case of continuous rainfall, at each point in time all area with travel time less than or equal to that time will be contributing.

Figure 5.3 shows the amount of area that should be contributing at each of 20 points in time for a short duration pulse of rainfall. If water traveled without loss and without attenuation, by simple translation, the outflow hydrograph from a single pulse of rainfall would closely resemble Figure 5.3. However, as noted by Clarke (1945), there is some difference in the shape of the hydrograph as compared to the time-area graph. Clarke explained it as *attenuation*. The model presented will implicitly explain it as the influence of varying survival rates from areas of varying time (distance).

Figures 5.2 and 5.3 contain the same information about the hypothetical time-area relation, each presenting that information differently. If the time steps in Figure 5.3 were dimensionalized by multiplication of the time increments by the total time of a real watershed, the width of each bar would represent 1/20 of the total time. If it were dimensionalized by multiplication of each area fraction (the bar height) by the topographic contributing area of the same real watershed, each bar would represent the area contributing between two adjacent isochrones.

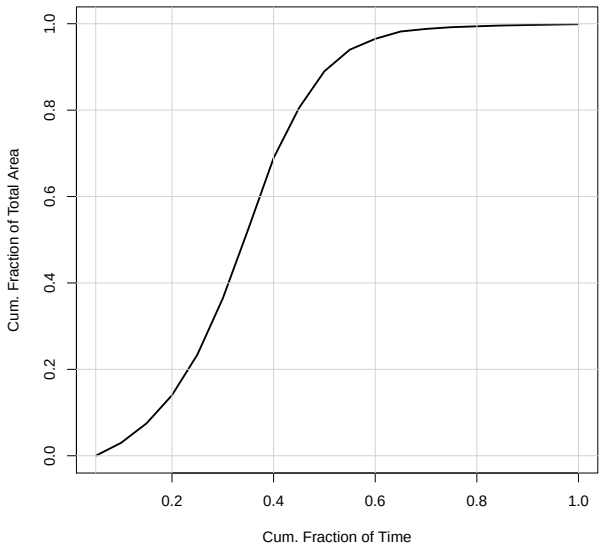


**Figure 5.2.** Cumulative Time-Area graph for an example watershed. This graph shows the amount of area contributing (as a fraction of the total topographic watershed) for a corresponding fraction of the total time of contribution of the topographic watershed.

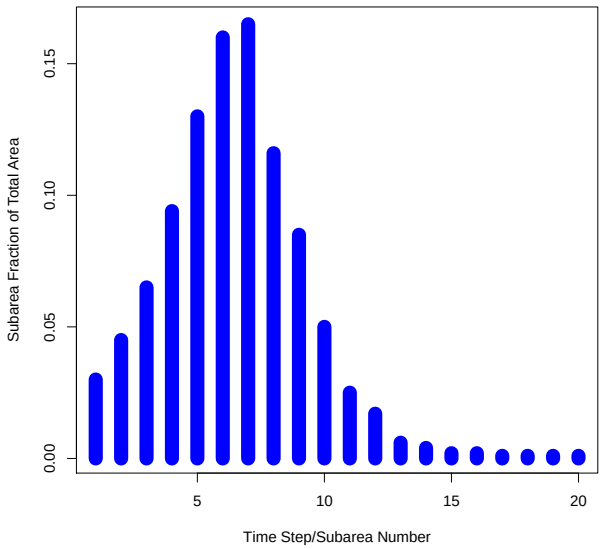


**Figure 5.3.** Incremental Time-Area histogram for the watershed shown in Figure 5.2.

### 5.7.2 Random Lifespans and Known Escape Times

For the second part of the model, the runoff process can be thought of in terms of a random process, as described in Section 5.6. If the identity of individual drops is considered to remain unique, a probability distribution can be assumed and a random value assigned to each of a sample of drops. The value assigned is not a probability; it is a dimensionless magnitude associated with a probability through the selected distribution. The magnitude can be declared to be the time (distance) the individual drop will travel, as a fraction of the total time of contribution of the topographic watershed (the lifespan of the drop). By appropriate selection of a probability distribution and parameters, the average lifespan of many drops can be controlled. A large number of drops can be generated, and divided into groups proportional in size to the bars in Figure 5.3. The lifespan of each drop can be compared to the time necessary for that drop to escape past the point of interest (escape time). Those drops with lifespans greater than the escape times of the group in which they fall are considered to survive; ther remainder are considered to have died on the journey. A simple accounting procedure allows both number and rate of surviving drops between each pair of adjacent isochrones to be determined. The result is a listing of time versus surviving drops, as well as time versus rate of survival of the drops.

## 5.8 Hypothetical Model Construction

This model was constructed in the **R** programming language (R Development Core Team, 2011). A set of functions were written to generate, capture, store, and present simulations of watershed processes. A time-area relationship based on real data was obtained from prior work, and was used as the prototype time-area graph. Cleveland et al. (2008) used a custom-written computer program that operated on digital elevation model (DEM) data to generate the time-area in Figure 5.2 for use in a particle tracking code. Future work using flow-accumulation features of a GIS at small spatial resolution is expected to be more efficient and scale as DEM resolution improves. Figures 5.2 and 5.3 are the result of the described particle tracking computation in dimensionless cumulative form, and incremental form, respectively.

### 5.8.1 Selection of a Probability Distribution

Because the interest is in how many conceptual raindrops survive a trip downstream and past the point of interest, reference to literature on statistical distributions for survival and reliability analysis was the source of information for this pursuit (Johnson et al., 1994). Both the Weibull and exponential distributions are common in survival analysis. The Weibull is found in two- and three-parameter forms. In the two-parameter form, the parameters are called shape and scale, both greater than 0. In the case where the shape parameter is 1, the result is, in fact, the exponential distribution. In a less commonly used three-parameter form, the third parameter (called a shift parameter) moves the distribution along the probability axis such as when there may be a minimum expected survival time. This concept may be useful in the context of an "initial abstraction", a loss accounting variable commonly discussed in watershed modeling, but is not explored here.

Equation 5.1 is the exponential distribution function.

$$F(x,\lambda) = \begin{cases} 1-\exp(-\lambda x) & \text{if } x \geq 0 \\ 0 & \text{if } x < 0 \end{cases} \tag{5.1}$$

The exponential distribution requires only 1 parameter. In the context of the **R** environment, that parameter is expressed as a rate, denoted $\lambda$. The $\lambda$ is often described in texts as the reciprocal of the mean of the distribution; when $\lambda$ increases, the mean, and thus the mean magnitude, of random variates generated on the distribution decreases. Figure 5.4 shows plots of the magnitudes versus probabilities for the exponential distribution with rates of 1, 2, and 5 for the purpose of illustrating the variation in values because of changes in $\lambda$. A $\lambda$ of 1 results in a mean value of magnitude of 1, and values ranging to nearly 5 when computed for $x$ (representing probability) very near 1. For a $\lambda$ of 5, the mean value is 0.2, and the range much smaller. A $\lambda$ of 2 produces a curve between those of 1 and 5. The graph is random variates on the abscissa versus probability on the ordinate.

Both the exponential distribution and the Weibull distribution are "exponential family" distributions. They thus both offer the ability to simulate the self-similar survival behavior mentioned at the end of 5.6.2.

The Weibull is found in forms with two and three parameters. The two-parameter form of the Weibull distribution is shown in Equation 5.2

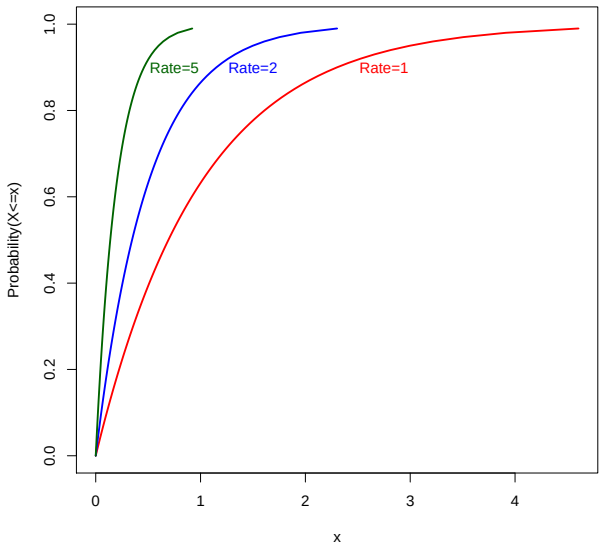


**Figure 5.4.** Graph of the Exponential Distribution for various $\lambda$ parameter values. Abscissa is magnitude of the variate corresponding to the probability values on the ordinate.

$$F(x,\lambda,k) = \begin{cases} \frac{k}{\lambda}(\frac{x}{\lambda})^{k-1}\exp(\frac{-x}{\lambda})^{k} & \text{if } x \geq 0 \\ 0 & \text{if } x < 0 \end{cases} \tag{5.2}$$

The Weibull possesses many of the same qualities as the exponential distribution. In the notation used, $\lambda$ for the Weibull distribution is called the *scale* parameter, and $k$ the *shape* parameter. Figure 5.5 is a plot of the Weibull distribution for scale parameter values of 1, $1/2$, and $1/5$, with the shape parameter held constant at 1. Note that curves in Figure 5.5 appear identical to those in Figure 5.4. The Weibull distribution with the shape parameter of 1 is, in fact, the exponential distribution, with the scale parameter of the Weibull equal to the reciprocal of the $\lambda$ (rate) in the exponential distribution. The use of $\lambda$ as a descriptor in both distributions can be confusing; however the fact that the influence of the variable on the distribution is similar and they are related reciprocally alleviates some of the confusion.

In this work, the exponential distribution will be chosen as the distribution to generate random variates to represent trips downstream of conceptual raindrops. The term $\lambda$ will henceforth be intended as the $\lambda$ (rate) of the exponential distribution rather than the $\lambda$ (scale) of the Weibull distribution, to avoid confusion.

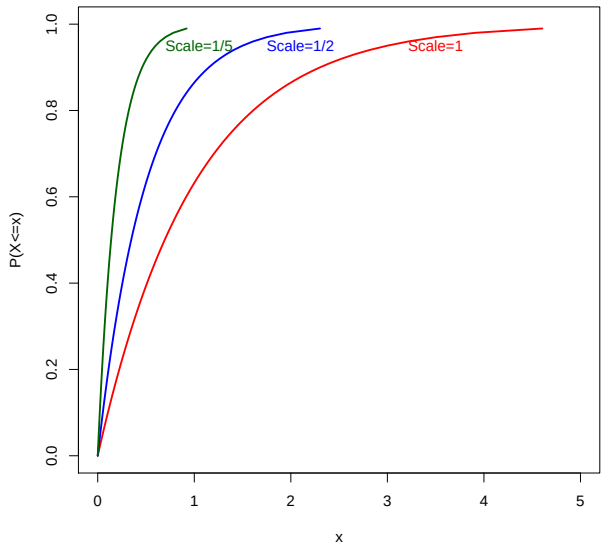


**Figure 5.5.** Graph of the Weibull Distribution for various scale parameter values, with the shape parameter held constant at 1. With shape parameter of one, the Weibull is identical to the exponential in shape. Abscissa is magnitude of the variate corresponding to the probability values on the ordinate.

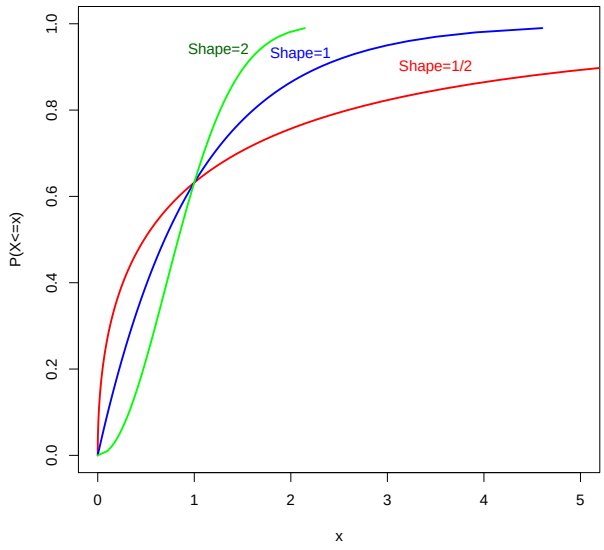


**Figure 5.6.** Graph of the Weibull Distribution for various shape parameter values. The scale parameter is held constant at 1 in the cases plotted here. Abscissa is magnitude of the variate corresponding to the probability values on the ordinate.

### 5.8.2 Specification of the Time-Area Relationship

Building a hypothetical model by this method proceeds in this manner: The first step in developing the model was the coding of the time-area information mentioned above as a vector of values representing isochronic fractions of the watershed area. In this case, 20 values were selected because that number produced a reasonable representation of a smooth curve, and allowed each fractional area to contain a large enough number of conceptual drops that oscillations from random noise were well suppressed. Any number of values could be chosen, but 20 seemed a good compromise between resolution and noise. Each of the elements of this vector is proportional in size to a bar on the incremental time-area graph, depicted on Figure 5.3. These values also represent the fraction of the raindrops in a pulse of rainfall that fall on areas with travel times corresponding to the each time step in the total travel time vector.

On a time-area graph, or a time-area table, each time step has associated with it a fraction of the total contributing area; the topographically defined watershed area. Thus, discussion of a step along the timeline can be thought of as synonymous with a fraction of the contributing area. For the purposes of this discussion the terms shall be associated in the context of the time-area relationship. The time step size will be expressed in minutes. The time step size is also the discrete computational interval, as well as the time interval between rainfall pulses. All of the temporal step sizes must be identical to avoid aliasing of computations.

Table 5.1 lists the time step-subarea number, the incremental fraction of total area contributing in that time step, and the cumulative fraction of total area contributing at the end of each time step. time step refers to the increment of the total time of contribution, subarea refers to the fraction of total area contributing in that time step. The two terms are an ordered pair (time, area)

### 5.8.3 The Escape Time of a Drop

The next step is to generate the travel time-distance vector. This vector will contain the same number of elements (conceptual drops) as the lifespan vector of random variates (discussed subsequently in Subsection 5.8.4). Fractions of this vector correspond to the time-area vector fractions defined in Subsection 5.8.2 are given values representing the average fraction of total time for each time step, from 0.025 to 0.975 at intervals of 0.05. The average values can be thought of as the *escape time*, or the time needed for the drop

**Table 5.1.** Table of fractions of total contributing area at each time interval from the time-area graph in Figure 5.3 and Figure 5.2. Incremental areas are area beginning contribution in each step, cumulative areas are the fraction of total area contributing at the end of each step.

| Time step (Subarea) | Subarea Incr. Frac. | Subarea Cum. Frac. |
|---|---|---|
| 1 | 0.03 | 0.03 |
| 2 | 0.045 | 0.075 |
| 3 | 0.065 | 0.14 |
| 4 | 0.094 | 0.234 |
| 5 | 0.13 | 0.364 |
| 6 | 0.16 | 0.524 |
| 7 | 0.165 | 0.689 |
| 8 | 0.116 | 0.805 |
| 9 | 0.085 | 0.89 |
| 10 | 0.05 | 0.94 |
| 11 | 0.025 | 0.965 |
| 12 | 0.017 | 0.982 |
| 13 | 0.006 | 0.988 |
| 14 | 0.004 | 0.992 |
| 15 | 0.002 | 0.994 |
| 16 | 0.002 | 0.996 |
| 17 | 0.001 | 0.997 |
| 18 | 0.001 | 0.998 |
| 19 | 0.001 | 0.999 |
| 20 | 0.001 | 1 |

to escape and survive from the subarea it falls in, as a fraction of total travel time of the topographically defined watershed. The escape time vector can be thought of as being composed of subsets of travel time proportional to the bars in Figure 5.3. Each individual variate represents the escape time of an individual "drop." The number of escape times in the first subset correspond to the fraction of total travel time in the first bar, and are assumed to fall very close to the point of interest, within 1/20 or 5 percent of the total time to traverse the watershed from the most distal point—an average of 2.5 percent (average of 0 and 5). The drops in the second subset represent those that fall at places that are between 5 and 10 percent of the total travel time distant from the point of interest, average 7.5 percent. The third, between 10 and 15, an average of 12.5, and so forth. The value of all elements in a subset is the same (the average). The number of elements in each subset represents the fraction of area that contributes in a given time step.

Table 5.2 lists values of the time step-subarea number, beginning and ending indices for each time step-subarea of a vector of 1 million escape distances, and the values of the escape vector for those index ranges. Table 5.2 represents the time-area relationship of Figure 5.3 for 1 million drops. A different time-area graph would result in a different distribution of indices; while a different depth of rainfall would result in a different, but proportional, set of indices representing each time step-subarea.

In the case presented, 1 million drops is equated to 1 inch of rainfall. It is implied that each conceptual drop represents a much larger population of raindrops. During the initial coding of the model in **R**, various numbers were evaluated. Numbers smaller than 1 million, when multiplied by a depth much less than 1 inch, produced erratic survival and inconsistent graphics. Larger numbers, 10 million and 100 million, were also evaluated. Whereas these numbers produced even smoother and consistent results, computational time was unacceptably long for application here. If the algorithm were coded in a more efficient (compiled) programming environment, a larger number such as 10 million would provide smoother results. The larger the number of drops, the smoother the results, but the longer the computational time.

### 5.8.4 The Lifespan of a Drop

The next step is to construct a long vector string (say, 1 million elements) of exponential random variates. The long vector is intended to represent a certain depth of rainfall. The individual variates each represent the *lifespan* of an individual drop. It will be assumed this rainfall pulse occurs only during a specific time step, and uniformly over the watershed, similar to the rainfall pulses used in UH modeling. Recall from Section 5.6 that discussion of time and distance will be considered synonymous. There are now two vectors that can be placed in 1:1 correspondence: a lifespan vector of random variates, and an escape vector of fractional times as described in Subsection 5.8.3.

### 5.8.5 Comparing Lifespans and Escape Times

Next, each element in the lifespan vector of random variates is compared to the escape time fractional time/distance corresponding to it by position in the time/distance vector. If the value of the lifespan variate is greater than the escape time, it is replaced with a value of 1. If it is less, it is replaced with a value of 0. The vector then contains only zeroes and ones.

**Table 5.2.** Table of time step-subarea ($Tstep/SA$) number and corresponding index numbers of values in both "lifespan" (random variate) vector and "escape time" vector

| Time step (Subarea) | Beginning Index | Ending Index | Escape time frac. |
|---|---|---|---|
| 1 | 1 | 30000 | 0.025 |
| 2 | 30001 | 75000 | 0.075 |
| 3 | 75001 | 140000 | 0.125 |
| 4 | 140001 | 234000 | 0.175 |
| 5 | 234001 | 364000 | 0.225 |
| 6 | 364001 | 524000 | 0.275 |
| 7 | 524001 | 689000 | 0.325 |
| 8 | 689001 | 805000 | 0.375 |
| 9 | 805001 | 890000 | 0.425 |
| 10 | 890001 | 940000 | 0.475 |
| 11 | 940001 | 965000 | 0.525 |
| 12 | 965001 | 982000 | 0.575 |
| 13 | 982001 | 988000 | 0.625 |
| 14 | 988001 | 992000 | 0.675 |
| 15 | 992001 | 994000 | 0.725 |
| 16 | 994001 | 996000 | 0.775 |
| 17 | 996001 | 997000 | 0.825 |
| 18 | 997001 | 998000 | 0.875 |
| 19 | 998001 | 999000 | 0.925 |
| 20 | 999001 | 1000000 | 0.975 |

Ones represent drops that survive the journey to the outlet, zeroes represent drops that do not survive.

The lengths of the respective subsets in the distance vector representing each time step are known, and the number of surviving drops in a time step is simply the sum of that subset. By associating the time step with the number of surviving drops in that time step, the elements of a conceptual outflow hydrograph exist. In addition, both the raw number and the fraction of drops surviving from each subarea can easily be computed.

Code to perform these tasks, written in the **R** Programming Language (R Development Core Team, 2011), is included and documented in the appendices on **R** code.

### 5.8.6 Elementary Example

To illustrate the workings of the survival model, a simple example is presented. A simple time-area relationship will be contrived, and a small number of exponential random variates generated, and a list of the escape times for the time steps will be used for comparison. A time-area curve with 5 time steps is shown in Figure 5.7. The values of the fractions of total area, that which would be the topographically defined watershed, for the graph are (0.16, 0.4, 0.24, 0.16, 0.04).

Table 5.3 shows the time step-subarea number for each "drop" in the first column. The second column contains the number of "drops" in each subarea, aligned with the last drop in that subarea. The third column is the "lifespan" of each drop, the exponential random variate for that "drop". The fourth column is the "escape time" column, the average time to excape from each subarea. For example, the first subarea begins at $time = 0$ and ends at $time = 0.2$, because there are 5 subareas and $1/5 = 0.2$. The average of 0 and 0.2 is 0.1, so the escape time for time step-subarea 1 is 0.1. The second time step-subarea begins at 0.2 and ends at 0.4; the average is 0.3. The third, 0.4 to 0.6 for an average of 0.5, and so forth. Thus, the escape times are (0.1, 0.3, 0.5, 0.7., 0.9).

The algebraic difference between the lifespan and the escape time is calculated for each "drop" by subtraction and placed in the fifth column. If the lifespan is greater than the escape time, the difference is greater than 0, a 1 is placed in the sixth column, if not, it is less than or equal to 0, and a 0 is placed in the sixth column. The seventh and last column shows the sum of survivals for each time step-subarea, which can be compared to the number of "drops" originally in it (the second column) to get a survival fraction from the time step-subarea.

Table 5.3, generated with a $\lambda$ of 1, has a very high survival rate. However, Table 5.4 is an identical table, other than that the "lifespan" of each "drop" was generated with a $\lambda$ of 5. Survival is much less from this value. In fact, the survival of the three later time step-subareas is nonexistent. Conceptually, the latter time step-subareas represent the distal areas of the topographic watershed. The lack of survival in later time step-subareas means that the distal areas are not contributing to the modeled runoff. In Tables 5.3 and 5.3, the "length" of each subarea (conceptually transformed from area to length) is proportional to the height of the subarea fraction in Figure 5.7. Thus, from 25 total drops, four are associated with subarea 1, ten with subarea 2, six with subarea 3, four with subarea 4, and one with subarea 5 (see "Num. Drops" column in Table 5.3).

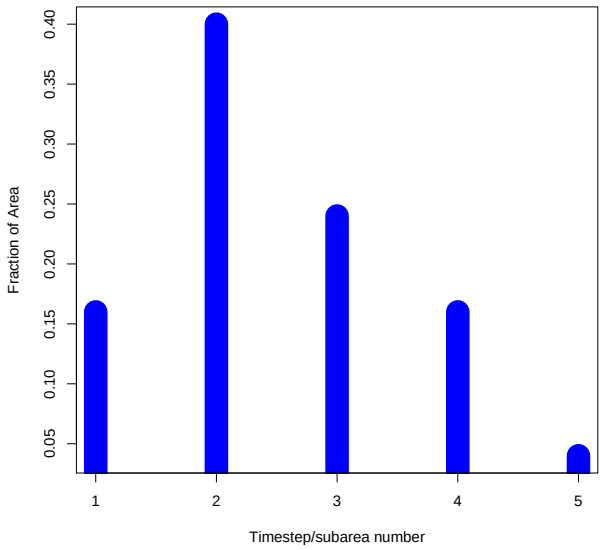


**Figure 5.7.** time-area graph for the simple example in Subsection 5.8.6. Five subareas for simplicity

The example in this subsection is greatly simplified for presentation, but demonstrates the principles of the survival model. As $\lambda$ is adjusted, survival is influenced; survival from the distal areas of a watershed is always less than from proximate areas. The variable or partial area representation can be represented by this model. By changing $\lambda$, the survival of water falling on the distal areas of the watershed can be manipulated.

### 5.8.7 Discussion of the Survival Model Concept

The magnitude of each random variate has been considered to be the time, as a fraction of the total time, that it will travel before it is lost in some way. Each magnitude has been checked against the time it must travel to escape and survive. If the magnitude is less than the time from that subarea, it is considered lost and is discarded, these are changed to 0 in the vector. Those that are larger are considered to have survived to pass the point of interest, and are counted as runoff. They are changed to 1 in the vector. The number of drops surviving is interpreted as the magnitude of runoff from a given isochronic subarea. These magnitudes are summed and assembled into a vector of values representing a conceptual direct runoff hydrograph from a pulse of rainfall of duration 1/20 of the conceptual travel

**Table 5.3.** Table of values for a simple example with exponential distribution $\lambda$ value of 1. Sample size of 25 drops, according to the time-area graph in Figure 5.7.

| Timestep-Subarea | Num. Drops | Lifespan | Escape Time | Diff. | Life Death | Num. Surv. |
|---|---|---|---|---|---|---|
| 1 | - | 0.3862 | 0.1 | 0.2862 | 1 | - |
| 1 | - | 0.2890 | 0.1 | 0.1890 | 1 | - |
| 1 | - | 0.2146 | 0.1 | 0.1146 | 1 | - |
| 1 | 4 | 1.0154 | 0.1 | 0.9154 | 1 | 4 |
| 2 | - | 0.0458 | 0.3 | -0.2542 | 0 | - |
| 2 | - | 0.7413 | 0.3 | 0.4413 | 1 | - |
| 2 | - | 1.7530 | 0.3 | 1.4530 | 1 | - |
| 2 | - | 0.5928 | 0.3 | 0.2928 | 1 | - |
| 2 | - | 0.4485 | 0.3 | 0.1485 | 1 | - |
| 2 | - | 1.1743 | 0.3 | 0.8743 | 1 | - |
| 2 | - | 0.1545 | 0.3 | -0.1455 | 0 | - |
| 2 | - | 0.7841 | 0.3 | 0.4841 | 1 | - |
| 2 | - | 0.6819 | 0.3 | 0.3819 | 1 | - |
| 2 | 10 | 1.2286 | 0.3 | 0.9286 | 1 | 8 |
| 3 | - | 0.8926 | 0.5 | 0.3926 | 1 | - |
| 3 | - | 1.0133 | 0.5 | 0.5133 | 1 | - |
| 3 | - | 2.0399 | 0.5 | 1.5399 | 1 | - |
| 3 | - | 0.8522 | 0.5 | 0.3522 | 1 | - |
| 3 | - | 0.5894 | 0.5 | 0.0894 | 1 | - |
| 3 | 6 | 1.7412 | 0.5 | 1.2412 | 1 | 6 |
| 4 | - | 0.4665 | 0.7 | -0.2335 | 0 | - |
| 4 | - | 0.9269 | 0.7 | 0.2269 | 1 | - |
| 4 | - | 0.6465 | 0.7 | -0.0535 | 0 | - |
| 4 | 4 | 3.3069 | 0.7 | 2.6069 | 1 | 2 |
| 5 | 1 | 0.2635 | 0.9 | -0.6365 | 0 | 0 |

time from the most distal point on the watershed, the time usually interpreted as "time of concentration."

Figure 5.8 is the plot of three such vectors, with $\lambda$s of 1, 2, and 5. The graph shows the time step number (out of 20) versus the fraction of drops landing in the area between isochrones that survive, (areas from Figure 5.3) for that time step. For a $\lambda$ of 1, the mean value of the lifespan of a drop is 1, therefore half of them will be greater than 1 in magnitude. If they are greater than 1, they are certain to exceed the escape time; thus a large fraction of them survive. For a $\lambda$ of 2, the mean is 0.5, and for a $\lambda$ of 5, the mean is 0.2. Therefore, much smaller fractions of the lifespan variates are greater than the escape time. As the time step increases in value, the escape time increases in value, and a smaller fraction

**Table 5.4.** Table of values for a simple example with exponential distribution $\lambda$ value of 5. Sample size of 25 drops, according to the time-area graph in Figure 5.7.

| Timestep-Subarea | Num. Drops | Lifespan | Escape Time | Diff. | Life Death | Num. Surv. |
|---|---|---|---|---|---|---|
| 1 | - | 0.0312 | 0.1 | -0.0688 | 0 | - |
| 1 | - | 0.0881 | 0.1 | -0.0119 | 0 | - |
| 1 | - | 0.0819 | 0.1 | -0.0181 | 0 | - |
| 1 | 4 | 0.2194 | 0.1 | 0.1194 | 1 | 1 |
| 2 | - | 0.0504 | 0.3 | -0.2496 | 0 | - |
| 2 | - | 0.0023 | 0.3 | -0.2977 | 0 | - |
| 2 | - | 0.1407 | 0.3 | -0.1593 | 0 | - |
| 2 | - | 0.1205 | 0.3 | -0.1795 | 0 | - |
| 2 | - | 0.3281 | 0.3 | 0.0281 | 1 | - |
| 2 | - | 0.0815 | 0.3 | -0.2185 | 0 | - |
| 2 | - | 0.1176 | 0.3 | -0.1824 | 0 | - |
| 2 | - | 0.0797 | 0.3 | -0.2203 | 0 | - |
| 2 | - | 0.2301 | 0.3 | -0.0699 | 0 | - |
| 2 | 10 | 0.1184 | 0.3 | -0.1816 | 0 | 1 |
| 3 | - | 0.2247 | 0.5 | -0.2753 | 0 | - |
| 3 | - | 0.0203 | 0.5 | -0.4797 | 0 | - |
| 3 | - | 0.2295 | 0.5 | -0.2705 | 0 | - |
| 3 | - | 0.3263 | 0.5 | -0.1737 | 0 | - |
| 3 | - | 0.3629 | 0.5 | -0.1371 | 0 | - |
| 3 | 6 | 0.0448 | 0.5 | -0.4552 | 0 | 0 |
| 4 | - | 0.0866 | 0.7 | -0.6134 | 0 | - |
| 4 | - | 0.3440 | 0.7 | -0.3560 | 0 | - |
| 4 | - | 0.0423 | 0.7 | -0.6577 | 0 | - |
| 4 | 4 | 0.1104 | 0.7 | -0.5896 | 0 | 0 |
| 5 | 1 | 0.0473 | 0.9 | -0.8527 | 0 | 0 |

of drops survive. In that way, Figure 5.8 shows that time and distance from the point of interest control the rate of survival of drops; smaller time step numbers (shorter distances) have a greater rate of survival than larger time step numbers. Smaller time step numbers correspond to areas more proximate, and larger time step numbers correspond to areas more distal, of the topographic watershed.

From general UH theory the model borrows the idea of discrete time steps for analysis, and from IUH theory the model also borrows the idea of a time-area graph. Those theories can again be used to supply the idea to generate a series of these outflow hydrographs and sum the fractions contemporaneously, producing a composite hydrograph resulting from a sequence of rainfall pulses not necessarily of the same rainfall depth.

The difference in depth in each pulse can be simulated by the number of variates generated for the rainfall pulse associated with the particular time step. For instance, $X$ variates might be one unit of depth, $2X$ two units, and so forth. For variates generated using the same parameters, similar fractions can be expected to survive in each time slot, even with different overall numbers. The model is built assuming that survival will be linearly proportional to depth.

Earlier, it was discussed that UH computations require three basic parts; a hyetograph, a loss model, and a response model. In the survival model, a hyetograph can be applied in the same way as done for UH computations. The response model is represented by the interaction between the time-area graph and the survival probability of the exponential random variates. One of the most interesting aspects of the alternative model is in the loss process. The idea of a "loss model" removing rain from the gross rainfall has been eliminated and instead is replaced it by the idea that only under certain, special conditions does a raindrop survive the trip downstream.

It is known that the removal of water from surface runoff can occur by many causes. Classical loss models typically attempt to assign physical cause, simulated by equations, to those processes. Even if a portion of those processes are intimately known, and very good parameters for the equations can be developed, this accounts for only one, or at most two, of those processes. Typically, modeling estimates an "initial abstraction" prior to which no runoff occurs. A parameterized equation such as Green-Ampt or Horton's is used to estimate a time-dependent loss component (USACE-HEC, 2012). For UH calculations, methods and parameters must be averaged over a watershed (or subwatershed in the case of subdivided or distributed modeling). Under the best of practical modeling circumstances, many other components of the loss process are neglected, for instance flow into the ground, both soil and rock, through macroscopic features. These components of loss are seldom represented at all in practical modeling.

In the presence of rainfall-runoff data, it is common to advocate the "calibration" of models, i.e. the adjustment of model parameters until modeled results match measured data. Experience has shown that this process often results in model parameters that are difficult to justify physically. Losses implied by measured data are often greater than would be calculated by models using infiltration loss methods alone. This inconsistency may be explained by the neglect of the effects of macroscopic features as mentioned earlier, and is mentioned only to illustrate the potential lack of completeness in the application of traditional loss models as part of engineering watershed modeling methodology (Wiles and Sharp, 2008).

In the presence of rainfall-runoff data, it is common to advocate the "calibration" of models, i.e. the adjustment of model parameters until modeled results match measured data. Experience has shown that this process often results in model parameters that are difficult to justify physically. Losses implied by measured data are often greater than would be calculated by models using infiltration loss methods alone. This inconsistency may be explained by the neglect of the effects of macroscopic features as mentioned earlier, and is mentioned only to illustrate the potential lack of completeness in the application of traditional loss models as part of engineering watershed modeling methodology.

The survival model replaces all of those ideas with a single, simple, parsimonious one—the longer a drop of water remains on the watershed, the more likely it is to suffer a fate that removes it from the runoff process. In addition, the model allows for the influence of the loss process upon the shape of the outflow hydrograph. In this model, contribution to the outflow hydrograph, and therefore influence on its shape, is greatest from area located proximate to the point of interest. Distal areas of the watershed exert less influence on the shape and timing of the hydrograph. At this point, no attempt is being made to ascribe loss magnitude to any particular physical cause, the model simply acknowledges that losses occur, and are only related to residence time on the watershed.

The fraction of drops surviving to escape the watershed is clearly proportional to the average magnitude of random variates. By changing $\lambda$, the average magnitude changes, thus changing the fraction of drops that survive the journey. Clearly, a change in survival is also inversely proportional to the conceptual distance to the point of interest. As $\lambda$ increases, survival rate diminishes overall, and survival rate from the distal areas of the conceptual watershed diminish more than those proximate to the point of interest. In this can be seen an analog to what would be expected from several causes such as soil type, antecedent moisture, or land use/land cover. Thus, by use of the $\lambda$ in generating random variates, the model can be fit to the same physical conditions on a real watershed that the physically-based infiltration loss models attempt to simulate.

Increasing $\lambda$ diminishes the number (and correspondingly the fraction) of drops that escape the watershed. In this way, $\lambda$ can be considered in the same light as a loss parameter, although what is actually occurring is that those drops that survive the journey out of the watershed are being counted. It is also evident that the number of particles surviving that originated (fell, as it were) in the distal areas of the watershed is comparatively small. This result would be expected if for no other reason than, according to Figure 5.3, limited area actually contributes in the final few time steps. However, if the number of drops surviving from each subarea are counted, and a fraction surviving from the number that

"fell" computed, a plot of survival versus residence time on the watershed can be obtained. Figure 5.8 is such a graph. The graph shows that the fraction of drops surviving the journey to the outlet diminishes with travel time (and thus distance) from the point of interest, regardless of the $\lambda$ for random variates.

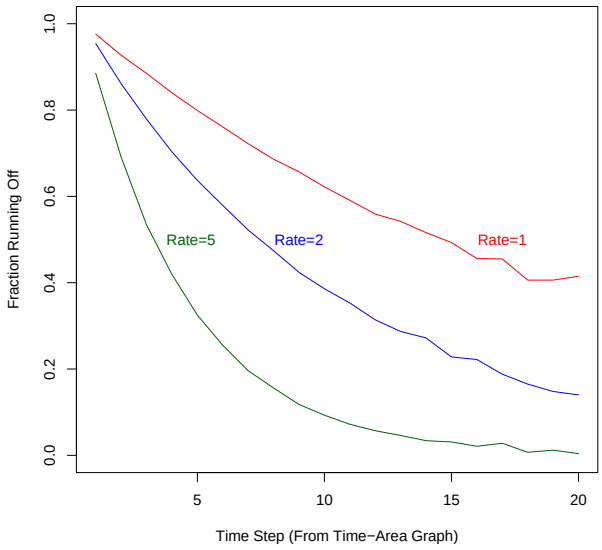


**Figure 5.8.** Graph of the fraction of drops surviving the journey to the outlet with time step. The outlet is assumed to be at time=0.

Thus far, a conceptual model of watershed runoff generation has been developed around the time-area relationship, a single pulse of conceptual rainfall, and the survival of raindrops, based on residence time on the watershed. This modeling has been done by way of a function in the **R** programming environment. Now taking another idea from UH methods, that of adding together the simultaneously occurring results from multiple rainfall pulses distributed in time according to regular time steps, the model can be extended to simulate incremental conceptual storm events. The computations to accomplish that will be done by way of an R function that "wraps around" the previous function, evaluates it for a series of values, stores the results, and sums the values in individual time steps from each pulse.

Comparing Figure 5.8 and a conceptual watershed map with an appropriately numbered set of isochrones, Figure 5.9 (similar to Figure 5.1), it can be seen by examination that, for a $\lambda$ of 1 in the exponential distribution, the fraction of the drops falling that run off is around 60 percent for time step-subarea 10, whereas for a $\lambda$ of 2, it is approximately 40 percent, and for a $\lambda$ of 5, approximately 25 percent. The interpretation is that in the case of a single

pulse of rainfall, at a time of one-half of the watershed response time, runoff seen would consist of 60, 40, and 25 percent, respectively, of the drops that fell in the area between the T9 ( not shown) and T10 isochrones on Figure 5.9. The remaining 40, 60, and 75 percent, respectively, have undergone *death* from the standpoint of runoff; they have succumbed to loss processes and are not seen as direct runoff.

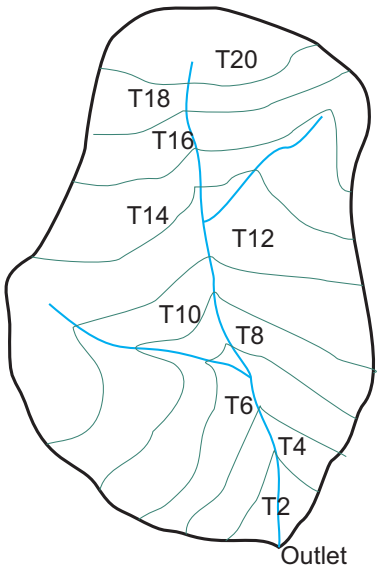


**Figure 5.9.** Conceptual Picture of Time-Area relationship, adapted to reflect 20 time steps. To avoid clutter, odd numbered isochrones are not shown. This drawing is conceptual, and areas are not proportional to those used in the example.

To this point, the product of computations has been a count of surviving drops, useful for conceptual purposes, but not very representative of real rainfall. However, if it is assumed that an appropriate scale factor relating number of conceptual drops, for instance the one million mentioned before, to a sample drawn from one unit depth of rainfall, the move can be made from drops to depth. In order to interpret this model in a meaningful way, it must be able to represent different rainfall depths in different pulses. This representation is easily accomplished by use of a vector of conceptual depth values in the wrapper function, by which the reference one million drops is multiplied in order to arrive at a number of

variates generated in a pulse. There are now two parameters; magnitude representing conceptual depth of rainfall through number of variates generated, and the survival likelihood controlled by the $\lambda$ for the exponential variates.

## 5.9 Hypothetical Model Results

For the purposes of demonstration and discussion, conceptual events with only three rainfall pulses will be simulated. Figure 5.10 represents three pulses at unit depth and a constant rate parameter. The results of each pulse is the same; the fourth graph is the sum of the other three, as in UH methods. Both the number and rate of survival graphs are similar for all three pulses.

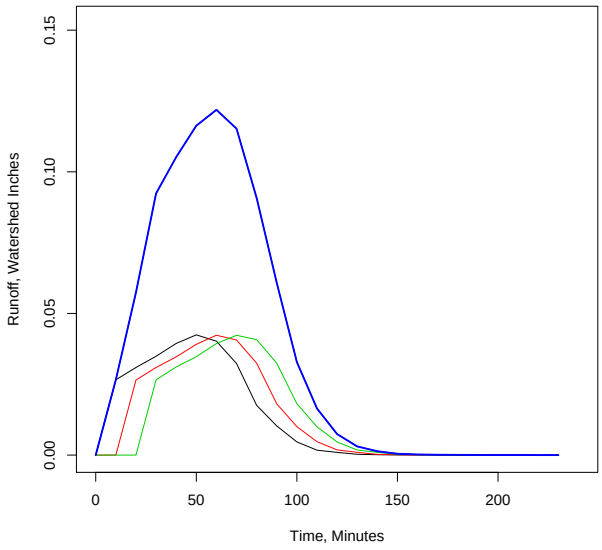


**Figure 5.10.** Graph of the individual, sequential rainfall pulse hydrographs (black, red, and green) with the same rate parameter, and the aggregated conceptual outflow hydrograph (blue). Ordinates represent watershed inches per time step.

As has already been demonstrated, increasing the $\lambda$results in diminished survival, both in number and rate, from a given conceptual depth. Increasing the depth should increase the number of surviving drops, but should not alter the rate at which they survive. Figures 5.11–5.13, respectively, show the results of a run with depths of 1, 1.5, and 2 units. Each subarea is a different fraction of the total contributing area. Increasing subarea number also means

increasing travel time. Note that survival fraction diminishes with subarea number and time, but survival fraction at each step is the same for all three pulses, and note that depth of rainfall surviving diminishes with time.

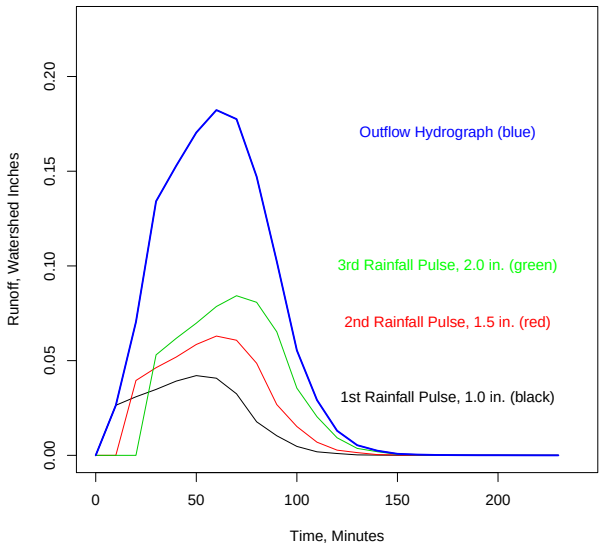


**Figure 5.11.** Graph of the result of three sequential rainfall pulses with conceptual depths of 1, 1.5, and 2 inches of rainfall (black, red, and green respectively) and the aggregated conceptual outflow hydrograph (blue). Ordinates represent watershed inches per time step.

As suspected, numbers of surviving drops change, but rates do not. Figure 5.11 shows the conceptual outflow hydrograph generated by the aggregation of rainfall pulses of 1, 1.5, and 2 inches of conceptual rainfall, represented as 1 inch being 1 million drops. Time begins at the first rainfall pulse, generating a response consisting of 20 time steps, each of 1/20 of he total time of contribution of the topographic watershed ($T_c$). At a time of 1/20 $T_c$ later, a second pulse occurs, this pulse of larger magnitude (1.5 inches). The second pulse results in a similar response, larger by proportion. At a time of 2/20 $T_c$, a third pulse occurs, with a similar, proportional response. The ordinates of all three responses are aggregated at the remaining time steps to construct a hydrograph resulting from 3 rainfall pulses of different depths. Figure 5.12 shows the number of drops from each time step (subarea) surviving from each of the three pulses of different depths. Larger depths result in more survival, but as Figure 5.13 shows, the rate of survival is indistinguishable. For a constant $\lambda$ value in the exponential distribution, rate of survival is indistinguishable.

At this point, the question might arise what advantage this process offers over UH computations. The answer is contained in Figures 5.11–5.13. From graphs such as these (and the numbers they are composed of) it can be seen that contribution of runoff is not uniform in terms of area—rain that falls on the distal areas of the watershed is much less likely to survive the journey to the point of interest than is rain that falls close to the point of interest. The effect under discussion, rather than the assumption that the entire watershed contributes uniformly, accounts for diminishing influence with time and distance. The advantages in real watershed simulation might be in representing the effects of land-use changes, urbanization, vegetation management, and many other of the uses of watershed modeling.

Another advantage that might not be evident immediately is that the idea of "critical duration" for watershed response is relaxed, at least to some extent. A consequence of the partial area concept occasionally cited (Wong, 2007), but often not mentioned, is that acknowledgment that watershed area does not contribute uniformly, fundamentally alters the characteristic time of response. The need of having storm duration match travel time from the most remote point is less acute. Because, in the survival model, areas closer to the point of interest contribute a larger proportion of the rainfall they receive than do more

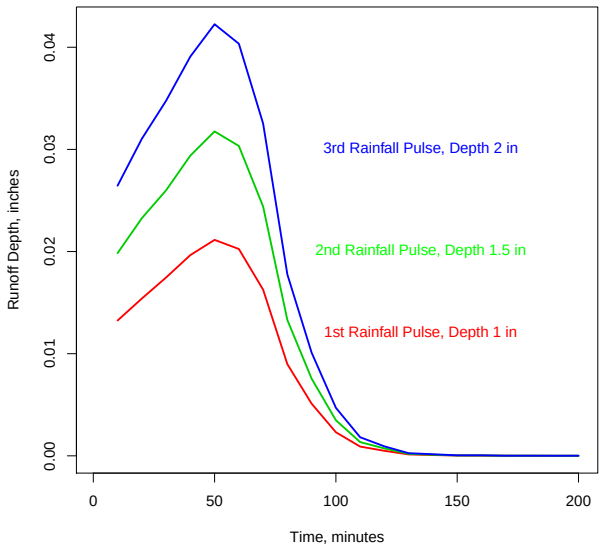


**Figure 5.12.** Graph of the depth of conceptual rainfall surviving for three sequential rainfall pulses with conceptual depths of 1, 1.5, and 2 inches of rainfall. Ordinates represent watershed inches per time step.

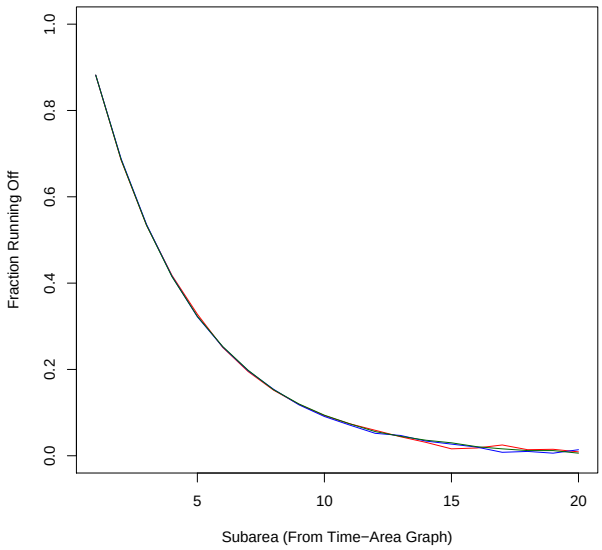


**Figure 5.13.** Graph of the fraction of conceptual drops surviving for three sequential rainfall pulses with conceptual depths of 1, 1.5, and 2 inches of rainfall. Ordinates represent watershed inches per time step.

than distal areas, shorter duration, more intense events may result in larger discharges than those of duration closer to total travel time, that might be assumed to engage full watershed contribution.

## 5.10 Case Study

As further illustration of the concept, a case study is shown using time-area information and real rainfall-runoff data from Ash Creek near Dallas, Texas. These data originated in a previous study (Cleveland et al., 2008) and were used for continuity.

Time-area data as obtained were cumulative, in even grid cell increments (from GIS) with associated travel time to the outlet. Total travel time to the outlet was shown as 192 minutes. Time-area data were depopulated in a way to provide cumulative area for 20 even time increments, rounded to 10 minutes each, for a total travel time to the outlet of 200 minutes. Cumulative data were then differenced to obtain incremental area data for each 10 minute time step. A cumulative time-area graph is shown in Figure 5.14 and an incremental time-area histogram is shown in Figure 5.15.

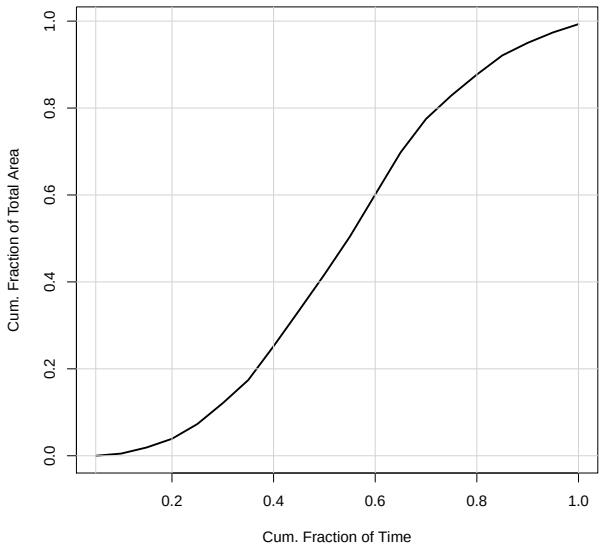


**Figure 5.14.** Cumulative time-area graph for the Ash Creek watershed. This graph is comparable to that of Figure 5.2, but for a different watershed.

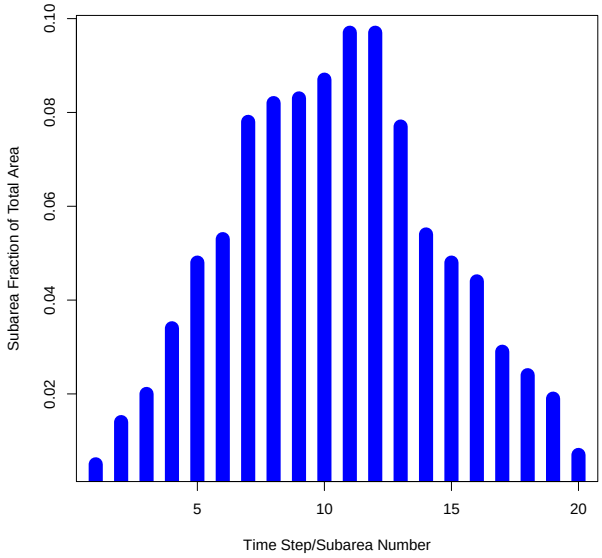


**Figure 5.15.** Time-area histogram for Ash Creek. Some minor smoothing has been done by examination to eliminate a pronounced double peak in the raw data. This graph is comparable to Figure 5.3, but for a different watershed.

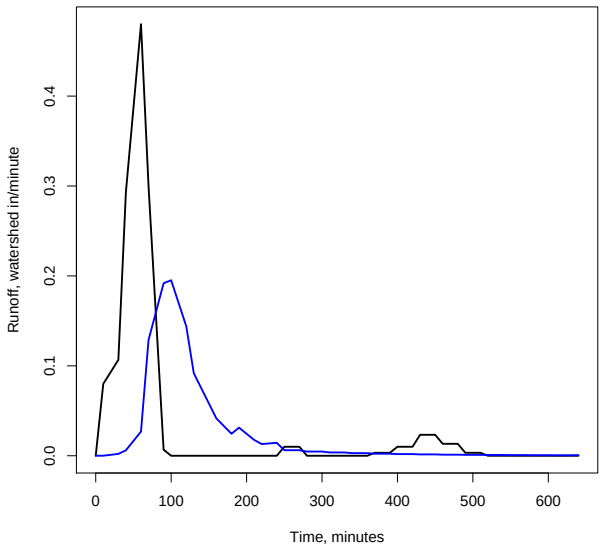


**Figure 5.16.** Graph of measured rainfall (black) and runoff (blue) from the Ash Creek Watershed for a simple event. These are the data strings used for the first case study. Ordinates represent watershed inches per time step.

Rainfall and runoff data as obtained were cumulative inches, in one minute increments. These data were depopulated to 10-minute increments, to match the time step size of the time-area data. Two different sets of rainfall-runoff data were selected for study, one 24-hour dataset with a single main event, and one 48-hour dataset with multiple rainfall and runoff events. Both datasets were reduced to a length smaller and more convenient than a full 24 and 48 hours for simplicity. Graphs of the rainfall and runoff from the simple event on the Ash Creek watershed is shown in Figures 5.16.

The prospective model requires parameter input in vector form, with each vector representing different parameter values for each rainfall pulse. Inputs are a rainfall pulse depth vector and a vector of $\lambda$ values for the exponential distribution, with one value for each rainfall pulse values. The modeling program as described previously was run with a vector of rainfall values as shown in Figure 5.17, and a vector of $\lambda$ values all equal to 7.5. The individual hydrographs resulting from rainfall pulses are shown in Figure 5.17 in various colored light curves, with the convolved conceptual runoff hydrograph shown as the heavy blue curve. It is worthy of note that the only quantity varied in this case study was rainfall depth; $\lambda$ values are uniform at 7.5.

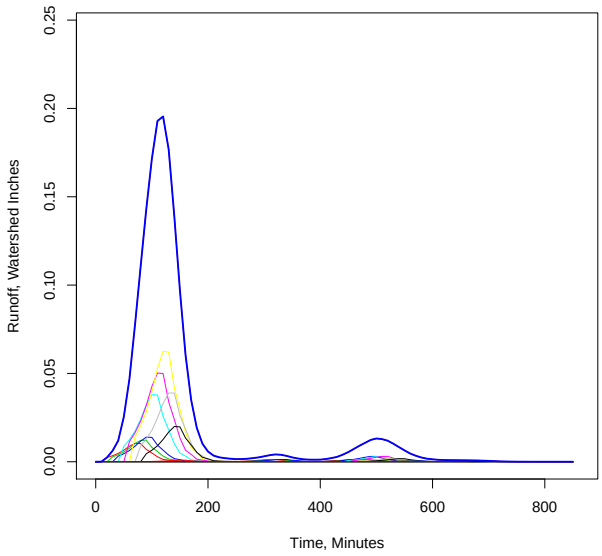


**Figure 5.17.** Model results using the Ash Creek time-area graph, a constant $\lambda$ of 7.5, and measured rainfall depths. Ordinates represent watershed inches per time step.

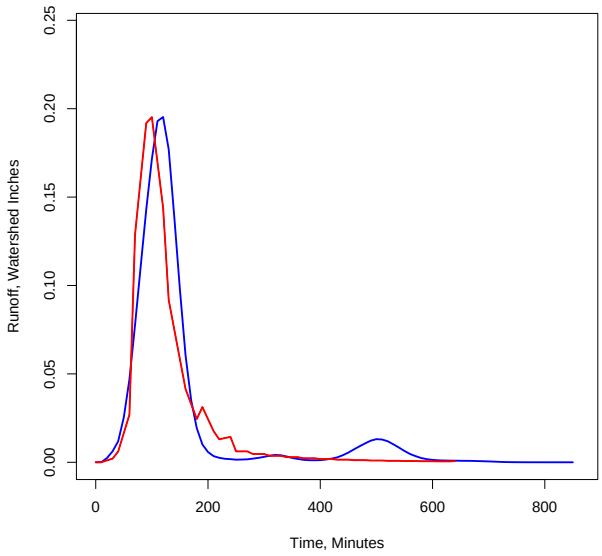


**Figure 5.18.** Comparison of measured (red) and computed (blue) hydrographs for Ash Creek for a simple event. Watershed inches of measured runoff is compared to watershed inches of computed runoff per time step.

Both rainfall and flow data are in units of depth (inches). In the conceptual model, one inch of rainfall is represented by 1 million conceptual rain drops distributed over the 20 time steps as per the time-area graph, resulting in varying amounts of conceptual rain in each rainfall pulse. A graph showing conceptual runoff compared with real runoff is shown in Figure 5.18. Whereas not a precise fit, this comparison shows fit similar to what often is observed in the calibration of traditional models. It is emphasized that the fit seen was obtained with minimal parameter adjustment; $\lambda$ was held constant. For clarity, graphs and discussion are based on the conversion of conceptual drops to inches being 1 million drops to one inch.

The second case study is the same watershed, Ash Creek, using data that involve a more complicated series of events. Figure 5.19 shows raw rainfall and runoff data for this time series.

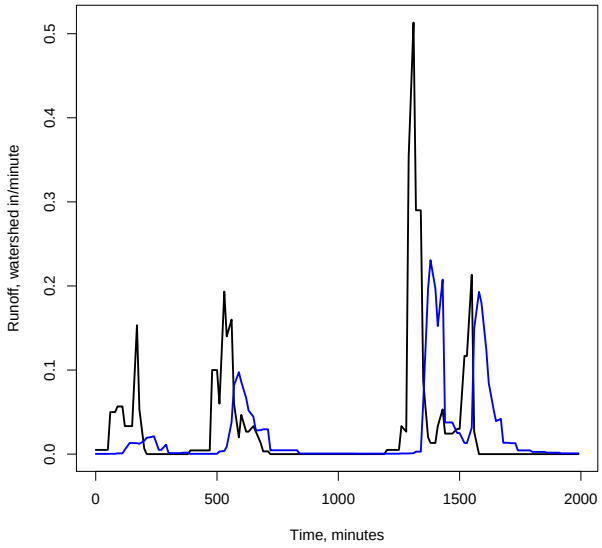


**Figure 5.19.** Graph of measured rainfall (black) and runoff (blue) from the Ash Creek Watershed for a string of events. These are the data strings used for the second case study. Ordinates represent watershed inches per time step.

Figure 5.20 shows the results of model runs with the results of individual rainfall pulses shown in various colors, while Figure 5.21 shows model results compared to actual runoff. In this case of 200 rainfall pulses, fit was obtained for the majority of the time series with value of 1 in the rate vector. However, the first small pulse showed larger computed than actual discharge.

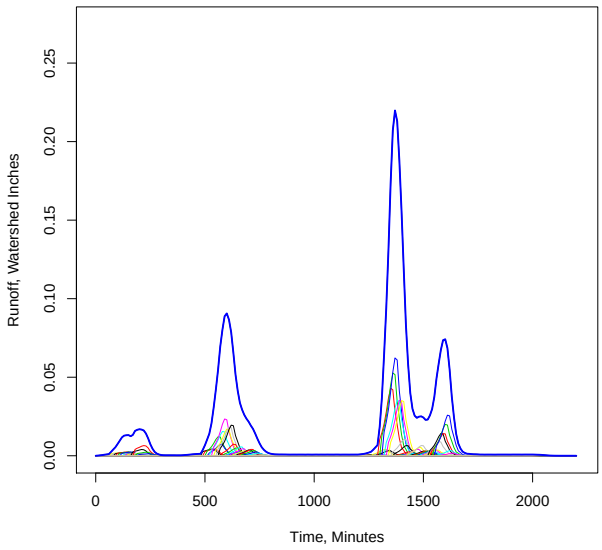


**Figure 5.20.** Model results using the Ash Creek time-area graph, a constant $\lambda$ of .75, and measured rainfall depths.

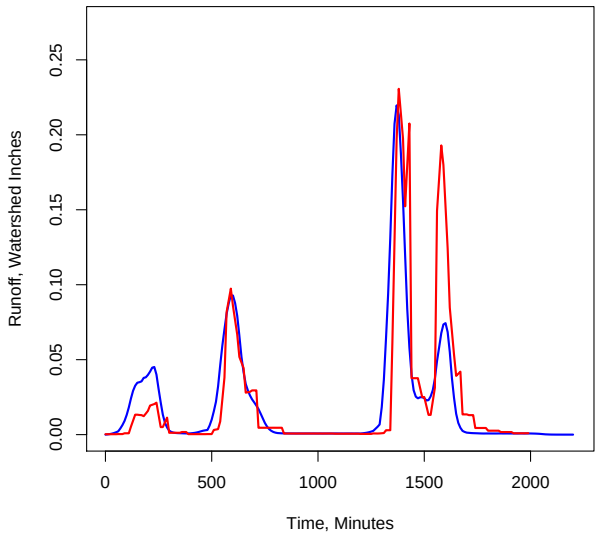


**Figure 5.21.** Initial comparison of measured (red) and computed (blue) hydrographs for Ash Creek for a series of events. Rate value for the entire series is 1. Note that the model overestimates survival for the first pulse of runoff. Ordinates represent watershed inches per time step.

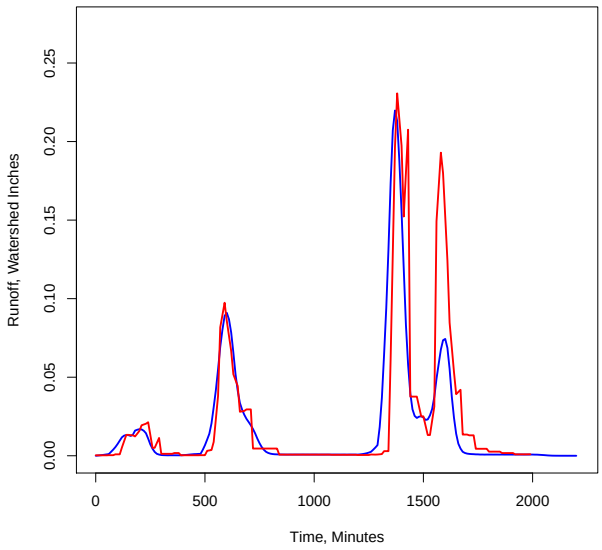


**Figure 5.22.** Comparison of measured (red) and computed (blue) hydrographs for Ash Creek for a series of events with the rate value varied. Rate for the first 50 pulses of rainfall was raised from 1 to 5, resulting in better fit for the first pulse. Ordinates represent watershed inches per time step.

Fit for the first pulse was enhanced by coding the first 50 of 200 values in the rate vector at a value of 5, a relatively simple adjustment that reduced survival during the early part of the time series, as shown in Figure 5.23. An attempt was made to obtain better fit for the last large runoff pulse by reducing values in the rate vector to very small, enhancing survival in the latter part of the time series. This attempt was not successful; it appears that rainfall recorded was insufficient to account for the magnitude of that pulse, as raising survival to nearly 100 percent in the latter stages did not result in a better fit.

Compared with many watersheds, the Ash Creek data displays a very high runoff production— the volumetric runoff coefficient for the simple event used is 0.746. Thus, Ash Creek cannot be considered an arid watershed. The Survival Model is thought by the author to be most applicable to arid watersheds with large loss rates and small runoff rates. The application of the model to such watersheds will await future research

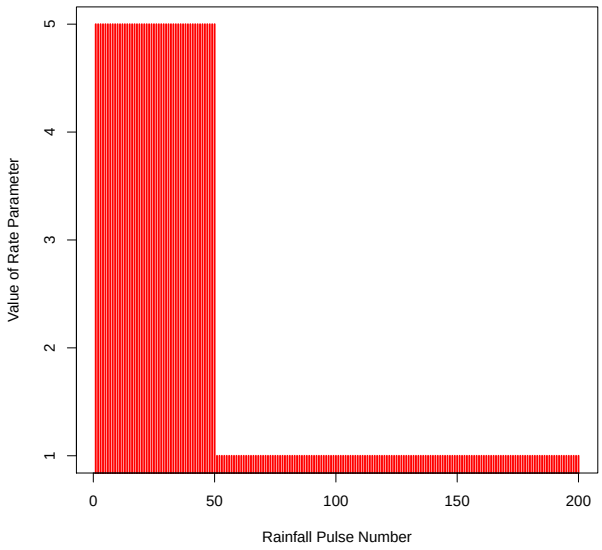


**Figure 5.23.** Rate values used to fit the series of events represented in Figures 5.20 and 5.22 for the Ash Creek watershed

## 5.11 Discussion of the Survival Model

Traditional UH methods (dealing with other than base flow) are based on five basic assumptions: (Chow et al., 1988)

1. The excess rainfall has a constant intensity within the effective duration (within a time step);
2. The excess rainfall is uniformly distributed throughout the whole drainage basin;
3. The base time of the direct runoff hydrograph (DRH; the duration of direct runoff) resulting from an excess rainfall of a given duration is constant;
4. The ordinates of all DRH's of a common time base are directly proportional to the total amount of direct runoff represented by each hydrograph; and
5. For a given watershed, the hydrograph resulting from a given excess rainfall reflects the unchanging characteristics of the watershed.

Chow et al. (1988) then continue:

> Under natural conditions, the above assumptions cannot be perfectly satisfied. However, when the hydrologic data to be used are carefully selected so that they come close to meeting the

> above assumptions, the results obtained by the UH model are generally acceptable for practical purposes ...

The assumptions listed begin with the assumption of excess (effective) precipitation; total rainfall is assumed to have been subjected to a loss model prior to the applicability of the assumptions; the property of distinct segregation of excess precipitation from total precipitation is a cornerstone of UH theory. Assumptions of linearity of the UH, uniform precipitation over the drainage basin, and time base are all necessary assumptions.

In truth, the survival model is subject to very similar assumptions. Paraphrasing the above assumptions and adapting them to the survival model:

1. The total rainfall has a constant intensity within the effective duration (within a time step);
2. The total rainfall is uniformly distributed throughout the whole drainage basin;
3. The base time of the DRH resulting from an rainfall pulse of a given duration is constant, but shape changes by survival weights of each subarea of the time-area graph;
4. The ordinates of all DRH's of a common time base are proportional to the depth of rainfall *and the survival weights of each subarea of the time-area graph;* and
5. For a given watershed, the hydrograph resulting from a given excess rainfall reflects the unchanging characteristics of the watershed *weighted by the time-dependence of the loss process.*

The survival model integrates the time-dependent loss process into the stepwise response simulation process, allowing time weighting of contribution from the watershed according to the time-area graph. The time-area graph provides the time invariant anchor; because if the nature of the graph, the time base of runoff is defined in the same way as for traditional UH modeling. Time invariance of the time-area graph and a constant time base of runoff allow the aggregation of runoff from subsequent rainfall pulses as in traditional UH computations. The survival model is able to *simulate* partial and variable area because of the time dependent weighting of contribution from proximal/distal subareas. The shape of the response to each pulse of rainfall is not necessarily the same or proportional to any other response, it is proportional to the time-area graph and to the survival from the various subareas, controlled by the distributional specification. The survival model does not depend on the property of distinct segregation of excess precipitation from total precipitation. This property alone is a unique aspect of the method. The segregation of effective precipitation from total precipitation has long been a complication of linking measured with modeled runoff (Asquith et al., 2005; Asquith and Roussel, 2007).

In both of the examples above, the proposed method produces results that are consistent with expectation for a watershed model. Differences between this and traditional methods include the ability of this model to easily and simply simulate partial or variable area contribution, to present varying time-to-peak, and to simulate non-uniformity of contribution from areas in the watershed. The role of partial area contribution in the context of loss models is discussed in Betson (1964). As an alternative to considering equations such as Horton's to explain infiltration with time, Betson alludes to such ideas as ways to explain an increase in contributing area with time. The discussion in Betson is very close in concept to the model under discussion.

All of these differences are difficult to simulate with lumped models currently in use. Subdivision of watersheds for modeling, even to the degree of gridded models, is commonplace in the profession order to provide some simulation of these complications. Even such distributed models continue some of the simplifying assumptions that depart from reality; for instance, in-transit loss of continuity is seldom, if ever, considered. As with conventional lumped models, uniformity of contribution is assumed; the membrane analogy persists.

A distinct advantage of a model that simulates non-uniformity of contribution may well lie in the area of simulating advective transport; sediment and contaminants spring immediately to mind. Simulating, even in a rudimentary manner, the relative contribution from proximate versus distal areas of the watershed may provide considerable insight into erosion and sources of sediment, as well as the spread of contaminants from sources within a watershed. Developed further, a model of this nature could provide some simulation of contaminant transport distance and distribution within a watershed, not just out of it. The central question asked in the model shown is "How many drops survive the journey to the outlet?" Simulating the transport of contaminants by use of this model would only require modification of the central question to the following: "How far does each drop travel, and bear contaminants, before it suffers fatality, depositing contaminants?"

Because this modeling technique uses a time-area curve as a major component, it may be well adapted to simulating urbanization. Traditional methods consider increase in "impervious area" as a major variable, as well as contraction of the time of contribution. Both of these quantities imply increased transport efficiency. The derivation of pre- and post-development time-area curves, as well as isochrone maps similar to Figure 5.1, could provide information not only on changes in volume, timing, and peak rate of runoff, but changes in contaminant movement path, distribution, and concentration over time. Currently, such information is subject to the same simplifying assumptions as runoff itself.

Versions of the model were developed using both the exponential and two-parameter Weibull distributions, and both were compared side by side. The Weibull, having two parameters (scale and shape), was thought to be more flexible in fitting. Comparing the two, the scale parameter of the Wiebull compares with the $\lambda$ of the exponential; in fact, the Weibull with the shape parameter of 1 becomes the exponential. The shape parameter appeared in this case to be of no practical value in assisting fit. Code for both is included in the section on **R** code. The exercises shown were accomplished using the Exponential distribution only. It is thought that the high survival rate (large runoff fraction) of the Ash Creek data may curtail advantages of the Weibull distribution as compared to the exponential distribution. Case studies on arid watersheds may return different results.

## 5.12 Chapter Summary, Conclusions, and Observations

### 5.12.1 Summary

In this chapter, the author has examined traditional watershed modeling techniques, critiqued them, and made note of certain core concepts that are recognized as gross simplifications. The idea that all areas of a watershed contribute uniformly under storm conditions has been called into question, along with the necessity and utility of that idea as a modeling constraint. A detailed examination of the literature on partial and variable area contribution is given.

Substituted for the ideas in traditional UH modeling is an idea that is equally elegant, but uncommon and more difficult to analyze. The idea presented is that the likelihood of a drop of rain traveling to the outlet is inversely proportional to residence time on the watershed. Residence time for a traveling raindrop is dependent on the distance it must travel to reach the outlet, therefore raindrops landing on areas far removed from the outlet are thought to have a much smaller chance of traveling to the outlet than do those that land closer. A computer model based on this assumption has been constructed, has been shown it to produce results that are consistent with the core concepts and ideas.

Whereas these ideas have been demonstrated as useful and viable, much work remains before they can be considered fully functioning tools. In particular, the investigation of more complex probability distributions should be undertaken. Some link between $\lambda$ values and traditional loss rates might be drawn from additional case studies

### 5.12.2 Conclusions

The attraction of a model of this type is that it might better represent the runoff generation process as it really exists, particularly in arid areas. The traditional technique of UH modeling implies that rainfall frequency maps to flood frequency in a 1:1 manner, and the idea that full watershed contribution should be assumed in frequency-based modeling (attempts to estimate discharges of specific probabilities) is still the prevailing notion (Boughton, 1987). Statistical analysis of stream gauge data results in values that very often do not correlate well to those produced by rainfall-runoff modeling. When watershed modeling is performed in arid- and semi-arid areas and is compared to the statistics of observed streamflow, it is common to encounter poor fit between the two. Forcing a match at infrequent (large magnitude) events by parameter manipulation of the watershed model usually results in over-estimation of discharge at more frequent event magnitudes as compared to the results of statistical procedures.

A possible source of this inconsistency is that full watershed contribution is not associated with the probabilities of interest, and that partial area contribution could be a dominant occurrence. In effect the watershed is behaving as if it is smaller because distal areas are not contributing significantly. In such a case, characteristic time of response would be shorter, rainfall depth associated with critical duration would be smaller, but rainfall intensity associated with critical duration would be larger.

### 5.12.3 Observations

The survival model weights contribution from area close to the point of interest more than that further away, in effect emphasizing partial area and variable area effects, as well as de-emphasizing the value of full watershed contribution. It does so in a simple, parsimonious way. The need to attempt to delineate the areas of partial or variable contribution is circumvented, as is the need for detailed physical process parameters in those areas; the model uses the *topographic watershed* as do traditional models, as the beginning unit, and accounts for variable or partial area contribution by inverse area weighting. Alleviation of the need to distinguish the *topographic watershed* from the *hydrologic watershed* is a conceptual leap forward in practical techniques that capitalizes on the partial/variable area idea. Characteristic time can begin with time associated with the topographic watershed, and be adjusted to that of the hydrologic watershed after initial trial results.

In UH modeling as it is currently undertaken, there are certain parameters that must be specified. For instance, the popular SCS method (also known as NRCS method) requires:

- A rainfall distribution,
- Watershed area,
- A time parameter called "basin lag time,"
- A "curve number" to specify loss, and
- A response kernal—the UH.

The shape of the UH is specified by the fact that it is the SCS method; the shape of the SCS Dimensionless UH (DUH), either the curvilinear version or the triangular version, has traditionally been fixed. Watershed area and basin lag time dimensionalize the DUH. The SCS method works best when the rainfall distribution is one of those recommended by the originating agency, also called SCS distributions. These are typically constrained to 24 hour durations and depths of rainfall.

With the Survival model, other parameters must be specified. These include:

- A rainfall distribution,
- Watershed area—not yet incorporated into the code, but necessary to fully dimensionalize runoff,
- A time step size—the code provided uses $1/20$ of the total time of contribution of the topographic watershed,
- A time-area graph, and
- A vector of rate parameters for the exponential version; vectors of scale and shape parameters for the Weibull version.

Experience has shown that the performance of the SCS method is questionable if used with rainfall distributions other than those recommended by the SCS; the method seems "tuned" to work best together. The Survival model can accomodate any rainfall distribution.

The Survival model, therefore, is similar in parsimony to the SCS method. If the Weibull version is used, one additional piece of information is needed. However, constraints on response kernel shape and rainfall distribution shape and duration are relaxed for the Survival model. The role of the response kernel in UH modeling has been divided between the time-area graph and the survival rates of various subareas.

Thus it can be said that for similar parsimony, the Survival model offers fewer constraints, and because of the division of the response kernel, it can simulate partial area/variable area response. These advantages alone hold considerable promise.

At this time, no link between distributional parameter values and useful watershed property metrics is known. It has been shown that the model can be fitted to real data, but synthetic modeling is the subject of future work.

This model has been discussed under the name "Survival model" during this discussion. The literature on "survival" from a statistical standpoint is rich in depth, but was not very helpful in the case of this model. The model in question is really too simplistic to benefit from the survival literature. The Survival model is more closely mirrored in residence time distribution modeling, however even in that context, it is an example of elementary simplicity. It is, in truth, a simple expression of a "washout" function as discussed in residence time. However, the very simplicity that places it at the bottom of the heap of problems associated with survival and residence time is one of the most attractive aspects of the model.

The beauty of this model is the potential ability to represent partial/variable area contribution simply enough to be of practical use to the working engineering community. Research into and interest in the areas of partial/variable area has been ongoing for over four decades, since Betson (1964) with limited progress toward the goal of making it a useful engineering tool.

In principle further research along this path could develop procedures and correlations with real data to allow repeatable simulation of partial area effects, including critical duration of rainfall.

# Chapter 6
# Overall Conclusions

The four topical chapters included in this dissertation all pivot on a common theme. The primary theme is the relationship among geomorphology, stream behavior, and hydrologic response. The author's interest in this topic dates back many years prior to beginning a personal and academic association with engineering and hydrology. Because of that interest, focusing on that theme for a doctoral dissertation seems poetic.

The author had taken two professional level training courses in fluvial geomorphology in the five years prior to encountering the issues at Guadalupe Arroyo. The first was given in Austin to TxDOT personnel only by Craig Fischenich, Ph.D., of the U.S. Army Corps of Engineers. That course was an epiphany; in particular it pointed out how much information was available from streams themselves—the streams themselves tell a story and that story was being overlooked by practicing engineers. The second was the introductory course of a series given by David Rosgen, Ph.D., of Wildland Hydrology (Fort Collins, Colorado, USA). Both of the courses were very valuable.

The Guadalupe Arroyo study, and the subsequent paper, began a line of thought and reinforced how geomorphology, hydrology, hydraulics, and sediment transport are coupled and inseparable. It also demonstrated that very unusual combinations of difficult factors can be encountered in the real world. Engineers, especially those with special expertise and advanced knowledge, are often called upon to deal with chronic problem sites. It seems logical to assume that if a particular site exhibits severe, chronic problems, that site is probably unusual in some way. In the opinion of the author, with many years of experience as a practicing engineer in the field, recognition of extraordinary problems is something that engineers are not trained or educated for as a matter of general academic and professional development. For that matter, academic and professional development seldom even acknowledge the possibility and existence of extraordinary problems other than by oblique reference. Experience dealing with these issues institutionally indicates

that many engineers are uncomfortable with the existence of extraordinary problems. For these reasons, ordinary solution techniques are often applied to extraordinary problems, often with poor results. Guadalupe Arroyo is such a case, and has been for decades.

The Guadalupe Arroyo paper (Chapter 2) documented an extraordinary case, as well as stimulating questions that echoed for several years. Chapter 3 discusses an article published in October, 2013, which resulted in part from the inquiry into Guadalupe Arroyo. The article in question is included in its entirety in Appendix A. The techniques developed for that paper may well provide guidance for similar, future studies. The implications for hydraulic modeling review, as well as abbreviated bridge scour analyses, are far reaching. The most important lesson learned by the work on this paper is that the physical shape of a stream may tell us more about the behavior of that stream than any model. There is some elegance in that fact; the physical shape of a stream is the result of its behavior, so it make sense that the shape contains information about the behavior.

Chapter 4 illustrates another extraordinary case, this time on the scale of a large watershed. The behavior of the river examined appears to be a result of the influence of rugged terrain, exacerbated by proximity, on the flood characteristics of a large and well-known stream. The detection of this phenomenon was permitted by the fact that it is a large stream with multiple streamgauges and heterogeneous terrain. It is unknown how these issues may manifest themselves on smaller watersheds, The idea of proximity being an important factor in hydrologic response appears not to be a new one, but literature dealing specifically with it is sparse, except in the context of partial area contribution. Hydrologic modeling methodology that treats different parts of a watershed separately, such as distributed watershed modeling, could in theory be adapted to do so, but guidance in the literature was not found.

Chapter 5 was stimulated by both a long standing mental picture of watershed processes in the context of time dependent losses, and the idea of proximity stemming from the issues that drove the case study in Chapter 4. A model was conceived by the author that accounted for inverse distance effects. Several of the standard paradigms of watershed modeling are challenged by this modeling concept; yet the concept appears sound and is executable. This model has been discussed under the name "survival model" for some time among the author and colleagues. The literature on “survival” from a statistical standpoint was not very helpful in this case, and the term may be slightly misleading. The model in question is really too simplistic to benefit from the survival literature. It is really a simple, “decay” model. It is more closely mirrored in residence time distribution modeling, however even in that context, it is an example of elementary simplicity. However, the very simplicity that

places it at the bottom of the heap of problems associated with survival and residence time is one of the most attractive aspects of the model.

Chapters 4 and 5 constitute the bulk of the uniquely original work exclusive to the author not previously published. There are many issues that remain unresolved. Among those are the specific identification of sites that exhibit behavior converse to the behaviour of the watersheds shown in Chapter 4. The development of a useful metric of terrain ruggedness awaits discovery or validation and acceptance, and the influence of such a metric on flood frequency analysis is speculative. In the context of Chapter 5, the use of other distributions should be investigated, as well as complete investigation of parameterization issues. Practical methods of assigning parameter values that correspond to physical variables representing runoff production is essential. Whereas the presentation of this model conceivably constitutes a paradigm shift with respect to watershed modeling techniques, at this time it remains an experimental method.

With the exception of the paper presented in Appendix A, the works presented here are, implicitely or explicitely, geared towards arid environments. Guadalupe Arroyo and the lower Pecos River are both located in arid environments at the place investigated. The Survival model grew from the context of an arid environment, where survival of rainfall may be the exception, rather than the rule. In environments with more rainfall, the interesting aspects of survival and inverse distance weighting may be of less significance. The environments studied in this dissertation, arid climate and rugged terrain, are consistent with the primary interests of the author.

*George R. Herrmann, P.E., P.H., CFM, SIT, Lubbock, Texas, Fall, 2013*

# References

American Society of Civil Engineers (1996). *River Hydraulics: Technical Engineering and Design Guides*. New York: ASCE Press.

Amerman, C. R. (1965). The Use of Unit-Source Watershed Data for Runoff Prediction. *Water Resources Research 1*, 499–508.

Arneson, L. A., L. W. Zevenberger, P. F. Lagasse, and P. E. Clopper (2013). *Evaluating Scour at Bridges*. Washington, DC, USA: USDOT-FHWA.

Asquith, W. H. (1998). Peak-Flow Frequency and Extreme Flood Potential for Tributaries of the Colorado River Downstream of Austin, Texas. Water-Resources Investigations Report 98–4015, U.S. Geological Survey.

Asquith, W. H. (2001). Effects of Regulation on L-moments of Annual Peak Streamflow in Texas. Water-Resources Investigations Report 01–4243, U.S. Geological Survey.

Asquith, W. H., G. R. Herrmann, and T. G. Cleveland (2013). Generalized Additive Regression Models of Discharge and Mean Velocity Associated with Direct–Runoff Conditions In Texas: Utility of the U.S. Geological Survey Discharge Measurement Database. *Journal of Hydrologic Engineering 18*, 1331–1348.

Asquith, W. H. and M. C. Roussel (2004). Atlas of Depth-Duration Frequency of Precipitation Annual Maxima for Texas. Scientific Investigations Report 2004–5041, U.S. Geological Survey.

Asquith, W. H. and M. C. Roussel (2007). An Initial-Abstraction, Constant-Loss Model for Unit Hydrograph Modeling for Applicable Watersheds in Texas. Scientific Investigations Report 2007–5243, U.S. Geological Survey.

Asquith, W. H. and M. C. Roussel (2009). Regression Equations for Estimation of Annual Peak-Streamflow Frequency for Undeveloped Watersheds in Texas Using an L-moment-based, PRESS-minimized, Residual-adjusted Approach. Scientific Investigations Report 2009–5087, U.S. Geological Survey.

Asquith, W. H., M. C. Roussel, T. G. Cleveland, X. Fang, and D. B. Thompson (2006). Statistical Characteristics of Storm Interevent Time, Depth, and Duration for Eastern New Mexico, Oklahoma, and Texas. Professional Paper 1725, U.S. Geological Survey.

Asquith, W. H., M. C. Roussel, and J. Vrabel (2006). Statewide Analysis of the Drainage-area Ratio Method for 34 Streamflow Percentile Ranges in Texas. Scientific Investigations Report 2006–5286, U.S. Geological Survey.

Asquith, W. H. and R. M. Slade (1997). Regional Equations for Estimation of Peak-Streamflow Frequency for Natural Basins in Texas. Water-Resources Investigations Report 96–4307, U.S. Geological Survey.

Asquith, W. H., R. M. Slade, and J. Lanning-Rush (1996). Peak-Flow Frequency and Extreme Flood Potential for Streams in the Vicinity of the Highland Lakes, Central Texas. Water-Resources Investigations Report 96–4072, U.S. Geological Survey.

Asquith, W. H. and D. B. Thompson (2008). Alternative Regression Equations for Estimation of Annual Peak-Streamflow Frequency for Undeveloped Watersheds in Texas Using PRESS Minimization. Scientific Investigations Report 2008–5084, U.S. Geological Survey.

Asquith, W. H., D. B. Thompson, T. G. Cleveland, and X. Fang (2005). Unit Hydrograph Estimation for Applicable Texas Watersheds. Research Report 0-4193-4, Texas Tech University, Center for Multidisciplinary Research in Transportation;.

Barnes, H. H. (1967). Roughness Characteristics of Natural Channels. Water Supply Paper 1849, U.S. Geological Survey.

Betson, R. P. (1964). What is Watershed Runoff? *Journal of Geophysical Research 69*, 1541–1552.

Beven, K. J. and M. J. Kirkby (1979). A Physcially Based, Variable Contributing Area Model of Basin Hydrology. *Hydrological Sciences Bulletin 24*, 43–69.

Bomar, G. W. (1994). *Texas Weather*. Austin, Texas: University of Texas Press.

Botter, G., E. Bertuzzo, and A. Rinaldo (2011). Catchment Residence and Travel Time Distributions: The Master Equation. *Geophysical Research Letters 38*.

Boughton, W. C. (1987). Evaluating Partial Areas of Watershed Runoff. *Journal of Irrigation and Drainage Engineering 113*, 356—366.

Box, G. E. P. and D. R. Cox (1964). An Analysis of Transformations (with discussion). *J. Royal Stat. Soc., Series B 26*, 211–252.

Briaud, J., H. C. Chen, K. A. Chang, Y. A. Chung, N. Park, W. Wang, and P. H. Yeh (2007). Establish Guidance for Soil Properties–Based Prediction of Meander Migration Rate. Research Report 0-4378-1, Texas Department of Transportation.

Briaud, J., H. C. Chen, Y. Li, P. Nurtjahyo, and J. Wang (2003). Complex Pier Scour and Contraction Scour in Cohesive Soils. Research Report 24-15, National Cooperative Highway Research Program.

Briaud, J., A. V. Govindasamy, D. Kim, P. Gardoni, F. Olivera, H. C. Chen, C. Mathewson, and K. Elsbury (2009). Simplified Method for Estimating Scour at Bridges. Research Report 0-5505-1, Texas Department of Transportation.

Bull, L. J. and E. Kirkby, M. J. (2002). *Dryland Rivers; Hydrology and Geomorphology of Semi-arid Channels*. Chichester, West Sussex, England: John Wiley and Sons, LTD.

Castro, J. M. and P. L. Jackson (2001). Bankfull Discharge Recurrence Intervals and Regional Hydraulic Geometry Relationships: Patterns in the Pacific Northwest, USA. *Journ. Amer. Wat. Res. Assoc. 37*(5), 1249–1262.

Chow, V. T., D. R. Maidment, and L. W. Mays (1988). *Applied Hydrology*. New York, NY, USA: McGraw-Hill.

Clark, G. M., D. K. Mueller, and M. A. Mast (2001). Nutrient Concentrations and Yields in Undeveloped Stream Basins of the United States. *J. Amer. Wat. Res. Assoc. 36*(4), 849–860.

Clark, M. M. (1996). *Transport Modeling for Environmental Engineers and Scientists*. New York, NY, USA: John Wiley and Sons.

Clarke, C. O. (1945). Storage and the Unit Hydrograph. *Transactions of the American Society of Civil Engineers 100*, 1419–1488.

Cleveland, T. and D. Thompson (2009). Subdivision of Watersheds for Hydrologic Modeling. Research Report 0-5822-01-2, Texas Department of Transportation.

Cleveland, T. G., D. B. Thompson, and X. Fang (2011). Use of the Rational and Modified Rational Method for Hydraulic Design. Research Report 0-6070-1, Texas Department of Transportation.

Cleveland, T. G., D. B. Thompson, X. Fang, and X. He (2008). Synthesis of Unit Hydrographs From a Digital Elevation Model. *Journal of Irrigation and Drainage Engineering 34*, 212–221.

Coffman, D. K., G. Malstaff, and F. T. Heitmuller (2011). Characterization ofGgeomorphic Units in the Alluvial Valleys and Channels of Gulf Coastal Plain Rivers in Texas, with Examples from the Brazos, Sabine, and Trinity Rivers. Scientific Investigations Report 2011–5067, U.S. Geological Survey.

Cooley, S. W. (2013). GIS 4 Geomorphology.

Corradini, C., R. Morbidelli, and F. Melone (1998). On the Interaction Between Infiltration and Hortonian Runoff. *Journal of Hydrology 204*, 52–67.

Dalrymple, T. and M. A. Benson (1967). Measurement of Peak Dscharge by the Slope-Area Method. Techniques of Water Resources Investigations Book 3, Chapter A2, U.S. Geological Survey.

Devulapalli, R. S. and J. B. Valdes (1996). Volume-Duration-Frequencies for Ungaged Catchments in Texas: Volume 1, Calculation of Regional Regression Equations. Technical Report 173, Texas Water Resources Institute, Texas A&M University, College Station, Texas.

Dooge, J. C. I. (1959). A General Theory of the Unit Hydrograph. *Journal of Geophysical Research 64*, 241–256.

Dooge, J. C. I. and M. Bruen (1989). Unit Hydrograph Stability and Linear Algebra. *Journal of Hydrology 111*, 377–390.

Drever, J. I. (1997). *The Geochemistry of Natural Waters* (3 ed.). Upper Saddle River, NJ, USA: Prentice Hall.

Dunne, T. and R. D. Black (1970). Partial Area Contributions to Storm Runoff in a Small New England Watershed. *Water Resources Research 6*, 1296–1311.

Eagleson, P. S., R. Mejia-R, and F. March (1966). Computation of Optimum Realizable Unit Hydrographs. *Water Resourcesl Research 2*(4), 755–764.

Engman, E. T. (1974). Partial Area Hydrology and Its Application to Water Resources. *Water Resources Bulletin 10*, 512–521.

Engman, E. T. and A. S. Rogowski (1974). A Partial Area Model for Storm Flow Synthesis. *Water Resources Research 10*, 464–472.

Fang, X., T. Cleveland, C. A. Garcia, D. Thompson, and R. Malla (2005). Literature Review on Timing Parameters for Hydrographs. Research Report 0-4696-01, Texas Department of Transportation.

Faraway, J. J. (2005). *Linear Models with R*. Boca Raton, Florida: Chapman & Hall/CRC.

Faraway, J. J. (2006). *Extending the Linear Model with R—Generalized Linear, Mixed Effects and Nonparametric Regression Models*. Boca Raton, Florida: Chapman & Hall/CRC.

Graf, W. L. (2002). *Fluvial Processes in Dryland Rivers* (2 ed.). Caldwell, NJ, USA: The Blackburn Press.

Hastie, T. J. and R. J. Tibshirani (1990). *Generalized Additive Models*. Boca Raton, Florida: Chapman & Hall/CRC.

Heitmuller, F. T. (2009). Downstream Trends of Alluvial Sediment Composition and Channel Adjustment in the Llano River Watershed, Central Texas, USA: The Roles of a Highly Variable Flow Regime and a Complex Lithology.

Heitmuller, F. T. and W. H. Asquith (2008). Potential for Bed-Material Entrainment in Selected Streams of the Edwards Plateau, Edwards, Kimble, and Real Counties, Texas, and Vicinity. Scientific Investigations Report 2008–5017, U.S. Geological Survey.

Heitmuller, F. T. and L. E. Greene (2009). Historical Channel Adjustment and Estimates of Selected Hydraulic Values in the Lower Sabine River and Lower Brazos River Basins, Texas and Louisiana. Scientific Investigations Report 2009–5174, U.S. Geological Survey.

Helsel, D. R. and R. M. Hirsch (2002). Statistical Methods in Water Resources. Techniques of Water-Resources Investigations Book 4, Chapter A3, U.S. Geological Survey.

Herrmann, G. R. (2007). Report of Observations and Recommendations: RM 335 and Unnamed Stream.

Herrmann, G. R. (2008). Supplementary Report: Subsequent Actions, Observations, and Conditions, RM 335 and Unnamed Stream.

Herrmann, G. R. and T. G. Cleveland (2010). Moving Substrate in an Ephemeral Stream: A Case Study in Bridge Survival. *Transportation Research Record: Journal of the Transportation Research Board 2201*, 3–9.

Hewlett, J. D. and A. R. Hibbert (1967). Factors Affecting the Response of Small Watersheds to Precipitation in Humid Areas. pp. 253–275. 1st International Symposium on Forest Hydrology.

Horton, R. E. (1933). The Role of Infiltration in the Hydrologic Cycle.

House, P. K., R. H. Web, V. R. Baker, and D. R. Levish (2001). *Ancient Floods, Modern Hazards, Principles and Applications of Paleoflood Hydrology*. Washington DC, USA: American Geophysical Union.

Huggett, R. J. (2007). *Fundamentals of Geomorphology* (2nd ed.). New York, NY, USA: Routledge.

IASH (1969). Symposium on Analog and Digital Computers in Hydrology. In *Symposium of Tucson*. International Association of Scientific Hydrology: Taylor and Francis.

Jain, S. C. (2001). *Open Channel Flow*. New York: John Wiley.

Johnson, N. L., S. Kotz, and N. Balakrishnan (1994). *Continuous Univariate Distributions, Vol. 1* (2 ed.). New York, NY, USA: Wiley Interscience.

Kirkby, M. J. and R. J. Chorley (1967). Overland Flow, Throughflow, and Erosion. *Intl. Assoc. Sci. Hydrol. Bulletin 12*, 5–21.

Koutsoyiannis, D. (2009). Seeking Parsimony in Hydrology and Water Resources Technology. EGU General Assembly: EGU.

Langmuir, D. (1997). *Aqueous Environmental Geochemistry*. Upper Saddle River, NJ, USA: Prentice Hall.

Lanning-Rush, J. (2000). Regional Equations for Estimating Mean Annual and Mean Season Runoff for Natural Basins in Texas. Water-Resources Investigations Report 00–4064, U.S. Geological Survey.

Lee, K. T. and J. K. Huang (2013). Runoff Considering Time-Varying Partial Contributing Area Based On Current Precipitation Index. *Journal of Hydrology 486*, 443–454.

Leopold, L. B. (1994). *A View of the River*. Cambridge, Mass., USA: Harvard University Press.

Leopold, L. B. and T. Maddock (1953). The Hydraulic Geometry of Stream Channels and Some Physiographic Implications. Professional Paper 242, U.S. Geological Survey.

Lienhard, J. H. (1964). A Statistical Mechanical Prediction of the Dimensionless Unit Hydrograph. *Journal of Geophysical Research 69*, 5231–5238.

Maidment, D. R. e. a. (1993). *Handbook of Hydrology*. New York, NY, USA: McGraw-Hill.

Minka, T. P. (2011). Maps: Draw Geographic Maps.

Morehead, M. D., J. P. Syvitski, E. W. H. Hutton, and S. D. Peckham (2003). Modeling the Temporal Variability in the Flux of Sediment from Ungauged River Basins. *Global and Planetary Change 39*(1–2), 95–110.

Nash, J. E. (1957). The Form of the Insantaneous Unit Hydrograph. In *General Assembly of Toronto*, pp. 114–121. International Association of Scientific Hydrology.

Nash, J. E. (1959). Systematic Determination of Unit Hydrograph Parameters. *Journal of Geophysical Research 64*, 241–256.

National Research Council (1999). *Hydrologic Hazards Science at the U.S. Geological Survey*. Washington, D.C.: National Academies Press.

National Research Council (2004). *Assessing the National Streamflow Information Program—Committee on Review of the USGS National Dtreamflow Information Program*. Washington, D.C.: The National Academies Press.

Oceaninc, N. and A. Administration (2013). Hurricane Alice, June 24–27 1954.

Ockerman, D. J. and F. T. Heitmuller (2010). Simulation of Streamflow and Suspended-Sediment Concentrations and Loads in the Lower Nueces River Watershed, Downstream from Lake Corpus Christi to the Nueces Estuary, South Texas, 1958–2008. Scientific Investigations Report 2010–5194, U.S. Geological Survey.

O'Connor, J. E. and J. E. Costa (2003). Large Floods in the United States: Where They Happen and Why. Circular 1245, U.S. Geological Survey.

Pappenberger, F. and K. J. Beven (2006). Ignorance is Bliss; Or Seven Reasons Not To Use Uncertainty Analysis. *Water Resources Research 42*.

Potter, K. W. and J. F. Walker (1981). A Model of Discontinuous Measurement Error and its Effects on the Probability Distribution of Flood Discharge Measurements. *Water Resour. Res. 17*(5), 1505–1509.

PRISM Climate Group (2010, July 1, 2010). PRISM Data Explorer.

R Development Core Team (2011). ***R****: A Language and Environment for Statistical Computing*. Vienna, Austria: R Foundation for Statistical Computing. ISBN 3-900051-07-0.

Ragan, R. M. (1968). An Experimental Investigation of Partial Area Contributions. *Intl. Assoc. Sci. Hydrol. Publ. 76*, 241–249.

Raines, T. H. (1998). Peak-Discharge Frequency and Potential Extreme Peak Discharge for Natural Streams in the Brazos River Basin, Texas. Water-Resources Investigations Report 98–4178, U.S. Geological Survey.

Raines, T. H. and W. H. Asquith (1997). Analysis of Minimum 7-day Discharges and Estimation of Minimum 7-day, 2-year Discharges for Streamflow-Gaging Stations in the Brazos River Basin, Texas. Water-Resources Investigations Report 97–4117, U.S. Geological Survey.

Ramsey, K. L. (2011, August). Personal interview.

Rifai, H. S., S. M. Brock, K. B. Ensor, and P. B. Bedient (2000). Determination of Low-Flow Characteristics for Texas streams. *J. of Water Resour. Plan. Manag. 126*(5), 310–319.

Riggs, H. C. (1976). A Simplified Slope-area Method for Estimating Flood Discharges in Natural Channels. *J. Res. USGS 4*(3), 285–291.

Riley, S. J., S. D. DeGloria, and R. Elliot (1999). A Terrain Ruggedness Index That Quantifies Topographic Heterogeneity. *Intermountain Journal of Sciences 5*, 23–27.

Rosgen, D. (1996). *Applied River Morphology* (2 ed.). Pagosa Springs, Colorado: Wildland Hydrology.

Sayama, T. and J. J. McDonnell (2009). A New Space-Time Acounting Scheme to Predict Stream Water Residence Time and Hydrograph Source Components at the Watershed Scale. *Water Resources Research 45*.

Sherman, L. (1932). Streamflow From Rainfall by the Unit-Graph Method. *Engineering News-Record 108*, 501–505.

Shreve, R. L. (1966). Statistical Law of Stream Numbers. *J. Geol. 74*, 17–37.

Slade, R. M., W. H. Asquith, and G. D. Tasker (1995). Multiple Regression Rquations to Estimate Peak-Flow Frequency for Streams in Hays County, Texas. Water-Resources Investigations Report 95–4019, U.S. Geological Survey.

Smakhtin, V. Y. and B. Massey (2000). Continuous Daily Hydrograph Simulation Using Duration Curves of a Precipitation Index. *Hydrological Processes 14*, 1083–1100.

Soulsby, c., D. Tetzlaff, P. Rodgers, S. Dunn, and S. Waldron (2013). Runoff Processes, Stream Water Residence Times and Controlling Landscape Characteristics in a Mesoscale Catchment: An Inital Evaluation. *Journal of Hydrology 2005*.

Sposito, G. (1998). *Scale Dependence and Scale Invariance in Hydrology*. Cambridge, UK, New York, NY: Cambridge University Press.

Strahler, A. N. (1957). Quantitative Analysis of Watershed Geomorphology. *Trans. Am. Geophys. Union 8*(6), 913–920.

Sturm, T. W. (2010). *Open Channel Hydraulics* (2nd ed.). New York: McGraw-Hill.

Texas Commission on Environmental Quality (TCEQ) and Texas Parks and Wildlife Department (TPWD) and Texas Water Development Board (TWDB) (2008). Texas Instream Flow Studies: Technical Overview. Report 369, Texas Water Development Board, Austin, Texas.

Texas Senate Bill 3 Science Advisory Committee for Environmental Flows (TSAC) (2009, August 17, 2011). Texas Instream Flow Studies: Technical Overview.

The Division of Bridges and Structures Hydraulics Section (1993). *Texas Secondary Evaluation and Analysis for Scour (TSEAS)*. Austin, TX, USA: Texas Department of Transportation.

Thompson, D. B. (2001, September). Surface Water Hydrology, C.E. 5361 .

Thompson, D. B., T. G. Cleveland, X. Fang, and K. H. Wang (2009). Design Guidance for Low-Water Crossings in Areas of Extreme Bed Mobility, Edwards Plateau, Texas. Research Report FHWA/TX-09/0-4695-3, FHWA, U.S. Department of Transportation.

Turnipseed, D. P. and V. B. Sauer (2010). Discharge Measurements at Gaging Stations. Techni. and Meth. Book 3, Chapter A8, U.S. Geological Survey.

U. S. Geological Survey (2013). The StreamStats Program.

U.S. Geological Survey (2009a, March 1, 2009). Daily Mean Streamflow Values for Texas.

U.S. Geological Survey (2009b, March 1, 2009). Streamflow Measurements for Texas.

USACE-HEC (2012). User Manual for HEC-HMS.

USDA-SCS (1972). *National Engineering Handbook, Part 4*. Washington, DC, USA: U.S. Department of Agriculture Soil Conservation Service.

Van De Griend, A. A. and E. T. Engman (1985). Partial Area Hydrology and Remote Sensing. *Journal of Hydrology 81*, 211–251.

Venables, W. N. and B. D. Ripley (2002). *Modern Applied Atatistics with S* (4th ed.). New York: Springer.

Viessmann, W. and G. L. Lewis (2003). *Introduction to Hydrology* (5 ed.). New Jersey: Prentice Hall.

Vogel, R. M. and N. M. Fennessey (1994). Flow-Duration Curves I: New Interpretation and Confidence Intervals. *J. Wat. Res. Plan. Managment 120*(4), 485–504.

Wiles, T. J. and J. M. Sharp (2008). The Secondary Permeability of Impervious Cover. *Environmental and Engineering Geoscience*, 251—265.

Williams-Sather, T., W. H. Asquith, D. B. Thompson, T. G. Cleveland, and X. Fang (2004). Empirical, Dimensionless, Cumulative-Rainfall Hyetographs Developed From 1959–86 Storm Data for Selected Small Watersheds in Texas. Scientific Investigations Report 2004-5075, U.S. Geological Survey.

Wong, T. S. (2007). Influence of Loss Model on Design Discharge of Homogeneous Plane. *Journal of Irrigation and Drainage Engineering 131*, 210–217.

Wood, S. N. (2006). *Generalized Additive Models—An Introduction with R*. Boca Raton, Florida: Chapman & Hall/CRC.

Wood, S. N. (2009, March 1, 2009). mgcv: GAMs with GCV/AIC/REML Smoothness Estimation and GAMMs by PQL.

Wurbs, R. A. and T. J. Kim (2011). River Flows for Alternative Conditions of Water Resources Development. *J. Hydro. Eng. 16*(2), 17–37.

# Appendix A

# Generalized Additive Regression Models of Discharge and Mean Velocity associated with Direct-Runoff Conditions in Texas: The Utility of the U.S. Geological Survey Discharge Measurement Database

## A.1 Abstract

A database containing more than 17,700 discharge values and ancillary hydraulic properties was assembled from summaries of discharge measurement records for 424 U.S. Geological Survey streamflow-gaging stations (streamgages) in Texas. Each discharge exceeds the 90th-percentile daily mean streamflow as determined by period-of-record, streamgage-specific, flow-duration curves. Each discharge therefore is assumed to represent discharge measurement made during direct-runoff conditions. The hydraulic properties of each discharge measurement included concomitant cross-section flow area, water-surface top width, and reported mean velocity. Systematic and statewide investigation of these data in pursuit of regional models for the estimation of discharge and mean velocity has not been previously attempted. Generalized additive regression modeling is used to develop readily implemented procedures by end users for estimation of discharge and mean velocity from select predictor variables at ungaged stream locations. The discharge model uses predictor variables of cross-section flow area, top width, stream location, mean annual precipitation, and a generalized terrain and climate index (OmegaEM) derived for a previous flood-frequency regionalization study. The mean velocity model uses predictor variables of discharge, top width, stream location, mean annual precipitation, and OmegaEM. The discharge model has an adjusted R-squared value of about 0.95 and a residual standard error (RSE) of about 0.22 base-10 logarithm (cubic meters per second); the mean velocity model has an adjusted R-squared value of about 0.67 and an RSE of about 0.063 fifth root (meters per second). Example applications and computations using both regression models are provided.

## A.2 Introduction

The U.S. Geological Survey (USGS) for the operational support of the streamflow-gaging station (streamgage) network in Texas collected and digitally archived about 140,000 discharge measurements (including zero-flow values) and streamgage inspections for more than 600 streamgages for the approximate period Dec. 1897–Feb. 2009. These discharge measurements, which are actually individual summaries of extensive field-collected data, reside within the USGS National Water Information System (NWIS) and are readily obtained U.S. Geological Survey (2009b) by streamgage number (a unique numerical identifier). The vast majority of the data represent discharges $Q$ measured from current-meter-based (velocity-meter) techniques Turnipseed and Sauer (2010). For most of the discharge measurements concomitant hydraulic properties are also available, these are cross-section flow area $A$, water-surface top width $B$, reported mean velocity $V$, and other details. The basic relation between $Q$, $A$, and $V$ is $Q = AV$. The basic relation between hydraulic (mean) depth $D$ and $A$ and $B$ is $D = A/B$.

The National Research Council (1999, p. 29) stated that a "wealth of information on geomorphology could be extracted from the USGS's vast discharge measurement file." This paper demonstrates that the imposing number of records, flow-condition range, and large number of streamgages contained just within the USGS discharge measurement database in Texas facilitates the regionalization of $Q$ and $V$. The term "regionalization" in the hydrologic sciences is a framework for statistical analyses that produce procedures for estimation of various properties, such as discharge, at ungaged or unmonitored locations from select characteristics at those locations. The regional models of $Q$ and $V$ reported here demonstrate that indeed a wealth of generalized hydraulic information can be associated with simple metrics of channel morphology and stream location as anticipated by the National Research Council (1999). The National Research Council (2004, p. 122–123) stated "surprisingly, the USGS and other groups have not published hydraulic geometry relationships [...] for hydroclimatic regions of the United States. A consequence of this is that [situations requiring] hydraulic geometry try [to] use either 'average' hydraulic geometry relationships, which are often the data from Leopold and Maddock (1953) or stream classifications schemes[.]"

### A.2.1 Purpose, Scope, and Organization

The purpose of this paper is to document the first systematic and statewide investigation, conducted in cooperation with the Texas Department of Transportation, of principle features of the USGS discharge measurement database in Texas to regionalize (1) the relation between $Q$ and selected predictor variables and (2) the relation between $V$ and selected predictor variables. The objective of the regionalization is to create readily used procedures for engineers and scientists so that they may readily implement the parametric and semi-parametric models presented in this paper.

The scope of this paper is limited to discharge measurement records for streamgages in Texas that are anticipated to represent direct-runoff conditions (see Figure A.1). The regionalization is based on generalized additive models or modeling (GAM) in which selected predictor variables include those associated with fundamental hydraulics and other predictor variables that are readily determined from maps and graphical plots or special "smoothing" functions. These maps and plots are provided herein.

This paper is organized as follows. Previous studies having either conceptual association or those with salient hydraulic analysis are summarized in Section A.2.2. The regional analyses of $Q$ and $V$ are intended to be used in applied circumstances; various applications are discussed in Section A.3. In particular, some applications of a $Q$ regional model are discussed in Section A.3.1, and some applications of a $V$ regional model are discussed in Section A.3.2. Section A.4 discusses the data manipulation required to create a unified discharge measurement database in Texas that contains discharge measurements spanning low- to high-flow conditions. For this paper, the unified database went through a subsequent paring into anticipated high-magnitude $Q$ to create a database with general association to direct-runoff conditions. The definition of high-magnitude $Q$ and other details are provided in Section A.4, which further scope the statistical analyses herein.

The regional analysis framework using GAMs is introduced in Section A.5, and a brief introduction to GAM and the basic model forms chosen are provided in Section A.5. The preprocessing and preliminary analyses are described in Section A.5.2, and in particular, that section describes two non-hydraulic predictor variables selected for regionalization and the topic of selection of suitable variable transformation. The final regional model of $Q$ is presented in Section A.5.3, and the final regional model of $V$ is presented in Section A.5.4. A discussion on limitations and thoughts for model improvement follows in Section A.5.5.

The regional models of $Q$ and $V$ herein are intended for use in applied circumstances. Therefore, Section A.6 provides some example applications with extensive example com-

putations to help guide the user. In particular, Section A.6.1 provides an example of $Q$ computation, whereas, Section A.6.2 provides an example of $V$ computation as well as a method to approximate the distribution of a given prediction. Additional discussion of results is provided in Section A.7.

### A.2.2 Previous Studies

A conceptual precursor for discharge estimation from channel properties is provided by Riggs (1976), who describes a "simplified" slope-area method for estimation of peak discharge $Q_p$ in natural channels in the Pacific Northwest, USA. The slope-area method Dalrymple and Benson (1967) can be used to estimate postdirect-runoff peak discharge based on evidence of peak water-surface elevation or extent and corresponding cross-section geometric properties. Water-surface elevations are assumed to represent friction slopes $S$ necessary for hydraulic computations in a selected stream reach, and when $S$ are combined with topographic surveys (see Figure A.2) providing multiple cross-sectional areas and other hydraulic properties, an estimate of $Q_p$ results from the slope-area method. Unfortunately, the slope-area method is labor intensive and expensive. Riggs (1976) sought a quick, reproducible, and inexpensive alternative or compliment to the slope-area method. Arguing that Manning n-values and water-surface slopes are coupled relations, Riggs (1976) proposed that discharge $Q$ can be estimated by:

$$Q = c_1 A^{c_2} S^{c_3} \tag{A.1}$$

where $A$ is cross-section flow area, $S$ is water-surface slope, and $c_k$ are regression coefficients for a particular study area with $k = 1,\ 2,\ 3$. Riggs (1976) continues with a "further simplification" and argued that the contribution of the water-surface slope term can be removed.

Castro and Jackson (2001) investigated statistical relations between various hydraulic elements for 76 USGS streamgages in the Pacific Northwest, USA. Their primary objectives were to: (1) test the validity of the assumption that the 1.5-year (0.67 annual exceedance probability, AEP) discharge represents bankfull conditions; (2) define alternative relations of the $T$-year bankfull discharge in the study area; and (3) define statistical relations for discharge and channel hydraulics by geographic region. Castro and Jackson (2001, table 4) list ensembles of regression equations for four geographic regions. Some of these equations have algebraic similarity to the regression models presented in this paper. Those authors

developed four regression equations of top width $B$ in the form $B = d_1 Q^{d_2}$ for two regression coefficients $d_k$. The weighted mean of the exponent $d_2$ on $Q$ for the four equations is 0.497, which was computed from the tabulated exponents in Castro and Jackson (2001, table 4). Fitting the Castro and Jackson statistical model to the database described near the end of Section A.4 results in a $d_2$ value of 0.459, which is similar to the weight-mean exponent computed from Castro and Jackson (2001) of $d_2 = 0.497$ for rivers in the Pacific Northwest, USA. The exponent similarity is interesting because the study areas and the underlying databases are different. Castro and Jackson (2001) used site visits and hydraulic analyses; the analyses in this paper are based exclusively on statistical processing of discharge measurements.

An extensive number of studies have been done related to a regionalization of a range of streamflow statistics in Texas Slade et al. (1995); Asquith et al. (1996); Devulapalli and Valdes (1996); Asquith and Slade (1997); Raines and Asquith (1997); Asquith (1998); Raines (1998); Lanning-Rush (2000); Rifai et al. (2000); Asquith (2001); Asquith and Thompson (2008); Asquith and Roussel (2009) including a study on the drainage-area ratio method by Asquith et al. (2006). However, these studies generally are focused on the classical problem of estimation of a streamflow statistic (such as the median 7-day low flow, the mean annual streamflow, or the 0.1 annual exceedance probability peak streamflow). Wurbs and Kim (2011) discuss and provide extensive background and citations concerning monthly streamflow estimation as part of Texas water availability modeling to support planning and water rights analysis; the water availability modeling represents a fundamentally different thematic scope than the studies cited at the beginning of this paragraph. In total, all of these studies are fundamentally different from the current (2012) study, which is explicitly focused on regionalization of summaries of USGS discharge measurements and not the estimation of a particular statistic derived from time series of streamflow, such as the mean annual streamflow derived from annual mean streamflow values.

## A.3 Regionalization of Discharge Measurement Databases: Potential Applications

This section provides description of two interrelated applications of regionalized discharge measurement databases. The applications have distinct circumstances of use that are demonstrated by numerical examples in Section A.6.

### A.3.1 Potential Applications of a Regional Model of Discharge

The regionalization of $Q$ has potential applications for: (1) estimation of peak discharge $Q_p$ from readily field-surveyed cross-section topography after high-magnitude discharge events, (2) provisional stage-discharge relations from cross-section topography, and (3) other applications. After substantial flooding, evidence, such as debris lines on embankments or seed lines on trees, of peak water-surface elevation often remains. A regional model of $Q$ based on $A$, $B$, $D$, and other factors could provide for a relatively straightforward means to estimate $Q_p$ using measured or estimated values of $A$, $B$, and $D$ for the event with potentially less labor and expense, albeit with potentially greater uncertainty, compared to a slope-area computation of discharge.

When streamgages are activated there is a period of time in which the initial development of the stage-discharge relations is needed. Regionalization of $Q$ could facilitate the creation of provisional stage-discharge relations prior to actual measurements being made and subsequently used to initially define the relation between discharge and stage (also referred to as a "rating curve" or corresponding "rating table") at new streamgages. Typical direct discharge measurements have a potential error of about 5 to 8 percent—the potential errors associated with regionalized $Q$ from direct measurements likely are much larger than 8 percent. Indirect measurements of discharge errors are "probably several times larger" than those for direct measurements Potter and Walker (1981). Stage-discharge relations can be based on both types of discharge measurements, and Potter and Walker (1981) provide extensive discussion of the effects of this fundamental shift in relative error on the peak-streamflow frequency curve.

Other applications of regionalization of $Q$ are foreseen. Estimation of $Q$ (as well as $V$) for ungaged stream cross sections in Texas has obvious connections to hydraulic modeling but also connection to "instream-flow assessments" for aquatic and riparian habitats. For example, hydraulic values derived from cross-section and longitudinal surveys of selected, ungaged stream reaches in the Edwards Plateau, Texas have been used to predict magnitude and frequency of bed-material entrainment flows for purposes of mitigating maintenance costs associated with gravel bombardment of road crossings Heitmuller and Asquith (2008). Other hydrologic programs in Texas, notably those to quantify environmental flows Texas Senate Bill 3 Science Advisory Committee for Environmental Flows (TSAC) (2009), mandate hydraulic assessments of ungaged stream reaches for purposes of aquatic and riparian habitat conservation Texas Commission on Environmental Quality (TCEQ) and Texas Parks and Wildlife Department (TPWD) and Texas Water Development Board (TWDB) (2008).

In an expression of the utility of discharge measurements and attendant characteristics for instream-flow assessments, Heitmuller and Greene (2009) rendered historical cross sections and computed hydraulic values at 15 USGS streamgages in the Brazos and Sabine River basins. The historical cross sections and computed hydraulics are useful for detecting geomorphic and hydraulic conditions associated with instream habitat structure and function. Heitmuller and Greene (2009) as well as Coffman et al. (2011) describe geomorphic associations and properties of select reaches of various Texas riverine systems (Brazos, Sabine, and Trinity) from spatial and temporal perspectives. These two reports provide information as to the complexities of Texas river systems and their responses to flood-control measures, channel modifications, landscape changes, and other activities.

The general assessment or regionalization of hydraulic characteristics for ungaged stream locations provides needed flexibility to support conservation efforts Texas Senate Bill 3 Science Advisory Committee for Environmental Flows (TSAC) (2009). Finally, various efforts to model runoff, contaminant loads, and sediment loads commonly are needed for ungaged stream locations Clark et al. (2001); Morehead et al. (2003); Ockerman and Heitmuller (2010). These types of studies might benefit from regionalization of discharge measurement databases.

### A.3.2 Potential Applications of a Regional Model of Mean Velocity

The regionalization of $V$ has potential uses for rapid and reliable review of $\overline{V} = Q/A$ (mean velocity) that can emanate from one-dimensional backwater models. These models often are used to model peak water-surface elevations of high-magnitude discharge, for computations of bridge scour or bank protection, and for other applications. The authors observe that it is common for engineers involved in one-dimensional backwater modeling to have been taught to assemble models based on generalizations of parameter values from textbooks Jain (2001); Sturm (2010) or literature of the method American Society of Civil Engineers (1996), from computer program documentation, and from experience. However, the aforementioned "experience" often is exclusive to *prior modeling experience*—an example of circular logic. The authors also observe that conventional engineering education, as well as practice, lacks physical (observational) experience with or even exposure to streamflow metrology as exemplified by the discharge measurements supporting operation of the nationally consistent USGS streamgage network.

In one-dimensional, open-channel computations, parameters such as Manning n-values are selected from tables such as Sturm (2010, table 4.1), graphs, other published procedures, and ideally from visual site assessments Barnes (1967). For certain parameters, such as coefficients for expansion or contraction losses, the default values are often used. This practice (understandably) is made because typically there is scant information on which to base alternative values. As a result, modeling efforts by even experienced modelers are assembled and often judged to be valid based entirely on experiences from earlier modeling efforts for hydraulically similar settings.

Unfortunately, unless model calibration is influenced by data from one or more streamgages, there is seldom any independent information to assess the validity of a given model. Many assessments of, and discussions about, hydraulic model validity necessarily begin and end as expressions of individual professional opinion with often scant quantification to discriminate between valid and invalid models. A regional model of $V$ could provide a fundamental link to physical reality and potentially could provide an authoritative and independent measure of consistency that will allow for enhanced assessment of one-dimensional, open-channel computations and general model reliability. A regional model of $V$ would provide a tool to flag severely inconsistent situations and identify these for further scrutiny.

A regional model of $V$ could also serve as a means for straightforward computation of real-time velocity information to augment real-time discharge data from USGS streamgages in the context of stream-spill scenarios and attendant emergency response.

## A.4 Database of Discharge Measurements

This section provides background information to elucidate various nuances concerning observed values of $Q$ and other channel characteristics in Texas. Further, this section discusses various data gaps and information barriers that hinder systematic regionalization of $Q$ and $V$ relations in Texas. These gaps and barriers are not exclusive to the USGS discharge measurement records in Texas; they are likely endemic to other historic or emergent discharge measurement records elsewhere by the USGS or other entities.

A **unified database of discharge measurements in Texas** was prepared by the authors from the USGS National Water Information System U.S. Geological Survey (2009b). The database contains 89,874 discharge records for the approximate period Dec. 1897–Feb. 2009 for 437 selected Texas streamgages. The 437 streamgages were selected as a prerequisite for this paper based on preliminary screening of more than 600 streamgages

and select preprocessing that included factors such as consideration of streamflow data type, record length, number of discharge measurements, and regional setting or location of the streamgage. In general, a candidate streamgage needed to be a continuous-record type and represent streamgages that are considered examples of conventional (traditional) USGS streamgaging operation and not special projects (perhaps streamgages operated with theoretical weir stage-discharge relations), partial duration streamgages (perhaps flood hydrograph, or conversely, low-flow streamgages), or peak-only streamgages.

This unified discharge measurement database provides the foundational basis for the analysis reported here and contains the following attributes: discharge, reported mean velocity, cross-section flow area, water-surface top width, Froude number, and estimated flow-duration probability of the discharge. Unlike the approach by Castro and Jackson (2001) in their study of regional bankfull relations, no site visits to any of the 437 Texas streamgages were made for this study. The unified discharge measurement database was assembled through the following steps:

1. Daily Mean Streamflow Values—For the large and reasonably comprehensive list (437) of continuous-record (daily mean values of streamflow) streamgages in Texas, the daily mean streamflow values were retrieved from U.S. Geological Survey (2009a);
2. Streamflow Measurements—For the 437 streamgages, the discharge measurement file for each streamgage was retrieved from U.S. Geological Survey (2009b);
3. Complete Records—The measured discharge $Q$ in cubic meters per second ($\mathrm{m}^3/\mathrm{s}$), "channel velocity" (referred to herein as "reported mean velocity") $V$ in meters per second ($\mathrm{m}/\mathrm{s}$), "channel area" (referred to herein as "cross-section flow area") $A$ in square meters ($\mathrm{m}^2/\mathrm{s}$), and "channel width" (referred to herein as "water-surface top width" or just "top width") $B$ in meters (m) were extracted and only those records with $Q > 0$ were retained;
4. Computed Mean Velocity—Computed mean velocity $\overline{V}$ in $\mathrm{m}/\mathrm{s}$ was computed by $\overline{V} = Q/A$. The adjective "computed" (as opposed to "reported" mean velocity in Step 3) in this paper refers to $Q$ divided by $A$ irrespective of the source of $Q$ or $A$;
5. Velocity Consistency—The computed $\overline{V}$ was compared to the reported $V$, and if the absolute difference was greater than 0.03 $\mathrm{m}/\mathrm{s}$ (chosen by the authors), then the record (a single discharge measurement) was rejected for inclusion in the unified discharge measurement database and thus not retained for the analysis reported here;
6. Froude Number—The Froude number was computed by $\mathrm{Fr} = V(gA/B)^{-1/2}$ where $g$ is acceleration of gravity. For this paper, Fr is not used but is retained in the unified discharge measurement database;

7. Flow-Duration Curve—The entire period of record of daily mean streamflow for each streamgage referenced in Step 1 was converted to a streamgage-specific, flow-duration curve Vogel and Fennessey (1994); and
8. Individual Discharge Probabilities—The probability of each $Q$ was determined from the respective streamgage-specific, flow-duration curve of daily mean streamflow values using linear interpolation as necessary.

Further discussion of selected details of the 8 steps is needed to provide additional context for various decisions or observations that are important to communicate:

- On Greater than Zero Discharge—Step 3 excludes reverse flow ($Q < 0$) in tidal and zero-flow conditions ($Q = 0$);
- On Incomplete Attributes—To clarify, any discharge measurements (direct or indirect) lacking any core attributes ($Q$, $V$, $A$, and $B$) or in violation of Step 5 were not retained for the unified discharge measurement database;
- On Streamflow Probability—Step 7 states that the *entire* record of each streamgage was used to compute each streamgage-specific, flow-duration curve. This explicitly means that no attempt was made to define periods of stationary (unchanging statistical properities) streamflow or more importantly statistics of hydraulic relations. For example, no differentiation between pre- and post-reservoir conditions (if applicable) for a given streamgage was made. Such streamgage-specific investigation is beyond the scope of this paper;
- On Streamgage Location—USGS streamgages are only very rarely located in settings in which backwater conditions occur because a unique stage-discharge relation is desired. Also, a given streamgage is not anticipated to permanently exist at the exact same location along a stream during the course of the streamgage's operational time frame; however, many streamgages remain more-or-less sited at their original locations. Streamgage locations are referenced to the nearest town or locality with a postal code, for example, USGS streamgage 08167000 Guadalupe River near Comfort, Texas. Streamgages are periodically relocated to nearby locations, but adjustments to identity (number and name) are not made, because of channel migration; channel rectification/restoration; bridge maintenance, decommission, and new construction; property access (landowner changes); and changes in safety policy and practices. Changes in bridge characteristics are likely the most common cause of relocation because many streamgages in Texas often are located along Texas Department of Transportation right-of-way;

- On Measurement Location—A fact, which likely hampers many streamgage-specific investigations of geomorphic processes using USGS measurement databases, is that the precise cross-section location of an individual discharge measurement is neither reported or fully documented in USGS discharge measurement summaries used herein. Furthermore, the measurement location is not expected to coincide with the same location either over the years or over a range of discharge conditions. There are many discipline- and technically-specific reasons discharge measurements might be not made at precisely the same geographic stream location because of discharge magnitude and year-over-year streamgage operation;
- On Bankfull Conditions and Floodplain Engagement—The discharge measurements (summaries) available from U.S. Geological Survey (2009b) do not provide consistent and, even when available, only limited details identifying whether the measurement summary is applicable for a partially to full channel or whether the floodplain (if it exists in a classical sense) is engaged by the water surface near the measurement location. Because of generally more favorable conditions for measurement, discharge measurements are often performed, whenever possible, in places with flow conditions lacking substantial floodplain inundation. Also, many streamgages are located near bridges because of the more favorable conditions for truck-mounted-crane, high-magnitude discharge measurement;

A discussion is needed that concerns components of the well known Manning's equation for computation of simplified open-channel hydraulics in the context of USGS discharge measurement databases. Manning's equation is:

$$Q = ([\text{n-value}]^{-1})\, A\, (A/WP)^{2/3}\, S^{1/2} \tag{A.2}$$

where the equation provides a useful mathematical structure to statistically evaluate $Q$ and $V$ through intrinsic relations between $A$, $B$, wetted perimeter $WP$, and a friction slope $S$. However, several limitations excluded application of Manning's equation in a statistical context for this paper:

- Friction slope—Friction slope is indisputably an important parameter because $Q$ and $V$ are proportional to the square root of slope. However, the friction slope is not available from U.S. Geological Survey (2009b). Channel slope often is used in place of friction slope in Manning's equation; channel slope also is not available from U.S. Geological Survey (2009b). Therefore, for this paper, a metric of channel slope near each

streamgage for statistical consideration is outside the scope but commented on further in Section A.5.5;

- Manning's n-value—The Manning n-value also is indisputably an important parameter in Equation A.2. Unfortunately, n-values, which are not direct measures of roughness, or other roughness parameters, such as median grain sizes, influencing channel hydraulics are not readily available for any of the streamgages in general or for individual discharge measurements across time in particular; and
- Wetted perimeter—The wetted perimeter $WP$, which is used to compute the hydraulic radius (the $A/WP$ term in Manning's equation), likely is useful as a direct predictor variable on $Q$ or $V$ or is useful as a predictor variable when expressed as hydraulic radius. The field-measured data for direct measurements of discharge by the USGS contain horizontal stationing and vertical sounding (depth) information. From these raw data, $WP$ for individual measurements could be estimated. Unfortunately at the present time (2012), the USGS discharge measurement database U.S. Geological Survey (2009b), being summaries of the field observations, lack either $WP$ values or the raw data to compute them. Hence, $WP$ values are not available for this study.

The unified discharge measurement database of 87,874 records for 437 streamgages in Texas was subsequently filtered or reduced to contain discharge measurements that could be reasonably associated with direct-runoff conditions. Specifically, discharge measurements exceeding the 90th-percentile daily mean streamflow as determined by the streamgage-specific, flow-duration curves were retained for the analysis reported herein. This **90th-percentile discharge measurement database**, is the database used for statistical analysis in Section A.5. The 90th-percentile database contains 17,753 discharge records for 424 of the original 437 streamgages. Each of the 424 streamgages has at least one measurement greater than the 90th-percentile daily mean streamflow for that streamgage.

Summary statistics of $A$, $Q$, $V$, Fr, and $B$ of the 90th-percentile discharge measurement database were computed. After filtering for high-magnitude discharge considerable variation or range remains in $A$ (about 6 orders of magnitude), $Q$ (about 7 orders of magnitude), $V$ (about 2 orders of magnitude), Fr (about 2 orders of magnitude), and $B$ (about 5 orders of magnitude). These tabulated statistics of their respective distributions could be used for additional data screening and record rejection prior to regionalization. For example, the maximum $B = 14{,}000$ m is almost certainly too large, the minimum $\text{Fr} = 0.00610$ is almost certainly too small, and the maximum $\text{Fr} > 1$ (indicative of supercritical flow conditions) is seemingly high for natural channel flow. Additional data screening and record rejection

was not made prior to statistical analysis except for the removal of a few extreme outliers as described in Section A.5.2.3.

## A.5 Generalized Additive Models and Regionalization of Discharge and Mean Velocity

### A.5.1 Generalized Additive Models

Complex relations between both $Q$ and $V$ and available predictor variables (described in Section A.5.2) were anticipated. Therefore, in lieu of conventional multi-linear regression modeling Faraway (2005), generalized additive modeling (GAM) Hastie and Tibshirani (1990); Wood (2006) was chosen. A GAM is a statistical model between a response variable and an additive combination of various parametric terms and smooth terms (functions). The incorporation of smooth functions can be an advantage to GAMs over simpler multi-linear regression because appropriately configured smooth functions accommodate otherwise difficult to "linearly model" components of a prediction-response model. A Gaussian family for the generalized linear model Faraway (2006) was used to estimate the GAM models reported here using mostly default arguments of the `gam` function in the R environment R Development Core Team (2011) from the `mgcv` package by Wood (2009). The model fitting is based on maximum likelihood (not conventional least-squares) for parameter fitting (optimization). The basic form of a GAM model:

$$y_i = \mathbf{X}_i\Theta + f_1(x_{1i}, x_{2i}) + f_2(x_{3i}) + \ldots + \varepsilon_i \tag{A.3}$$

where $y_i$ is a suitably transformed response variable for the $i$th observation, $\mathbf{X}_i$ is a model matrix for strictly parametric and suitably transformed predictor variables, $\Theta$ is a parameter matrix, the $f_k$ are "smooth functions" of the predictor variables $x_{ik}$, and $\varepsilon_i$ are error terms taken as independently and identically distributed $N(0, \sigma^2)$ (Gaussian distribution or normal distribution) random variables. The $\mathbf{X}_i\Theta$ term is the familiar multi-linear regression component of a GAM.

For this paper, separate GAM analyses of $Q$ and $V$ were conducted. The GAM model of $Q$ is referred to as QGAM, and similarly, the GAM model of $V$ is referred to as VGAM. As further described and justified in Section A.5.2, the basic form of the QGAM reported in Section A.5.3 is:

$$\log(Q) = b_1 + a_1 \log(A) + a_2 \log(B) + a_3 \Omega + f_5(\text{longitude}, \text{latitude}) + f_6(P) \quad \text{(A.4)}$$

and the basic form of the VGAM reported in Section A.5.4 is:

$$V^{1/5} = b_2 + a_4 \log(Q) + a_5 \log(B) + a_6 \Omega + f_9(\text{longitude}, \text{latitude}) + f_{10}(P) \quad \text{(A.5)}$$

where log is base-10 logarithm, $Q$ is discharge in $m^3/s$, $V$ is mean velocity in $m/s$, $b_k$ are intercepts, $a_k$ are regression coefficients, $A$ is cross-section flow area in $m^2/s$, $B$ is top width in m, $\Omega$ is the OmegaEM parameter from Asquith and Roussel (2009) and is described in Section A.5.2, $f_k$ are smooth functions in one or two dimensions as indicated and the numerical value of the subscript references the applicable figure of this paper, and $P$ is mean annual precipitation in millimeters (mm) and is described in Section A.5.2. The QGAM and VGAM are respectively presented in Sections A.5.3 and A.5.4. Lastly, the predictive potential of watershed drainage area was found to be unsuitable as a predictor variable for the $Q$ and $V$ regionalization of the 90th-percentile discharge measurement database. Select predictor variables are discussed in the next section along with choice of variable transformation.

## A.5.2 Preprocessing and Preliminary Analysis

### A.5.2.1 OmegaEM Parameter

Asquith and Roussel (2009) developed regional equations to estimate annual peak-streamflow frequency for undeveloped watersheds in Texas. As part of that analysis, those authors created a generalized residual of the 10-year (0.10 AEP) discharge equation that is referred to as the OmegaEM parameter. This parameter represents a generalized terrain and climate index that expresses peak-streamflow potential not otherwise represented in the watershed characteristics of drainage area, main-channel slope, and $P$. The OmegaEM parameter is gridded by 1-degree quadrangles Asquith and Roussel (2009, p. 14) and is reproduced and shown in Figure A.3. Although developed from analysis of undeveloped

watersheds, the parameter captures generalized terrain and climate influences on channel conveyance properties affecting discharge magnitude.

The authors hypothesize that OmegaEM should be a useful, but minor, predictor of $Q$ and $V$ because OmegaEM expresses regional variation in otherwise difficult to quantify variations in high-magnitude discharge. Using the latitude and longitude of each of the 424 streamgages, the OmegaEM parameter was computed for each streamgage by bilinear interpolation from the gridded values in Figure A.3.

#### A.5.2.2 Mean Annual Precipitation

Climatological conditions in Texas are diverse. Bomar (1994) provides a review of Texas weather and climate and details historically important rainfall and resulting floods, the characteristics of the atmosphere, and general weather statistics for Texas. For the 424 streamgages, $P$ ranges from about 292 mm for a streamgage in the extreme western part of Texas to 1,571 mm for a streamgage in the extreme southeastern part of Texas.

Using the latitude and longitude of each of the 424 streamgages, mean annual precipitation $P$ in mm was retrieved for each streamgage from PRISM Climate Group (2010) for the 1971–2000 normals. The PRISM Climate Group (2010) source was chosen for expediency. Given the many sources of uncertainty both in GAM development and implementation by end users, the authors consider that any general and authoritative source of $P$ for any suitably long period (perhaps 30 years) is sufficient for GAM development or substitution into the QGAM and VGAM that are reported here. This statement concerning the source of $P$ reiterates the position by Asquith and Roussel (2009, p. 3) in a similar context.

The authors hypothesize that $P$ should be a useful, but minor, predictor of $Q$ and $V$ because $P$ exerts considerable influence on vegetation communities both across the greater watershed as well as for the riparian zone near stream channels such as an identifiable riparian might exist. General erosional and attendant geomorphologic settings as represented by stream channel shapes are also affected by $P$. Channel shape in turn influences relations between discharge and mean velocity through the hydraulic characteristics of cross-section flow area and top width.

The authors also considered other climate normals available from PRISM Climate Group (2010) including mean July high and mean January low temperatures and their difference. These climate indices seem to be no better predictors or contributors to the explanation $Q$ or $V$ variance than $P$.

#### A.5.2.3 Variable Transformation

The authors hypothesize for the objective of $Q$ regionalization that the hydraulic parameters of $A$ and $B$ should be critically important parameters. A preliminary issue at hand is the choice of transformation in the GAM analysis. Analysis through multi-linear regression, Box-Cox power transformations Box and Cox (1964) (the `boxcox` function in R from the `MASS` package by Venables and Ripley (2002)), and preliminary GAM analysis showed that logarithmic transformation on $Q$, $A$, and $B$ was appropriate.

The authors also hypothesize for the objective of $V$ regionalization that the hydraulic parameters of $Q$ and $B$ should be critically important parameters. The use of $A$ is not appropriate or even possible in the context here because the reported $V$ values are effectively, if not exactly, the ratio of $Q$ to $A$. A preliminary issue at hand is the choice of transformation in the GAM analysis. Analysis through multi-linear regression, Box-Cox power transformations, and preliminary GAM analysis showed that fifth-root transformation on reported $V$ (or $V^{1/5}$) and logarithmic transformation on $Q$ and $B$ was appropriate.

Preliminary QGAM and VGAM were fit following the algebraic structure of Equations A.4 and A.5 and were used to identify a few extreme outliers. The minimum of the absolute value of the range of the residuals was separately computed for the preliminary QGAM and VGAM. The $Q$ and $V$ records having residuals in absolute value greater than the respective minimums subsequently were removed; summary of these removals (very few) is made in Sections A.5.3 and A.5.4. The effect of outlier removal was to enhance the centering of the residuals in the final QGAM and VGAM models.

### A.5.3 Generalized Additive Model of Discharge

The final QGAM in R output is shown in Figure A.4. For the QGAM, each of the predictor variables is statistically significant. The adjusted R-squared value is about 0.95, and the residual standard error is about $s = 0.22$ base-10 logarithm of $\mathrm{m}^3/\mathrm{s}$, which is the square root Wood (2006, p. 61) of the "Scale est." because a Gaussian family was used for this GAM. For the final QGAM model, 26 discharge measurements for 13 streamgages (USGS station numbers: 07295500, 08018730, 08047500, 08080700, 08110325, 08129300, 08166000, 08185000, 08186500, 08190500, 08197500, 08202700, and 08210400) were removed but the overall streamgage count remained at 424 (see discussion at end of Section A.4). The QGAM with the coefficients shown in Figure A.4 can be written as:

$$\log(Q) = -0.2896 + 1.269\log(A) - 0.2247\log(B) + 0.2865\Omega + f_5(\text{longitude}, \text{latitude}) + f_6(P) \quad \text{(A.6)}$$

where log is base-10 logarithm, $Q$ is discharge in $m^3/s$, $A$ is cross-section flow area in $m^2$, $B$ is top width in m, $\Omega$ is the OmegaEM parameter from Figure A.3, $P$ is mean annual precipitation in mm, and $f_5$ and $f_6$ are "smooth functions" of the indicated predictor variables in Figures A.5 and A.6, respectively. For Figure A.5, the base map and superimposed smooth lines were created in R using graphic capabilities of packages by Minka (2011) and Wood (2009), and Figure A.6 was created using graphic features by Wood (2009). The red, green, and black lines as ensembles of three for each numerical value shown in Figure A.5 are not all shown for reasons such as grid resolution for the graphic, nonuniform distribution of streamgages, and general statistical magnitude of the two-dimensional smooth surface.

The `k=14` argument (shown in Figure A.4) to the $f_5(\text{longitude}, \text{latitude})$ or $f_5(l,k)$ smooth function of location represents the dimension of the isotropic thin plate regression spline Wood (2006, p. 225). The `bs="cr", k=5` arguments (shown in Figure A.4) to the $f_6(P)$ smooth function represent cubic regression splines (`bs="cr"`) with the dimension `k=5` representing "knots" of the spline Wood (2006, p. 226). The spline dimensions were chosen through visual evaluation of figures similar to Figures A.5 and A.6.

The residuals of the discharge model are shown in Figure A.7, and summary statistics of the residuals are shown in Figure A.4. Because of overplotting, gray transparency was used for Figure A.4 to enhance visual density of the data point distribution. The Akaike Information Criterion is a measure of information content of a regression model. The statistic accounts for a trade off between the number of parameters and the fit of the model; small values are sought. The Akaike Information Criterion is $-3{,}830$ for the model in Equation A.6 but $-281$ for the model lacking $f_5$ and $f_6$. The percent change in residual standard error from the model lacking $f_5$ and $f_6$ to the model in Equation A.6 is $-9.6$ percent. A preference for the more complex model involving the smooth functions $f_5$ and $f_6$ is made.

Lastly, loose interpretation of the parametric coefficients can be made that are consistent with well-known hydraulic constraints. The positive coefficient on $A$ shows that $Q$ increases with increasing $A$; the negative coefficient on $B$ shows that $Q$ decreases with increasing $B$. The positive coefficient on OmegaEM indicates that $Q$ increases in proportion to OmegaEM. OmegaEM takes on a positive value in the central part of Texas (the region demarked by positive OmegaEM values) and is greatest along the Balcones escarpment in south central Texas. O'Connor and Costa (2003, p. 9) identify this region (Balcones escarpment) of the nation as having "concentrations of large floods." Asquith and Roussel (2009, p. 23)

provide further and relevant discussion. Thus, OmegaEM acts to increase $Q$ in QGAM near the central part of Texas and reduce $Q$ in other parts. The smooth function $f_5(l,k)$ of location also shows a tendency for larger $Q$ in the central part of Texas. The smooth function $f_6(P)$ shows that there is a subtle relation between $P$ and $Q$ that is difficult to interpret given the presence of the two other spatially varying parameters (OmegaEM and $f_5$).

### A.5.4 Generalized Additive Model of Mean Velocity

The final VGAM in R output is shown in Figure A.8. For VGAM, each of the predictor variables is statistically significant. The adjusted R-squared value is about 0.67, and the residual standard error is about $s = 0.063$ fifth root of m/s, which is the square root of the "Scale est." because a Gaussian family was used for this GAM. For the final VGAM model reported here, two discharge measurements for two streamgages (USGS station numbers: 08105000 and 08176500) were removed but the overall streamgage count remained at 424 (see discussion at end of Section A.4). The VGAM with the coefficients shown in Figure A.8 can be written as:

$$\begin{aligned} V^{1/5} = {} & 0.9758 + 0.1588\log(Q) - 0.1820\log(B) + 0.0854\Omega \\ & + f_9(\text{longitude}, \text{latitude}) + f_{10}(P) \end{aligned} \tag{A.7}$$

where log is base-10 logarithm, $V$ is mean velocity in m/s transformed by the fifth root, $Q$ is discharge in $\text{m}^3/\text{s}$, $B$ is top width in m, $\Omega$ is the OmegaEM parameter from Figure A.3, $P$ is mean annual precipitation in mm, and $f_9$ and $f_{10}$ are "smooth functions" of the indicated predictor variables in Figures A.9 and A.10, respectively. For Figure A.9, the base map and superimposed smooth lines were created in R using graphic capabilities of packages by Minka (2011) and Wood (2009), and Figure A.10 was created using graphic features by Wood (2009). The red, green, and black lines as ensembles of three for each numerical value shown in Figure A.9 are not all shown for reasons such as grid resolution for the graphic, nonuniform distribution of streamgages, and general statistical magnitude of the two-dimensional smooth surface.

The `k=14` argument (shown in Figure A.8) to the $f_9(\text{longitude}, \text{latitude})$ or $f_9(l,k)$ smooth function of location represents the dimension of the isotropic thin plate regression spline Wood (2006, p. 225). The `bs="cr", k=5` arguments (shown in Figure A.8) to the

$f_{10}(P)$ smooth function represent cubic regression splines (`bs="cr"`) with the dimension `k=5` representing "knots" of the spline Wood (2006, p. 226). The spline dimensions were chosen through visual evaluation of figures similar to Figures A.9 and A.10.

The residuals of the mean velocity model are shown in Figure A.11, and summary statistics of the residuals are shown in Figure A.8. Because of overplotting, gray transparency was used for Figure A.8 to enhance visual density of the data point distribution. The Akaike Information Criterion is $-47{,}700$ for the model in Equation A.7 but $-42{,}100$ for the model lacking $f_9$ and $f_{10}$. The percent change in residual standard error from the model lacking $f_9$ and $f_{10}$ to the model in Equation A.7 is $-14$ percent. A preference for the more complex model involving the smooth functions $f_9$ and $f_{10}$ is made.

Again, loose interpretation of the parametric coefficients can be made that are consistent with well-known hydraulic constraints. The positive coefficient on $Q$ shows that $V$ increases with increasing $Q$; the negative coefficient on $B$ shows that $V$ decreases with increasing $B$. The positive coefficient on OmegaEM indicates that $V$ increases in proportion to OmegaEM. This finding was anticipated (see discussion in Section A.5.3). The smooth function $f_9(l,k)$ of location also shows a tendency for smaller $V$ in the eastern part of Texas. The authors hypothesize that this observation is consistent with greater vegetation density in the riparian zones in the eastern parts of Texas than in the western parts, and vegetation is associated with larger $P$ and other physiographic factors. The smooth function $f_{10}(P)$ shows that there is a subtle relation between $P$ and $V$ that is difficult to interpret given the presence of two other spatially varying parameters (OmegaEM and $f_9$).

### A.5.5 Limitations of QGAM and VGAM and Thoughts for Improvement

According to the National Research Council (2004, p. 123) "a limitation of [the discharge measurement database] is that [streamgages] are chosen to have particular channel characteristics, such as the existence of a control section that will ensure a unique rating curve." The National Research Council (2004, p. 123) continues, "the channel characteristics of [streamgage] locations may thus not be representative of randomly selected locations at any point along the entire length of a stream or river." This last statement is particularly relevant for regional analysis of discharge measurement databases in that many high-magnitude discharge measurements are made at bridge crossings; the primary end-user application for VGAM is foreseen to be at or near bridge crossings in Texas. The general applicability

or unapplicability of QGAM and VGAM for other cross sections of streams in Texas is difficult to quantitatively assess.

Assuming that the QGAM and VGAM do have acceptable applicability for other cross sections in Texas, additional discussion of applicability in terms of location is needed. The far western part of Texas is a mountainous region (Figures A.5 and A.9) with few USGS streamgages. The applicability of QGAM and VGAM is uncertain, but the models might retain some but difficult to quantify applicability in far western Texas. The number of streamgages diminishes rapidly towards the southernmost part of Texas; however because of the low-relief terrain, similarity in soils and vegetation, and orientation of the region with respect to the Gulf of Mexico, the authors suggest that QGAM and VGAM remain applicable. Lastly, the far north-northwestern parts of Texas also have few streamgages. By consideration of the physiographic features and the preponderance of branded sand channels in that general region, the authors suggest that QGAM and VGAM might retain some but difficult to quantify applicability.

As discussed in Section A.4, the structure of Manning's equation and thus the potential influence of $S$ on computation of $Q$ or $V$ is important, but such "proximal-to-streamgage" $S$ data are lacking for this paper. The eventual inclusion of a $S$ (friction, channel, or other slope) as a predictor variable in QGAM and seemingly more importantly in VGAM (because of the smaller adjusted R-squared) should further enhance the regionalization of the discharge measurement database used here. Other potentially useful characteristics of the stream network or the channel near the streamgage include stream order Strahler (1957); Shreve (1966), drainage density, and sinuosity. The authors hypothesize that the inclusion of additional "channel-specific characteristics" that are near the streamgage could serve as measurably important predictor variables for alternative QGAM and VGAM. Presumably, model diagnostics will improve as near-the-streamgage characteristics are included in the regionalization.

General enhancement to the GAM diagnostics should be attainable through deliberate and systemic review of the summary statistics of $A$, $Q$, $V$, Fr, and $B$. It might be possible for analysts to select particular variable thresholds. For example, all discharge measurements with $0.1 \leq \text{Fr} < 1$ or $1 \leq B \leq 2{,}000$ m could be retained and the regional analysis proceeding from there.

A suggested approach beyond conventional residual or standardized residual plots would be an evaluation of the inherently coupled relations between $Q$ and $V$ on a per-streamgage basis. For example, it is known that the $Q$ and $V$ for most streamgages show positive association ($Q$ increasing with $V$ and vice versa); however, a not insubstantial number

of streamgages do show negative association between $Q$ and $V$. Could the generalized association (positive or negative) of $Q$ and $V$ for a given streamgage be used for further statistical enhancement?

## A.6 Example Applications

### A.6.1 Post-Event Discharge Estimation

Two example applications of the QGAM and VGAM are presented in this section. Suppose that a direct-runoff event occurred and an analyst is interested in estimating the $Q_p$ for a particular stream located at about 31.5° north and −98.5° west. A postdirect-runoff event survey measures that the top width of the peak water surface at about 100 m and the average depth is estimated as 4.5 m. The estimated cross section area is thus 450 $m^2$. The $P$ for the location is about 744 mm PRISM Climate Group (2010), and the OmegaEM parameter in Figure A.3 for the location is about −0.106.

The smooth function $f_5(l,k)$ of the location for QGAM is judged to be about 0.15 from Figure A.5 using interpretation and interpolation of the smooth function lines (black lines) and the lower and upper standard error lines (green and red lines, respectively) as available. The smooth function $f_6(P)$ of $P$ for QGAM is about −0.02 from Figure A.6. The $Q_p$ can now be readily computed by variable substitution in Equation A.6:

$$\begin{aligned}\log(Q_p) &= -0.2896 + 1.269\log(450) - 0.2247\log(100) \\ &\quad +0.2865(-0.106) + 0.15 - 0.02 \qquad \text{(A.8)}\\ \log(Q_p) &= 2.728 \qquad \text{(A.9)}\\ Q_p &= 535 \text{ m}^3/\text{s} \qquad \text{(A.10)}\end{aligned}$$

For this estimate of $Q_p$, the $\overline{V}$ is:

$$\overline{V} = \frac{535\ [\text{m}^3/\text{s}]}{450\ [\text{m}^2]} = 1.19 \text{ m/s} \qquad \text{(A.11)}$$

The VGAM provides an alternative estimate of $V$ for a $Q$ of 535 $m^3/s$. The smooth function $f_9(l,k)$ of the location for VGAM is judged to be about 0.06 from Figure A.9 using interpretation and interpolation of the smooth function lines (black lines) and the

lower and upper standard error lines (green and red lines, respectively) as available. The smooth function $f_{10}(P)$ of $P$ for VGAM is about $-0.02$ from Figure A.10. The $V$ can be readily computed by variable substitution in Equation A.7:

$$V^{1/5} = 0.9758 + 0.1588\log(535) - 0.1820\log(100) + 0.0854(-0.106) + 0.06 - 0.02 \quad \text{(A.12)}$$

$$V^{1/5} = 1.076 \quad \text{(A.13)}$$

$$V = 1.44 \text{ m/s} \quad \text{(A.14)}$$

Lastly, the authors observe that the two estimates of $V$ (1.19 m/s versus 1.44 m/s) are seemingly consistent with each other. Consistency between either a computed (from known or design discharge and known cross sectional area) or modeled $\overline{V}$ and $V$ predicted by VGAM is the subject of the next section.

### A.6.2 Review of Mean Velocity from a Hydraulic Model

The previous example application guides a user in computing $Q$ given cross-section properties and other characteristics. The focus of the computations was on QGAM. For another example application, the focus is on VGAM. Suppose for the same location that an analyst has a design discharge $Q_T$ of 800 $\text{m}^3/\text{s}$ for a 0.02 AEP or recurrence interval of $T = 50$ years, and a hydraulic model predicts a $B$ of 100 m and an $A$ of 450 $\text{m}^2$ as used in the previous example for simplicity. The hydraulic model is thus predicting a computed $\overline{V}$ of 1.78 m/s. The VGAM can be used to independently evaluate the $\overline{V}$ from the hydraulic model. The $V$ estimate from VGAM is 1.44 m/s as computed in the previous example.

Wood (2009) provides the `predict.gam` function Wood (2006, p. 243), which is designed for use in R. This function computes standard errors of a prediction for a GAM using a Bayesian posterior covariance matrix. However, without a digital presentation of the GAM object from R as well as R running on a host computer, the computations of standard error are tedious and error prone for desktop application by anticipated end users. A convenient means for end-user implementation to only approximate the distribution of a prediction from VGAM (or QGAM by association) thus is needed.

The prediction percentile for a multi-linear regression Helsel and Hirsch (2002, p. 295–322) can be computed by:

$$y(\Pi/100) = y_o + s \times t_{[\Pi/100,n-p]} \sqrt{1+h_o} \tag{A.15}$$

where $y(\Pi/100)$ is the predicted response for the $\Pi$ percentile, $y_o$ is a prediction from the regression model, $n$ is the sample size, $p$ is the number of parameters, $t_{[\Pi/100,n-p]}$ is the quantile distribution function (qdf) of the t-distribution, $s$ is the residual standard error, and $h_o$ is the leverage of the prediction. The sample size for VGAM is large ($n$ =17,751, Figure A.8) and the parameter count is small ($p$ =7, Figure A.8); as a result, the qdf of the standard normal distribution $\Phi(F)$ for nonexeedance probability $F$ can be substituted for the t-distribution.

Although the specific leverage or its equivalence of a GAM for ungaged locations is extremely difficult to represent or approximate, the average leverage of a conventional multi-linear regression model is $p/n$. The average leverage for VGAM is effectively zero because the ratio $7/17{,}751$ is small. Therefore, $h_o$ is approximately zero because of the enormous degrees of freedom and thus $\sqrt{1+h_o} \approx 1$. The residual standard error is $s =$ 0.0630 (Figure A.8). The prediction percentile of the 1.78 m/s velocity can thus be loosely approximated, recalling use of the fifth-root transformation and Equation A.15, by:

$$y(\Pi/100) \approx 1.78^{1/5} \approx 1.44^{1/5} + 0.0630\ \Phi(\Pi/100) \tag{A.16}$$

$$\Phi(\Pi/100) \approx 0.739 \tag{A.17}$$

$$\Pi/100 \approx \phi(0.739) \approx 0.77 \tag{A.18}$$

where $\phi(x)$ is the cumulative distribution function of the standard normal distribution for value $x$. The results show that $\overline{V}$ of the hydraulic model is at the 77th percentile. The project reviewer would naturally conclude that the $\overline{V}$ of the hydraulic model is consistent with VGAM.

To further demonstrate VGAM application, suppose that an analyst wants to apply for the same location a design $Q_T$ of 2,100 $m^3/s$. Suppose also that the analyst has run or is reviewing a hypothetical hydraulic model predicting $B$ of 100 m and $A$ of 450 $m^2$ (as used in previous examples for simplicity). The hydraulic model is thus predicting a computed $\overline{V}$ of 4.67 m/s. The prediction percentile for 4.67 m/s can be estimated, recalling use of the fifth-root transformation, by:

$$y(\Pi/100) \approx 4.67^{1/5} \approx 1.44^{1/5} + 0.0630\ \Phi(\Pi/100) \tag{A.19}$$

$$\Phi(\Pi/100) \approx 4.53 \tag{A.20}$$

$$\Pi/100 \approx \phi(4.53) > 0.999 \tag{A.21}$$

The results show that the hydraulically modeled $V$ is in excess of the 99.9th percentile of VGAM. The analyst running or reviewing the hydraulic model would naturally conclude that the $\overline{V}$ is inconsistent with VGAM and by extension is inconsistent with more than 17,700 measurements of high-magnitude discharge in Texas. The apparent absence of congruence between the two $V$ values could be a sign that enhancements to the reliability of the hydraulic model through changes in model assumptions, parameter values, or select cross-section representations might be possible.

The previous computations considered a large hydraulically modeled $\overline{V}$. The problem could also be in the opposite direction. Suppose for the same location that the design $Q_T$ is 210 $\mathrm{m}^3/\mathrm{s}$ and again a hydraulic model is predicting a $B$ of 100 m and an $A$ of 450 $\mathrm{m}^2$. The hydraulic model is thus predicting a computed $\overline{V}$ of 0.467 $\mathrm{m}/\mathrm{s}$. The prediction percentile for 0.467 $\mathrm{m}/\mathrm{s}$ can be estimated, recalling use of the fifth-root transformation, by:

$$y(\Pi/100) \approx 0.467^{1/5} \approx 1.44^{1/5} + 0.0630\ \Phi(\Pi/100) \tag{A.22}$$

$$\Phi(\Pi/100) \approx -3.44 \tag{A.23}$$

$$\Pi/100 \approx \phi(-3.44) < 0.0003 \tag{A.24}$$

The results show that the hydraulically modeled $\overline{V}$ is less than the 0.03th percentile. Again, the analyst running or reviewing the hydraulic model would naturally conclude that the $\overline{V}$ is inconsistent with VGAM and by extension is inconsistent with more than 17,700 measurements of high-magnitude discharge in Texas. The apparent absence of congruence between the two $V$ values could be a sign that enhancements to the reliability of the hydraulic model through changes in model assumptions, parameter values, or select cross-section representations might be possible.

The procedures shown to compute the distribution of a prediction from VGAM in this section are also applicable by association to the distribution of a prediction from QGAM although example computations are not shown in this paper.

## A.7 Discussion

A 90th-percentile or high-magnitude discharge measurement database containing more than 17,700 discharge values and ancillary hydraulic properties was assembled from summaries of discharge measurement records for 424 U.S. Geological Survey streamflow-gaging stations (streamgages) in Texas. These discharge measurements therefore are assumed to represent discharge measurements made during direct-runoff conditions at each streamgage.

Systematic and statewide investigation of these high-magnitude discharges in pursuit of regional models for the estimation of discharge and mean velocity has not been previously attempted. Generalized additive regression modeling is used to develop readily implemented procedures by end users for estimation of discharge and mean velocity from select predictor variables at ungaged stream locations. Example applications and computations using both regression models are provided.

The application of generalized additive model regression techniques created apparently useful almost statewide-applicable models of discharge and mean velocity. The diagnostics of the generalized additive models of discharge (QGAM) and mean velocity (VGAM) presented including adjusted R-squared, residual standard error, the wide ranges in predictor variable values, the large number of streamgages, and imposing number of discharge measurements indicate that reliable estimation of $Q$ and $V$ can be made from the parametric and smooth function components of QGAM and VGAM, respectively. The two smooth functions within QGAM and VGAM show a particular advantage of regionalization using GAM algorithms. Specifically, the smooth function variable fitting to otherwise difficult to incorporate predictor variables measurably enhances the regression model without the explicit need to find optimal transformations for each term with respect to the response variable. The application of generalized additive model regression techniques created apparently useful near-statewide applicable models of discharge and mean velocity.

The application of GAM for the regionalization of USGS discharge measurement database(s) could be enhanced by inclusion of potentially useful channel, soil, or vegetation properties near streamgages. Such properties could include proximal channel slope, cohesion classification of bed and bank soils, or channel vegetation classification or density measures. The imposing size of the Texas database suggests that statistical associations with these and other potential predictor variables could be found and statistical enhancements could be made for alternative QGAM and VGAM analyses.

This study focused on measurements of discharge related to direct-runoff conditions, which is determined by those $Q$ values exceeding the 90th-percentile daily mean streamflow.

It currently is unknown what changes or influence (sensitivity) in the basic QGAM or VGAM would manifest with alternative probability thresholding. It might be possible to include a factor variable of "low," "base," and "high" flow conditions as a predictor variable in the model building process to include all discharge measurements (more than 89,900 in Texas) and create more hydrologic-spectrum encompassing GAMs of $Q$ or $V$ than reported in this paper. Alternatively, a low-flow or drought regionalization of $Q$ and $V$ from perhaps a "10th-percentile discharge measurement database" could be more applicable for instream-flow assessments than the 90th-percentile discharge measurement (direct-runoff) database and the reported QGAM and VGAM.

The authors purposely constructed QGAM and VGAM to use $B$ instead of hydraulic depth $D = A/B$. The authors selected $B$ for the VGAM because the response variable reported $V$ was nominally computed as $Q/A$ and hence, use of either $A$ or the ratio $A/B$ as predictor variables in VGAM leads to conceptual and numerical problems. The $B$ was therefore retained in QGAM for some algebraic consistency with VGAM.

Following the availability of reliable QGAM and VGAM models, some other ideas have come to the authors attention. The authors suggest that QGAM or other similar statistical models when coupled with a stage (gage height, $h$) table of cross-section flow area $A(h)$ and a stage table of water-surface top width $B(h)$ could contribute to streamflow monitoring in which peak-stage records or stage-hydrograph recorders are used to support "an alternative data collection paradigm of collecting slightly less accurate [streamflow] information at more geographic sites" National Research Council (1999, p. 27). Further, QGAM or other statistical models have a natural application for "construction of stream rating curves" for which the National Research Council (1999, p. 28) deems an area where technique improvement is needed.

Further development and refinement of statistical approaches (GAM or otherwise) for regionalization of the extensive and nation-wide discharge measurement databases of the USGS also could produce viable and alternative regional models of $Q$ and $V$ measurements. Such models then could support "short-term [monitoring] of flows at street and highway crossings to generate design [discharge] data ... [which] might be done more appropriately by federal, state, or local highway administrations [than the USGS]" National Research Council (2004, p. 90). Such monitoring interlocks with the "alternative data collection paradigm" in the previous paragraph. Lastly, the incorporation of $B$ in the GAMs might make these models more compatible with sophisticated computer imaging and processing systems used for visually monitoring channel and streamflow conditions. Such systems could provide for objective detection of water-surface extent $B$ rather than water-surface

elevation $h$ from image sequences (video) and $A$ estimated in turn from $A(B)$ rating tables ($A$ as a function of $B$).

As regional models of $Q$ and $V$ become more sophisticated and refined, other applications might be identified. For instance, the $Q$ model could form the basis for assessment of the probability of roadway inundation during high-magnitude discharges at low-chord (low-roadway) elevation stream crossings in rural areas with low traffic volumes that may not warrant efforts towards rigorous hydraulic analysis. Suppose an analyst has estimates of the flood-frequency curves (discharge as a function of AEP) for these stream crossings, such as provided by the equations in Asquith and Roussel (2009), and $A(h)$ and $B(h)$ tables. A value for $h$ defined by the lowest low-chord elevation of the stream crossing could provide estimates of $A$ and $B$. These estimates could be used to compute $Q'$—the discharge for which over-topping of the stream crossing commences—from a model like QGAM. The analyst could then estimate the AEP value of $Q'$ from the flood-frequency curve; if this "estimated AEP of over-topping" is found to be too small according some institutional guidance or regulation, then the hydrologic hazard of the stream crossing could be deemed substantial and more rigorous hydraulic analysis conducted.

## Acknowledgements

The inspiration for this paper originated from discussions between G.R. Herrmann and W.H. Asquith in December 2008. The nexus was Herrmann's question "What can the USGS discharge measurement database in Texas tell the analyst running or reviewing a hydraulic model about the expected value or distribution of mean velocity for design discharges that emanate from hydraulic models within natural channels or near bridge openings?" Exploratory analyses (circa 2009–10) by Asquith and Herrmann were summarized in an unpublished whitepaper (now in Section 3.5 of this dissertation), which discussed the potential for regionalization of discharge measurement databases. The authors thank D.B. Thompson (R.O. Anderson) for constructive comments in an early draft of this paper. The authors thank M.C. Roussel (USGS) and R.M. Slade, Jr. (retired USGS Surface-Water Specialist in Texas) for providing thoughtful comments on early drafts of this paper. Lastly, the authors are grateful for the instructive anonymous peer reviews of this paper.


**Figure A.1.** U.S. Geological Survey (USGS) personnel conducting one of two high-magnitude discharge measurements on January 11, 2007 at USGS streamflow-gaging station 08156800 Shoal Creek at West 12th Street, Austin, Texas. Both measurements are represented in the database used for this paper. Photograph by W.H. Asquith and courtesy of USGS.

**Figure A.2.** U.S. Geological Survey (USGS) personnel surveying on December 15, 2004 one of four stream cross sections to support a slope-area computation of peak discharge for a historically important event at USGS streamflow-gaging station 08148500 North Llano River near Junction, Texas. Photograph by W.H. Asquith and courtesy of USGS.

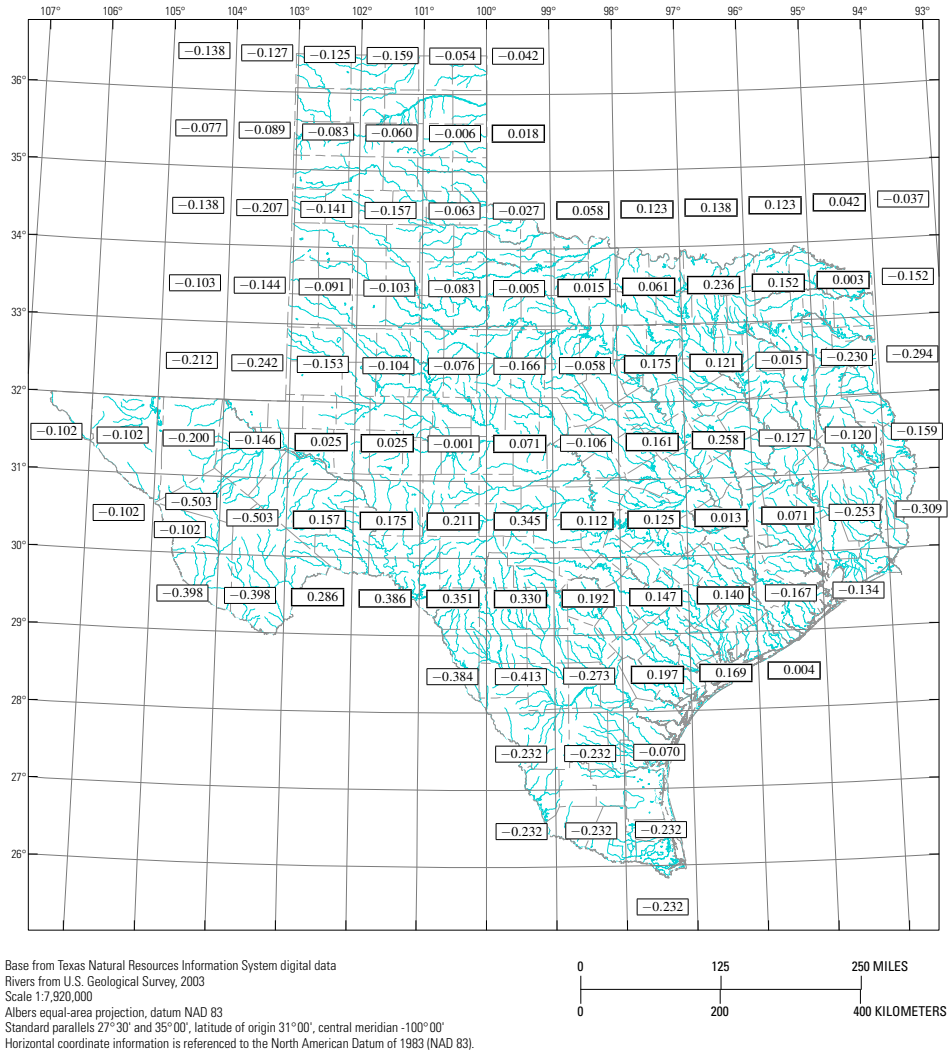


**Figure A.3.** OmegaEM parameter of Asquith and Roussel (2009) to be used in generalized additive model (GAM) of discharge (QGAM) shown in Figure A.4 and Equation A.6 and generalized additive model of mean velocity (VGAM) shown in Figure A.8 and Equation A.7. The OmegaEM parameter represents a generalized terrain and climate index expressing relative differences in peak-streamflow potential across Texas (reproduced from Asquith and Roussel (2009))

```
DISCHARGE GENERALIZED ADDITIVE MODEL (QGAM), SI UNITS

Select Abbreviations:
log = base-10 logarithm used on Q, A, and B
Q   = discharge in cubic meters per second
A   = cross-section area in square meters
B   = water-surface top width in meters
oem = OmegaEM parameter (Asquith and Roussel, 2009)

Family: gaussian
Link function: identity

Formula:
logQ ~ logA + logB + oem +
       s(LongitudeDegrees, LatitudeDegrees, k = 14) +
       s(MeanAnnualPrecipMillimeters, bs = "cr", k = 5)

Parametric coefficients:
             Estimate Std. Error t-value Pr(>|t|)
(Intercept) -0.289609   0.006156  -47.05   <2e-16
logA         1.269194   0.004927  257.59   <2e-16
logB        -0.224712   0.007641  -29.41   <2e-16
oem          0.286524   0.028057   10.21   <2e-16
---

Approximate significance of smooth terms:
                                       edf Ref.df      F p-value
s(LongitudeDegrees,LatitudeDegrees) 12.87  13.00 187.19  <2e-16
s(MeanAnnualPrecipMillimeters)       4.00   4.00  25.96  <2e-16
---

R-sq.(adj) =  0.949   Deviance explained = 94.9%
GCV score = 0.047158  Scale est. = 0.047103  n = 17727
Residual Standard Error (gaussian family) = 0.217032

RESIDUAL SUMMARY
    Min.  1st Qu.   Median     Mean  3rd Qu.     Max.
-1.04100 -0.12800  0.01848  0.00000  0.14320  1.05000
```

**Figure A.4.** Summary in R output of generalized additive model of base-10 logarithm of discharge based on statistical relations between the base-10 logarithms of discharge and water-surface top width, OmegaEM parameter by Asquith and Roussel (2009), and separate smooth functions of longitude and latitude $f_5(l,k)$ (figure A.5) and mean annual precipitation $f_6(P)$ (figure A.6)

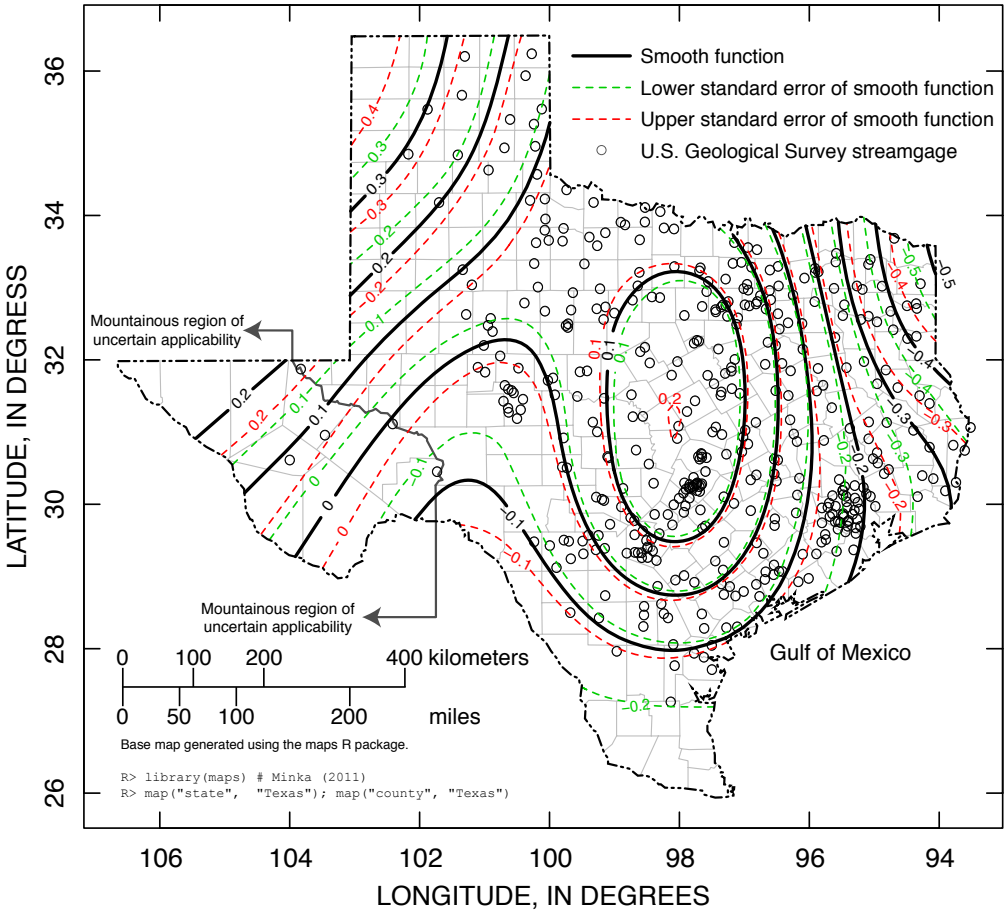


**Figure A.5.** Smooth function $f_5(l,k)$ of location in Texas for the discharge model shown in Figure A.4

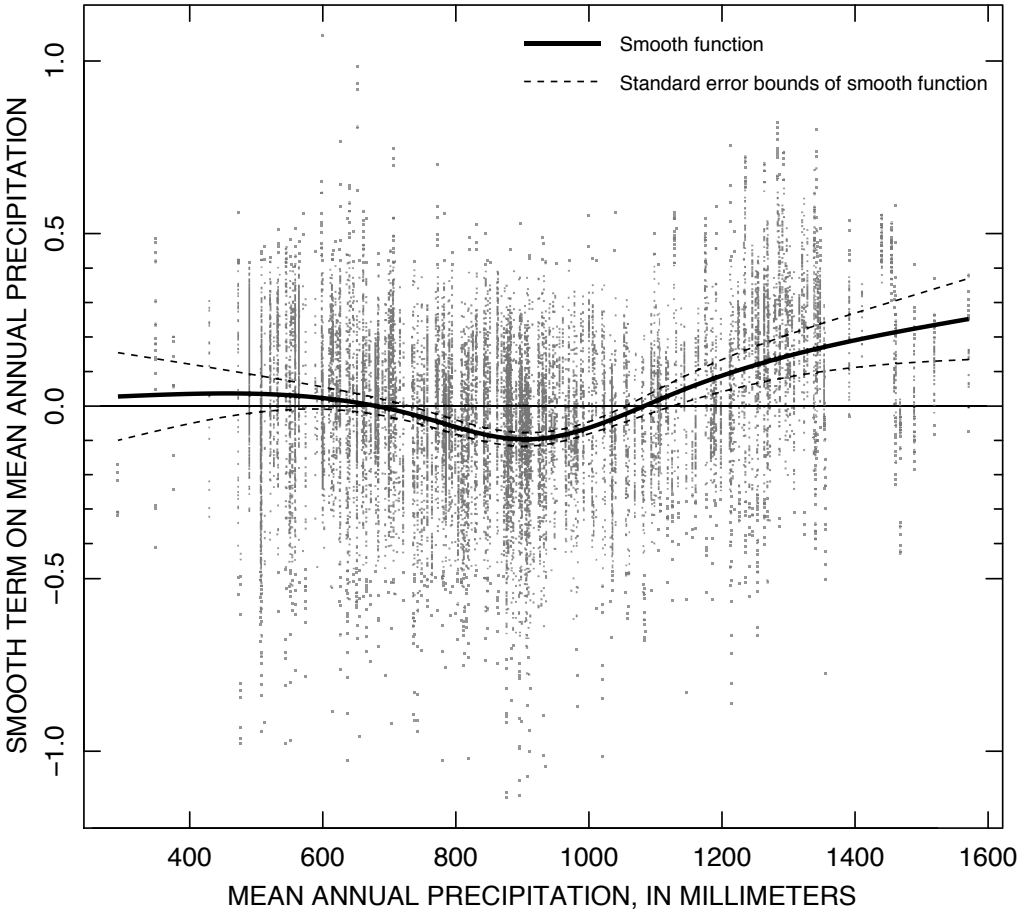


**Figure A.6.** Smooth function $f_6(P)$ of mean annual precipitation for the discharge model shown in Figure A.4

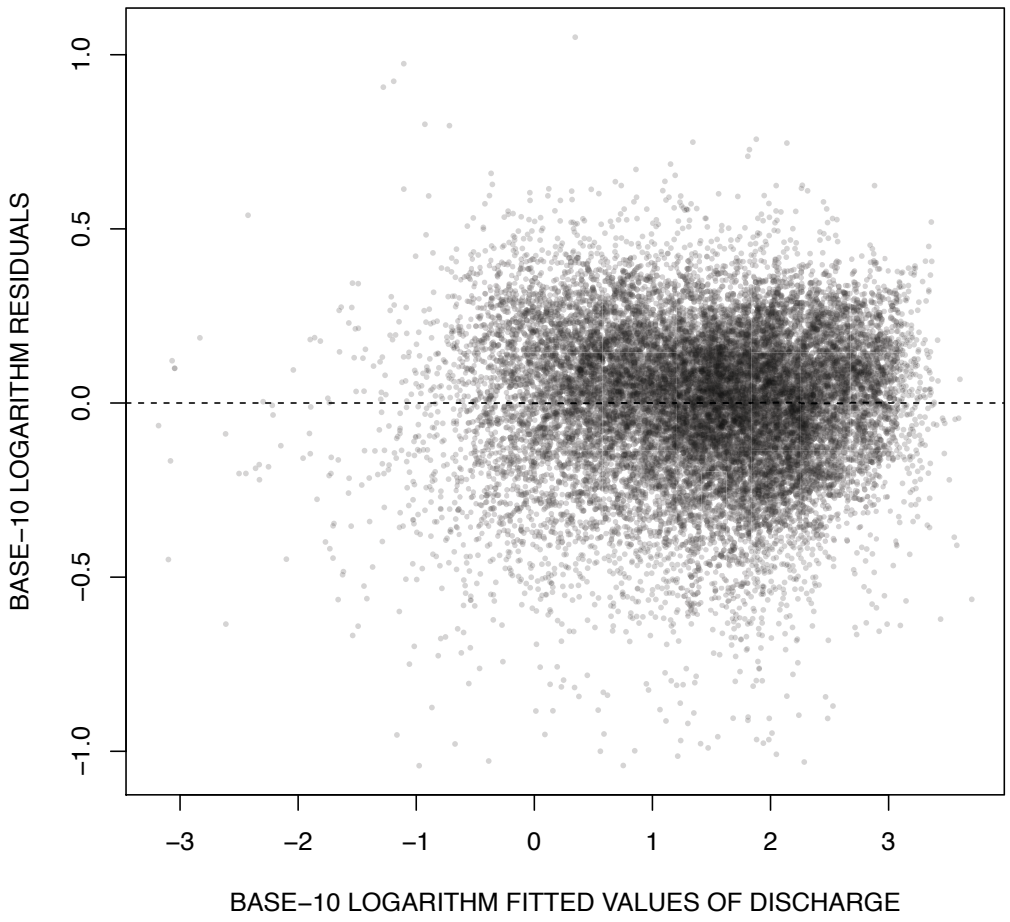


**Figure A.7.** Residuals for the discharge model shown in Figure A.4

```
VELOCITY GENERALIZED ADDITIVE MODEL (VGAM), SI UNITS

Select Abbreviations:
tV  = fifth-root of mean velocity in meters per second
log = base-10 logarithm used on Q and B
Q   = discharge in cubic meters per second
B   = water-surface top width in meters
oem = OmegaEM parameter (Asquith and Roussel, 2009)

Family: gaussian
Link function: identity

Formula:
tV ~ logQ + logB + oem +
     s(LongitudeDegrees, LatitudeDegrees, k = 14) +
     s(MeanAnnualPrecipMillimeters, bs = "cr", k = 5)

Parametric coefficients:
             Estimate Std. Error t-value Pr(>|t|)
(Intercept)  0.9758281  0.0018882  516.80   <2e-16
logQ         0.1588495  0.0009992  158.98   <2e-16
logB        -0.1819640  0.0018281  -99.54   <2e-16
oem          0.0853768  0.0081059   10.53   <2e-16
---

Approximate significance of smooth terms:
                                       edf Ref.df      F  p-value
s(LongitudeDegrees,LatitudeDegrees) 12.72  12.99 203.25  < 2e-16
s(MeanAnnualPrecipMillimeters)       4.00   4.00  11.33 3.52e-09
---

R-sq.(adj) =  0.671   Deviance explained = 67.1%
GCV score = 0.0039773  Scale est. = 0.0039727  n = 17751
Residual Standard Error (gaussian family) = 0.063029

RESIDUAL SUMMARY
      Min.    1st Qu.     Median       Mean    3rd Qu.       Max.
-0.3762000 -0.0389000 -0.0007972  0.0000000  0.0406300  0.4032000
```

**Figure A.8.** Summary in R output of generalized additive model of fifth root of mean velocity based on statistical relations between the base-10 logarithms of discharge and water-surface top width, OmegaEM parameter by Asquith and Roussel (2009), and separate smooth functions of longitude and latitude $f_9(l,k)$ (figure A.9) and mean annual precipitation $f_{10}(P)$ (figure A.10)

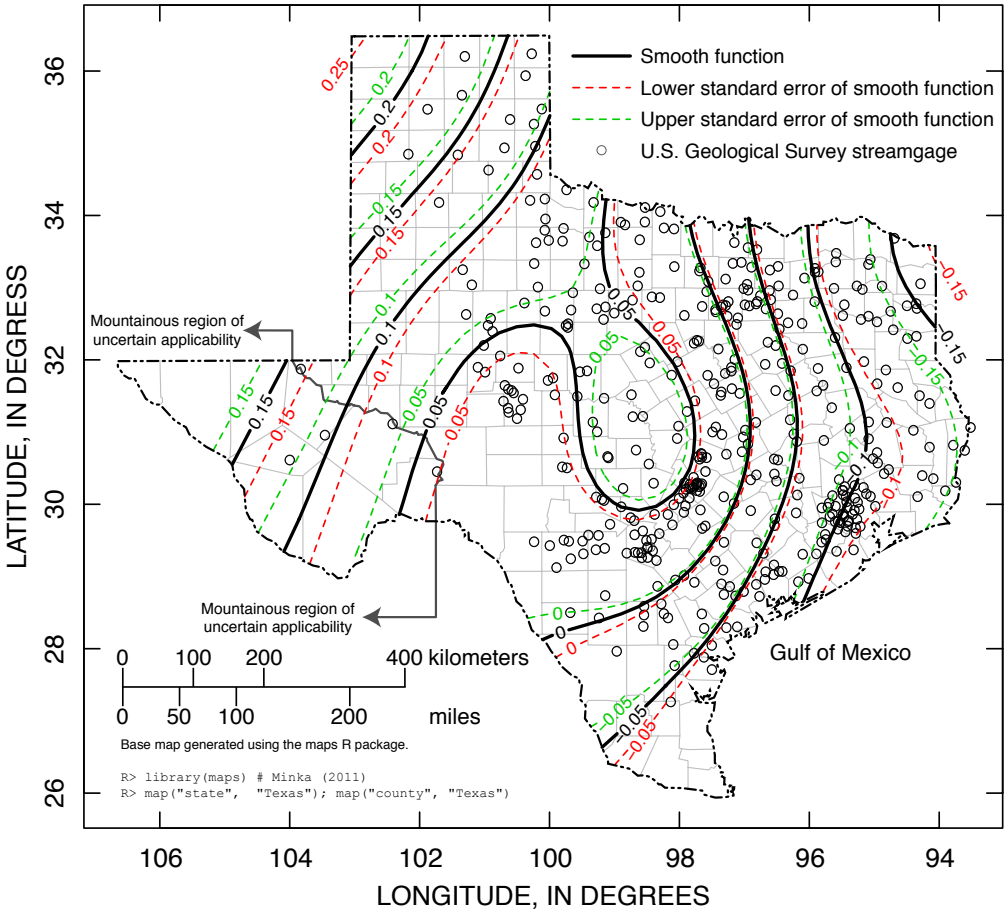


**Figure A.9.** Smooth function $f_9(l,k)$ of location in Texas for the mean velocity model shown in Figure A.8

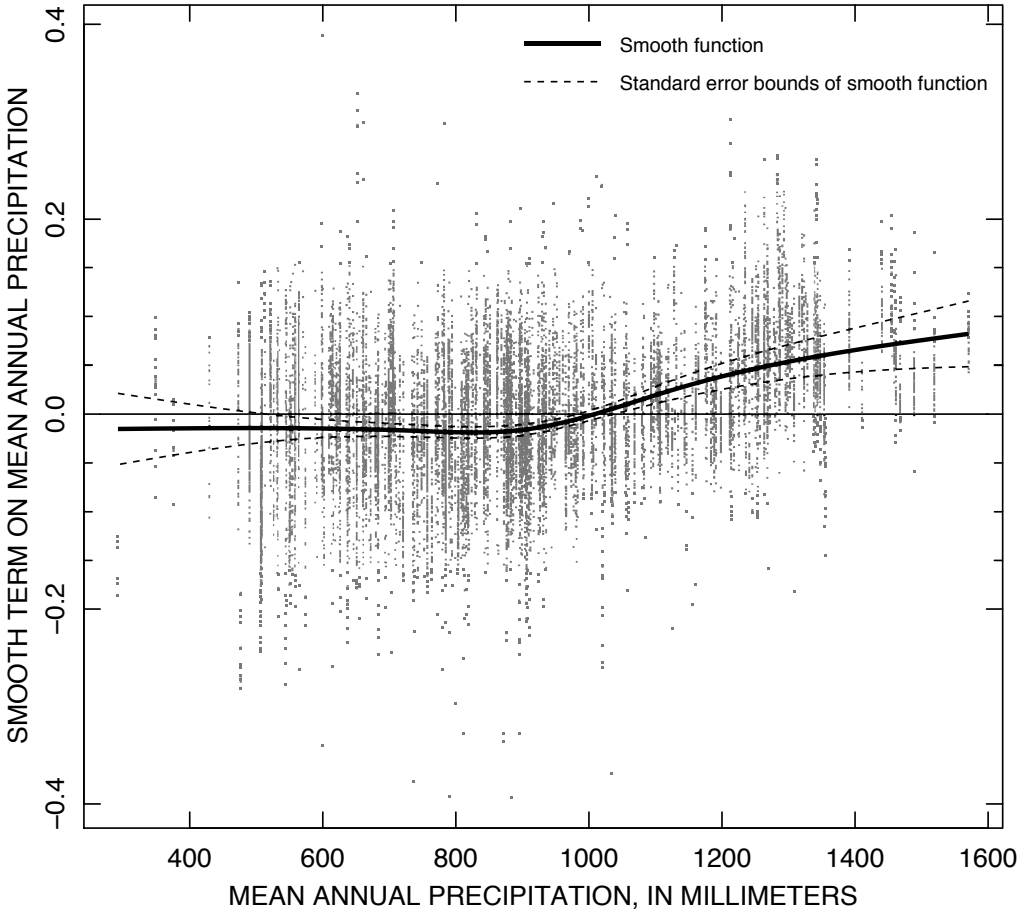


**Figure A.10.** Smooth function $f_{10}(P)$ of mean annual precipitation for the mean velocity model shown in Figure A.8

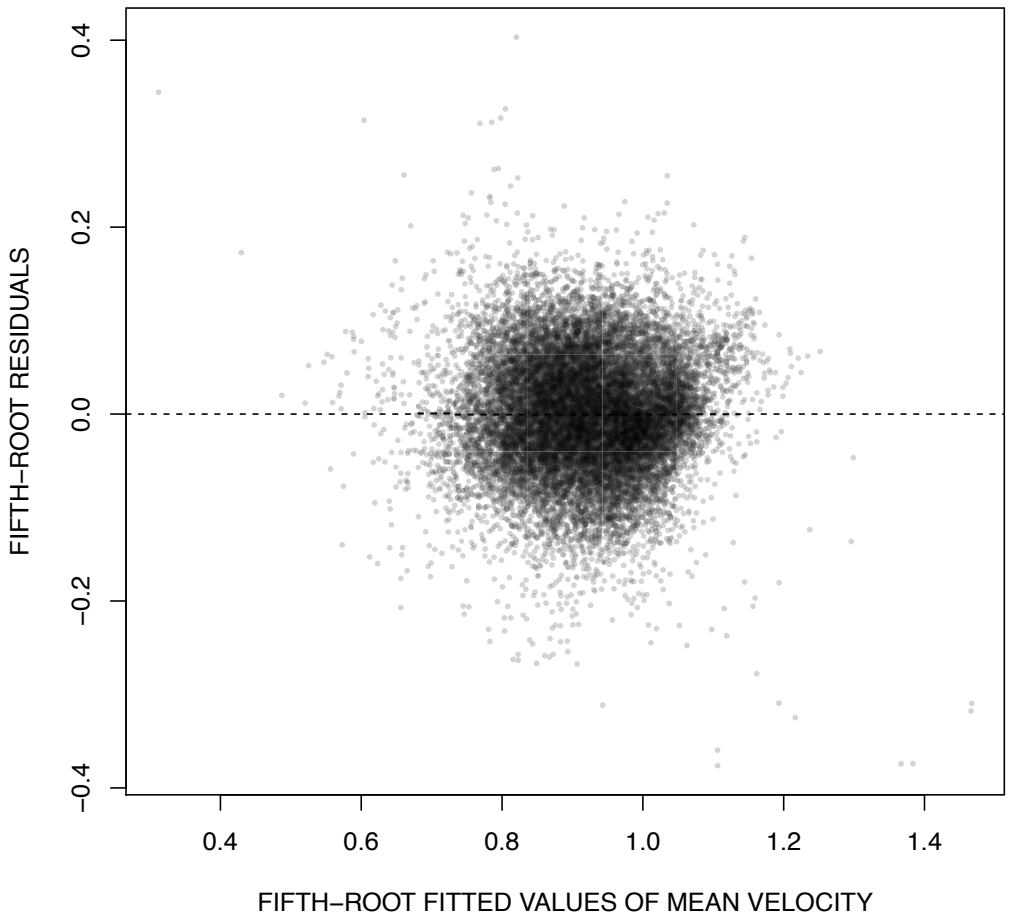


**Figure A.11.** Residuals for the mean velocity model shown in Figure A.8

# Appendix B
# Exponential Survival Code

## B.1 Instructions for the Use of Exponential Survival Model R Code

The **R** code necessary to perform the survival computations as done for the case studies is included in the appendices. This appendix includes the code using the exponential distribution as the random process approximation, while appendix C includes the code using the Weibull distribution. Both versions of the code can accept a 20-value vector of incremental time-area fractions. There are three such vectors that can be set as default by adding and removing pound signs.

The code below must be reproduced, normally in a text file or in the script editor of the **R** environment, and input at the command prompt of the **R** console window in order to load the functions. This can be done by copy/paste, by typing "source(filename)" at the command prompt, using the filename of the file storing the code, or by using a pull-down menu to access the "source" command, after which the file is selected from a list of files in the active directory. After sourcing the file or pasting the command string at the prompt, the functions are accessible to the user until the **R** session is terminated.

The exponential version requires a rainfall vector, a vector of $\lambda$ values, and a vector called *mfact*. Each must have the same number of elements. The mfact vector is a scalar multiplier that was intended as a tuning factor. It was not used in this context. The vectors used must all have the same number of elements.

The routine is invoked by typing

```
stormexp(rain=..., rate=..., mfact=..., tstep=...)
```

at the command line, and giving the appropriate names of the vectors. The code can be demonstrated by typing

```
stormexp()
```

at the command line. This will invoke a default of three rainfall pulses with default values for parameters. The "tstep" parameter specifies time step length, in minutes. The default value is 10 minutes. If not specified in the input, the default is used.

Results of the computations are stored in a data hash named "out.hash" and can be retrieved from the hash for further processing.

## B.2 Exponential R Code Listing

**Listing B.1.** Exponential Version

```
#Set up a hash to throw all of the output to
out.hash<-new.env(hash=TRUE)



#Generate a function to do the actual survival modeling
stormexp<-function(rain=NULL, mfact=NULL, rate=NULL, areas=NULL,
   tstep=NULL){

if(is.null(rain)        ==TRUE) {rain<-c(1, 1, 1)}
if(is.null(mfact)       ==TRUE) {mfact<-rep(1, length(rain))}
if(is.null(rate)        ==TRUE) {rate<-rep(5, length(rain))}
if(is.null(tstep) ==TRUE)       {tstep<-10}

out.hash$frac   <-0
out.hash$numsin <-0
out.hash$numsout        <-0

#Populate a vector of 20 time-area fractions
#An alternative vector can be input manually

if(is.null(areas)       ==TRUE){

#areas<-c(.005,.014,.020,.034,.048,.053,.078,.082,
.083,.087,.097,.097,.077,.054,.048,.044,.029,.024,.019,.007)

areas<-c(.03,.045,.065,.094,.130,.16,.165,.116,.085,
.05,.025,.017,.006,.004,.002,.002,.001,.001,.001,.001)

#areas<-c(.005,.014,.020,.034,.048,.053,.078,.082,
.083,.087,.097,.092,.082,.054,.048,.044,.029,.024,.019,.007)

}



#generate an escape value vector
```

```
radii           <-seq(.025, .975, .05)

#Check length of areas vector
if(length(areas)!=20){print("Length␣of␣areas␣vector␣must␣be␣20")}

#Set up an array for output values from the rainfall computations
rain.out<-c()


#Set up an array for hydrograph output
hydro.out<-matrix(nrow=(length(rain)), ncol=(length(rain)+20))

#Set up a loop that cycles through the rain, rate, and mfact
   vectors
#and invokes the drop function that actually computes the
   hydrograph from
#a set of parameters

k       <-1
while(k<=(length(rain))){
#check for zero rainfall value and replace with small value
        if(rain[k]<0.001)rain[k]<-0.001

#ndrops is the number of drops per unit of conceptual rainfall
        ndrops<-1000000*rain[k]

#Invoke the drop function, take output, and bind it together
        f<-drope(areas, ndrops, mfact=mfact[k], rate=rate[k],
           radii=radii, k=k)
        rain.out<-rbind(rain.out, f)
        k<-k+1
}

#Store the results in the output hash
out.hash$rain.out<-rain.out
```

```
m       <-1
        while(m<=(length(rain))){
        if(m==1){hydro.out[m,]<-c(rain.out[m,], (rep(0, length(
           rain))))}
        if(m>1){hydro.out[m,]<-c((rep(0, (m-1))), rain.out[m,], (
           rep(0, (length(rain)-m+1))))}
        m<-m+1
}

#
runoff  <-c()
p               <-1
while(p<=(length(hydro.out[1,]))){
        runoff[p]<-sum(hydro.out[,p])
        p<-p+1
}
hydro.out<-rbind(hydro.out, runoff)
z<-rep(0, length(hydro.out[,1]))
hydro.out<-cbind(z, hydro.out)
out.hash$hydrograph<-hydro.out


#Set up plotting routines
xval<-seq(, (length(hydro.out[1,])))
xval<-xval-1
xlm<-c(0, (length(hydro.out[1,])*tstep))
ylm<-c(0, ((max(runoff)*1.25)/1000000))
plot(NA, NA, xlim=xlm, ylim=ylm, xlab="Time, Minutes", ylab="
   Runoff, Watershed Inches")
q<-1
while(q<=length(hydro.out[,1])){
#points((xval*tstep), (hydro.out[q,]/1000000), type="l", col=q)
points((xval*tstep), (hydro.out[q,]/1000000), type="l", col="
   white")

q<-q+1
}
```

```
s2<-length(hydro.out[,1])
points((xval*tstep), (hydro.out[s2,]/1000000), type="l", col="
   blue", lwd=2)

#return(out.hash)
}









drope           <-function(areas, ndrops, mfact, rate, radii, k){

areas2  <-areas*ndrops

i               <-1
rads            <-c()


while(i<=20){
fake            <-rep(radii[i], areas2[i])
rads            <-c(rads, fake)
i               <-i+1
}

probs           <-rexp(ndrops, rate=rate)
        if(length(rads) <length(probs)){
rads[(length(rads)+1)]  <-rads[length(rads)]}
        if(length(rads) <length(probs)){
rads[(length(rads)+1)]  <-rads[length(rads)]}
```

```
probs           <-probs*mfact                                                  141
q               <-probs-rads                                                   142
j               <-1                                                            143
        while(j<=ndrops){                                                      144
        if(q[j]<0){q[j]<-0}                                                    145
        if(q[j]>0){q[j]<-1}                                                    146
j               <-j+1                                                          147
}                                                                              148
                                                                               149
escapes<-c()                                                                   150
r<-1                                                                           151
a<-0                                                                           152
b<-0                                                                           153
while(r<=20){                                                                  154
b<-b+areas2[r]                                                                 155
escapes[r]<-sum(q[a:b])                                                        156
a<-a+areas2[r]                                                                 157
r<-r+1                                                                         158
}                                                                              159
                                                                               160
#print(escapes)                                                                161
frac<-escapes/areas2                                                           162
frac<-round(frac, digits=3)                                                    163
out.hash$frac<-rbind(out.hash$frac, frac)                                      164
out.hash$numsin<-rbind(out.hash$numsin, areas2)                                165
out.hash$numsout<-rbind(out.hash$numsout, escapes)                             166
out.hash$depthsin<-out.hash$numsin/ndrops                                      167
out.hash$depthsout<-out.hash$numsout/ndrops                                    168
                                                                               169
print(sum(out.hash$numsin))                                                    170
print(sum(out.hash$numsout)/sum(out.hash$numsin))                              171
return(escapes)                                                                172
}                                                                              173
```

# Appendix C
# Weibull Survival Code

## C.1 Instructions for the Use of Weibull Survival Model R Code

The **R** code necessary to perform the survival computations as done for the case studies is included in the appendices. Appendix B includes the code using the exponential distribution as the random process approximation, while this appendix includes the code using the Weibull distribution. Both versions of the code can accept a 20-value vector of incremental time-area fractions. There are three such vectors that can be set as default by adding and removing pound signs.

The code below must be reproduced, normally in a text file or in the script editor of the **R** environment, and input at the command prompt of the **R** console window in order to load the functions. This can be done by copy/paste, by typing "source(filename)" at the command prompt, using the filename of the file storing the code, or by using a pull-down menu to access the "source" command, after which the file is selected from a list of files in the active directory. After sourcing the file or pasting the command string at the prompt, the functions are accessible to the user until the **R** session is terminated.

The Weibull version requires a rainfall vector, a vector of scale parameter values, and a vector of shape parameter values. If the shape parameter is 1, it is identical to the exponential. The vectors used must all have the same number of elements.

The routine is invoked by typing

```
stormwbl(rain=..., shape=..., scale=..., tstep=...)
```

at the command line, and giving the appropriate names of the vectors. The code can be demonstrated by typing

```
stormwbl()
```

at the command line. This will invoke a default of three rainfall pulses with default values

for parameters. The “tstep” parameter specifies time step length, in minutes. The default value is 10 minutes. If not specified in the input, the default is used.

Results of the computations are stored in a data hash named “out.hash” and can be retrieved from the hash for further processing.

## C.2 Wiebull R Code Listing

**Listing C.1.** Weibull Version

```
#Set up a hash to throw all of the output to
out.hash<-new.env(hash=TRUE)


#Generate a function to do the actual survival modeling
stormwbl<-function(rain=NULL, scale=NULL, shape=NULL, areas=NULL,
    tstep=NULL){

if(is.null(rain)        ==TRUE) {rain<-c(1, 1, 1)}
if(is.null(scale)       ==TRUE) {scale<-rep(.2, length(rain))}
if(is.null(shape)       ==TRUE) {shape<-rep(1, length(rain))}
if(is.null(tstep) ==TRUE)       {tstep<-10}

out.hash$frac   <-0
out.hash$numsin <-0
out.hash$numsout        <-0

#Populate a vector of 20 time-area fractions

if(is.null(areas)       ==TRUE){

#areas<-c(.03,.045,.065,.094,.130,.16,.165,.116,.085,
.05,.025,.017,.006,.004,.002,.002,.001,.001,.001,.001)
areas<-c(.005,.014,.020,.034,.048,.053,.078,.082,.083,
.087,.097,.092,.082,.054,.048,.044,.029,.024,.019,.007)



}
#Generate an escape value vector
radii           <-seq(.025, .975, .05)
```

```
#Check length of areas vector
if(length(areas)!=20){print("Length␣of␣areas␣vector␣must␣be␣20")}

#Set up an array for output values from the rainfall computations
rain.out<-c()

#Set up an array for hydrograph output

hydro.out<-matrix(nrow=(length(rain)), ncol=(length(rain)+20))

#Set up a loop that cycles through the rain, scale, and shape
   vectors
#and invokes the drop function that actually computes the
   hydrograph from
#a set of parameters


k       <-1
while(k<=(length(rain))){
#check for zero rainfall value and replace with small value
        if(rain[k]<0.001){rain[k]<-0.001}

#ndrops is the number of drops per unit of conceptual rainfall

        ndrops<-1000000*rain[k]
#Invoke the drop function, take output, and bind it together

        f<-dropw(areas, ndrops, scale=scale[k], shape=shape[k],
           radii=radii, k=k)
        rain.out<-rbind(rain.out, f)
        k<-k+1
}
#Store the results in the output hash
out.hash$rain.out<-rain.out

m       <-1
        while(m<=(length(rain))){
```

```
        if(m==1){hydro.out[m,]<-c(rain.out[m,], (rep(0, length(
           rain))))}
        if(m>1){hydro.out[m,]<-c((rep(0, (m-1))), rain.out[m,], (
           rep(0, (length(rain)-m+1))))}
        m<-m+1
}

runoff  <-c()
p               <-1
while(p<=(length(hydro.out[1,]))){
        runoff[p]<-sum(hydro.out[,p])
        p<-p+1
}
hydro.out<-rbind(hydro.out, runoff)
z<-rep(0, length(hydro.out[,1]))
hydro.out<-cbind(z, hydro.out)
out.hash$hydrograph<-hydro.out

#Set up plotting routines
xval<-seq(, (length(hydro.out[1,])))
xval<-xval-1
xlm<-c(0, (length(hydro.out[1,])*tstep))
ylm<-c(0, ((max(runoff)*1.25)/1000000))
plot(NA, NA, xlim=xlm, ylim=ylm, xlab="Time, Minutes", ylab="
   Runoff, Watershed Inches")
q<-1
while(q<=length(hydro.out[,1])){
#points(xval, hydro.out[q,], type="l", col=q)
points(xval, (hydro.out[q,]/1000000), type="l", col="white")

q<-q+1
}
s2<-length(hydro.out[,1])
points((xval*tstep), (hydro.out[s2,]/1000000), type="l", col="
   blue", lwd=2)

#return(out.hash)
}
```

```
dropw<-function(areas, ndrops, scale, shape, radii, k){

areas2<-areas*ndrops

i<-1
rads<-c()

while(i<=20){
fake<-rep(radii[i], areas2[i])
rads<-c(rads, fake)
i<-i+1
}
probs<-rweibull(ndrops, shape=shape, scale=scale)
if(length(rads)<length(probs)){
rads[(length(rads)+1)]<-rads[length(rads)]}

#probs<-probs*mfact
q<-probs-rads
j<-1
while(j<=ndrops){
        if(q[j]<=0){q[j]<-0}
#       if(q[j]=0){q[j]<-0}
        if(q[j]>0){q[j]<-1}
j               <-j+1
j<-j+1
}

escapes<-c()
r<-1
a<-0
```

```
b<-0                                                                    141
while(r<=20){                                                           142
b<-b+areas2[r]                                                          143
escapes[r]<-sum(q[a:b])                                                 144
a<-a+areas2[r]                                                          145
r<-r+1                                                                  146
}                                                                       147
                                                                        148
#print(escapes)                                                         149
frac<-escapes/areas2                                                    150
frac<-round(frac, digits=3)                                             151
out.hash$frac<-rbind(out.hash$frac, frac)                               152
out.hash$numsin<-rbind(out.hash$numsin, areas2)                         153
out.hash$numsout<-rbind(out.hash$numsout, escapes)                      154
out.hash$depthsin<-out.hash$numsin/ndrops                               155
out.hash$depthsout<-out.hash$numsout/ndrops                             156
                                                                        157
print(sum(out.hash$numsin))                                             158
print(sum(out.hash$numsout)/sum(out.hash$numsin))                       159
return(escapes)                                                         160
}                                                                       161
```